MEDICAL UNIVERSITY
OF OHIO

COLLEGE OF GRADUATE STUDIES

FINAL APPROVAL OF DISSERTATION
Doctor of Philosophy in Biomedical Sciences

The Rad51d DNA Repair Gene is Required for Chromosome and Telomere Stability in Mammalian Cells

Submitted by

Phillip G. Smiraldo

In partial fulfillment of the requirements for the degree of
Doctor of Philosophy in Medical Sciences

Date of Defense:

March 10, 2006

Major Advisor
Douglas Pittman, Ph.D.

Academic Advisory Committee
Kandace Williams, Ph.D.
George Cicila, Ph.D.
Mark Micale, Ph.D.
Han-Fei Ding, Ph.D.

Dean, College of Graduate Studies
Keith K. Schlender, Ph.D.

The *Rad51d* DNA Repair Gene is Required for Chromosome and Telomere Stability in Mammalian Cells

Phillip G. Smiraldo

Medical University of Ohio

2006

DEDICATION

This work is dedicated to my wife, Elaine, for her unconditional love and support. I could not have done this without you.

ACKNOWLEDGMENTS

I thank God for all of the gifts that I have been given. I am grateful to Dr. Douglas L. Pittman, my major advisor, for his guidance, patience, and continual support throughout my dissertation studies. He has, from the beginning, pushed me with encouragement to go beyond what I believed were within my limits. I also thank the members of my advisory committee: Dr. Steven L. Britton, Dr. George T. Cicila, Dr. Han-Fei Ding, Dr. Mark A. Micale, and Dr. Kandace J. Williams for their advice and assistance.

I thank Aaron M. Gruver, Dr. Steven L. Britton, Joshua C. Osborn, Aditi Nadkarni, Dr. Changanamkandath Rajesh, and Dr. Venkatesha Basrur for hours of discussion regarding homologous recombination and telomeres. Madalena Tarsounas provided data in Results, Figure 6. Purificación Muñoz and María A. Blasco provided data in Results, Figure 8D and Figure 9. I also thank Marianne Miller-Jasper and the faculty and staff of the Department of Physiology and Cardiovascular Genomics for support during these studies. I thank Mrs. Darl Perry for her thoughts and prayers. Finally, I would like to thank my wife, parents, and family for putting up with me and giving me constant love and support.

"We totally missed the possible role of enzymes in [DNA] repair although…I later came to realize that DNA is so precious that probably many distinct repair mechanisms would exist."

Francis Crick, (1974) The double helix: a personal view. Nature *248*, 766

TABLE OF CONTENTS

INTRODUCTION

DNA is constantly challenged by damage originating from environmental agents and endogenous mutagens (Wood et al., 2001). Cells must efficiently repair damaged DNA to prevent an accumulation of DNA mutations, which can confer loss of the ability to control cell division, senescence, or apoptosis. One of the most genotoxic forms of DNA lesions is the double-stranded break (DSB), because both sugar-phosphate backbones of the DNA double helix are broken. Errors in the repair of a DSB may result in deletion or insertion mutations at the site of damage or chromosome translocations, which may contribute to the initiation or progression of cancer (Pierce et al., 2001). Homologous recombination (HR) is a DNA repair pathway that accurately repairs DNA DSBs by using intact homologous DNA as a replication template. The work described in this dissertation investigates a mammalian protein involved in HR and demonstrates the importance of this repair pathway in maintaining the stability of the mammalian genome.

Homologous recombination mechanisms have been observed in all organisms studied and is of fundamental importance for life (Krogh and Symington, 2004). Homologous recombination is involved in repairing DNA damage, maintaining chromosome stability, and increasing genetic diversity. Additionally, DNA structures that protect the ends of chromosomes (telomeres) resemble HR intermediates, suggesting proteins that function in HR may also have roles in telomere protection. In mammals, HR is directed by the RAD51-family of proteins. This family consists of seven members, RAD51, RAD51B (RAD51L1), RAD51C (RAD51L2), RAD51D (RAD51L3, TRAD), XRCC2, XRCC3, and DMC1, and each is the product of its own respective gene

(Thacker, 1999). Each gene was identified by either cloning human DNA sequences that functionally complement mammalian mutant cell lines that were hypersensitive to DNA damaging agents (Thacker et al., 1995; Liu et al., 1998) or by searching for sequence similarity to *RAD51* or other *RAD51*-family members (Habu et al., 1996; Albala et al., 1997; Cartwright et al., 1998; Dosanjh et al., 1998; Kawabata and Saeki, 1998; Pittman et al., 1998). At the amino acid level, approximately 45% similarity and 25% identity is shared among the RAD51-family members (Thacker, 1999). Although the RAD51-family members share sequence similarity and function in HR, each protein is required for the repair of DNA DSBs and DNA interstrand crosslinks (ICLs), and each likely possesses non-redundant functions (for example, in addition to roles in DNA repair, the RAD51D protein is required for maintaining telomere stability) (see Literature and Results sections). It is an interesting, yet difficult, challenge to determine how each of the RAD51-family members functions in mammalian HR, and whether these proteins are involved in other cellular processes.

Besides the RAD51-family members, additional proteins are required for HR in mammals, including ATM, ATR, BLM, BRCA1, BRCA2, FANC(A-L), MRE11, NBS1, RAD50, RAD52, RAD54, and WRN. Heritable genetic defects in several of these genes confer cancer-prone human syndromes, including *ATM* (ataxia telangiectasia), *ATR* (Seckel syndrome), *BLM* (Bloom syndrome), *FANC*(*A-L*) (Fanconi anemia), *MRE11* (ataxia telangiectasia-like syndrome), *NBS1* (Nijmegen breakage syndrome), and *WRN* (Werner syndrome) (Thompson and Schild, 2002; O'Driscoll et al., 2004). One common feature among these syndromes is that each confers chromosomal instability. Cells

derived from patients with ataxia telangiectasia, ataxia telangiectasia-like syndrome, Nijmegen breakage syndrome, or Werner syndrome have increased sensitivity to ionizing radiation (Digweed et al., 1999; Lavin and Khanna, 1999; Stewart et al., 1999; Yannone et al., 2001), whereas cells from patients with Fanconi anemia or Seckel syndrome are hypersensitive to DNA interstrand crosslinking agents (Auerbach et al., 1981; O'Driscoll et al., 2004), consistent with the corresponding proteins having a roles in DNA repair by HR. A hallmark phenotype of cells from Bloom syndrome patients is an increased frequency of crossovers between sister chromatids (sister chromatid exchange) and increased levels of exchanges between homologous chromosomes (Chaganti et al., 1974; van Brabant et al., 2000). Interestingly, cells derived from patients with ataxia telangiectasia, Bloom syndrome, or Werner syndrome have accelerated telomere attrition *in vitro*, suggesting the ATM, BLM, and WRN proteins also function in telomere maintenance (Klapper et al., 2001). The *BRCA1* and *BRCA2* tumor suppressor genes were identified due to their high mutation frequency in inherited breast and ovarian cancers. Cells deficient for *BRCA1* or *BRCA2* have high levels of chromosomal instability and are hypersensitive to DNA interstrand crossliking agents (Thompson and Schild, 2002). Investigation of these heritable human diseases exemplifies the importance of HR at the cellular level by maintaining the integrity of the genome and repairing DNA damage, and at the organism level by protecting against cancer and maintaining overall health.

Because multiple genetic mutations are required to transform a normal cell to a cancerous cell, individuals who inherit defects in DNA response and repair genes are

likely prone to develop cancer due to the "hypermutability" of their cells (Pierce et al., 2001). This is consistent with the cancer predisposition of patients with the previously mentioned syndromes associated with defects in HR. Additionally, although there is no definite proof, preliminary clinical studies suggest a link between defects in the *RAD51*-family members and cancer susceptibility (Thacker, 2005). One study suggested *RAD51* defects are associated with bilateral breast cancer (Kato et al., 2000), and a separate study found that increased *RAD51* expression correlated with histological grading of sporadic invasive ductal breast cancer (Maacke et al., 2000). In addition, carriers of *BRCA2* mutations have a higher breast cancer risk due to presence of a polymorphism in *RAD51* (Levy-Lahad et al., 2001). Preliminary studies are also consistent with mutations in *RAD51*-like genes and associated cancer formation. Chromosome rearrangements included an amplification of *RAD51C* in breast cancer cell lines and breast tumors (Barlund et al., 2000; G.J. Wu et al., 2000). The *RAD51B* gene was implicated in uterine leiomyoma (a smooth muscle neoplasm) due to a chromosomal translocation between chromosomes 12 and 14, which disrupts the gene resulting in premature transcription termination (Ingraham et al., 1999; Schoenmakers et al., 1999; Takahashi et al., 2001). A common allelic variant of *XRCC3* has been associated with the development of malignant melanoma and bladder cancer (Winsey et al., 2000; Matullo et al., 2001). An allelic variant of *RAD51D* (E233G), which changes the glutamic acid at position 233 to glycine, was more highly represented in high-risk familial breast cancers not associated with defects in *BRCA1* or *BRCA2* genes (Rodriguez-Lopez et al., 2004). These results are

consistent with the hypothesis that defects in *RAD51* and *RAD51*-related genes are responsible for chromosomal abnormalities during the carcinogenesis process.

The focus of this dissertation is on investigating the RAD51-family members and how these proteins function to maintain genome stability. Particular attention has been placed on characterizing the phenotypes of mouse cells deficient for the *Rad51d* gene. The mammalian *RAD51D* gene was originally identified in 1998 (Cartwright et al., 1998; Kawabata and Saeki, 1998; Pittman et al., 1998b). When the studies, described here, were initiated in the fall of 2000, mice deficient for *Rad51d* had been generated (Pittman and Schimenti, 2000) and only two biochemical investigations had been reported (Braybrooke et al., 2000; Schild et al., 2000). In the Literature section, I provide a general overview of HR and telomeres, with special emphasis on the RAD51-related proteins.

The Results section consists of three research manuscripts and supplemental data. The hypothesis of Manuscript 1 proposes that both extensive chromosome instability and the inability to repair DNA damage are the causes of embryonic lethality conferred by a *Rad51d* disruption in mice. These data were published in the research article entitled, "Extensive Chromosomal Instability in *Rad51d*-Deficient Mouse Cells" in *Cancer Research* on March 15, 2005 (Smiraldo et al., 2005). Data presented in the next section were performed in collaboration with Stephen C. West's laboratory at the London Research Institute and María A. Blasco's laboratory at the Spanish National Cancer Center, and was published in the research article entitled, "Telomere Maintenance Requires the RAD51D Recombination/Repair Protein" in *Cell* on April 30, 2004

(Tarsounas et al., 2004). Specifically, the data described demonstrate telomere dysfunction in *Rad51d*-deficient mouse embryonic fibroblasts. The data in Manuscript 2 is part of a collaborative effort with Susan M. Bailey's laboratory at Colorado State University. My contributions to this work demonstrate that, in *Rad51d*-deficient mouse cells, telomeres have an increased frequency of being detected as DSBs and telomeres have long single-stranded, telomeric 3´ overhangs. I hypothesize that, in the absence of the RAD51D protein, protective telomere structures are not formed, which leaves chromosome ends vulnerable to excessive exonuclease degradation. The hypothesis of Manuscript 3 proposes that rats selectively bred based upon their low aerobic running capacity have shorter telomeres compared to rats selectively bred based upon their high aerobic running capacity. This work was performed in collaboration with Steven L. Britton and Lauren Gerard Koch of the University of Michigan, and will be submitted for publication. I was invited to write a commentary describing the nomenclature of telomerase; this manuscript was published in *International Union of Biochemistry and Molecular Biology Life* (*IUBMB Life*) in September, 2004 (Smiraldo, 2004) and is included as Appendix A. Finally, a Discussion and Summary of this research is presented which includes a model for the repair of interstrand crosslinks, and two models for telomere dysfunction in *Rad51d*-deficient cells.

LITERATURE

The purpose of this section is to present an overview of the literature describing the process of HR repair. I discuss the background information that is fundamental for our current understanding of HR, and how this pathway is involved in repairing DNA damage and protecting telomeres. The initial parts of this section describe the DNA repair pathways that cells use to repair DNA DSBs and provide molecular models of recombination. I then review the key proteins involved in each step of HR in *Escherichia coli* (*E. coli*), *Saccharomyces cerevisiae* (*S. cerevisiae*), and mammals. The next sections give an overview of telomeres, describe how recombination processes in *S. cerevisiae* and mammals protect chromosome ends, and discuss the potential physiological consequences of telomere dysfunction in complex organisms. These sections are followed by a synopsis of work presented in this dissertation.

DNA Double-strand Break Repair

DNA is constantly challenged by damage originating from environmental agents, such as ultraviolet light from the sun, radiation, and aromatic hydrocarbons that are found in cigarette smoke and burnt food. In addition, DNA lesions also can be caused by endogenous mutagens such as reactive oxygen species and water (Wood et al., 2001). Cells must efficiently repair damaged DNA to prevent an accumulation of DNA mutations, which can confer the loss of the ability to control cell division, irreversible cell growth arrest, or cell death. One of the most genotoxic forms of DNA lesions is the DSB (where both sugar-phosphate backbones of the double helix are broken), which prevents the use of an intact complementary DNA strand as a template for repair. Double-

stranded breaks can be caused exogenously (ionizing radiation or chemicals) and endogenously (free radicals, single-stranded breaks in DNA replication, collapsed replication forks, meiosis intermediates, or V(D)J recombination) (van Gent et al., 2001).

In mammalian cells, DSBs can be repaired by two mechanistically different pathways: non-homologous end-joining (NHEJ) and HR. The cellular decision to repair a DSB by HR or NHEJ is likely dependent upon the stage of the cell cycle; HR is most efficient in S and G2 phases of the cell cycle when the sister chromatid is present to use as a repair template, and NHEJ in G1 and G0 phases of the cell cycle in the absence of sister chromatids (Johnson and Jasin, 2001). The process of NHEJ consists of at least three steps, including (1) detection of the DSB, (2) processing of DNA ends into ligatable substrates, and (3) ligation. The DSB is initially recognized and bound by the Ku70/Ku80 protein heterodimer, which stimulates the recruitment of DNA-PKcs to the damage site. Although the enzyme(s) responsible for processing the ends of DSBs caused by environmental mutagens are not known, the protein, Artemis, binds to DNA-PKcs and processes DNA ends during V(D)J recombination. Lastly, free DNA ends are ligated together by the DNA ligase IV/XRCC4 protein complex (for reviews, see Weterings and van Gent, 2004; Hefferin and Tomkinson, 2005). The NHEJ repair pathway can be error-prone if nucleotides are lost at the site of the DSB, which could be deleterious if the missing bases are within a gene-coding region of the genome (Figure 1A). Additionally, if a cell sustains more than one DSB, DNA ends that were not previously linked could be joined, resulting in a chromosomal rearrangement (Weterings

Figure 1. DNA Double-strand Break Rpair

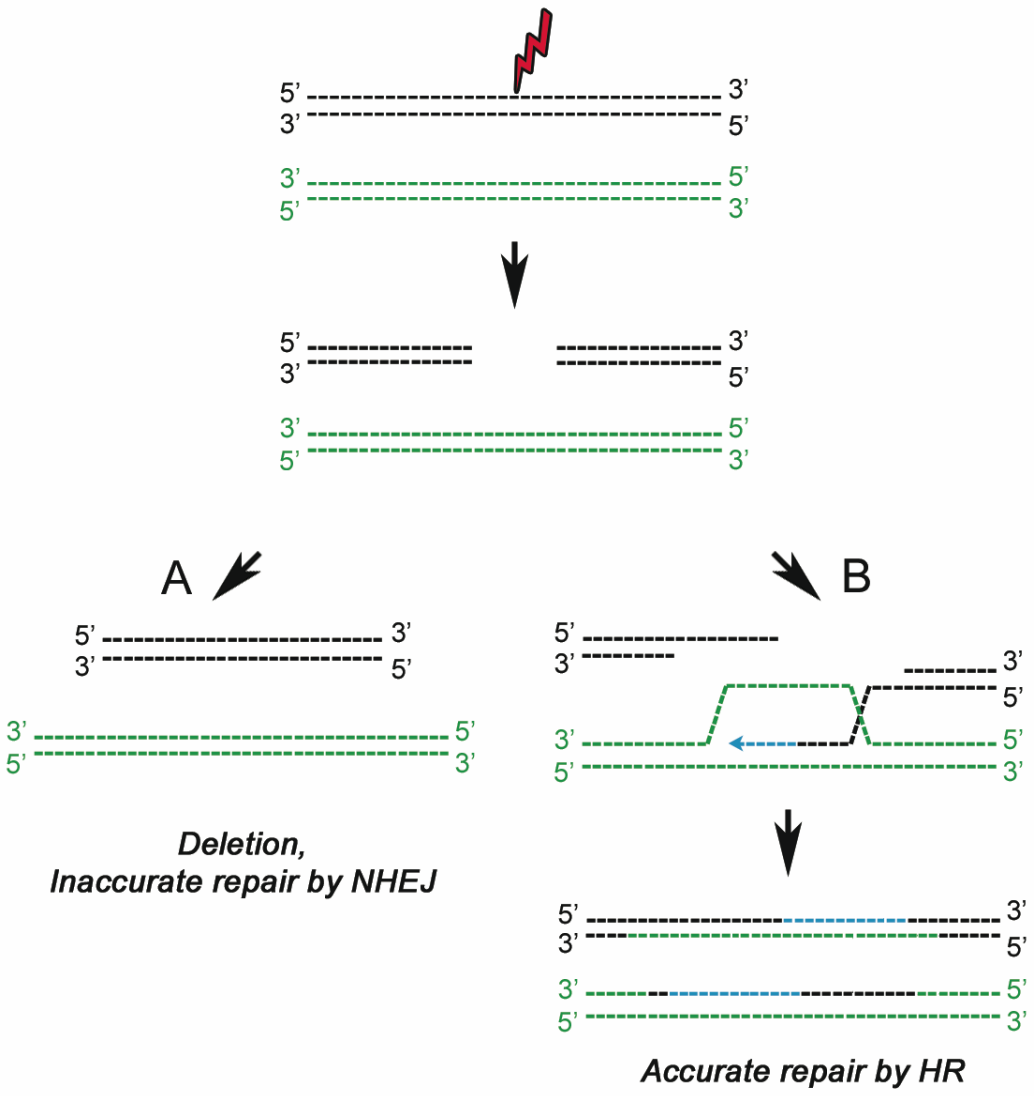

DNA DSBs can be repaired by either NHEJ or HR. The double black lines represent duplex DNA and the double green lines represent homologous duplex DNA. In this case, black DNA and green DNA are sister chromatids. DNA damage (lightning bolt) causes a DSB in the black DNA, conferring loss of DNA at the damage site. (A) Non-homologous end-joining (NHEJ) of the damaged strand ligates free DNA ends together. NHEJ can be error prone as, in this example, nucleotides are lost at the site of repair. The sister chromatid is shown in green only to exemplify the amount of lost DNA from the damaged black strand. (B) The HR repair pathway uses the intact sister chromatid (green) as a replication template to restore the original sequence that was lost due to the DSB.

and van Gent, 2004). In comparison to NHEJ, repair of DSBs by HR is considered accurate. To repair the DSB, the HR machinery uses the intact sister chromatid as a replication template to replace any missing bases at the damage site (Figure 1B) (for reviews, see Thompson and Schild, 2001; Helleday, 2003). Because the sister chromatids are identical, the damaged DNA is restored to its original sequence. Multiple models of how HR repairs DSBs are discussed below. Additionally, HR mechanisms have been observed for the restoration of stalled replication forks, telomere protection, and telomere lengthening, which will also be discussed.

Mechanisms of Homologous Recombination Repair

Homologous recombination refers to the exchange of genetic material between two DNA fragments that share sequence homology. The HR process is fundamentally important during meiosis for recombination among maternal and paternal chromosomes to increase genetic diversity, during mitosis to repair DNA lesions such as DSBs and ICLs, and during DNA replication to re-start stalled DNA replication forks. In mitotic cells, HR can theoretically occur between any homologous DNA sequences including homologous chromosomes, repetitive DNA elements, and sister chromatids. To ensure that DNA information is not lost or altered, the sister chromatid is the preferred template to repair DNA damages in mitotic cells (Johnson and Jasin, 2001).

Two models have been proposed as to how HR occurs using the sister chromatid as a replication template. In both models, the HR process is organized into four steps: (1) initiation (processing), (2) homologous pairing and DNA exchange, (3) DNA heteroduplex extension (branch migration), and (4) resolution. The first model for DNA

double-strand break repair (DSBR) (Figure 2) occurs when strand exchange and branch migration form two, four-way Holliday junctions (Resnick, 1976). These structures can be resolved in the same or opposite directions, resulting in non-crossover or crossover products, respectively. The second model, synthesis dependent strand annealing (SDSA) (Figure 3) occurs when strand exchange and synthesis occurs past the damaged region. However, instead of the formation of two Holliday junctions, the invading strand releases from the intact template and re-anneals to the damaged strand. The gaps that remain are then filled in. In this model, the only product is gene conversion without crossover (Strathern et al., 1982).

Figure 2. Repair of DSBs by "Double-strand Break Repair" Model

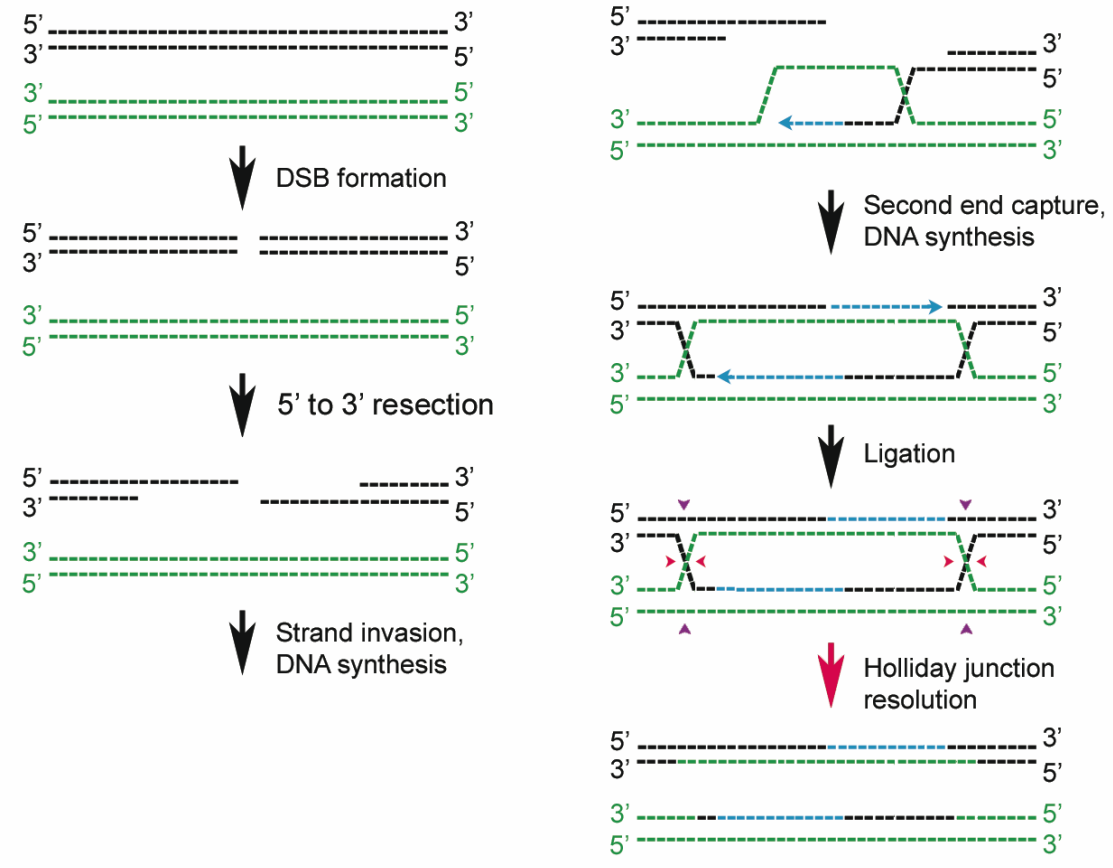

Repair of DSBs by the "double-strand break repair" (DSBR) model. The double black lines represent duplex DNA and the double green lines represent duplex DNA. In this case, black DNA and green DNA are sister chromatids. A DSB has occurred in the black DNA. Following DSB formation, exonuclease activity occurs at the DSB in a 5′ to 3′ direction to form a single-stranded, 3′ overhanging tails. The 3′ overhanging tail invades the intact sister chromatid and anneals to the homologous DNA sequence to prime DNA synthesis (new DNA is represented by the blue line). The second end of the broken chromatid is captured followed by DNA synthesis (new DNA is represented by the blue line) and ligation. Double Holliday junction resolution can occur in either plane at both junctions (small red and purple arrowheads) to generate noncrossover or crossover products. In this diagram, cuts of the Holliday junction occur at the small red arrowheads resulting in noncrossover products. Figure re-drawn with modifications from Szostak et al., 1983.

Figure 3. Repair of DSBs by "Synthesis Dependent Strand Annealing" Model

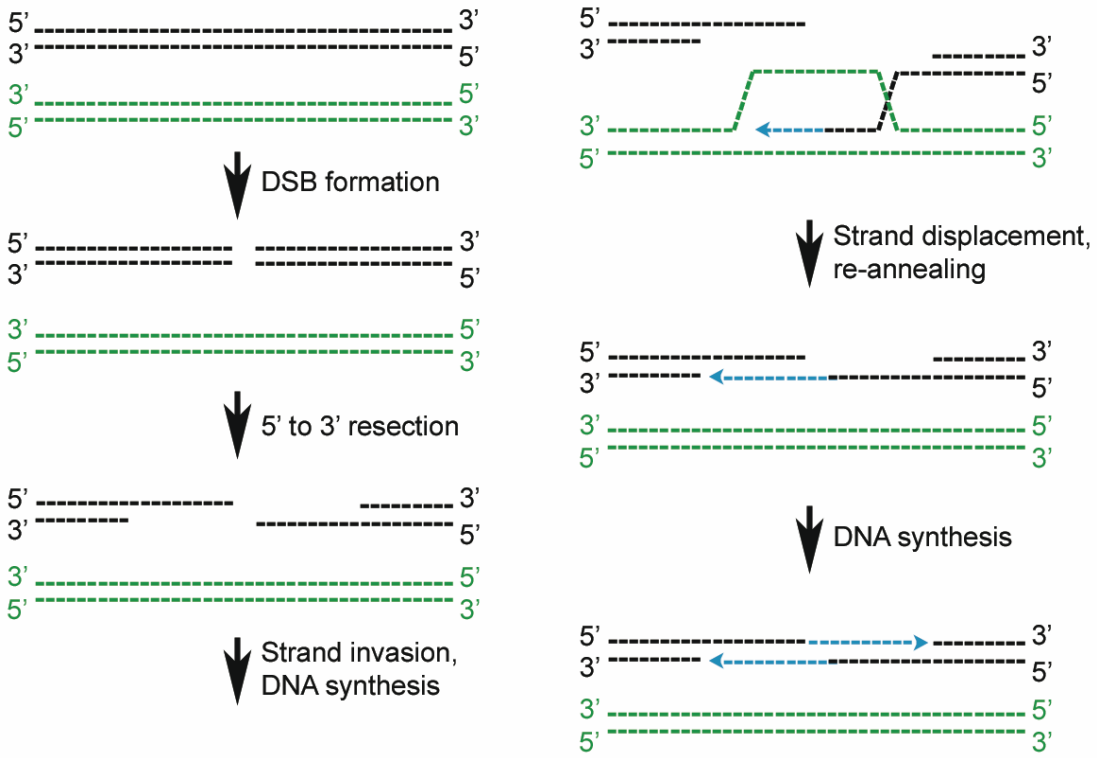

Repair of DSBs by "synthesis dependent strand annealing" (SDSA) model. The double black lines represent duplex DNA and the double green lines represent duplex DNA. In this case, black DNA and green DNA are sister chromatids. A DSB has occurred in the black DNA. Following DSB formation, exonuclease activity occurs at the DSB in a 5′ to 3′ direction to form a single-stranded, 3′ overhanging tails. The 3′ overhanging tail invades the intact sister chromatid and anneals to the homologous DNA sequence to prime DNA synthesis (new DNA is represented by the blue line). The invading strand then displaces, pairs with the other 3′ single-stranded tail, and DNA synthesis fills in the remaining gaps. The only products from this repair model are noncrossover products. Figure re-drawn with modifications from Ferguson and Holloman, 1996

Homologous recombination is also a mechanism for re-starting stalled replication forks caused by DNA lesions. Multiple models have been proposed and each depends upon whether the strand that is replicated by leading or lagging strand synthesis is damaged. In the first scenario, the parental DNA strand contains a single stranded break

(Figure 4). When the parental strand is unwound for replication, the single-stranded break becomes a DSB. The 3′ end of the DSB can invade the newly replicated sister strand and prime DNA synthesis to form a single Holliday junction. The Holliday junction is resolved and DNA replication resumes (reviewed by Krogh and Symington, 2004). In the second scenario, a DNA lesion is present on the parental strand replicated by leading strand synthesis (Figure 5). To avoid the possibility of incorporating an incorrect nucleotide to pair with the damaged nucleotide, leading strand synthesis stops. Lagging strand synthesis proceeds past the DNA lesion. The newly replicated strands denature and anneal to form a "chicken foot" structure, which allows the leading strand to use the lagging strand as a template to prime replication (Higgins et al., 1976). The newly replicated strands denature from each other and re-nature to the parental strand, which allows DNA replication to proceed. The lesion is then be repaired by an excision repair pathway (reviewed by Krogh and Symington, 2004). In the third scenario, a DNA lesion occurs on the parental strand replicated by lagging strand synthesis (Figure 6). DNA replication occurs downstream of the DNA lesion by formation of an Okasaki fragment. The short lagging strand fragment invades the newly replicated leading strand to prime DNA synthesis. Similar to SDSA, the lagging strand denatures from the intact strand and re-anneals to the parental strand, which bypasses the DNA lesion. DNA synthesis can continue and the lesion repaired by an excision repair pathway (reviewed by Krogh and Symington, 2004).

Figure 4. Re-starting Stalled Replication Caused by a Nick in the Parental DNA.

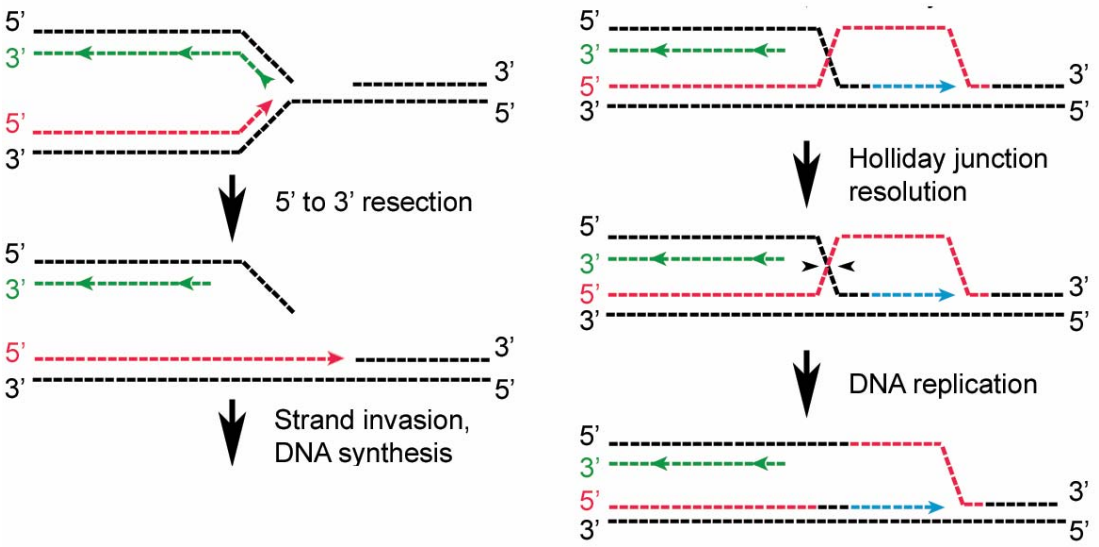

Re-starting stalled replication caused by a nick in the parental DNA. The double black lines represent parental DNA. The red line represents leading strand DNA synthesis and the green line represents lagging strand DNA synthesis. The DNA replication machinery encounters a single-stranded break on the template strand. Leading strand synthesis continues through the damaged region. Exonuclease activity occurs at the DSB in a 5′ to 3′ direction to form a single-stranded, 3′ overhanging tail. The 3′ overhanging tail invades the sister chromatid and anneals to the homologous DNA sequence to prime DNA synthesis (new DNA is represented by the blue line). The Holliday junction is resolved and DNA replication continues. Figure re-drawn with modifications from Krogh and Symington, 2004.

Figure 5. Re-starting Stalled Replication Caused by a Lesion in the Parental DNA Replicated by Leading-strand Synthesis

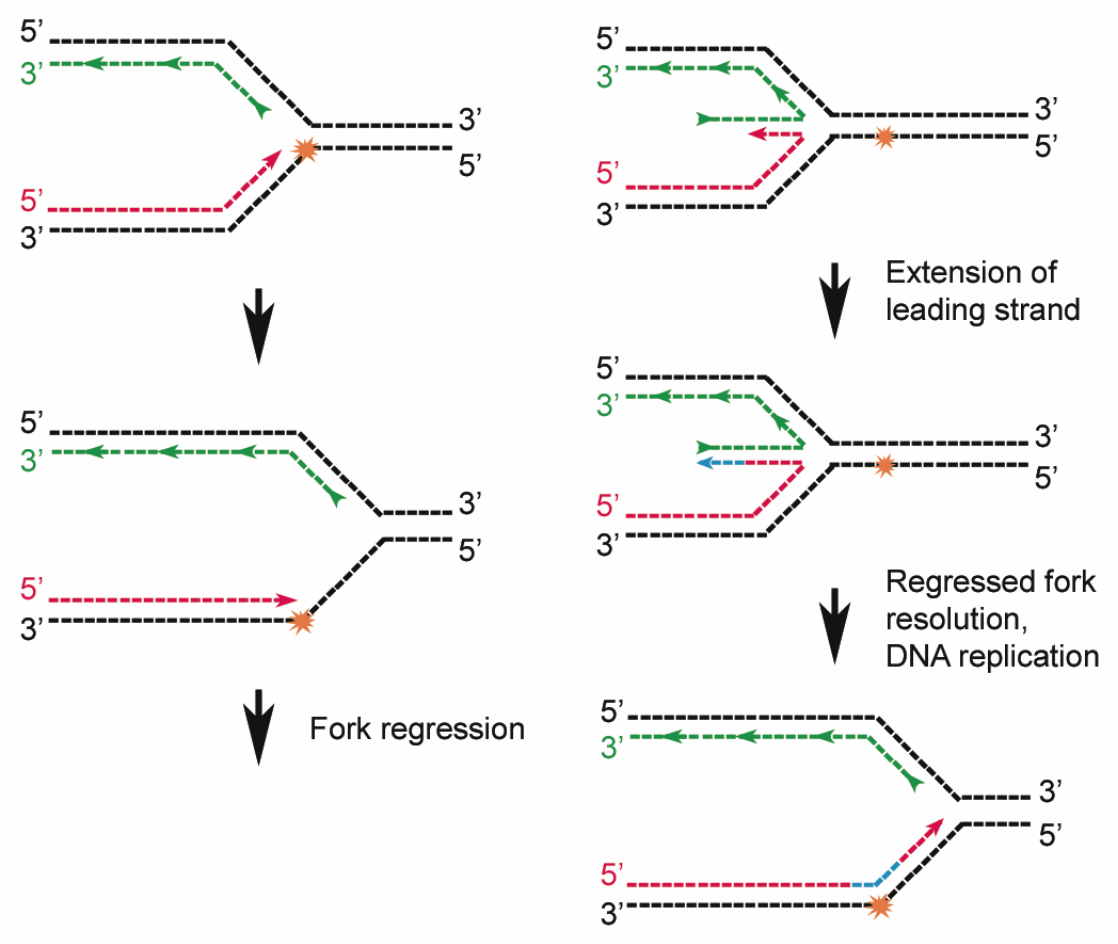

Re-starting stalled replication caused by a lesion in the parental DNA replicated by leading strand synthesis. The double black lines represent parental DNA. The red line represents leading strand DNA synthesis and the green line represents lagging strand DNA synthesis. Leading strand synthesis stalls to avoid pairing an incorrect nucleotide to the damage site. Newly synthesized strands pair and reverse branch migrate to form a Holliday junction-like structure, also known as a regressed fork (chicken foot). Extension of the leading strand occurs by DNA synthesis (new DNA is represented by the blue line). The regressed fork is resolved, parental and daughter strands re-anneal, and DNA replication continues past the DNA lesion. Figure re-drawn with modifications from Krogh and Symington, 2004.

Figure 6. Re-starting Stalled Replication Caused by a Lesion in the Parental DNA Replicated by Lagging Strand Synthesis

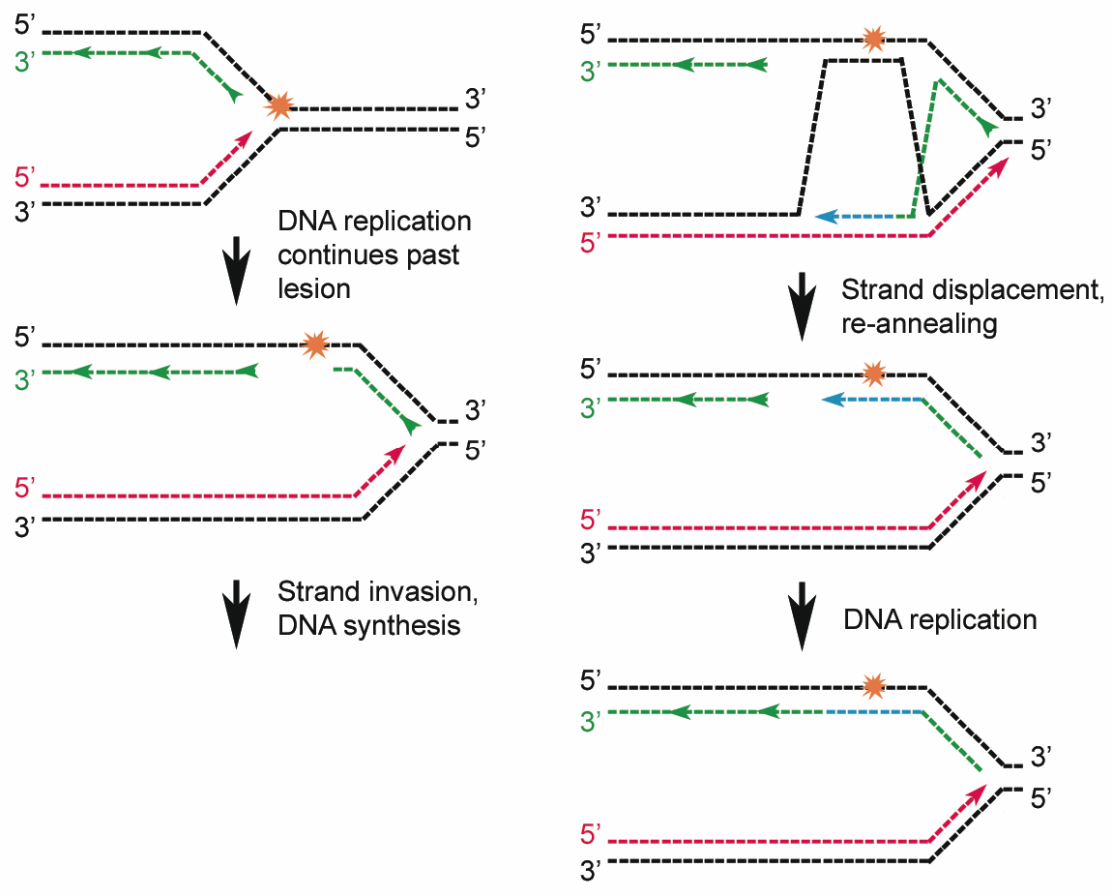

Re-starting stalled replication caused by a lesion in the parental DNA replicated by lagging strand synthesis. The double black lines represent parental DNA. The red line represents leading strand DNA synthesis and the green line represents lagging strand DNA synthesis. DNA replication continues past the DNA lesion. The 3′ end of the lagging strand invades, pairs to the homologous DNA replicated by leading strand synthesis, and primes DNA synthesis (new DNA is represented by the blue line). Similar to SDSA, the invading strand displaces to resolve the Holliday junction structure, pairs with the parental strand, and DNA replication continues. Figure re-drawn with modifications from Krogh and Symington, 2004.

Homologous Recombination in Escherichia coli

The basic understanding of HR mechanisms comes from studies of *E. coli*. At the sight of the DNA lesion, double-stranded DNA (ds-DNA) is initially processed to produce a single-stranded 3′ overhanging tail by the RecBCD protein complex (which consists of RecB, RecC, and RecD) (Taylor and Smith, 1980). The RecBCD heterotrimer is a helicase that unwinds ds-DNA and simultaneously degrades DNA to form a single-stranded 3′ overhang (MacKay and Linn, 1974). After the 3′ overhang is formed, the single-stranded DNA binding protein, SSB, binds along the single-stranded DNA (ss-DNA) to prevent DNA secondary structures. This allows RecA proteins to bind along the ss-DNA to form the presynaptic complex (Kowalczykowski and Krupp, 1987).

The RecA protein has multiple biochemical properties that are central to HR, including ATP binding and hydrolysis (through conserved Walker box A and Walker box B motifs), DNA binding, and the pairing and exchange of homologous DNA strands (McEntee et al., 1981b; West et al., 1981; Cox and Lehman, 1982). RecA binds ATP (which increases the affinity of RecA for DNA binding) and polymerizes along ss-DNA in a 5′ to 3′ direction to form a nucleoprotein filament (West et al., 1980; McEntee et al., 1981a; Register and Griffith, 1985). RecA then promotes the strand invasion of the 3′ ss-DNA into the non-damaged ds-DNA template, performs a homology search, and pairs homologous DNA molecules (synapsis) to form a DNA heteroduplex, referred to as a Holliday junction (West et al., 1981; Cox and Lehman, 1982). DNA polymerase I replaces any missing bases at the site of the DNA lesion using the non-damaged DNA as a replication template (Kowalczykowski et al., 1994).

Following synapsis, branch migration of the heteroduplex DNA region occurs by the RuvAB heterodimer. This complex, made up of the RuvA and RuvB proteins, functions as a molecular motor to catalyze the branch migration of Holliday junctions (Tsaneva et al., 1992; West and Connolly, 1992). To resolve the heteroduplex DNA, the RuvC endonuclease interacts with RuvAB at the Holliday junction and produces symmetric cuts at the point of the crossover (Connolly and West, 1990; Connolly et al., 1991). Lastly, the DNA strands are renatured by RecA and RecT, and the DNA phosphate backbone re-ligated by DNA ligase (Weinstock et al., 1979; Hall et al., 1993).

Homologous Recombination in Saccharomyces cerevisiae

Saccharomyces cerevisiae has proved to be a valuable system to investigate the mechanisms of HR in eukaryotic cells. The identification of more than 30 genes involved in yeast HR came from genetic screens for mutants with altered rates of recombination, hypersensitivity to DNA damaging agents, and reduced sporulation or spore viability (Krogh and Symington, 2004). Proteins encoded by the *RAD52* epistasis group of genes, which include *RAD50, RAD51, RAD52, RAD54, RAD55, RAD57, MRE11,* and *XRS2,* were found to play direct roles in HR.

Similar to HR mechanisms in *E.coli*, HR repair of DSBs in *S. cerevisiae* also requires the processing of DNA ends to form a 3′ ss-DNA tail capable of strand invasion. Following DSB formation, Mre11, Rad50, and Xrs2 proteins form a complex (MRX complex) that binds at the DNA damage site (the Mre11 protein is a 3′ to 5′ exonuclease, Trujillo et al., 1998; Trujillo and Sung, 2001). Consistant with a role in DNA repair, yeast *rad50, mre11,* or *xrs2* null mutant strains are hypersensitive to DNA-damaging

agents (Game and Mortimer, 1974; Tsubouchi and Ogawa, 1998; Bressan et al., 1999). The exonuclease directionality of Mre11 is opposite of the predicted 5′ to 3′ exonuclease activity required to form a single-stranded 3′ tail. Therefore, it is predicted that the MRX complex functions as an initiating nuclease to prepare DNA ends for an additional (unidentified) enzyme capable of 5′ to 3′ exonuclease activity (Fiorentini et al., 1997; Krogh and Symington, 2004). Consistent with this hypothesis, yeast *rad50, mre11,* or *xrs2* null mutant strains demonstrate slow resection at sites of induced DSBs (Ivanov et al., 1994). The 3′ ss-DNA is then bound by the ss-DNA binding protein, RPA, to stabilize and prevent DNA secondary structures of the single-stranded, 3′ overhang (Alani et al., 1992).

The 3′ ss-DNA tail is the substrate for Rad51 protein binding to form the presynaptic complex. The Rad51 protein in *S. cerevisiae* is a homolog of RecA in *E.coli*, and these two proteins share approximately 30% identity. The majority of homology between Rad51 and RecA occurs in the ATP binding/hydrolysis domains; both proteins contain the conserved Walker box A and Walker box B motifs (Aboussekhra et al., 1992; Basile et al., 1992). However, yeast Rad51 contains an amino-terminal extension of approximately 120 amino acids, which may be required for DNA binding, and a carboxyl-terminal truncation of approximately 90 amino acids (Aboussekhra et al., 1992; Basile et al., 1992). Like RecA, yeast Rad51 binds ATP, which increases its affinity to bind DNA, but the rate of ATP hydrolysis of yeast Rad51 is approximately 40-fold lower than RecA (Sung, 1994). The nucleoprotein filaments of Rad51 on the 3′ ss-DNA tail are almost identical in dimension and structure to filaments formed by RecA (Ogawa et

al., 1993; Sung and Robberson, 1995). However, in yeast, RPA bound to the 3′ ss-DNA tail prevents Rad51 from binding DNA, suggesting mediators are required for Rad51 nucleoprotein filament formation (Sung, 1997). The Rad52 protein interacts directly with RPA and Rad51; the localization of Rad51 to sites of DSBs requires Rad52, suggesting Rad52 delivers Rad51 to DNA damage, displaces RPA from ss-DNA, and loads Rad51 onto the 3′ ss-DNA tail (Song and Sung, 2000; Sugiyama and Kowalczykowski, 2002). Additionally, the Rad51 paralogs, Rad55 and Rad57, form a heterodimer that functions to form or stabilize Rad51 filaments (Hays et al., 1995; Johnson and Symington, 1995; Sung, 1997). In the absence of Rad55 or Rad57, assembly of Rad51 filaments at DSBs is delayed and there is no pairing between the 3′ ss-DNA tail and the intact donor template (Gasior et al., 2001; Sugawara et al., 2003; Wolner et al., 2003; Miyazaki et al., 2004). This suggests that, in the absence of the Rad55/Rad57 heterodimer, Rad51 filament assembly is not sufficient for the strand invasion step during HR or, alternatively, that the Rad55/Rad57 heterodimer has strand invasion and base pairing abilities (Sugawara et al., 2003).

Following formation of the Rad51 nucleoprotein filament, synapsis occurs. This includes the search and alignment of the nucleoprotein filament with the homologous donor strand, strand invasion, and base pairing (Krogh and Symington, 2004). With respect to the complementary strand of duplex DNA, the polarity of single-stranded exchange by yeast Rad51 is 5′ to 3′, opposite to the polarity observed for RecA, demonstrating a functional difference between yeast Rad51 and RecA in strand invasion (Radding, 1991; Sung and Robberson, 1995). The Rad54 protein binds ds-DNA

(presumably the duplex donor strand), has ds-DNA-specific ATPase activity, and the ability to translocate along duplex DNA to partially relax supercoiled DNA, which facilitates the search, alignment, and invasion of the Rad51 nucleoprotein filament and into the donor DNA (Petukhova et al., 1999; Mazin et al., 2000; Van Komen et al., 2000). Following DNA strand invasion and base pairing, the Rad54 protein displaces Rad51 from duplex DNA, which potentially uncovers the 3´ end to initiate DNA repair synthesis (Solinger and Heyer, 2001; Solinger et al., 2002). Consistent with Rad54 being involved in displacing Rad51 after homolous pairing, *rad54* mutant strains have increased sensitivity to DNA damage and DSB induced Rad51 foci persist for longer periods of time compared to Rad54 proficient strains (Miyazaki et al., 2004).

Branch migration and Holliday junction resolution in *S. cerevisiae* have not been characterized as well as the prior HR steps. Homologs of the *E.coli* RuvAB or RuvC proteins have not been identified in *S. cerevisiae* (Krogh and Symington, 2004). Recent data suggest the Sgs1 helicase promotes branch migration of Holliday junctions (Gangloff et al., 1994). Top3, a topoisomerase, is proposed to make the single-strand incisions required to resolve Holliday junction structures (Wallis et al., 1989; Gangloff et al., 1994). Although little is known about resolution, it remains possible that different proteins are required to resolve double- (as shown in DSBR model, Figure 2) or single- (as shown in SDSA model, Figure 3) Holliday junction intermediates, regressed forks (Figure 5), or to form crossover or noncrossover products (Krogh and Symington, 2004).

Homologous Recombination in Mammals

As in yeast, a similar general mechanism of HR exists in mammals. Although homologs of the yeast proteins have been identified in humans, DNA repair by HR in mammals is less understood. Additionally, defects in DNA repair genes in humans have been associated with hereditary diseases and susceptibility to cancer, demonstrating HR is fundamentally important for health in complex organisms (Thompson and Schild, 2002).

Sensory systems monitor genomic DNA for all types of DNA lesions. Once a lesion is identified, a signal is transduced to activate the appropriate biological response. These responses include the activation of DNA repair mechanisms to correct damaged nucleotides and triggering of G1/S, intra-S, G2, or M checkpoints to stop progression of the cell cycle. The exact mechanism for detection of DNA DSBs is an area of ongoing research and, because many of the techniques used require visualization of microscopically visible DNA repair foci, the initial detection of the lesion is not known. In undamaged cells, the ATM kinase typically forms a homo-multimer and is inactive (Bakkenist and Kastan, 2003). Immediately following DSB formation, an unknown signal activates the autophosphorylation of ATM at Ser1981 and the homo-multimer is disrupted to release activated ATM monomers (Bakkenist and Kastan, 2003). Activated ATM phosphorylates proteins involved in HR repair including NBS1 (X. Wu et al., 2000), histone H2AX (Burma et al., 2001), and BRCA1 (Cortez et al., 1999). Phosphorylated H2AX (typically referred to as γ-H2AX) accumulates at sites of DSBs and is thought to be critical for mediating the assembly of DNA repair complexes on

DSB sites (Paull et al., 2000; van Gent et al., 2001). The MRE11-RAD50-NBS1 (MRN) complex also binds immediately to DSB sites and is thought to play a role in processing broken DNA ends for repair (Maser et al., 1997). The MRN complex functions in both of the HR and NHEJ repair pathways (van Gent et al., 2001); the cellular decision to repair a DSB by HR or NHEJ is likely dependent upon the stage of the cell cycle (HR is most efficient in S and G2 phases of the cell cycle and NHEJ in G1 and G0 phases of the cell cycle) (Johnson and Jasin, 2001; Bassing and Alt, 2004). Biochemically, the MRE11 protein is a single- and double-strand DNA endonuclease and a 3′ to 5′ exonuclease; both activities are stimulated by the binding of RAD50 and NBS1 to MRE11 (Paull and Gellert, 1998; Trujillo et al., 1998). Because of the biochemical properties of this complex, the MRN hetero-trimer is a candidate enzyme to process broken DNA ends into single stranded 3′ overhangs, which are the substrates for HR repair. However, like the MRX complex (Mre11-Rad50-Xrs2) in *S. cerevisiae*, the exonuclease directionality of the MRN complex in mammals conflicts the predicted 5′ to 3′ exonuclease activity required to form a single-stranded 3′ tail. Therefore, like in *S. cerevisiae*, an additional (unidentified) enzyme capable of 5′ to 3′ exonuclease activity may be required (Fiorentini et al., 1997; Krogh and Symington, 2004).

The RAD51 protein in mammals is the structural and functional homolog of RecA in *E.coli* and Rad51 in *S. cerevisiae* (Thompson and Schild, 1999). At the amino acid level, the human RAD51 protein is 80% similar to yeast Rad51 and 30% similar to RecA. All three proteins can form protein filaments on ss-DNA and contain conserved Walker box A and Walker box B motifs that are involved in ATP binding and hydrolysis (Ogawa

et al., 1993; Benson et al., 1994; Sung and Robberson, 1995). Like yeast Rad51, the human RAD51 protein hydrolyzes ATP at a significantly slower rate than RecA (Benson et al., 1994; Sung, 1994) and, with respect to the complementary strand of duplex DNA, the polarity of single-stranded exchange by human RAD51 is 5′ to 3′, opposite to the polarity observed for RecA (Radding, 1991; Sung and Robberson, 1995; Baumann and West, 1997). Purified human RAD51 is able to form homologous joint molecules between ss-DNA and ds-DNA, but is not able to perform strand exchange, suggesting that mammalian RAD51 plays a primary role in the search for homologous DNA sequences and the formation of joint molecules, but requires additional protein factors for strand exchange (Gupta et al., 1999).

Mammalian RAD51 requires additional proteins for filament formation along ss-DNA. Like in *S. cerevisiae*, mammalian RAD52 interacts directly with RAD51 (Shen et al., 1996) and may function to displace the RPA ss-DNA binding complex to allow for the binding of RAD51 to ss-DNA (Benson et al., 1998). The RAD51 protein also interacts directly with the breast cancer susceptibility protein, BRCA2, at conserved "BRC" repeats (Pellegrini et al., 2002). Cells deficient for *BRCA2* are defective for the formation of ionizing radiation-induced RAD51 foci (Yuan et al., 1999; Yu et al., 2000) and are deficient for homology-directed repair of DSBs (Moynahan et al., 2001), but not deficient for NHEJ (Xia et al., 2001). The BRCA2 protein binds ss-DNA and stimulates RAD51-mediated recombination in vitro (Yang et al., 2002). Transport of RAD51 into the nucleus is defective in cells carrying a cancer-associated BRCA2 truncation (Davies et al., 2001). *Brca2*-deficient or *Rad51*-deficient mice confer embryonic lethality (Lim

and Hasty, 1996; Tsuzuki et al., 1996; Ludwig et al., 1997; Sharan et al., 1997; Suzuki et al., 1997) and cells with mutations in, or deficient for, the *BRCA2* gene have chromosome instability, mild sensitivity to IR, high sensitivity to DNA crosslinking agents, and decreased levels of HR (Abbott et al., 1998; Patel et al., 1998; Tutt et al., 1999; Yuan et al., 1999; Moynahan et al., 2001; Kraakman-van der Zwet et al., 2002). Together, these data demonstrate that BRCA2 plays a role in HR by mediating the localization and assembly of RAD51 onto sites of DNA DSBs. However, the mechanism that re-locates BRCA2-RAD51 complexes to the site of DNA damage and how RAD51 disassociates from BRCA2 onto ss-DNA is not known.

Mammalian cells also encode six *RAD51*-related genes: *RAD51D*, *RAD51B*, *RAD51C*, *XRCC2*, *XRCC3*, and *DMC1* (these genes, together with *RAD51*, comprise the *RAD51*-family). Each gene was identified by cloning human DNA sequences that functionally complement mammalian mutant cell lines that were hypersensitive to DNA damaging agents (Thacker et al., 1995; Liu et al., 1998) or by searching for sequence similarity to *RAD51* or other *RAD51*-family members (Habu et al., 1996; Albala et al., 1997; Cartwright et al., 1998; Dosanjh et al., 1998; Kawabata and Saeki, 1998; Pittman et al., 1998b). Each of the *RAD51*-like gene products contains the two highly conserved Walker box motifs, and has 20-30% sequence similarity to the RAD51 protein (Thacker, 1999). In mitotic cells, the RAD51-like proteins (except for DMC1, which is meiosis-specific) have been observed in two distinct complexes; one complex consists of RAD51B-RAD51C-RAD51D-XRCC2 (BCDX2 complex) and the other consists of RAD51C-XRCC3 (Masson et al., 2001a,b; Liu et al., 2002; Miller et al., 2002).

Biochemical analyses suggest these proteins may function as individual monomers or in complexes with specific activities (Table I).

Table I. Biochemical Properties of RAD51 Family Members and Complexes

Protein(s)	ss-DNA Binding	ATPase Activity	Homologous Pairing
RAD51	Yes[1]	Yes[2]	Yes[3]
RAD51D	Yes[4]	Yes[4]	Not reported
RAD51B	Yes[5]	Yes[5]	No[5]
RAD51C	Yes[5]	Yes[5]	Yes[5, 6]
XRCC2	Not reported	Not reported	Not reported
XRCC3	Not reported	Not reported	Not reported
RAD51D-XRCC2	Yes[7, 8]	Yes[7, 8]	Yes[7]
RAD51B-RAD51C	Yes[9]	Yes[9]	No[9]
RAD51C-XRCC3	Yes[10]	Not reported	Yes[6]
RAD51B-RAD51C-RAD51D-XRCC2	Yes[11]	Yes[11]	Not reported

[1] (Tombline et al., 2002), [2] (Tombline and Fishel, 2002), [3] (Baumann et al., 1996), [4] (Braybrooke et al., 2000), [5] (Lio et al., 2003), [6] (Kurumizaka et al., 2001), [7] (Kurumizaka et al., 2002), [8] (Braybrooke et al., 2003), [9] (Sigurdsson et al., 2001), [10] (Masson et al., 2001a), [11] (Masson et al., 2001b)

Although the *RAD51*-family members share some of the same biochemical properties alone or in complex, targeted disruption of *Rad51*, *Rad51b*, *Rad51d*, or *Xrcc2* in mice confers embryonic lethality (Table II), demonstrating that these proteins are essential for mouse viability and that they do not have overlapping or redundant functions.

Table II. Mouse Phenotypes Conferred by Disruptions of HR Genes in Mice			
Gene[Ref]	**Viable Mouse**	**Age of Death**	**Distinguishing Phenotypes of Mutants**
Rad51[1]	No	E6.5-8.5	Embryos are developmentally delayed with elevated levels of cellular apoptosis.
Rad51b[2]	No	E6.5-8.5	Embryos are decreased in size and developmentally delayed.
Rad51c	N/A	----	----
Rad51d[3]	No	E8.5-11.5	Embryos are decreased in size and developmentally delayed.
Xrcc2[4]	No	E10.5-birth	Embryos are decreased in size and developmentally delayed. Neonatal lethality is due to respiratory failure.
Xrcc3	N/A	----	----
Dmc1[5]	Yes	N/A	Adult males and females are sterile.
Rad50[6]	No	E6.5-7.5	Embryos are decreased in size and developmentally delayed.
Mre11	N/A	----	----
Nbs1[7]	No	< E7.5	Embryos are decreased in size and developmentally delayed.
Rad52[8]	Yes	N/A	Mutant mice are not different compared to normal littermates.
Rad54[9]	Yes	N/A	Mutant mice are not different compared to normal littermates.
Blm[10]	No	E9.5-13.5	Embryos are decreased in size and have severe anemia.
Blm[11]	Yes	N/A	Mice are susceptible to a wide spectrum of cancers.
Brca1[12]	No	E10.5-13.5	Embryos are decreased in size and developmentally delayed.
Brca1 mammary gland-specific disruption[13]	Yes	N/A	Increased levels of apoptosis, abnormal mammary gland development, and mammary tumors associated with chromosomal instability. Loss of p53 accelerated tumor formation.
Brca2[14]	No	E7.5-8.5	Embryos are decreased in size and developmentally delayed.
Brca2 various epithelial-specific disruption[15]	Yes	N/A	High incidence of mammary carcinomas and skin cancer in *Trp53*-deficient background.

Gene[Ref]	Viable Mouse	Age of Death	Distinguishing Phenotypes of Mutants
Atm[16]	Yes	N/A	Mice are growth retarded, sterile, and susceptible to thymic lymphomas.
Atr[17]	No	< E7.5	Embryos are developmentally delayed with elevated levels of cellular apoptosis.
H2AX[18]	Yes	N/A	Mice are radiation sensitive, growth retarded, immune deficient, and infertile.

[1] (Lim and Hasty, 1996; Tsuzuki et al., 1996), [2] (Shu et al., 1999), [3] (Pittman and Schimenti, 2000), [4] (Deans et al., 2000), [5] (Pittman et al., 1998a), [6] (Luo et al., 1999), [7] (Zhu et al., 2001), [8] (Rijkers et al., 1998), [9] (Essers et al., 1997), [10] (Chester et al., 1998), [11] (Luo et al., 2000), [12] (Gowen et al., 1996; Hakem et al., 1996; Liu et al., 1996; Ludwig et al., 1997), [13] (Xu et al., 1999a), [14] (Ludwig et al., 1997; Sharan et al., 1997; Suzuki et al., 1997), [15] (Jonkers et al., 2001), [16] (Barlow et al., 1996; Elson et al., 1996; Xu et al., 1996), [17] (Brown and Baltimore, 2000; de Klein et al., 2000), [18] (Celeste et al., 2002)

A disruption in any of the *RAD51*-family members in mitotic chicken, hamster, or mouse cells results in global chromosome instability, hypersensitivity to ionizing radiation and DNA interstrand crosslinking agents, defective RAD51 foci formation, and decreased HR activities (Table III) (see Results chapter), consistent with these proteins functioning in DNA repair by HR. Evidence also demonstrates that in the absence of RAD51C, protein levels of XRCC3 are decreased, suggesting that the formation of the RAD51C-XRCC3 heterodimer stabilizes XRCC3 (Lio et al., 2004). It remains possible that absence of a different RAD51-like protein could de-stabilize other RAD51-family members. Because disrupting any of the *Rad51*-like genes confers a decreased ability to form RAD51 foci, it is proposed that the RAD51-like proteins function like Rad55/Rad57 in *S. cerevisiae* to form the presynaptic complex. How BRCA2 and the RAD51-like proteins function together to load RAD51 onto sites of DNA damage is not known. It remains possible that the RAD51-like proteins direct BRCA2/RAD51 to sites of DNA damage, prepare the site of DNA damage for BRCA2/RAD51 docking, or interact with

BRCA2 to unload RAD51 onto single-stranded DNA. Although the RAD51-like proteins do not interact with BRCA2 at the third BRC domain (BRC3) by yeast two-hybrid analysis, their interaction with other BRC repeats *in vivo* remains possible (Wiese et al., 2002).

Table III. Cell Phenotypes Conferred by Disruptions of HR Genes

Gene[Ref]	**Cell type**	**Genome instability**	**Ionizing radiation sensitivity**	**DNA cross-linking agent sensitivity**	**RAD51 foci status**	**HR activities**
Rad51[1]	Murine embryonic stem cells, DT40[18]	Yes, CIN[24]	Increased[25]	Not determined	Not applicable	Decreased[26]
Rad51b[2]	DT40[18]	Yes, CIN[24]	Mild	High	Decreased	Decreased[26, 27]
Rad51c[3]	irs3[19], CL-V4B[19], DT40[18]	Yes, CIN[24]	Mild	High	Decreased	Decreased[26, 27]
Rad51d[4]	MEFs[20], DT40[18]	Yes, CIN[24]	Mild	High	Decreased	Decreased[26, 27]
Xrcc2[5]	MEFs[20], DT40[18]	Yes, CIN[24]	Mild	High	Decreased	Decreased[26, 27]
Xrcc3[6]	DT40[18]	Yes, CIN[24]	Mild	High	Decreased	Decreased[26, 27]
Dmc1	Not determined	----	----	----	----	----
Rad50[7]	Murine embryonic stem cells	Not determined	Increased[25]	Not determined	Not determined	Not determined
Mre11[8]	DT40[18]	Yes, CIN[24]	Mild	Mild	Normal	Decreased[27]
Nbs1[9]	Human NBS cells[21], Murine embryonic stem cells, DT40[18]	Yes, CIN[24]	Mild	Moderate	Normal	Decreased[26, 27]

Gene[Ref]	Cell type	Genome instability	Ionizing radiation sensitivity	DNA cross-linking agent sensitivity	RAD51 foci status	HR activities
Rad52[10]	Murine embryonic stem cells, DT40[18]	No	Normal	Normal	Normal	Slightly decreased[27]
Rad54[11]	Murine embryonic stem cells, DT40[18]	Yes, CIN[24]	Mild	Mild	Decreased	Decreased[27]
Blm[12]	Human BLM cells[22], Murine embryonic stem cells, MEFs[20]	Yes, CIN[24]	Mild	Mild	Increased	Increased[26]
Brca1[13]	Human cancer cells, Murine embryonic stem cells, MEFs[20]	Yes, CIN[24]	Mild	High	Decreased	Decreased[27]
Brca2[14]	Human cancer cells, Murine embryonic stem cells, MEFs[20]	Yes, CIN[24]	Mild	High	Decreased	Decreased[26, 27]
Atm[15]	Human AT cells[23], MEFs[20], DT40[18]	Yes, CIN[24]	Moderate	Mild	Delayed	Normal[26]
Atr[16]	Human cancer cells, Murine embryonic stem cells	Yes, CIN[24]	Mild	Moderate	Not determined	Not determined

Gene[Ref]	Cell type	Genome instability	Ionizing radiation sensitivity	DNA cross-linking agent sensitivity	RAD51 foci status	HR activities
H2AX[17]	Murine embryonic stem cells, MEFs[20]	Yes, CIN[24]	Mild	Mild	Normal	Decreased[27]

[1] (Lim and Hasty, 1996; Sonoda et al., 1998; Sonoda et al., 1999), [2] (Takata et al., 2000; Takata et al., 2001), [3] (Takata et al., 2001; French et al., 2002; Godthelp et al., 2002), [4] (Takata et al., 2001; Smiraldo et al., 2005), [5] (Takata et al., 2001; Deans et al., 2003), [6] (Takata et al., 2001), [7] (Luo et al., 1999), [8] (Yamaguchi-Iwai et al., 1999; Rosselli et al., 2003), [9] (Dong et al., 1999; Kang et al., 2002; Tauchi et al., 2002; Rosselli et al., 2003), [10] (Rijkers et al., 1998; Yamaguchi-Iwai et al., 1998), [11] (Bezzubova et al., 1997; Takata et al., 1998; Tan et al., 1999), [12] (Chester et al., 1998; Luo et al., 2000; Beamish et al., 2002; Slupianek et al., 2005), [13] (Shen et al., 1998; Abbott et al., 1999; Snouwaert et al., 1999; Bhattacharyya et al., 2000; Yun et al., 2005), [14] (Abbott et al., 1998; Patel et al., 1998; Tutt et al., 1999; Yuan et al., 1999; Moynahan et al., 2001; Kraakman-van der Zwet et al., 2002), [15] (Kohn et al., 1982; Elson et al., 1996; Takao et al., 1999; Morrison et al., 2000; Rosselli et al., 2003), [16] (Cliby et al., 1998; Wright et al., 1998; Brown and Baltimore, 2000), [17] (Celeste et al., 2002)

[18] DT40 is a chicken B lymphocyte cell line.

[19] Chinese hamster ovary (CHO) cells were treated with a DNA mutagen and then individual colonies were screened for hypersensitivity to irradiation and Mitomycin C (DNA crosslinking agent) (Thompson, 1998). Expression of human *RAD51C* rescued the hypersensitivity of irs3 and CL-V4B cell lines to DNA damaging agents. Therefore, irs3 and CL-V4B cell lines are presumably deficient for *RAD51C*.

[20] MEFs are mouse embryonic fibroblasts

[21] Human NBS cells were isolated from patients with Nijmegen breakage syndrome.

[22] Human BLM cells were isolated from patients with Bloom syndrome.

[23] Human AT cells were isolated from patients with ataxia telangiectasia.

[24] CIN refers to chromosomal instability. Characterized by gross structural chromosome abnormalities (for example, breaks, gaps, and translocations).

[25] Sensitivity determined by analyzing mouse blastocyst outgrowth after treatment.

[26] HR levels were analyzed the frequency of sister chromatid exchange (SCE).

[27] HR levels were analyzed by the frequency of gene targeting.

In eukaryotes, the knowledge of the late stages of HR (branch migration and resolution) is limiting. Most of our understanding and assumptions are based upon the bacterial RuvABC-Holliday junction complex to provide a mechanistic understanding for intermediate-processing enzymes from higher organisms (West, 1997). The BLM and WRN proteins are helicases that can unwind four-way DNA structures that mimic Holliday junctions (Karow et al., 1997; Constantinou et al., 2000; Mohaghegh et al., 2001). The BLM protein also interacts directly with RAD51 (Bischof et al., 2001; Wu et al., 2001) and after treatment with ionizing radiation, BLM co-localizes with RAD51 foci (Bischof et al., 2001; Wu et al., 2001). Consistent with a role in Holliday junction resolution, BLM and WRN interact directly with the topoisomerases, Topo IIIα (Johnson et al., 2000; L. Wu et al., 2000; Hu et al., 2001) and Topo I (Lebel et al., 1999), respectively. The RAD51-like proteins also have been implicated in the late stages of HR. RAD51D binds directly to BLM and the RAD51D-XRCC2 heterodimer stimulates BLM to resolve synthetic Holliday junctions (Braybrooke et al., 2003). The BCDX2 complex (RAD51B-RAD51C-RAD51D, XRCC2) binds to synthetic Holliday junctions implying that it can participate in the migration of joint structures in the cell (Yokoyama et al., 2004). The RAD51C and XRCC3 heterodimer or the BCDX2 complex can perform branch migration and resolution of synthetic Holliday junctions (Y. Liu et al., 2004).

In conclusion, much remains unknown about the complex mechanism of HR in mammals. The HR models derived from studies of unicellular organisms have provided a general mechanism, but are insufficient to fully understand this repair pathway in

mammals. For example, it is possible that, in unicellular organisms, HR between DNA molecules is less stringent than in mammals. This would potentially enhance the rate of mutation in unicellular organisms and increase the likelihood of adaptation to new environmental conditions. However, in multicellular organisms, an enhancement of mutation rate could be lethal or oncogenic. Therefore, further studies are necessary to fully appreciate HR in mammals and how this repair pathway maintains the stability of our genomes. Experimental data in Manuscript 1 describes phenotypes conferred by a disruption in the *Rad51d* gene in mouse cells. These data demonstrate the fundamental importance of the RAD51D protein and the HR repair pathway in maintaining chromosome stability and in repairing DNA damage. While these studies were being performed, it was discovered by Dr. Madalena Tarsounas who, at the time, was working with Dr. Stephen West at the London Research Institute, that the RAD51D protein localizes at telomeres. The purpose of the next section is to present an overview of the literature describing telomeres and how the ends of linear chromosomes are involved in cellular aging and maintaining genome stability. The initial parts of this section describe telomeres in *S. cerevisiae* and how the HR mechanism can function in telomere lengthening. The next sections describe mammalian telomeres and how they are protected by Holliday junction-like structures termed T-loops. Additionally, like in *S. cerevisiae*, HR can function to lengthen telomeres in mammals. The final section discusses the potential correlation of short telomeres and predisposition to complex genetic diseases associated with aging in humans.

Telomeres

In eukaryotes, the terminal ends of all chromosomes, which are referred to as telomeres, are composed of protein complexes that bind along stretches of a simple, tandemly repeated, G/C-rich sequence. These DNA/protein structures are essential for stabilizing the ends of chromosomes and masking free DNA ends from repair mechanisms. If the structural integrity of the telomere is lost, chromosome degradation may occur resulting in the loss of genetic information. If DNA repair mechanisms recognize telomere ends as DNA damage, recombination pathways can cause rearrangements conferring the net gain or loss of chromosome regions and end-joining mechanisms may fuse telomeres together. Telomere fusions, which form dicentric and/or ring chromosomes, are detrimental in actively dividing cells because they can initiate the chromosome "breakage-fusion-bridge cycle" (discussed later). Therefore, telomere integrity is essential to prevent the gain, loss, and/or rearrangements of genetic information in eukaryotes (Maser and DePinho, 2002).

DNA-replication presents an obstacle for telomeres. During lagging strand synthesis, DNA polymerase is unable to fully copy the ends of linear chromosomes (Figure 7) causing telomeres to shorten with each cellular division. This gradual loss of DNA theoretically places a limitation on the number of cellular divisions and, thus, the survival of all eukaryotic organisms. It is proposed that when telomeres become shortened to a critical length, cells stop dividing and enter senescence. Cells that

Figure 7. Inability of DNA Polymerase to Fully Synthesize the Lagging Strand Ends During DNA Replication

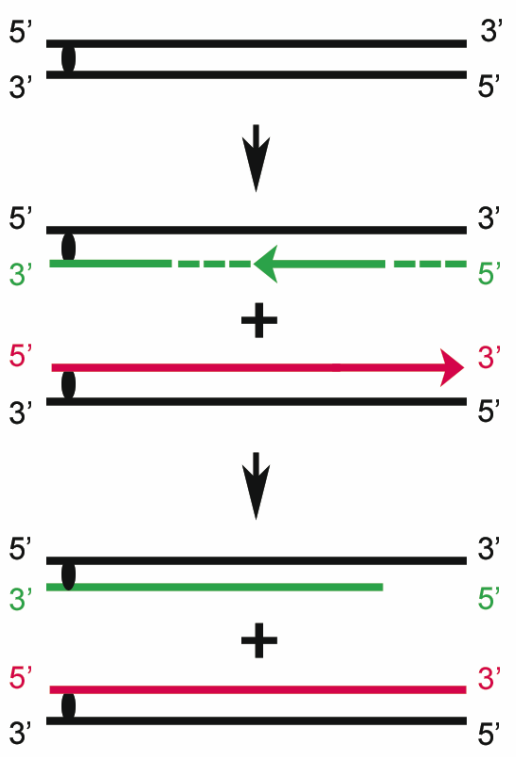

Inability of DNA polymerase to fully synthesize the lagging strand ends during DNA replication. The parental DNA duplex is shown in black (black ovals represent the centromeres). During DNA replication, leading strand synthesis (red) copies the parental strand to the last nucleotide. Discontinuous lagging strand synthesis (green) is primed by RNA primers (green dotted lines). When the final RNA primer is removed from the lagging strand terminus, a gap in the newly synthesized DNA remains. Figure re-drawn with modification from Blackburn, 1991.

can divide indefinitely (for example, single-cell eukaryotic organisms and cancerous cells) have the ability to maintain telomere length by expressing the ribonucleoprotein, telomerase. Functional telomerase is composed of an enzymatic protein and an essential RNA subunit. The RNA subunit serves as a template for the *de novo* elongation of

telomeric repeats at the chromosome ends (Figure 8). By this method, cells/organisms with linear chromosomes that express functional telomerase are able to maintain telomeric length and overcome the end replication problem (Dokudovskaya et al., 1997).

Figure 8. Schematic Diagram of Telomere Elongation by Telomerase

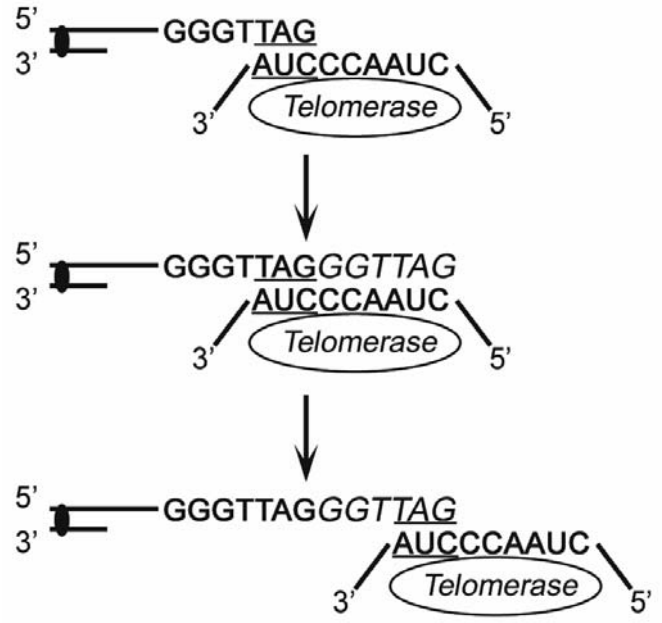

Schematic diagram of telomere elongation by telomerase. The RNA template of telomerase associates with the telomeric 3` tail (top). Using the RNA subunit as a template, the telomerase enzyme elongates the telomere by a reverse transcriptase mechanism (middle) (newly added nucleotides are italicized). Telomerase then translocates to the newly synthesized terminus (bottom) followed by several rounds of elongation and translocation. The black ovals represent centromeres. Figure re-drawn with modifications from Dokudovskaya et al., 1997.

Telomeres in Saccharomyces cerevisiae

Most of what is known about eukaryotic telomeres was discovered in the yeast, *S. cerevisiae*. Based upon the DNA sequence, each yeast telomere is divided into three regions. First, each chromosome end contains approximately 350 base pairs (bp) of the tandemly repeated $C_{1\text{-}3}A/TG_{1\text{-}3}$ sequence. Internal (centromere proximal) to the G/C rich region is a 6.7 kb sub-telomeric sequence, termed the Y` element. As opposed to satellite-like repeats, Y` elements contain a complex sequence of DNA and are often referred to as "telomere-associated" or "telomere-adjacent" sequences. Not all yeast

telomeres contain a Y` element, while some contain up to four tandemly repeated Y` elements. The third telomeric region is located internal (centromere proximal) to the Y` element (or internal to the G/C rich sequence in telomeres lacking Y` elements) and is referred to as the X` element. These exist as a single copy at all yeast telomeres. On chromosomes that contain both X` and Y` elements, approximately 100 bp of the G/C telomeric repeat sequence occurs at the junction. The functions of the Y` and X` elements are not known, although they contain "autonomously replicating sequences," or potential replication origins, which may ensure that DNA replication occurs all the way to the end of the chromosome (Chan and Tye, 1983).

In addition to the DNA sequences, a complex of proteins is associated at the ends of yeast telomeres. These complexes include the product of the telomerase-associated RNA coding gene (*TLC1*), the telomerase enzyme catalytic subunit (Est2), two telomere-associated proteins (Est1 and Cdc13), and a protein that binds only with the single-strand 3` overhang (Pot1). A gene disruption in *EST2* or *TLC1*, either of which disrupts telomerase, caused telomeres to gradually shorten with each cellular division. Continued growth in culture resulted in chromosome loss and cell death. These results are consistent with the end replication problem resulting in critically short telomeres to trigger telomere dysfunction, cell senescence, and cell death (Singer and Gottschling, 1994; Lendvay et al., 1996; Lingner et al., 1997). However, with prolonged growth in culture, colonies from each mutant strain form (Lendvay et al., 1996; Teng and Zakian, 1999). These "survivors" utilized a mechanism, which was Rad52-recombination dependent to lengthen telomere ends, despite the absence of functional telomerase. Yeast

strains that were deficient for telomerase (disruption of the telomerase-associated RNA coding gene, *TLC1*) and deficient for the *RAD52* gene were unable to generate survivors, demonstrating that an alternative pathway of telomere elongation exists, which is dependent upon HR (Le et al., 1999; Teng and Zakian, 1999; Chen et al., 2001).

Two methods of telomere elongation events can occur by recombination (in the absence of functional telomerase), which generate two types of survivors. Survivor types can be distinguished by Southern blot analysis using a probe specific against the G/C rich repeats. Type I survivors have amplification of the telomere-associated Y` elements and have very short $C_{1-3}A/TG_{1-3}$ tracts on the chromosome ends. Type II survivors show a highly variable pattern of long $C_{1-3}A/TG_{1-3}$ repeats with little amplification of the Y` elements (Lundblad and Blackburn, 1993). To better understand how these two types of survivors were generated by recombination, yeast strains deficient for functional telomerase and members of the *RAD52*-epistasis group were investigated. The *tlc1 rad51, tlc1 rad54,* or *tlc1 rad57* double mutants generated only type II survivors, demonstrating these proteins are required for the formation of type I survivors. Rad51, Rad54, and Rad57 proteins normally function in repairing chromosome breaks by HR, suggesting the generation of type I survivors requires the HR pathway. Type I survivors are likely generated by recombination events occurring between the Y` elements, which would require a high level of sequence identity. Alternatively, *tlc1 rad50, tlc1 xrs2,* or *tlc1 mre11* double mutants generated only type I survivors, demonstrating these proteins are required for the formation of type II survivors. In yeast, the Rad50, Xrs2, and Mre11 proteins function in end-joining and recombination repair of chromosome breaks. Type

II survivors likely arise by recombination events within the variable G/C rich sequences, which would require a low level of sequence identity for recombination. Similar to the *tlc1 rad52* double mutants, no *tlc1 rad50 rad51* triple mutant strains generated survivors, demonstrating HR is required for the generation of survivors in the absence of functional telomerase in *S. cerevisiae* (Le et al., 1999; Chen et al., 2001).

Although yeast contain multiple pathways to maintain telomere length, functional telomerase elongation is the preferred pathway. As mentioned previously, *tlc1* mutants have the ability to generate survivors by recombination. If wild-type *TLC1* is re-introduced into survivor strains, telomeres revert to wild-type length and the complemented strains are normal. Therefore, in *S. cerevisiae,* recombination-based telomere elongation is a secondary mechanism and only is required when functional telomerase is absent (Teng and Zakian, 1999).

Telomeres in Mammals

Like yeast, mammalian telomeres end with G/C rich sequences. This repeated sequence is approximately 3-5 kb and 5-150 kb long in humans and mice, respectively. The strand running 5′ to 3′ towards the chromosome end contains the sequence TTAGGG (this sequence is not variable), which is referred to as the G-rich strand. The telomeric G-rich strand in eukaryotes is longer than the complementary C-rich strand, thus forming a single-stranded 3′ overhanging tail at the terminus of each telomere (Zakian, 1995; Chakhparonian and Wellinger, 2003). Up to 25% of human chromosomes contain a conserved element of approximately 4 kb just internal (centromere proximal) to the G/C rich sequence. The function of this element is not known, and is absent at rodent

chromosome ends (de Lange et al., 1990). Mammalian telomeres form unique structures, referred to as T-loops, which have not been detected in *S. cerevisiae*. These protective structures form when the single-stranded 3` overhanging tail folds back, invades the duplex DNA, and binds internally to the complementary DNA strand (Figure 9). It is proposed that the mammalian telomere-associated proteins not only function to maintain telomere lengths, but also form, stabilize, and maintain the protective T-loop structure (Griffith et al., 1999).

In mammals, functional telomerase consists of a catalytic telomerase reverse transcriptase (TERT) and an RNA template encoded by the *TERC* gene to synthesize repetitive T_2AG_3 sequences at chromosome ends. However, differing from yeast, the expression of mammalian *TERT* is not detectable in most cells. Expression of *TERT* is limited to embryonic cells, male germ line cells, activated lymphocytes, and, at modest levels (insufficient for telomere maintenance), in hematopoietic and epithelial stem cells (expression of *TERC* is ubiquitous) (Shay, 1997). Because most mammalian somatic cells do not express detectable levels of *TERT*, with each cell division, 50-200 bp of DNA is lost (Harley et al., 1992). This gradual loss of DNA at the telomeric ends is thought to play a role in cellular senescence and "aging" of organisms. In support, telomere lengths decreased with each passage of primary cultures of human skin fibroblasts. Similarly, telomere length in fibroblasts derived from "older" individuals were, on average, shorter compared to telomeres derived from "younger" individuals (samples were taken from individuals ranging from 0-77 years old). Consistent with the expression of *TERT* in male germ line cells, telomere lengths were longer in sperm than

Figure 9. Proposed T-loop Structure

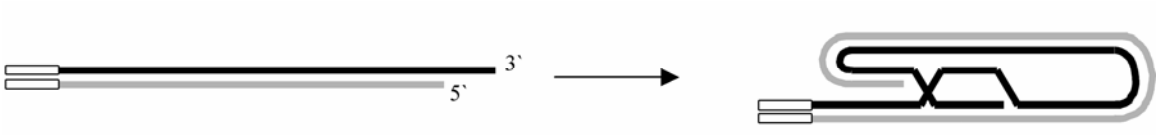

Proposed T-loop structure at the ends of mammalian telomeres. The single-stranded 3` overhanging tail folds back, invades the duplex DNA, and binds internally to the complementary DNA strand. Approximately 75-200 nucleotides of the single-stranded 3` overhang binds to its complement. White lines represent non-telomeric DNA, black line represents the G-rich telomeric strand, and gray line represents the C-rich telomeric strand.

in somatic cells isolated from the same donor (Harley et al., 1992). Several "aging" phenotypes have been associated with shortened telomere lengths, including decreased wound healing, decreased immune function, atherosclerosis, and an increased risk of developing cancer. Syndromes associated with accelerated aging and cancer predisposition, such as Werner syndrome, Bloom syndrome, Down syndrome, dyskeratosis congenita, and ataxia telangiectasia, also demonstrate alterations of telomere biology (Klapper et al., 2001).

Cell senescence in human fibroblasts occurs in two phases, mortality stage 1 (M1) and mortality stage 2 (M2). It was proposed that, after a limited number of cellular divisions, mammalian telomeres shorten to a recognizable length, which initiates a signal to stop cell division (M1) (Maser and DePinho, 2002). The signal into growth arrest is mediated by factors associated with both acute and chronic DNA damage checkpoint activities, such as p53, Rb, and p16 (INK4a) (Hara et al., 1991; Shay et al., 1991). If these checkpoints are bypassed, cells will leave M1 cell arrest and continue to divide resulting in further telomere erosion, telomere dysfunction, and entry into cellular crisis

(M2) (Maser and DePinho, 2002). When telomeres are eroded to critically short lengths, the protective T-loop structure may not be able to form leaving free DNA ends exposed. DNA repair mechanisms then can act upon these free DNA ends and create both intra- and inter-chromosome fusions, resulting in chromosome rings and dicentric chromosomes, respectively. During anaphase, the centromeres of ring and dicentric chromosomes are pulled to opposite spindle poles during chromosome segregation to form "anaphase bridges." This can cause chromosome non-disjunction leading to aneuploidy, or chromosome breaks. If chromosome breaks occur, and the daughter cells survive, the broken chromosomes are prone to be recognized by DNA repair mechanisms and may be fused together, forming another dicentric chromosome. This repetitive cycle is referred to as the breakage-fusion-bridge (BFB) cycle, which causes massive genetic instability and the "shuffling" of chromosome ends. This state of genetic instability likely causes cellular crisis observed during M2. However, as a consequence of this high level of genetic instability, tumor suppressor and proto-oncogenes may become altered causing an increased chance of malignant cellular transformation. In conclusion, telomere length and structure must remain intact to prevent telomere dysfunction and the BFB cycle to maintain genomic stability (Maser and DePinho, 2002).

Telomeres and Cancer

Mouse and human tumors typically have elevated levels of *TERT* expression, although the mechanism for how telomerase becomes expressed is unknown. The correlation of *TERT*-expression in cancerous cells suggests functional telomerase is a requirement for tumor growth. Primary human cells transfected with a *TERT* expressing

vector contained elongated telomeres and had an extended lifespan. However, expression of *TERT* alone is not capable of transforming fibroblast cells into cancerous cells (Bodnar et al., 1998). Because most cancers rely on functional telomerase to maintain telomere lengths, it was expected that the inhibition of telomerase could be used for cancer therapy. To test this hypothesis, mice deficient for the *Terc* gene (*Terc* encodes the RNA subunit of telomerase) were generated. Late generation mice had defects in high-renewal organ systems, such as the testes, bone marrow, and spleen (Lee et al., 1998). Contrary to expectations, $Terc^{-/-}$ mice had an increased rate of developing cancer in highly proliferative cell types, such as germ cells (teratocarcinomas), leukocytes (lymphomas), and keratinocytes (squamous cell carcinomas). Lymphocytes derived from late generation $Terc^{-/-}$ mice had high frequencies of aneupoidy and chromosome fusions. Therefore, the increased cancer incidence in $Terc^{-/-}$ mice was likely due to the genetic instability caused by excessive telomere shortening, the BFB cycle, and chromosome gain/loss. These results suggest that genomic instability conferred by telomere dysfunction promotes cancer initiation or progression. Interestingly, the cancerous cells had longer than normal telomeres (even in the absence of functional telomerase) and, despite progressive telomere shortening, mouse embryonic fibroblasts (MEFs) derived from $Terc^{-/-}$ mice had similar growth characteristics to wild-type MEFs, including the ability to overcome senescence/crisis (Blasco et al., 1997; Rudolph et al., 1999). These results were the first evidence that a second method of telomere lengthening is present in mammals. This is referred to as alternative lengthening of telomeres (ALT), and will be discussed later.

Proteins that Protect Telomeres in Mammals

Although it has been proposed that the length of DNA at chromosome termini is the cause of cellular aging, senescence, and telomere dysfunction, it is not the only culprit. Cell lines carrying defects in mammalian telomere-associated proteins demonstrate the inability to maintain telomere length, an increased frequency of telomeric fusions, and cell death. Therefore, telomere function is more likely to depend upon telomeric structure, rather than telomere length alone. A brief description of the initial telomere-associated proteins is given below.

Telomeric repeat binding factor 1 (TRF1) was first identified in mammals by its ability to specifically bind double-stranded telomeric (T_2AG_3/C_3TA_2) repeats. The TRF1 protein is found in all tissues and contains a single DNA binding domain. This protein functions as a homodimer to bind only telomeres in all stages of the cell cycle (Zhong et al., 1992; Chong et al., 1995). In a human fibrosarcoma cell line, over-expression of wild-type *TRF1* resulted in telomere shortening. Expression of a dominant-negative form of *TRF1*, which lacks the DNA binding domain, bound to endogenous TRF1, inhibited the binding of endogenous TRF1 to telomeres, and conferred telomere elongation. These data suggest that TRF1 normally functions to regulate telomere length, potentially by blocking telomerase from elongating telomeres (van Steensel and de Lange, 1997). Mice deficient for the *Trf1* gene die at embryonic stage E5-6 and, in contrast to expression of the dominant negative form of *TRF1* in human cells, telomeres in *Trf1*$^{-/-}$ MEFs were normal in length. The *Trf1*$^{-/-}$ MEFs underwent apoptosis, but there was no evidence of increased levels of telomere fusions (Karlseder et al., 2003). These data suggest that

TRF1 can act as a suppressor of telomere elongation and also has essential functions independent of telomere length regulation (van Steensel and de Lange, 1997; Karlseder et al., 2003).

Telomeric repeat binding factor 2 (TRF2) was identified by its ability to bind directly to T_2AG_3/C_3TA_2 repeats. The TRF2 protein is found in all tissues, contains a single DNA binding domain, and functions as a homodimer at chromosome ends (Bilaud et al., 1997; Broccoli et al., 1997). *In vitro,* TRF2 was required to form the T-loop structure on an artificial chromosome (Griffith et al., 1999). However, this reaction is not efficient, suggesting, *in vivo*, TRF2 is assisted by other factors that promote strand invasion of the single-stranded tail during the process of T-loop formation (Griffith et al., 1999; Stansel et al., 2001; de Lange, 2005). In human fibrosarcoma cells, expression of an inducible dominant-negative form of *TRF2* (*TRF2*$^{\Delta B \Delta M}$), which lacks an N-terminal basic region and the DNA binding domain, conferred removal of POT1 (a telomere-specific binding protein, see below) from telomeres, loss of the single-stranded 3´ overhanging tail, and a high number of telomere-telomere fusions (van Steensel et al., 1998; Karlseder et al., 1999, 2002). Expression of the dominant-negative form of TRF2 in mouse embryonic fibroblasts induced an immediate ATM/p53-dependent apoptotic pathway response, similar to the signaling pathway that is activated by DNA DSBs (Karlseder et al., 1999, 2002). Mice deficient for *Trf2* die before birth at E13.5, and embryonic lethality is not rescued in a *Trp53*$^{-/-}$ background. The *Trf2*$^{-/-}$ *Trp53*$^{-/-}$ MEFs had similar phenotypes as those observed when *TRF2*$^{\Delta B \Delta M}$ is expressed in human or mouse cells (Celli and de Lange, 2005). These data suggest TRF2 is required

for T-loop formation and to "mask" chromosome ends from DNA damage response mechanisms (van Steensel et al., 1998; Karlseder et al., 1999).

POT1 is one of the only mammalian telomere-associated proteins that has a homolog in the yeast, *Schizosaccharomyces pombe* (*S. pombe*). Both the yeast and human POT1 proteins bind specifically to the single-stranded 3` overhang of telomeres. In humans, expression of *POT1* is observed in all tissues. A *POT1* disruption in *S. pombe*, conferred immediate chromosome instability with a high frequency of chromosome mis-segregation, loss of telomeric G/C repeats, and chromosome circularization (Baumann and Cech, 2001). In human cells, reduction of POT1 by RNA interference conferred loss of the telomeric overhanging tail, increased levels of telomere fusions, and senescence (Veldman et al., 2004; Hockemeyer et al., 2005; Yang et al., 2005). Therefore, the POT1 protein may cap the 3` telomeric DNA end and, in humans, aid in the formation and stabilization of the T-loop. Alternatively, POT1 may act to recruit telomere-specific proteins to the single-stranded 3` overhang (Baumann and Cech, 2001).

Human RAP1 interacts directly with TRF2 and localizes to mammalian telomeres at all stages of the cell cycle. Overexpression of wild-type RAP1 in human fibrosarcoma cells resulted in the gradual elongation of telomeric ends. RAP1 does not appear to act directly with TERT, but likely regulates telomeric structure to enable functional telomerase to access the 3` overhanging end. Therefore, because of its interaction with TRF2, RAP1 may act in the regulation or formation of T-loop structures (Li et al., 2000).

Human TIN2 was found to interact directly with TRF1 and TRF2 (Kim et al., 1999; Liu et al., 2004a; Ye et al., 2004a). Expression of a mutant form of TIN2 in human cells conferred telomerase-dependent telomere elongation (Kim et al., 1999). *Tin2*-deficient mice die before embryonic stage E7.5 and the embryonic lethal phenotype is not rescued in a telomerase deficient (*Terc*$^{-/-}$) background (Chiang et al., 2004). Therefore, like TRF1, TIN2 can act as a suppressor of telomere elongation and also has essential functions independent of telomere length regulation (van Steensel and de Lange, 1997; Karlseder et al., 2003; Chiang et al., 2004). Although little is known about the biochemical functions of TIN2, it is required for protein complex formation among the mammalian telomere proteins (see below).

TPP1, previously named TINT1 (Houghtaling et al., 2004), PTOP (Liu et al., 2004b), and PIP1 (Ye et al., 2004b), was identified by a yeast two-hybrid screen for proteins that interact with TIN2 (Houghtaling et al., 2004). TPP1 also interacts directly with POT1 and recruits it to the telomere (Liu et al., 2004b; Ye et al., 2004b). Expression of a truncated form of TPP1 that lacked the TIN2 interacting domain, or inhibition of TPP1 by RNA interference, conferred progressive telomerase-dependent telomere elongation and failure of POT1 localization at telomeres (Houghtaling et al., 2004; Liu et al., 2004b). These data demonstrate that TPP1 recruits POT1 to telomeres and is also a regulator of telomere length.

The six previously mentioned telomere-binding proteins may interact to form a single complex in mammalian cells (Liu et al., 2004b; O'Connor et al., 2004; Ye et al.,

2004a) termed "shelterin" (de Lange, 2005) (Figure 10). Because each shelterin complex contains two TRF1 proteins, two TRF2 proteins, and one POT1 protein, shelterin contains five telomere-specific DNA binding domains, making this complex telomere specific (de Lange, 2005). Exactly how the shelterin complex protects chromosome ends is not known. Additional proteins, that are not telomere-specific, also play important roles at telomeres (de Lange, 2005) (see below).

Figure 10. Proposed Shelterin Complex Bound to Telomeric DNA

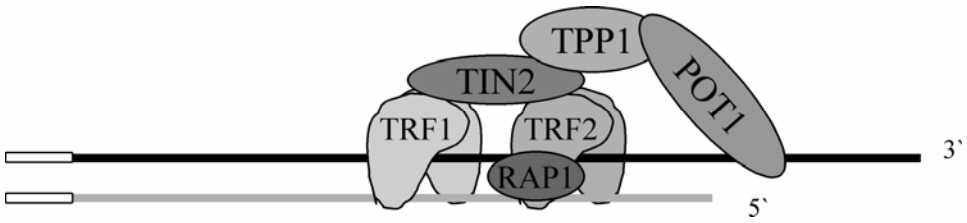

Proposed shelterin complex bound to telomeric DNA. Shelterin is composed of two TRF1 and TRF2 proteins, and one RAP1, TIN2, TPP1, and POT1 protein. White lines represent non-telomeric DNA, black line represents the G-rich telomeric strand, and gray line represents the C-rich telomeric strand. Figure re-drawn with modification from de Lange, 2005.

DNA Repair Proteins at Mammalian Telomeres

One function of telomere structure is to mask the ends of chromosomes from DNA repair proteins, especially proteins that are involved in repairing DSBs. Recently, several proteins that function in DSB repair were identified to normally associate with telomeres. Initial evidence from *S. cerevisiae* strains deficient for Ku70 or Ku80, two proteins that function in the repair of DSBs by NHEJ, had abnormally short telomeres and underwent senescence (Boulton and Jackson, 1996; Laroche et al., 1998). It was later reported that these proteins normally interact directly at yeast telomeres, although their role in telomere maintenance is not understood (Gravel et al., 1998).

As observed in *S. cerevisiae,* proteins involved in the mammalian NHEJ repair pathway, Ku70, Ku80, and DNA-PKcs, function in telomere maintenance. In human and rodent cells, Ku70 and Ku80 bind to TRF2 and TRF1, respectively, and localize at telomeres (Hsu et al., 1999; K. Song et al., 2000). Primary MEFs deficient for Ku70 or

Ku80 have normal length telomeres, but high levels of telomeric fusions. These data suggest Ku70 and Ku80 play a role in capping mammalian telomeres to prevent end joining (Bailey et al., 1999; Hsu et al., 1999; Samper et al., 2000). Lastly, although DNA-PKcs has not been reported to localize at telomeres, primary MEFs deficient for DNA-PKcs have an increased frequency of telomeric fusions (Bailey et al., 1999; Goytisolo et al., 2001). It has been proposed that DNA-PKcs, together with TRF2, are required for strand processing of telomeres after DNA replication (Bailey et al., 2001).

Mammalian RAD50, MRE11, and NBS1, proteins involved in both DSB repair pathways (NHEJ and HR) in mammals, also may have responsibilities at chromosome ends. In HeLa cells and primary human fibroblasts, the RAD50/MRE11/NBS1 (MRN) complex localizes (by the binding of RAD50 to TRF2) at telomeres (Zhu et al., 2000). Although telomere dysfunction in mammalian cells deficient for RAD50, MRE11, or NBS1 has not been reported, in *Drosophila melanogaster*, a gene disruption in *mre11* or *rad50* confers increased levels of telomere fusions, demonstrating that the MRN complex is required for telomere protection (Ciapponi et al., 2004). In HeLa cells, the RAD50 and MRE11 proteins remained at telomeres throughout G1, S, and G2, and may be required for the maintenance of T-loops at all stages of the cell cycle whereas NBS1 localized to telomeres in S-phase. This transient recruitment of NBS1 to telomeres suggests it plays a role during telomere replication. Because NBS1 has helicase activity, the MRN complex may regulate an unfolding of the T-loop to allow replication machinery to copy chromosome ends (Zhu et al., 2000).

The HR protein, RAD51D, localizes to telomeres in mitotic and meiotic cells and, in the absence of RAD51D, telomeres are dysfunctional (see Results) (Tarsounas et al., 2004). The mechanism of T-loop formation at mammalian telomeres is similar to how DSBs are repaired by HR. In this conception, T-loop formation is a specialized "intra-chromosomal DNA repair event." The potential roles of RAD51D at telomeres will be discussed in further detail (see Results and Discussion).

Telomere Lengths and Disease

Patients with ataxia telangiectasia, Bloom syndrome, or Werner syndrome inherit genetic defects in the *ATM*, *BLM*, or *WRN* genes, respectively. Each of these syndromes confers increased sensitivity to DNA damaging agents, chromosomal instability, and cancer predisposition. Interestingly, cells derived from patients with ataxia telangiectasia, Bloom syndrome, or Werner syndrome have accelerated telomere attrition *in vitro*, suggesting that the diseases associated with defects in the *ATM*, *BLM*, or *WRN* genes are partially due to telomere problems. However, it is not understood if the differences in telomere lengths contribute to the phenotypes associated with these syndromes (Klapper et al., 2001). It is likely that alterations in telomere structure or length will be identified in additional human syndromes (for example, in addition to its roles in DNA repair, the NBS1 protein functions at telomeres, and inherited mutations in the *NBS1* gene confer Nijmegen breakage syndrome).

The previously mentioned syndromes, which are associated with decreased telomere lengths, are caused by mutations in single genes. Recent data suggest that decreased telomere lengths also may be associated with genetically complex, age-related

diseases. In humans, decreased telomere lengths have been correlated with increased pulse pressure (Jeanclos et al., 2000; Benetos et al., 2001), atherosclerosis (Samani et al., 2001; Obana et al., 2003; Benetos et al., 2004), heart failure (Oh et al., 2003), type 1 and type 2 diabetes (Jeanclos et al., 1998; Adaikalakoteswari et al., 2005), insulin resistance (Gardner et al., 2005), obesity (Valdes et al., 2005), and stress (Epel et al., 2004). Although these studies have demonstrated an association of telomere length with disease, a causal or effectual relationship remains to be established. Mice in which telomeres are critically short due to a targeted gene disruption in telomerase have increased levels of heart failure, suggesting decreased telomere lengths confer cardiac disease (Leri et al., 2003). However, because age-related diseases are genetically complex and determined by the expression of combinations of allelic variants sensitive to a given environment (Mootha et al., 2003), animal models to test their relationship with telomere lengths are limiting.

Alternative Lengthening of Telomeres in Mammals

In cultured human and mouse primary cells, *TERT* expression is activated during cellular immortalization, and telomerase activity is present in approximately 90% of human tumors (Kim et al., 1994). Interestingly, tumor cells typically have shorter telomeres compared to other surrounding cell types. It was proposed that tumor cells initially acquire mutations that allow rapid, unregulated division. During this time, telomere shortening occurs and, at a later point, expression of telomerase is activated (Kass-Eisler and Greider, 2000). However, recall that mice deficient for the RNA subunit of functional telomerase, *Terc*, are prone to developing cancer (Blasco et al.,

1997; Rudolph et al., 1999). Additionally, approximately 10% of human tumors do not express detectable levels of telomerase (Kim et al., 1994). These data support an alternative mechanism for maintaining telomere length. Like in yeast, a recombination-based mechanism is thought to play an important role in alternative lengthening of telomeres (ALT). A model of a telomerase-independent mechanism of telomere lengthening has been proposed and is shown in Figure 11.

Telomerase-negative human cancer cells typically have extremely long and hypervariable telomeres ranging from ~10-50 kb in length. In these cells, telomeres gradually shorten until a critical limit followed by a sudden increase in telomere length. At critically short telomeres, it is possible that recombination is activated causing the 3` DNA end to invade a second chromosome to use as a template for telomere replication/elongation (Bryan et al., 1995; Kass-Eisler and Greider, 2000). In an immortalized telomerase negative human tumor cell line, it was demonstrated that a tagged telomeric DNA sequence was copied from telomere to telomere during growth in culture, supporting that ALT occurs by HR (Dunham et al., 2000).

All telomerase-negative human cancer cell lines contain a novel type of promyelocytic leukemia (PML) body, referred to as ALT-associated PML body (APB). The APBs are donut-shaped nuclear complexes containing the PML protein (Yeager et al., 1999). Although the function of the PML protein is not known in untransformed cells, evidence suggests that it activates the Fas- and caspase-dependent apoptotic pathways in response to ionizing irradiation (Wang et al., 1998). Interestingly, APBs in telomerase-negative ALT cell lines also contain RAD51D, RAD51, RAD52, and

Figure 11. Model of Alternative Telomere Lengthening in Mammals.

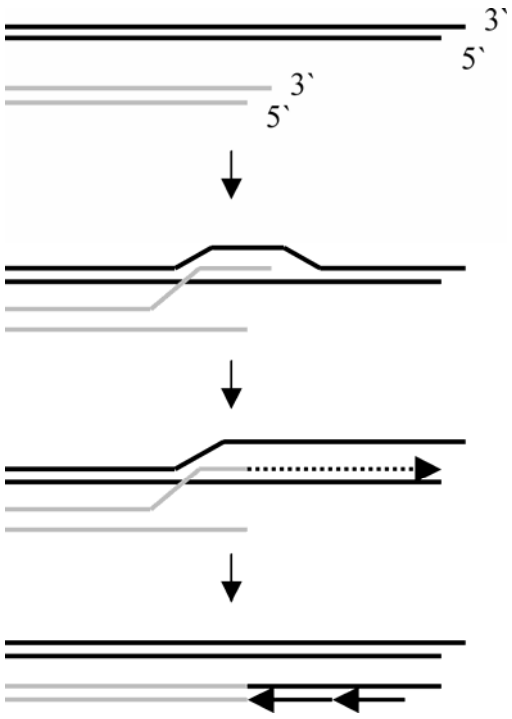

The 3´ telomeric end of a short chromosome (shown in gray) can invade a second longer chromosome (shown in black) and use its telomere as a template for elongation. The lagging strand can then be filled in by standard DNA replication machinery. Figure re-drawn with modifications from Dunham et al., 2000.

replication factor A (RPA), all of which are involved in HR (Yeager et al., 1999; Tarsounas et al., 2004). In ALT cell lines, APBs localized with TRF1 and TRF2 during G2/M phases of the cell cycle. This co-localization was not detected in mortal or telomerase-positive immortal cells (Grobelny et al., 2000). During *in vitro* immortalization of human fibroblasts isolated from a patient with Li-Fraumeni syndrome (*TP53*$^{+/-}$), APBs became detectable at telomeres at the same population doubling in which long heterogeneous telomeres appeared, characteristic of ALT cells (Yeager et al.,

1999). These data demonstrate telomere lengthening in ALT cells is dependent upon APBs and likely requires HR.

Telomere maintenance and elongation appear to be a requirement for cancer cell survival. Understanding how ALT occurs will give insights to how telomeres are elongated in the absence of functional telomerase. This knowledge could then be applied to comprehending cancer progression and may be useful in cancer treatment strategies.

In conclusion, telomeres are structures that primarily function to protect the ends of chromosomes from fusion and degradation. Although this seems like an easy task, telomere dynamics are complex. In mammalian cells, telomeres can be found in multiple conformations, which likely depend upon cell cycle: (1) the protective T-loop structure that is likely formed in G1, G2, and M phases, (2) unwound T-loops that form during S phase to allow for DNA replication, and (3) engaged with the telomere elongating enzyme telomerase (in telomerase expressing cells) during S and, possibly, G2 phases of the cell cycle. The telomere-specific proteins, which form the protein complex named shelterin, bind to the telomeric DNA and likely alter the telomeric DNA structure during the cell cycle. How exactly these proteins perform this function is not known. Additional proteins that are not telomere-specific, for example RAD51D, Ku70/Ku80, and the MRN protein complex, function in telomere protection. Again, how these proteins protect the ends of chromosomes is not known. Understanding the biology of mammalian telomeres is offered little help from prokaryotic organisms because the genomes lack telomeres (their chromosomes are circular). Additionally, telomeres from lower eukaryotic organisms, such as *S. cerevisiae*, do not form T-loop structures and

homologs of yeast telomere proteins are absent in mammals. Therefore, as of now, the simplest organism to study mammalian telomere biology is in mammalian cells themselves. Dr. Madalena Tarsounas demonstrated that the RAD51D protein localizes at telomeres in (1) human HeLa cells (telomerase positive) by dual indirect immunofluorescence and chromatin immunoprecipitation (ChIP) analysis, (2) human WI38-VA13/2RA cells (telomerase negative) by dual indirect immunofluorescence, and (3) mouse spermatocytes by dual indirect immunofluorescence, electron microscopic visualization by immunogold labeling, and ChIP analysis (Tarsounas et al., 2004). The data described in the Results section demonstrate telomere dysfunction in *Rad51d*-deficient mouse embryonic fibroblasts. Manuscript 2 demonstrates that, in *Rad51d*-deficient mouse cells, telomeres have an increased frequency of being detected as DSBs and the telomeres have long single-stranded, telomeric 3´ overhangs. In this work, I hypothesize that, in the absence of the RAD51D protein, protective telomere structures are not formed, which leaves chromosome ends vulnerable to excessive exonuclease degradation.

The progressive telomere shortening in somatic cells is proposed to be a mechanism of cellular aging. In human studies, decreased telomere lengths have been correlated to the development of age-related diseases; however, the cause-effect relationship is not known. Rats selectively bred based upon their aerobic running capacity have emerged as models that display multiple cardiovascular and metabolic disease risks when young adults. The hypothesis of Manuscript 3 proposes that rats selectively bred based upon their low aerobic running capacity have shorter telomeres

compared to rats selectively bred based upon their high aerobic running capacity. Following the Results section, a combined Discussion and Summary section addresses all of the data presented in this dissertation.

MATERIALS AND METHODS

The section describes materials and methods relating to studies presented in the Results section of this dissertation that are not included in the manuscripts. Detailed explanations of all protocols have been included as Appendices. Materials and methods describing additional dissertation research are included as parts of Manuscript 1, Manuscript 2, and Manuscript 3.

Southern Blot Genotyping of Mouse Embryonic Fibroblasts

This method was used to determine the genotype of the *Rad51d* gene in MEFs and to verify the results obtained by PCR using primers specific for the wild-type and disrupted *Rad51d* alleles (for primer sequences and PCR conditions, see Results section of Manuscript 1). Genomic DNA from primary MEFs (< passage 4) was digested with BamH1 and separated by size on a 0.8% agarose gel at 50 volts for 15 h. Gels containing DNA were depurinated in 0.2M HCl for 15 min at room temperature, denatured in 0.5M NaOH, 1.5M NaCl for 30 min at room temperature, and neutralized in 0.5M Tris, 1.5M NaCl, pH 7.6 for 30 min at room temperature. DNA was transferred to a nylon membrane (Schleicher & Schuell, Nytran® SPC) overnight in 10xSSC at room temperature. The membrane was rinsed in 0.5M Tris, 1.5M NaCl, pH 7.6, dried, and crosslinked with 600 J/m^2 using a UV Stratalinker® 2400 (Stratagene). The membrane was pre-hybridized in hybridization solution (6xSSC, 0.01M EDTA, 5x Denhardts reagent, 100 μg/ml sheared salmon sperm, 0.5% SDS) for 60 min at 63°C and probed with the downstream Probe B (Pittman and Schimenti, 2000) in fresh hybridization solution overnight at 63°C. The membrane was washed in 1xSSC 0.1% SDS two times

for 20 min each at room temperature with constant shaking and two times in 0.1xSSC 0.1% SDS for 20 min each at 65°C. The membrane was wrapped in plastic wrap and exposed to phosphorimager screen overnight at room temperature. The phosphoimager screen was developed using a Typhoon 8600 Variable Mode Imager (Molecular Dynamics, Amersham Pharmacia Biotech). Contrast of the image was enhanced using Adobe® Photoshop® version 7.0. Bands at 20.0- and 8.6-kb represent the disrupted and wild-type *Rad51d* alleles, respectively.

Detecting Anaphase Bridges in Primary Mouse Embryonic Fibroblasts

This method was used to obtain data described in Results: Telomere Dysfunction in *Rad51d*-Deficient Mouse Embryonic Fibroblasts. Primary MEFs were seeded onto ethanol-sterilized glass coverslips in 12-well plates at $8x10^4$ cells per well. Two independent primary wild-type, *Trp53*$^{-/-}$, and *Rad51d*$^{-/-}$ *Trp53*$^{-/-}$ MEFs were investigated. The following day, cells were washed twice with 1xPBS, fixed with 4% paraformaldehyde for 20 min at 4°C, washed twice with 1xPBS, and incubated in 1xPBS 0.3% Triton X solution for 10 min at 4°C. Cells then were washed twice with 1xPBS, stained with 100ng/ml DAPI (excitation = 360 nm, emission = 450 nm) solution for 10 min at room temperature, and washed twice with 1xPBS. Coverslips were mounted onto glass slides, sealed, and viewed at 1000x magnification using a Nikon Eclipse E800 fluorescent microscope equipped with a mercury lamp light-source (provided by W. Maltese, Medical University of Ohio, Department of Biochemistry & Cancer Biology, Toledo, Ohio) (Filter used, UV-2E/C excitation 330-380 nm). Images were captured

using Image-Pro® Plus version 4.0 for Windows. Contrast of the images was enhanced using Adobe® Photoshop® version 7.0 for Macintosh®.

Labeling Telomeres from Metaphase Chromosome Spreads with a Fluorescent Peptide Nucleic Acid Probe

This method was used to obtain data described in Results: Telomere Dysfunction in *Rad51d*-Deficient Mouse Embryonic Fibroblasts. Metaphase chromosome spreads were prepared as described (Appendix B). Chromosome spreads from two independent primary wild-type, *Trp53*$^{-/-}$, and *Rad51d*$^{-/-}$ *Trp53*$^{-/-}$ MEFs were investigated. Slides containing chromosome spreads were incubated in 0.005% Pepsin working solution at 37°C for 7.5 min and washed in 1xPBS for 5 min. Slides then were dehydrated through 70%, 85%, and 100% ethanol for at 4°C (1 min in each ethanol solution) and air-dried. Twelve µl of telomere specific peptide nucleic acid probe Cy3-$(CCCTAA)_3$ (Applied Biosciences) (Cy3: excitation = 552 nm, emission = 568-574 nm) was added to each slide. Slides were covered with a glass coverslip, placed at 70°C for 7 min, and then incubated at room temperature for 30 min. Slides were washed in 1xPBS 0.1% Tween 20 for 20 min at room temperature, washed in 1xPBS 0.1% Tween 20 for 20 min at 57°C, and washed in 2xSSC 0.1% Tween 20 for 1 min at room temperature. Slides were then stained in 200ng/ml DAPI (excitation = 360 nm, emission = 450 nm) for 5 min at room temperature, washed in 2xSSC 0.1% Tween 20 for 1 min at room temperature, covered with a glass coverslip, sealed with nail polish, and viewed at 1000x magnification using a Nikon Eclipse E800 fluorescent microscope equipped with a mercury lamp light-source (provided by W. Maltese, Medical University of Ohio, Department of Biochemistry &

Cancer Biology, Toledo, Ohio) (filter used to visualize DAPI stain: UV-2E/C excitation 330-380 nm, filter used to visualize Cy3 probe: G-2E/C TRITC excitation 528-553 nm). Images were captured and merged using Image-Pro® Plus version 4.0 for Windows. Contrast of the images was enhanced using Adobe® Photoshop® version 7.0 for Macintosh®.

Determining the Integral (Area Under the Curve) from DNA Damage Survival Curves from Mouse Embryonic Fibroblasts

This analysis was used to determine the fold differences in sensitivity of *Rad51d*-deficient MEFs to DNA damaging agents compared to control MEFs (see Results: Table 3, Supplemental data for Manuscript 1). Data from Results: Figure 4, Manuscript 1, was used for these analyses. A polynomial trend-line was calculated using Microsoft® Excel X for Macintosh® for each genotype, from each DNA damaging agent tested. The equation of the trend-line was input into the Y_1 of a Texas Instruments TI-81 graphing calculator. The integral from D100 (untreated cells, dose of the DNA damaging agent that corresponds to 100% survival) to D37 (dose of the DNA damaging agent that corresponds to 37% survival) and the integral from D100 to D10 (dose of the DNA damaging agent that corresponds to 10% survival) were calculated by running the program "SIMPSON" (see below) with 75 parabolas.

Program: "SIMPSON"

:Disp_"L.ENDPOINT_(A)"

:Input_A

:Disp_”R.ENDPOINT_(B)”

:Input_B

:Disp_”PARABOLAS”

:Input_P

:(B-A)/(2P) →H

:A→X

:Y_1→S

:1→J

:Lbl_1

:X+H→X

:S+4Y_1→S

:X+H→X

:S+2Y_1→S

:IS>(J,P-1)

:GOTO_1

:X+H→X

:S+4Y_1→S

:X+H→X

:S+Y_1→S

:HS/3→C

:Disp_”INTEGRAL”

:Disp_C

For an example of this program, see Appendix B. Fold differences in sensitivity were calculated by (D100-D37 integral of *Trp53*$^{-/-}$ cells) / (D100-D37 integral of *Rad51d*$^{-/-}$ *Trp53*$^{-/-}$ cells) and by (D100-D10 integral of *Trp53*$^{-/-}$ cells) / (D100-D10 integral of *Rad51d*$^{-/-}$ *Trp53*$^{-/-}$ cells).

RESULTS

MANUSCRIPT 1

Cancer Research. 2005 Mar 15;65(6):2089-96

Extensive Chromosomal Instability in *Rad51d*-Deficient Mouse Cells

Phillip G. Smiraldo, Aaron M. Gruver, Joshua C. Osborn, and Douglas L. Pittman

Department of Physiology, Medical College of Ohio, Toledo, Ohio

Financial Support: The March of Dimes Birth Defects Foundation and the American Cancer Society

Corresponding author:

Douglas L. Pittman

Department of Physiology

Medical College of Ohio

Block Health Science Building

3035 Arlington Avenue

Toledo, OH, 43614-5804

Telephone 419-383-4370

Fax 419-383-6168

Email: dpittman@mco.edu

Running Title: CHROMOSOME INSTABILITY IN *Rad51d*-DEFICIENT MICE

Keywords: Homologous recombination/RAD51/mouse/spectral karyotyping/genetic instability/aneuploidy

Abbreviations: Homologous recombination (HR), mouse embryonic fibroblast (MEF), sister chromatid exchange (SCE), interstrand crosslink (ICL), double strand break (DSB)

ABSTRACT

Homologous recombination (HR) is a double-strand break repair pathway required for resistance to DNA damage and maintaining genomic integrity. In mitotically dividing vertebrate cells, the primary proteins involved in HR repair are RAD51 and the five RAD51 paralogs, RAD51B, RAD51C, RAD51D, XRCC2, and XRCC3. In the absence of *Rad51d*, human and mouse cells fail to proliferate, and mice defective for *Rad51d* die prior to birth, likely as a result of genomic instability and p53 activation. Here, we report that a p53 deletion is sufficient to extend the lifespan of *Rad51d*-deficient embryos by up to 6 days and rescue the cell lethal phenotype. The *Rad51d*$^{-/-}$ *Trp53*$^{-/-}$ mouse embryo derived fibroblasts were sensitive to DNA-damaging agents, particularly interstrand crosslinks, and exhibited extensive chromosome instability including aneuploidy, chromosome fragments, deletions, and complex rearrangements. Additionally, loss of *Rad51d* resulted in increased centrosome fragmentation and reduced levels of radiation-induced RAD51-focus formation. Spontaneous frequencies of sister chromatid exchange (SCE) were not affected by the absence of *Rad51d*, but SCE frequencies did fail to be induced upon challenge with the DNA cross-linking agent mitomycin C. These findings support a crucial role for mammalian RAD51D in normal development, recombination, and maintaining mammalian genome stability.

INTRODUCTION

Genetic defects in DNA repair genes are likely responsible for chromosome rearrangements associated with the evolution of cancer (1). One type of DNA damage,

the double-strand break (DSB), is formed during DNA replication, antigen receptor rearrangements, or upon exposure to environmental or cancer therapy agents. Conventional two-ended DSBs are repaired by nonhomologous end joining or homologous recombination repair pathways, and defects in either pathway lead to a failure to properly repair damaged DNA which contributes to chromosome unstable phenotypes (2).

Homologous recombination (HR) is primarily directed by the RAD51 recombination/repair family (3, 4). Altered expression and mutations in *RAD51* genes are associated with chromosome rearrangements in human cancers and selected resistance to chemotherapeutic agents (1, 5-7). The RAD51D protein is approximately 39% similar in sequence and structure to RAD51 and contains two conserved Walker box motifs that predicted binding and hydrolysis of ATP (8-11). Biochemical analysis of RAD51D demonstrated DNA-stimulated ATPase activity independently and in complex with XRCC2 (12, 13). RAD51D:XRCC2 heterodimers have the ability to form filamentous structures along single-stranded DNA that promote homologous pairing between single- and double-stranded DNA molecules (14), and the RAD51D:XRCC2 complex interacts with the N-terminal domain of the BLM helicase protein to stimulate resolution of synthetic Holliday junctions (13). These data suggest RAD51D is involved in at least two aspects of HR, strand invasion and Holliday junction resolution.

Mice carrying a homozygous targeted deletion in the *Rad51d* gene die during embryo development, surviving up to 10.5 days post-conception. Mutant embryos have a range of phenotypes and increased levels of cell death, suggestive of random mutations in

cell and developmental regulatory genes (15). Supporting a role for RAD51D in genome maintenance in vertebrates, chicken B lymphocyte DT40 cell lines carrying a *rad51d* disruption accumulated chromosomal breaks and had increased levels of dead cells (16). Similarly, when RAD51D synthesis was inhibited by siRNA in human cells, cultures died within 7 days (17). Here, we report on mice and isogenic mouse embryo fibroblasts (MEFs) deficient for both *Rad51d* and *Trp53*. Double mutant embryos survive up to 16.5 days post-conception and unlike *Rad51d*$^{-/-}$ MEFs, *Rad51d*$^{-/-}$ *Trp53*$^{-/-}$ MEFs proliferate in culture. By generating viable *Rad51d*$^{-/-}$ *Trp53*$^{-/-}$ cell lines, we, for the first time, have been able to investigate cellular phenotypes conferred by a *Rad51d* disruption in mammalian cell lines and perform detailed analyses of chromosomal instability in primary, non-immortalized, *Rad51d*-deficient cells by multiple methods, including spectral karyotype analysis. Mutant cells had elevated levels of chromosome instability, increased centrosome fragmentation, were hypersensitive to DNA damaging agents, and failed to form radiation-induced RAD51 foci. These results demonstrate that RAD51D plays a critical role in maintaining the integrity of the mammalian genome and loss of p53 is sufficient for proliferation of these highly compromised and chromosomally unstable cells.

MATERIALS AND METHODS

Breeding Scheme and Genotyping. Mice heterozygous for *Rad51d* (15) and *Trp53* (18), obtained from The Jackson Laboratory, were crossed to generate mice heterozygous for both genes. Both lines of mice were in a C57BL6/J strain background. Following timed matings, embryos from E9.5 to E16.5 were dissected and either fixed in

10% formalin or homogenized for generating cell lines. *Rad51d* genotyping and genders for embryos were determined as described (15, 19). To genotype *Trp53*, a three primer PCR reaction was used, recommended by the Induced Mutant Resource Facility at The Jackson Laboratory: IMR36 (W5`) (18), IMR37 (W3`) (18), and IMR265 (5`-TCCTCGTCCTTTACGGTATC-3`). IMR36-IMR37 amplifies the wild-type *Trp53* allele (450bp) and IMR37-IMR265 amplifies the disrupted *Trp53* allele (600bp). Amplification conditions for the IMR36-IMR37-IMR265 reaction were 30 rounds of 95˚C, 1 min., 60˚C (-0.5ºC/cycle), 1 min., 72˚C, 2 min., and 15 rounds of 94˚C, 1 min., 50˚C, 1 min. 30 sec., 72˚C, 2 min. All animal procedures were performed in compliance with federal and institutional guidelines.

Cell Culture, Growth, and Chromosome Analysis. Primary cultures of E13.5 to E14.5 embryos were prepared by homogenizing whole embryos in DMEM supplemented with 7.5% FBS, 7.5% NCS, and antibiotics, to single cell suspension and plating to a 60mm dish. For cell growth analysis, MEFs were seeded onto 6-well plates at $8x10^4$ cells per well. Cells were counted using a Coulter counter (Coulter Beckman). Flow cytometric analysis (Coulter Beckman) was carried out on two independent exponentially growing primary MEF cultures per genotype stained with propidium iodide.

Giemsa stained metaphase chromosome spreads were prepared from primary MEF cells. Two independent MEF cell lines per genotype were scored for chromatid and chromosome abnormalities as described (20) ($Rad51d^{+/+}$ $Trp53^{+/+}$ n=206, $Rad51d^{+/+}$ $Trp53^{-/-}$ n=200, $Rad51d^{-/-}$ $Trp53^{-/-}$ n=204 spreads). Spectral karyotype analysis from two independent primary MEF cell lines per genotype was performed and scored by the

Germline Modification Laboratory at the Van Andel Research Institute (Grand Rapids, MI) using Applied Spectral Imaging software (*Rad51d*$^{+/+}$ *Trp53*$^{+/+}$ n=21, *Rad51d*$^{+/+}$ *Trp53*$^{-/-}$ n=31, *Rad51d*$^{-/-}$ *Trp53*$^{-/-}$ n=13 spreads). For sister chromatid exchange (SCE) analysis, 3x10^{6} high passage (passage > 15) MEF cells were seeded onto 150mm dishes and grown in McCoy's 5A medium supplemented with 15% FBS and antibiotics for 24 hours. Bromodeoxyuridine (Sigma) was added to a final concentration of 10μM for two cell cycles. Digitally captured images of 20 differentially stained metaphase chromosome spreads per genotype were scored. To determine the frequency of mitomycin C (MMC) induced SCEs, MMC (Novaplus) was added at 20.0 ng/ml for *Rad51d*$^{+/-}$ *Trp53*$^{+/-}$ and *Trp53*$^{-/-}$ cell lines for one cell cycle prior to harvesting. To adjust for the increased sensitivity of *Rad51d*-deficient cells to this DNA damaging agent, MMC was added at 2.0 ng/ml for *Rad51d*$^{-/-}$ *Trp53*$^{-/-}$ cell lines for one cell cycle prior to harvesting. 20 metaphase chromosome spreads per genotype were scored.

Expression and *Rad51d* cDNA cloning. 1μg of total RNA from MEF cells was used for cDNA synthesis by reverse transcription using random hexamers (Invitrogen). Presence of *Rad51d* cDNA was determined using primers 51dSS1 (5` GCGAGCGCCCAAGTGACAGA 3`) and 51dSS2 (5` GCTACCTGGGCCACCCACAA 3`), which are specific to exons one and four, and amplify a 386bp fragment. Amplification conditions for 51dSS1 and 51dSS2 were 35 rounds at 94°C, 30 sec., 57°C, 30 sec., 72°C, 1 min. Expression of *G3PDH* was used as a control (Clontech).

A full length *MmRad51d* cDNA was cloned in frame into HA-pCMV5 provided by W. Maltese (Medical College of Ohio, Toledo, OH), and the N-terminal tagged

sequence subsequently cloned into the *Nhe*I and *Bam*HI sites of pcDNA3.1 hygro+ (Invitrogen). High passage *Rad51d*$^{-/-}$ *Trp53*$^{-/-}$ MEFs were transfected using Lipofectamine Plus (Invitrogen) and selected with 250 μg/ml hygromycin B. Resistant colonies were screened by Western blotting with 0.1 μg/ml primary antibody raised against the HA epitope (12CA5) (Roche). Two independent clones expressing detectable levels of HA-RAD51D protein were tested for MMC resistance. A polyclonal population of empty vector control cells was used as a control.

DNA Damage Survival Assays. High passage cells were seeded onto 6-well dishes at 500-3500 cells per well. Cells were treated with cisplatin (Novaplus) or methylmethane sulfonate (MMS; Sigma) for one hour at the concentrations indicated. Cells were treated with MMC at the indicated concentrations for the duration of the experiment. To measure sensitivity to UV light, cells were treated using a UV Stratalinker® 2400 (Stratagene). To determine X-ray sensitivity, MEFs were treated with a Varian Clinac 1800 X-Ray machine at 400cGy/min. Following treatments, all cells were grown for 8-11 days before counting Giemsa stained colonies. Fold differences were calculated using the D37 values (21). Correction efficiency was calculated by comparing the dose of the agent that resulted in a 37% survival rate of the complemented (*Rad51d*$^{-/-}$ *Trp53*$^{-/-}$ HA-*MmRad51d*) cell lines with that of mutant (*Rad51d*$^{-/-}$ *Trp53*$^{-/-}$) and control (*Trp53*$^{-/-}$) cell lines. Briefly, correction efficiency = [(B-A) / (C-A)] x 100%, where A is the D37 value for mutant (*Rad51d*$^{-/-}$ *Trp53*$^{-/-}$) cell lines, B is the D37 value for the complemented (*Rad51d*$^{-/-}$ *Trp53*$^{-/-}$ HA-*MmRad51d*) cell lines, and C is the D37 value for the control (*Trp53*$^{-/-}$) cell lines (22).

Immunofluorescence. Cells were seeded onto glass coverslips, grown to sub-confluent levels, and, for the RAD51 foci experiments, treated with 10 Gy of irradiation. After 5 hours recovery, cells were fixed with 4% paraformaldehyde, permeablized with a 0.3% Triton X-100 solution, blocked with 5% dry milk in 1xPBS, and incubated with a 1:1200 dilution (diluted in block solution) of anti-HsRAD51 polyclonal antibody (Calbiochem) overnight at room temperature. Cells were then washed with 1xPBS and incubated with the Oregon Green 488 goat anti-rabbit IgG secondary (1:1200) (Molecular Probes) (diluted in block solution) for one hour at room temperature. Cells were washed with 1xPBS, stained with 4', 6-diamidino-2-phenylindole dihydrochloride hydrate (DAPI) (Sigma) (200ng/ml) for 10 min., coded, and mounted onto glass slides. Two methods were used to score RAD51 foci. Cells containing five or more distinct RAD51 foci were scored positive (untreated, *Rad51d*$^{+/-}$ *Trp53*$^{+/-}$ n=452, *Trp53*$^{-/-}$ n=812, *Rad51d*$^{-/-}$ *Trp53*$^{-/-}$ n=850 cells; treated with 10 Gy, *Rad51d*$^{+/-}$ *Trp53*$^{+/-}$ n=437, *Trp53*$^{-/-}$ n=756, *Rad51d*$^{-/-}$ *Trp53*$^{-/-}$ n=891 cells) and, in a separate analysis, the numbers of RAD51 foci/cell were scored (50 cells/genotype). For RAD51 protein expression analysis, whole cell MEF extracts were run on a 12% SDS PAGE gel and transferred to nitrocellulose membranes. The membranes were probed overnight with a 1:2000 dilution of anti-HsRAD51 primary and visualized by ECL detection. The membranes were stripped and re-probed with 1:2500 dilution of mouse anti-β-tubulin mAb obtained from Santa Cruz Biotechnology (sc-5274).

Centrosomes and microtubules were detected using anti-γ-tubulin-Cy3 (Sigma) and anti-α-tubulin-FITC (Sigma) antibodies following manufacturer instructions.

Primary MEFs were seeded onto glass coverslips, grown to sub-confluent levels, and fixed with methanol at -20°C. Coverslips were washed twice and rehydrated in 1xPBS 1% BSA block solution followed by incubation with a 1:600 dilution of anti-γ-tubulin-Cy3 in blocking solution for one hour at room temperature. Cells were then washed and incubated with a 1:300 dilution of anti-α-tubulin-FITC in blocking solution for 1 hour at room temperature. Cells were then washed with 1xPBS, stained with DAPI (200ng/ml) for 10 min., coded, and mounted onto glass slides. Mitotic cells from two independent primary MEF cell lines per genotype were scored (*Rad51d*$^{+/+}$ *Trp53*$^{+/+}$ n=144, *Rad51d*$^{+/-}$ *Trp53*$^{+/-}$ n=162, *Rad51d*$^{+/+}$ *Trp53*$^{-/-}$ n=248, *Rad51d*$^{-/-}$ *Trp53*$^{-/-}$ n=245 cells).

Statistical Analysis. Significance of the experimental data was determined using SPSS® version 11.5 for Windows. From Giemsa stained chromosomes and spectral karyotype analysis, the mean numbers of each chromosome abnormality/chromosome for each spread were compared using a Kruskal-Wallis test followed by pairwise comparisons using Mann-Whitney *U* tests. For SCE analysis, the mean numbers of SCEs/chromosome for each mitotic spread were compared by ANOVA. For RAD51 foci analysis, the mean percentage of foci positive cells were compared by ANOVA. To determine differences in centrosome numbers, *P* values were obtained from a 2-by-2 contingency table analyzed by the chi-square test.

RESULTS

Eliminating p53 Rescues the Lethality of *Rad51d*-Deficient Mouse Embryonic Fibroblast Cells. *Rad51d* is essential in the mouse for embryo and cell viability (15). Here, we report phenotypes of *Rad51d Trp53* double mutant embryos and embryo fibroblast cells, after performing timed matings of $Rad51d^{+/-}$ $Trp53^{+/-}$ heterozygous mice and embryo dissections. Lethality of *Rad51d*-deficient embryos was bypassed up to six days by deletion of the *Trp53* gene (Table 1) (the *Rad51d* and *Trp53* genes are 9.5cM apart on mouse chromosome 11, and for these experiments, the targeted gene disruptions were in the *cis*-formation). Mutant and wild-type embryos appear grossly similar at the midgestational stages, but by E13.5, $Rad51d^{-/-}$ $Trp53^{-/-}$ embryos are developmentally delayed and decreased in length by up to 50%. Double mutant embryos had non-consistent phenotypes of varying severity, suggestive of random mutations in developmental regulatory genes (Fig. 1*A*). Distinguishing features were blood islands, tissue necrosis, female specific exencephaly, and spinal and craniofacial malformations. To date, no $Rad51d^{-/-}$ $Trp53^{-/-}$ live pups have been identified and no increase in spontaneous tumors observed in more than 120 $Rad51d^{+/-}$ $Trp53^{+/-}$ mice up to 12 months of age.

Unlike mouse and human cells deficient for *Rad51d* (15, 17), $Rad51d^{-/-}$ $Trp53^{-/-}$ primary mouse embryonic fibroblasts (MEFs), isolated from E13.5-E14.5 embryos, were able to proliferate in culture. To confirm the cells were derived from double mutant embryos, the genotypes and absence of *Rad51d* expression were verified following several passages (Fig. 1*B*). Primary double mutant cells had delayed growth rates (Fig.

1*C*), but no senescence or crises were observed, likely due to absence of p53 (23). Growth rates of mutant cells did increase to wild-type levels upon passaging (data not shown). Flow cytometric analysis of early passage mutant cells suggested increased cell death, as high levels of sub-G1 signals are observed, and the percentage of S/G2 and hyperploid cells is consistent with genome instability (Fig. 1*D*).

Chromosome Instability in *Rad51d*-Deficient MEFs. To assay for chromosome defects, Giemsa stained metaphase spreads were scored from primary MEFs (Table 2). *Rad51d*-deficient cells had significantly increased levels of spontaneous chromatid breaks (11.3-fold) and gaps (4.7-fold), chromosome exchanges (24-fold), which likely result from inappropriate recombination, and end-to-end fusions (6.2-fold). Additionally, chromosomes at least two times the length of normal chromosomes, termed giant marker chromosomes, were observed at an increased frequency in the double mutants (9.2-fold). The frequencies of spontaneous chromosome gaps or breaks did not significantly increase in *Rad51d*-deficient cells. Consistent with the chromosome instability phenotype being directly related to loss of *Rad51d*, high passage *Rad51d*$^{-/-}$ *Trp53*$^{-/-}$ MEFs stably expressing a full-length, *HA-Rad51d* mouse cDNA had significantly lower levels of each chromosome abnormality compared with *Rad51d*$^{-/-}$ *Trp53*$^{-/-}$ cells transfected with an empty vector (data not shown).

To measure forms and frequencies of chromosomal rearrangements, spectral karyotype (SKY) analysis was performed (Fig. 2). A majority of identified abnormalities included nonreciprocal heterologous chromosome rearrangements, deletions, and fragments. The total number of chromosome aberrations in *Rad51d*$^{-/-}$ *Trp53*$^{-/-}$ cells was

increased 39.7-fold and 12.1-fold compared to homozygous wild-type and *Trp53*$^{-/-}$ cells, respectively (wild-type vs. *Trp53*$^{-/-}$ $P = 0.208$, wild-type vs. *Rad51d*$^{-/-}$ *Trp53*$^{-/-}$ $P < 0.001$, *Trp53*$^{-/-}$ vs. *Rad51d*$^{-/-}$ *Trp53*$^{-/-}$ $P < 0.001$) (Fig. 2*B*). *Rad51d*$^{-/-}$ *Trp53*$^{-/-}$ MEFs had a high frequency of detached centromeres (wild-type=0.0012 ± 0.0012, *Trp53*$^{-/-}$=0.0007 ± 0.0007, *Rad51d*$^{-/-}$ *Trp53*$^{-/-}$=0.0172 ± 0.0064 detached centromeres/chromosome) and increased levels of chromosome gain and loss (wild-type=0.762 ± 0.269, *Trp53*$^{-/-}$=0.677 ± 0.329, *Rad51d*$^{-/-}$ *Trp53*$^{-/-}$=2.69 ± 0.936 chromosomes/spread).

Decreased Levels of DNA Damage Induced Sister Chromatid Exchange and RAD51-Focus Formation in *Rad51d*-Deficient Cells. As a measure of homologous recombination, spontaneous and DNA damage induced sister chromatid exchange (SCE) frequencies were determined (Fig. 2*C*). Because RAD51D is an HR protein demonstrated to perform strand invasion (14) and *rad51d*$^{-/-}$ DT40 cells have decreased SCE levels (16), we anticipated that *Rad51d* deficient MEFs would have a reduced SCE frequency. However, spontaneous SCE levels in *Rad51d*$^{-/-}$ *Trp53*$^{-/-}$ cells were not significantly different compared with *Rad51d*$^{+/-}$ *Trp53*$^{+/-}$ controls (*Rad51d*$^{+/-}$ *Trp53*$^{+/-}$ vs. *Rad51d*$^{-/-}$ *Trp53*$^{-/-}$ $P = 0.979$). Upon treatment with MMC, SCE frequencies increased approximately 3-fold in control *Rad51d*$^{+/-}$ *Trp53*$^{+/-}$ and *Trp53*$^{-/-}$ cells, but failed to increase in *Rad51d*$^{-/-}$ *Trp53*$^{-/-}$ cells (*Rad51d*$^{-/-}$ *Trp53*$^{-/-}$: treated vs. untreated $P = 0.238$). Although treating the mutant and control cells at different concentrations of MMC complicates the interpretation of the data, these results suggest that in mouse cells, RAD51D is not essential for the rescue of stalled replication forks during DNA

replication (24), but is critical for DNA strand invasion of the homologous sister chromatid during the repair of ICLs.

To investigate whether RAD51D is necessary to recruit RAD51 to damaged DNA in mouse, MEFs were treated with X-rays and monitored for the presence of RAD51 foci (Fig. 3*A*). No significant difference was observed between non-irradiated *Rad51d*$^{+/-}$ *Trp53*$^{+/-}$ and *Trp53*$^{-/-}$ control cells ($P = 0.172$). However, there was a significant decrease in the percentage of non-irradiated *Rad51d*$^{-/-}$ *Trp53*$^{-/-}$ RAD51 foci positive cells (*Rad51d*$^{+/-}$ *Trp53*$^{+/-}$ vs. *Rad51d*$^{-/-}$ *Trp53*$^{-/-}$ $P < 0.001$, *Trp53*$^{-/-}$ vs. *Rad51d*$^{-/-}$ *Trp53*$^{-/-}$ $P < 0.001$) (Fig. 3*B*). Following treatment with 10 Gy of irradiation, the percentage of RAD51 foci positive *Rad51d*$^{-/-}$ *Trp53*$^{-/-}$ cells failed to be induced to control levels (*Rad51d*$^{+/-}$ *Trp53*$^{+/-}$ vs. *Rad51d*$^{-/-}$ *Trp53*$^{-/-}$ $P < 0.001$, *Trp53*$^{-/-}$ vs. *Rad51d*$^{-/-}$ *Trp53*$^{-/-}$ $P < 0.001$). Western analysis confirmed protein levels of RAD51 were similar among all cell lines tested (data not shown). Similar results were obtained by scoring the number of RAD51 foci per cell (data not shown). These data support that the mouse RAD51D protein is necessary for the recruitment of RAD51 to DNA damage sites following exposure of mammalian cells to X-rays.

Increased Levels of Centrosome Fragmentation in *Rad51d*-Deficient Cells. MEF cell lines deficient for *Xrcc2* and Chinese hamster ovary (CHO) cell lines deficient for *Xrcc2* or *Xrcc3* have increased frequencies of centrosome fragmentation linked to chromosome non-disjunction (25, 26), but *Rad51c* defects did not influence formation of centrosomes (27). To examine whether loss of *Rad51d* affects centrosome stability, centrosome numbers were analyzed in early passage MEFs. A significant increase in the

percentage of mitotic *Rad51d*$^{-/-}$ *Trp53*$^{-/-}$ cells having an abnormal number of centrosomes, compared to *Trp53*$^{-/-}$ cells ($P = 0.003$) and wild-type cells ($P < 0.001$), was observed (Fig. 3*C*). In contrast to the centrosome instability observed in *Xrcc2*$^{+/-}$ compared to wild-type MEFs (26), the frequency of abnormal centrosomes in *Rad51d*$^{+/-}$ *Trp53*$^{+/-}$ cells was not significantly different compared to wild-type controls (P=0.900). These data suggest that genome instability in absence of RAD51D confers centrosome fragmentation, potentially through the process of mitotic catastrophe (28).

Sensitivity to DNA Damaging Agents. The DNA repair capacity of high passage cell lines was assessed by colony survival assays following treatment with DNA damaging agents (Fig. 4). *Rad51d*$^{-/-}$ *Trp53*$^{-/-}$ cell lines were most sensitive to the DNA interstrand crosslinking agents, MMC (17.6-fold) and cisplatin (9.0-fold), and the DNA alkylating agent, methyl methanesulfonate (6.3-fold). The *Rad51d*-deficient cells were mildly sensitive to X-rays (1.5-fold), which induce DNA double-strand breaks directly and indirectly by producing increased levels of free radicals, and ultraviolet light (1.4-fold), which can induce low amounts of interstrand crosslink dimers (29) that may lead to double strand breaks during DNA replication (30). A full-length *HA-Rad51d* cDNA complemented the sensitivity phenotypes in *Rad51d Trp53*-deficient cells for each DNA damaging agent tested, with the exception of the alkylating agent, MMS. These data suggest that RAD51D plays a significant role in DNA crosslink repair and support that homologous recombination is the primary repair pathway of DNA interstrand crosslinks (4). Additionally, there is no indication for haploinsufficiency for *Rad51d*.

DISCUSSION

Homologous recombination (HR) is critical for a number of biological systems: the generation of genetic diversity, growth and development, chromosome segregation during meiosis, and repair of complex forms of DNA damage. Recently, HR defects have been associated with cancer formation and progression (1, 5, 7). The data presented here demonstrate that loss of the HR gene *Rad51d* disrupted genome integrity in mouse cells, increasing levels of chromatid breaks and gaps, aneuploidy, and chromosome rearrangements. Additionally, RAD51D was essential for repairing a number of DNA lesions, particularly interstrand crosslinks (ICLs).

Eliminating the *Trp53* gene was sufficient to increase the lifespan of *Rad51d*-deficient embryos up to 6 days and rescue cell lethality, despite such extensive chromosome instability. Previous reports also describe partial or complete bypass of embryonic lethality by a *Trp53* deficiency in mice carrying targeted disruptions in DSB repair genes (31-35). Mice deficient for the NHEJ genes, *Xrcc4* or *Lig4*, die during late embryonic development (E16.5) (36-38), and mutant phenotypes include increased neuronal cell death, impaired lymphocyte development, and growth deficiency. A *Trp53* disruption rescued the neuronal cell death phenotype conferred by each gene disruption and completely rescued embryonic lethality (31, 32). In contrast, mice deficient for the HR genes *Rad51* or *Rad51b* die during early gestation (E6.5-8.5) (33, 34, 39) and when crossed into a *Trp53*$^{-/-}$ background, embryo lethality was bypassed at least 1-2 days (33, 34). The BRCA2 protein has roles in HR and interacts directly with RAD51 through BRC motifs (40-43). BRCA2 null mouse embryos die approximately 7.5-8.5 days post-

conception (35, 44, 45) and, as observed in the *Rad51* knockout mouse, embryo lethality was bypassed approximately 1-2 days by a *Trp53*-disruption (35). These results, together with the data presented here, suggest HR proteins play a more universal and vital role than NHEJ-associated proteins during high rates of cell proliferation, such as embryogenesis.

Recently, it was demonstrated that RAD51D localizes at telomeres. Human and mouse cells lacking RAD51D have shorter telomeric DNA and an increased frequency of telomere fusions (17). In *Rad51d*-deficient mouse embryos, telomere dysfunction is likely one source for p53 mediated growth arrest (46). The increased frequency of chromosome fusions and giant marker chromosomes in *Rad51d*$^{-/-}$ *Trp53*$^{-/-}$ MEFs likely resulted, in part, from telomere fusions and chromosome translocations via the breakage-fusion-bridge cycle. Increased levels of telomere fusions were not observed in mouse fibroblasts deficient for *Xrcc2* (26). Similarly, in chromatin immunoprecipitation analyses, antibodies specific to RAD51D, but not RAD51 or the RAD51D interacting proteins RAD51C and XRCC2, pulled down significant levels of telomeric DNA (17). These data suggest that RAD51D is unique among the RAD51-family of proteins in maintaining genomic integrity by telomere protection.

Rad51d-deficient mice die at approximately 10.5 days post conception (15), compared to *Xrcc2*-deficient mice, which can survive to birth (47). Despite both mutant MEF cell lines having increased levels of genome instability, *Xrcc2*-deficient MEFs containing functional p53 could be immortalized whereas the *Rad51d*-deficient MEFs failed to proliferate (26). *Rad51d*$^{-/-}$ *Trp53*$^{-/-}$ MEFs had similar phenotypes to *Xrcc2*-

deficient MEFs and the *rad51d*-deficient chicken DT40 cell lines, including hypersensitivity to DNA crosslinking agents and ionizing radiation, failure to form radiation-induced RAD51 foci, and accumulated chromosomal breaks (16, 26). However, spontaneous SCE levels were not affected by loss of *Rad51d* in mouse cells, whereas the *Xrcc2*-deficient MEFs and *rad51d* mutant DT40 cells had a 1.4 and 1.9-fold decreased level of spontaneous SCEs, respectively. This suggests that mouse RAD51D is not essential to restart stalled DNA replication forks using the sister chromatid, but is critical for HR repair of ICLs using the sister chromatid as a replication template. Additionally, *Rad51d*-deficient MEFs and *Xrcc2*-deficient MEFs were 17.6- and 4.5-fold more sensitive to the DNA crosslinking agent MMC, respectively, suggesting a more vital role for RAD51D in repairing ICLs (26).

In this study, a full-length mouse *Rad51d* cDNA complemented the cell sensitivity phenotypes of *Rad51d*$^{-/-}$ *Trp53*$^{-/-}$ MEFs to MMC, cisplatin, X-Rays, and UV light, but failed to complement sensitivity to the alkylating agent MMS. We speculate that the engineered N-terminal epitope tag may be interfering with formation of recombinosome complexes specific to repairing MMS-associated DNA lesions (8, 48). Alternatively, variant splicing (49) or regulated expression of *Rad51d* might be necessary for HR repair of alkylation DNA damage.

The increase in spontaneous chromosomal aberrations in *Rad51d*$^{-/-}$ *Trp53*$^{-/-}$ MEFs may result from a failure to resolve HR-associated DNA intermediates as opposed to defects in strand invasion. RAD51D is part of a protein complex with RAD51B, RAD51C, and XRCC2, termed BCDX2 (50-53). Interestingly, the recent implication of

the BCDX2 complex in branch migration (54) and the direct interaction of RAD51D with the BLM helicase protein to stimulate the resolution of synthetic Holliday junctions (13), suggest a function for the RAD51 paralogs in resolving Holliday junction intermediates. We propose dual roles for RAD51D in both homologous recombination and telomere protection. For recombination, biochemical and SCE data support RAD51D is involved in strand invasion during the processing of interstrand crosslinks (14, 16) and in resolving recombination-associated DNA intermediates (13, 54). Because RAD51D is the only RAD51 paralog known to be present at telomeres (17), it may have a unique and independent role in the strand invasion step during formation of the protective T-loop structure, when the 3'single-stranded G-rich overhang invades duplex telomeric DNA and pairs with the complementary C-rich strand (55). As an alternative or additional role, RAD51D may function in concert with the BLM protein at the telomere (56) to catalyze the resolution of the Holliday junction-like T-loops, allowing for chromosome end replication.

In summary, these data demonstrate that RAD51D is critical for maintaining chromosome integrity in the mouse and for accurate repair of DSBs and ICLs. The absence of p53 is sufficient to bypass the cell lethal phenotype, permitting accumulation of complex genome rearrangements. These cell lines may help define mechanisms for tumor cells to continue proliferating even though genomic integrity has been substantially compromised. Such chromosome instability and continued cellular proliferation is observed in Fanconi anemia, Bloom syndrome, ataxia telangiectasia, and solid tumors (5). Clinical data suggest that defects in the *RAD51* paralogs contribute to the formation

of breast, uterine, skin, or bladder cancer (1, 5, 7) and telomere attrition promotes epithelial cancers in p53-deficient mice (57). The *Rad51d*-deficient MEF cell lines will be useful for structure and function analysis, determining RAD51D-dependent homologous recombination mechanisms, and may serve as a model for understanding the episodic genome instability phenotype during early carcinogenesis. Such investigations will further define the function of RAD51D in maintaining chromosome stability, which may underlie protection against tumorigenesis.

ACKNOWLEDGEMENTS

We thank the Laboratory of Germline Modification at the Van Andel Research Institute for SKY analysis and Debra Buchman for statistical advice. This manuscript is dedicated in memory of Jonathan David Judge who courageously battled cancer from age 7 to 18.

REFERENCES

1. Pierce AJ, Stark JM, Araujo FD, Moynahan ME, Berwick M, Jasin M. Double-strand breaks and tumorigenesis. Trends Cell Biol 2001;11:S52-9.
2. Mills KD, Ferguson DO, Alt FW. The role of DNA breaks in genomic instability and tumorigenesis. Immunol Rev 2003;194:77-95.
3. Pastink A, Eeken JC, Lohman PH. Genomic integrity and the repair of double-strand DNA breaks. Mutat Res 2001;480-481:37-50.
4. Dronkert ML, Kanaar R. Repair of DNA interstrand cross-links. Mutat Res 2001;486:217-47.
5. Thompson LH, Schild D. Recombinational DNA repair and human disease. Mutat Res 2002;509:49-78.
6. Slupianek A, Schmutte C, Tombline G, et al. BCR/ABL regulates mammalian RecA homologs, resulting in drug resistance. Mol Cell 2001;8:795-806.
7. Rodriguez-Lopez R, Osorio A, Ribas G, et al. The variant E233G of the RAD51D gene could be a low-penetrance allele in high-risk breast cancer families without BRCA1/2 mutations. Int J Cancer 2004;110:845-9.
8. Miller KA, Sawicka D, Barsky D, Albala JS. Domain mapping of the Rad51 paralog protein complexes. Nucleic Acids Res 2004;32:169-78.
9. Cartwright R, Dunn AM, Simpson PJ, Tambini CE, Thacker J. Isolation of novel human and mouse genes of the recA/RAD51 recombination-repair gene family. Nucleic Acids Res 1998;26:1653-9.

10. Kawabata M, Saeki K. Sequence analysis and expression of a novel mouse homolog of Escherichia coli recA gene. Biochim Biophys Acta 1998;1398:353-8.

11. Pittman DL, Weinberg LR, Schimenti JC. Identification, characterization, and genetic mapping of Rad51d, a new mouse and human RAD51/RecA-related gene. Genomics 1998;49:103-11.

12. Braybrooke JP, Spink KG, Thacker J, Hickson ID. The RAD51 Family Member, RAD51L3, is a DNA-stimulated ATPase that Forms a Complex with XRCC2. J Biol Chem 2000;275:29100-6.

13. Braybrooke JP, Li JL, Wu L, Caple F, Benson FE, Hickson ID. Functional interaction between the Bloom's syndrome helicase and the RAD51 paralog, RAD51L3 (RAD51D). J Biol Chem 2003;278:48357-66.

14. Kurumizaka H, Ikawa S, Nakada M, et al. Homologous pairing and ring and filament structure formation activities of the human Xrcc2:Rad51D complex. J Biol Chem 2002;277:14315-20.

15. Pittman DL, Schimenti JC. Midgestation lethality in mice deficient for the RecA-related gene, Rad51d/Rad51l3. Genesis 2000;26:167-73.

16. Takata M, Sasaki MS, Tachiiri S, et al. Chromosome instability and defective recombinational repair in knockout mutants of the five Rad51 paralogs. Mol Cell Biol 2001;21:2858-66.

17. Tarsounas M, Munoz P, Claas A, et al. Telomere maintenance requires the RAD51D recombination/repair protein. Cell 2004;117:337-47.

18. Jacks T, Remington L, Williams BO, et al. Tumor spectrum analysis in p53-mutant mice. Curr Biol 1994;4:1-7.

19. Sah VP, Attardi LD, Mulligan GJ, Williams BO, Bronson RT, Jacks T. A subset of p53-deficient embryos exhibit exencephaly. Nat Genet 1995;10:175-80.

20. Savage J. Classification and relationships of induced chromosomal structural changes. J Med Genet 1975;12:103-22.

21. Jones NJ, Cox R, Thacker J. Isolation and cross-sensitivity of X-ray-sensitive mutants of V79-4 hamster cells. Mutat Res 1987;183:279-86.

22. Cleaver JE. Do we know the cause of xeroderma pigmentosum? Carcinogenesis 1990;11:875-82.

23. Harvey M, Sands AT, Weiss RS, et al. In vitro growth characteristics of embryo fibroblasts isolated from p53-deficient mice. Oncogene 1993;8:2457-67.

24. Helleday T. Pathways for mitotic homologous recombination in mammalian cells. Mutat Res 2003;532:103-15.

25. Griffin CS, Simpson PJ, Wilson CR, Thacker J. Mammalian recombination-repair genes XRCC2 and XRCC3 promote correct chromosome segregation. Nat Cell Biol 2000;2:757-61.

26. Deans B, Griffin CS, O'Regan P, Jasin M, Thacker J. Homologous recombination deficiency leads to profound genetic instability in cells derived from xrcc2-knockout mice. Cancer Res 2003;63:8181-7.

27. Godthelp BC, Wiegant WW, van Duijn-Goedhart A, et al. Mammalian Rad51C contributes to DNA cross-link resistance, sister chromatid cohesion and genomic stability. Nucleic Acids Res 2002;30:2172-82.

28. Takada S, Kelkar A, Theurkauf WE. Drosophila checkpoint kinase 2 couples centrosome function and spindle assembly to genomic integrity. Cell 2003;113:87-99.

29. Nejedly K, Kittner R, Pospisilova S, Kypr J. Crosslinking of the complementary strands of DNA by UV light: dependence on the oligonucleotide composition of the UV irradiated DNA. Biochim Biophys Acta 2001;1517:365-75.

30. Dunkern TR, Kaina B. Cell proliferation and DNA breaks are involved in ultraviolet light-induced apoptosis in nucleotide excision repair-deficient Chinese hamster cells. Mol Biol Cell 2002;13:348-61.

31. Frank KM, Sharpless NE, Gao Y, et al. DNA ligase IV deficiency in mice leads to defective neurogenesis and embryonic lethality via the p53 pathway. Mol Cell 2000;5:993-1002.

32. Gao Y, Ferguson DO, Xie W, et al. Interplay of p53 and DNA-repair protein XRCC4 in tumorigenesis, genomic stability and development. Nature 2000;404:897-900.

33. Lim DS, Hasty P. A mutation in mouse rad51 results in an early embryonic lethal that is suppressed by a mutation in p53. Mol Cell Biol 1996;16:7133-43.

34. Shu Z, Smith S, Wang L, Rice MC, Kmiec EB. Disruption of muREC2/RAD51L1 in mice results in early embryonic lethality which can be partially rescued in a p53(-/-) background. Mol Cell Biol 1999;19:8686-93.

35. Ludwig T, Chapman DL, Papaioannou VE, Efstratiadis A. Targeted mutations of breast cancer susceptibility gene homologs in mice: lethal phenotypes of Brca1, Brca2, Brca1/Brca2, Brca1/p53, and Brca2/p53 nullizygous embryos. Genes Dev 1997;11:1226-41.

36. Barnes DE, Stamp G, Rosewell I, Denzel A, Lindahl T. Targeted disruption of the gene encoding DNA ligase IV leads to lethality in embryonic mice. Curr Biol 1998;8:1395-8.

37. Frank KM, Sekiguchi JM, Seidl KJ, et al. Late embryonic lethality and impaired V(D)J recombination in mice lacking DNA ligase IV. Nature 1998;396:173-7.

38. Gao Y, Sun Y, Frank KM, et al. A critical role for DNA end-joining proteins in both lymphogenesis and neurogenesis. Cell 1998;95:891-902.

39. Tsuzuki T, Fujii Y, Sakumi K, et al. Targeted disruption of the Rad51 gene leads to lethality in embryonic mice. Proc Natl Acad Sci U S A 1996;93:6236-40.

40. Wong AK, Pero R, Ormonde PA, Tavtigian SV, Bartel PL. RAD51 interacts with the evolutionarily conserved BRC motifs in the human breast cancer susceptibility gene brca2. J Biol Chem 1997;272:31941-4.

41. Chen PL, Chen CF, Chen Y, Xiao J, Sharp ZD, Lee WH. The BRC repeats in BRCA2 are critical for RAD51 binding and resistance to methyl methanesulfonate treatment. Proc Natl Acad Sci U S A 1998;95:5287-92.

42. Chen CF, Chen PL, Zhong Q, Sharp ZD, Lee WH. Expression of BRC repeats in breast cancer cells disrupts the BRCA2-Rad51 complex and leads to radiation hypersensitivity and loss of G(2)/M checkpoint control. J Biol Chem 1999;274:32931-5.

43. Pellegrini L, Yu DS, Lo T, et al. Insights into DNA recombination from the structure of a RAD51-BRCA2 complex. Nature 2002;420:287-93.

44. Sharan SK, Morimatsu M, Albrecht U, et al. Embryonic lethality and radiation hypersensitivity mediated by Rad51 in mice lacking Brca2 [see comments]. Nature 1997;386:804-10.

45. Suzuki A, de la Pompa JL, Hakem R, et al. Brca2 is required for embryonic cellular proliferation in the mouse. Genes Dev 1997;11:1242-52.

46. Chin L, Artandi SE, Shen Q, et al. p53 deficiency rescues the adverse effects of telomere loss and cooperates with telomere dysfunction to accelerate carcinogenesis. Cell 1999;97:527-38.

47. Deans B, Griffin CS, Maconochie M, Thacker J. Xrcc2 is required for genetic stability, embryonic neurogenesis and viability in mice. EMBO J 2000;19:6675-85.

48. Hays SL, Firmenich AA, Berg P. Complex formation in yeast double-strand break repair: participation of Rad51, Rad52, Rad55, and Rad57 proteins. Proc Natl Acad Sci U S A 1995;92:6925-9.

49. Kawabata M, Saeki K. Multiple alternative transcripts of the human homologue of the mouse TRAD/R51H3/RAD51D gene, a member of the rec A/RAD51 gene family. Biochem Biophys Res Commun 1999;257:156-62.

50. Liu N, Schild D, Thelen MP, Thompson LH. Involvement of Rad51C in two distinct protein complexes of Rad51 paralogs in human cells. Nucleic Acids Res 2002;30:1009-15.

51. Masson JY, Tarsounas MC, Stasiak AZ, et al. Identification and purification of two distinct complexes containing the five RAD51 paralogs. Genes Dev 2001;15:3296-307.

52. Schild D, Lio YC, Collins DW, Tsomondo T, Chen DJ. Evidence for simultaneous protein interactions between human Rad51 paralogs. J Biol Chem 2000;275:16443-9.

53. Miller KA, Yoshikawa DM, McConnell IR, Clark R, Schild D, Albala JS. RAD51C interacts with RAD51B and is central to a larger protein complex in vivo exclusive of RAD51. J Biol Chem 2002;277:8406-11.

54. Liu Y, Masson JY, Shah R, O'Regan P, West SC. RAD51C is required for Holliday junction processing in mammalian cells. Science 2004;303:243-6.

55. Griffith JD, Comeau L, Rosenfield S, et al. Mammalian telomeres end in a large duplex loop. Cell 1999;97:503-14.

56. Schawalder J, Paric E, Neff NF. Telomere and ribosomal DNA repeats are chromosomal targets of the bloom syndrome DNA helicase. BMC Cell Biol 2003;4:15.

57. Artandi SE, Chang S, Lee SL, et al. Telomere dysfunction promotes non-reciprocal translocations and epithelial cancers in mice. Nature 2000;406:641-5.

FIGURES

Figure 1

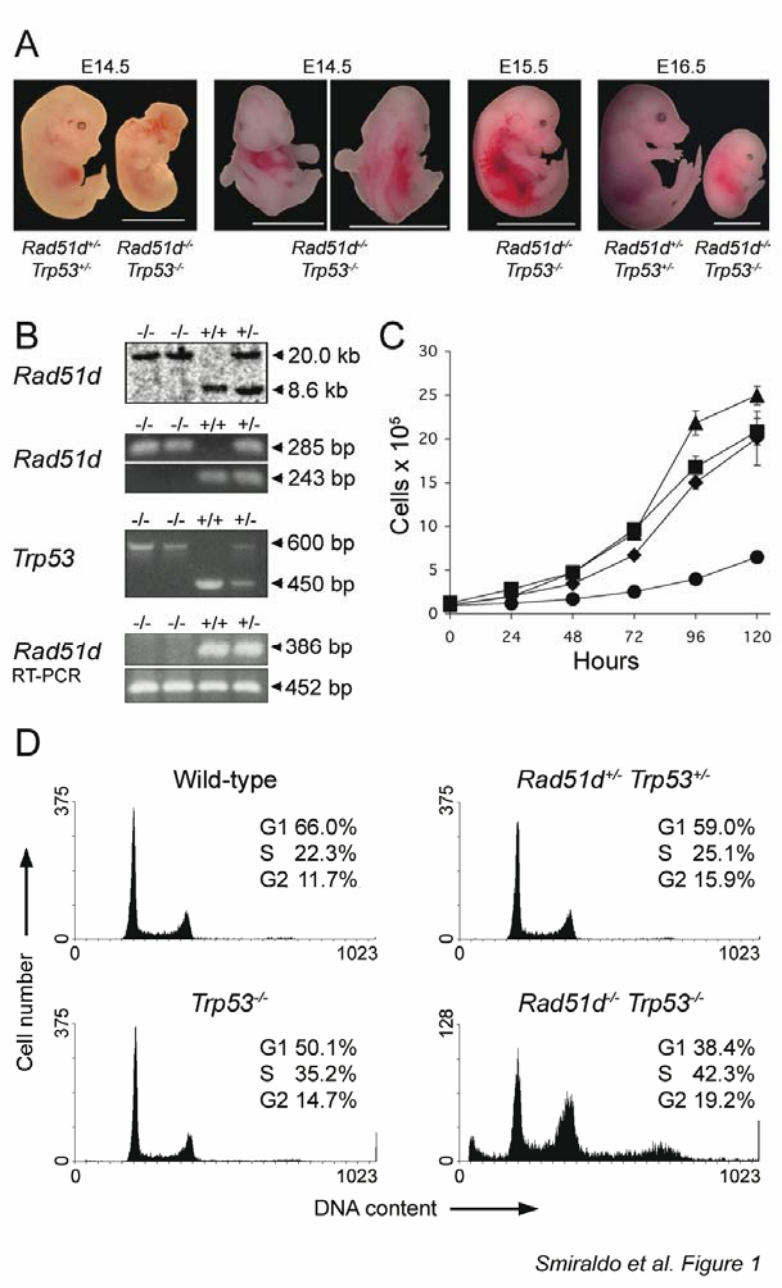

Figure 2

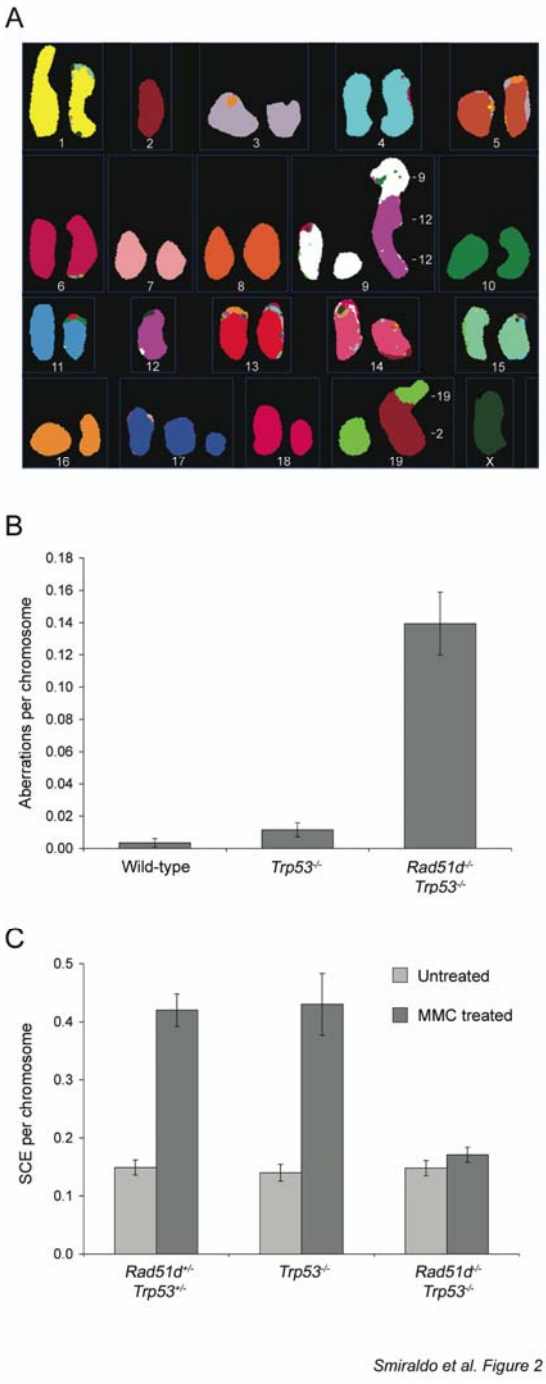
A
1
2
3
4
5
6
7
8
9
10
11
12
13
14
15
16
17
18
19
X
-9
-12
-12
-19
-2
B
Aberrations per chromosome
0.18
0.16
0.14
0.12
0.10
0.08
0.06
0.04
0.02
0.00
Wild-type
Trp53-/-
Rad51d-/-
Trp53-/-
C
SCE per chromosome
0.5
0.4
0.3
0.2
0.1
0.0
Untreated
MMC treated
Rad51d+/-
Trp53+/-
Trp53-/-
Rad51d-/-
Trp53-/-
Smiraldo et al. Figure 2

Figure 3

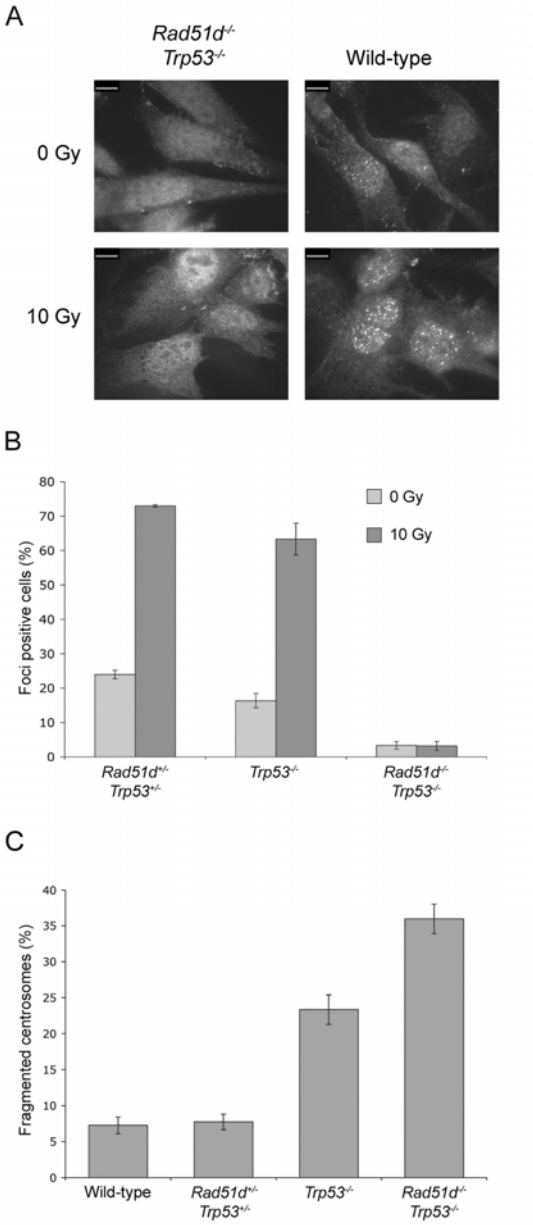

Smiraldo et al. Figure 3

Figure 4

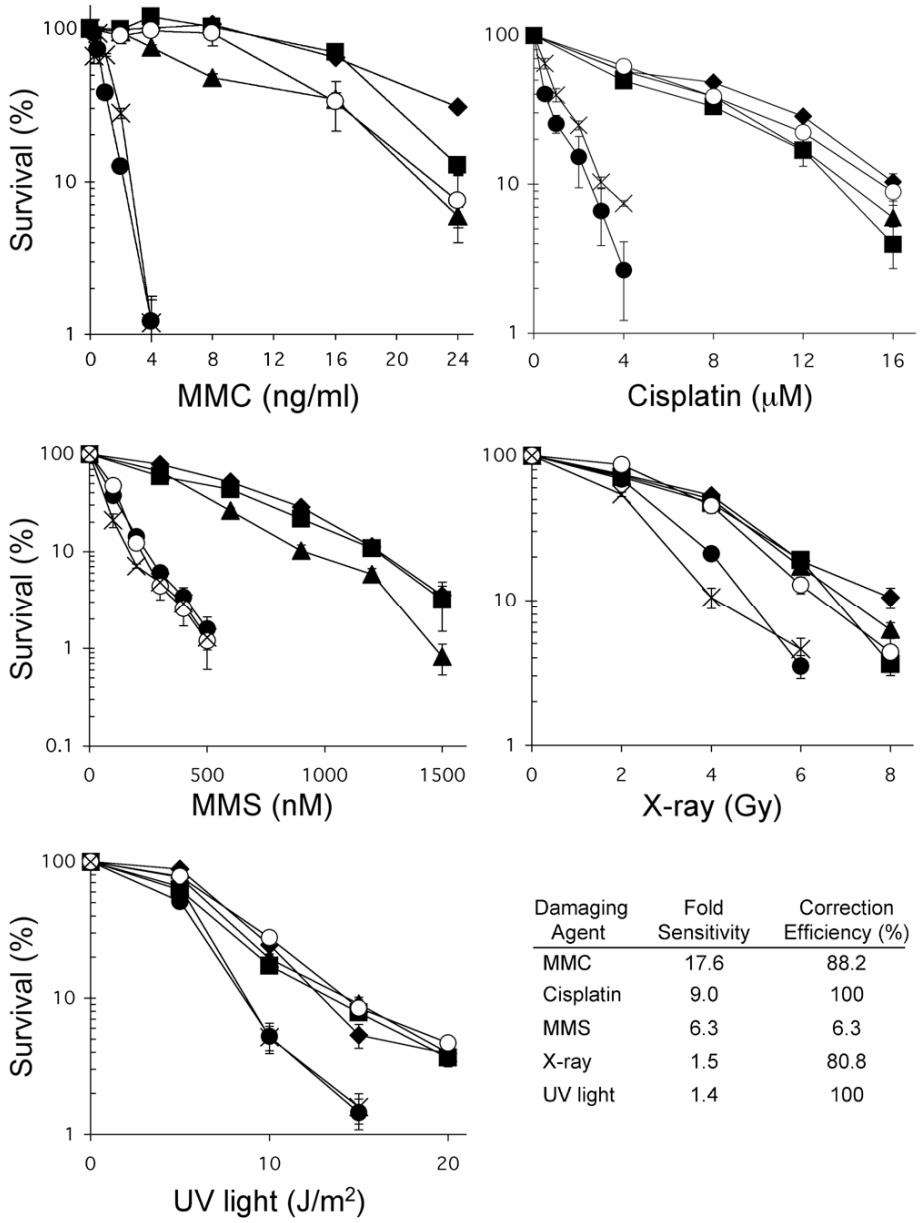

Damaging Agent	Fold Sensitivity	Correction Efficiency (%)
MMC	17.6	88.2
Cisplatin	9.0	100
MMS	6.3	6.3
X-ray	1.5	80.8
UV light	1.4	100

Smiraldo et al. Figure 4

TABLES

Table 1

Table 1 *Genotypes of progeny from Rad51d$^{+/-}$ Trp53$^{+/-}$ intercrosses*[a]

		Trp53$^{-/-}$		
Stage	Total	*Rad51d*$^{+/-}$	*Rad51d*$^{-/-}$	Resorbed Embryos
E9.5	17	1 (0.7)	4 (3.5)	1
E10.5	22	1 (0.9)	6 (4.5)	0
E11.5	19	0 (0.8)	3 (3.9)	0
E12.5	25	2 (1.1)	2 (5.1)	1
E13.5	85	2 (3.7)	14 (17.4)	12
E14.5	61	0 (2.6)	8 (12.5)	11
E15.5	35	0 (1.5)	4 (7.2)	2
E16.5	37	0 (1.6)	5 (7.6)	8
Live Pups	139	2 (6.0)	0 (28.5)[b]	Not Applicable

[a] Note that the *Rad51d* and *Trp53* genes are 9.5cM apart on mouse chromosome 11, and the targeted gene disruptions are in the *cis*-formation. The expected number of embryos for the reported genotypes is shown in parentheses.

[b] The observed number of progeny is significantly different compared to the expected number of progeny from χ^2 test, $P < 0.05$.

Table 2

Table 2 *Chromosome aberrations in primary MEF cells*

Genotype	Spreads scored	Total chromosomes	Chromatid[a]		Chromosome[a]				Giant marker chromosomes[a]
			Breaks	Gaps	Breaks	Gaps	Fusions	Exchanges	
Wild-type	206	9063	9.93	21.0	7.72	3.31	11.0	1.10	0
Trp53$^{-/-}$	200	9511	6.31	11.6	6.31	0	17.9	3.15	1.05
Rad51d$^{+/-}$ *Trp53*$^{-/-}$	204	11365	91.5*	77.4*	13.2	2.64	89.7*	51.0*	9.68*

[a]Data represent the total number of aberrations per chromosome x 10^{-4} from two independent cell lines for each genotype.
*Significant compared to wild-type and *Trp53*$^{-/-}$ cells at $P < 0.05$.

Figure Legends

Fig. 1. Characterization of *Rad51d*-deficient mouse embryos and MEF cell lines. *A*, representative normal and mutant mouse embryos. *Rad51d*$^{-/-}$ *Trp53*$^{-/-}$ embryos, from left to right, with exencephaly (E14.5), craniofacial and spinal defects (E14.5), hemorrhaging (E15.5), and decreased size (E16.5). Line represents 5 mm. *B*, for genotyping, genomic DNA from primary MEF cell lines was digested with *Bam*HI and analyzed by Southern blotting (probe B), as described (15) (20.0 kb and 8.6 kb fragments represent the disrupted and wild-type *Rad51d* alleles, respectively). *Rad51d* genotypes were further verified by PCR (15) (285 bp and 243 bp fragments identify the disrupted and wild-type alleles, respectively). The status of *Trp53* was determined by PCR genotyping (600 bp and 450 bp fragments identify the disrupted and wild-type *Trp53* alleles, respectively), and absence of *Rad51d* message confirmed by RT-PCR. Primers specific to *Rad51d* cDNA amplify a 386 bp fragment (control primers were *G3PDH*, which amplify a 452 bp fragment). *C*, growth curves of primary MEF cells, homozygous wild-type (♦), *Rad51d*$^{+/-}$ *Trp53*$^{+/-}$ (■), *Trp53*$^{-/-}$ (▲), and *Rad51d*$^{-/-}$ *Trp53*$^{-/-}$ (●). Data are from two independent cell lines per genotype (error bars = SEM). *D*, representative FACs profiles from primary cells of the indicated genotype.

Fig. 2. Chromosome instability in *Rad51d*$^{-/-}$ *Trp53*$^{-/-}$ MEFs. *A*, representative pseudocolor SKY image of a primary *Rad51d*$^{-/-}$ *Trp53*$^{-/-}$ cell [39, X, -Y, dic(3), +del(9)(B-F), der(9)t(9;12;12), +12, csb(17), del(18)A, der(19)t(2;19)(A;D)]. *B*, total chromosome aberration frequencies from primary MEF cells by SKY analysis (wild-type n=21, *Trp53*$^{-/-}$ n=31, *Rad51d*$^{-/-}$ *Trp53*$^{-/-}$ n=13 spreads), excluding chromosome gains and

losses (error bars = SEM of abnormalities/chromosome for each metaphase investigated). *C*, frequency of SCEs per chromosome in untreated and MMC treated MEFs (error bars = SEM of SCEs/chromosome).

Fig. 3. Decreased levels of RAD51 focus formation and increased levels of centrosome fragmentation in *Rad51d*$^{-/-}$ *Trp53*$^{-/-}$ MEFs. *A*, immunofluorsecence visualization of spontaneous and irradiation (10 Gy) induced RAD51 foci in wild-type and *Rad51d*$^{-/-}$ *Trp53*$^{-/-}$ MEFs. Line represents 10 μm. *B*, percentage of cells containing five or more distinct RAD51 foci (error bars = SEM of three independent experiments for each genotype). *C*, the percentage of mitotic cells with centrosome abnormalities in primary MEF cells (error bars = SEM of two independent cell lines for each genotype).

Fig. 4. Sensitivity of MEF cell lines to DNA damage. The fraction of surviving colonies following treatment with MMC, cisplatin, MMS, X-rays, and UV light are shown, homozygous wild-type (♦), *Rad51d*$^{+/-}$ *Trp53*$^{+/-}$ (■), *Trp53*$^{-/-}$ (▲), *Rad51d*$^{-/-}$ *Trp53*$^{-/-}$ (●), *Rad51d*$^{-/-}$ *Trp53*$^{-/-}$ HA-*MmRad51d* (○), and *Rad51d*$^{-/-}$ *Trp53*$^{-/-}$ vector control (X) cell lines. Data are the means from at least six independent experiments for each agent tested (error bars represent SEM). A summary of fold sensitivity of *Rad51d*$^{-/-}$ *Trp53*$^{-/-}$ cell lines to DNA damaging agents and the correction efficiency of complemented cell lines (both based upon D37 levels) is shown in the lower right.

SUPPLEMENTAL DATA FOR MANUSCRIPT 1

Experimental data presented in this section are in addition to the research article entitled "Extensive Chromosomal Instability in *Rad51d*-Deficient Mouse Cells" appearing in *Cancer Research* on March 15, 2005 (Smiraldo et al., 2005). The data included here provides a more detailed or alternative comparison of the phenotypes observed in *Rad51d*-deficient MEFs.

Cells deficient for *Rad51d* demonstrate chromosome instability, as determined by investigation of metaphase chromosome spreads (Takata et al., 2001; Tarsounas et al., 2004; Smiraldo et al., 2005). To determine the origin of giant marker chromosomes and to measure the frequencies of chromosome deletions, translocations, duplications, and end-to-end fusions, spectral karyotype (SKY) analysis was performed. In the *Rad51d*$^{-/-}$ *Trp53*$^{-/-}$ MEFs, a significant increase in chromosome deletions (wild-type vs. *Trp53*$^{-/-}$ p= 0.856, wild-type vs. *Rad51d*$^{-/-}$ *Trp53*$^{-/-}$ p≤0.001, *Rad51d*$^{-/-}$ *Trp53*$^{-/-}$ vs. *Trp53*$^{-/-}$ p p≤0.001), translocations (wild-type vs. *Trp53*$^{-/-}$ p=0.513, wild-type vs. *Rad51d*$^{-/-}$ *Trp53*$^{-/-}$ p≤0.001, *Rad51d*$^{-/-}$ *Trp53*$^{-/-}$ vs. *Trp53*$^{-/-}$ p≤0.001), end-to-end fusions (wild-type vs. *Trp53*$^{-/-}$ p=0.958, wild-type vs. *Rad51d*$^{-/-}$ *Trp53*$^{-/-}$ p=0.006, *Rad51d*$^{-/-}$ *Trp53*$^{-/-}$ vs. *Trp53*$^{-/-}$ p=0.006), and loss of centromeres (wild-type vs. *Trp53*$^{-/-}$ p=0.992, wild-type vs. *Rad51d*$^{-/-}$ *Trp53*$^{-/-}$ p≤0.001, *Rad51d*$^{-/-}$ *Trp53*$^{-/-}$ vs. *Trp53*$^{-/-}$ p≤0.001) was observed compared to homozygous wild-type or *Trp53*$^{-/-}$ control MEFs (Fig. 5). The presence of giant marker chromosomes (wild-type vs. *Trp53*$^{-/-}$ p=0.911, wild-type vs. *Rad51d*$^{-/-}$ *Trp53*$^{-/-}$ p=0.076, *Rad51d*$^{-/-}$ *Trp53*$^{-/-}$ vs. *Trp53*$^{-/-}$ p=0.117) or duplications (wild-type vs. *Trp53*$^{-/-}$ p=0.757, wild-type vs. *Rad51d*$^{-/-}$ *Trp53*$^{-/-}$ p=0.062, *Rad51d*$^{-/-}$ *Trp53*$^{-/-}$ vs. *Trp53*$^{-/-}$ p=0.009) was not

significantly different in this sample. However, when the types of chromosome abnormalities that collectively confer giant marker chromosomes, such as translocations, duplications, and end-to-end fusions, were combined, a significant increase was observed in the *Rad51d*$^{-/-}$ *Trp53*$^{-/-}$ MEFs compared to wild-type and *Trp53*$^{-/-}$ MEFs (wild-type vs. *Trp53*$^{-/-}$ $p=0.760$, wild-type vs. *Rad51d*$^{-/-}$ *Trp53*$^{-/-}$ $p\leq0.001$, *Rad51d*$^{-/-}$ *Trp53*$^{-/-}$ vs. *Trp53*$^{-/-}$ $p\leq0.001$). These data demonstrate that the giant marker chromosomes observed in *Rad51d*$^{-/-}$ *Trp53*$^{-/-}$ MEFs are likely due to a combination of chromosome translocations, duplications, and end-to-end fusions (Fig. 5).

Figure 5. Frequency of chromosome aberrations from primary MEF cells by spectral karyotype analysis

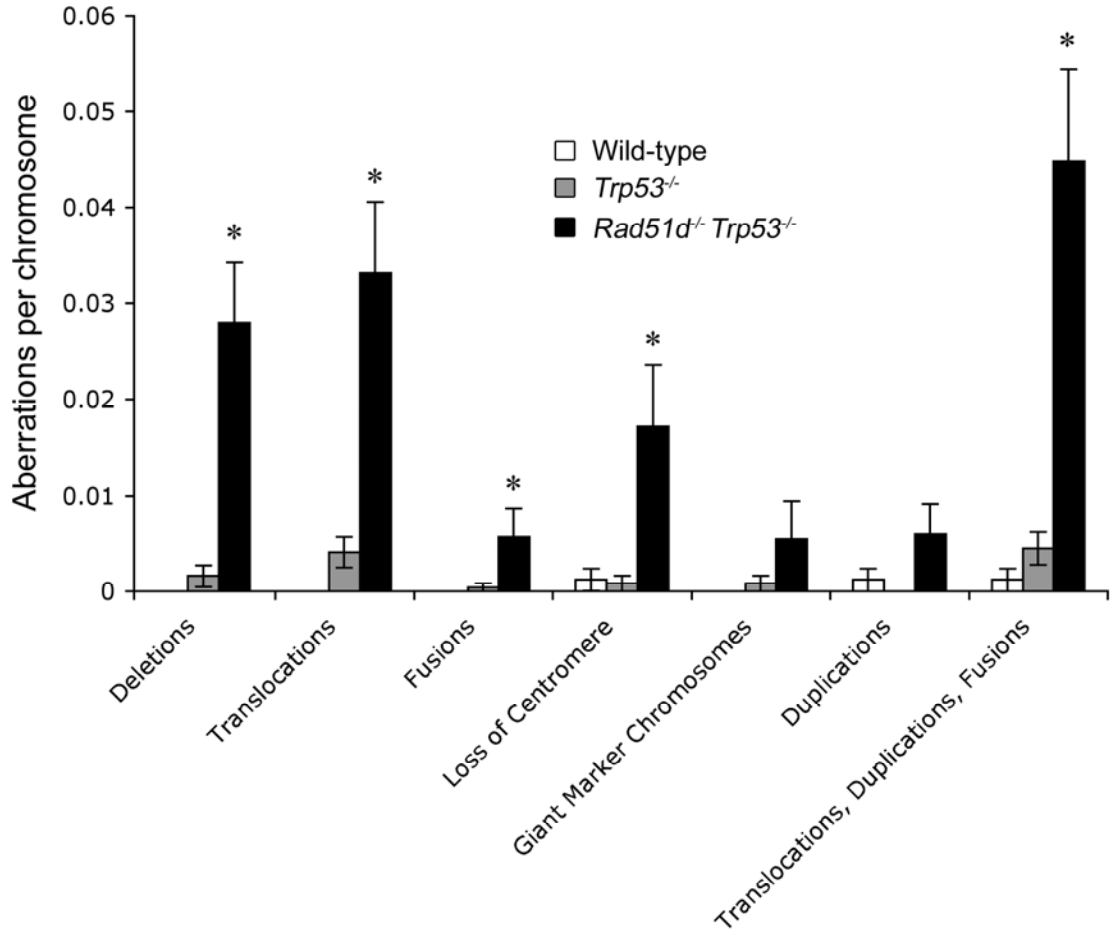

Frequency of chromosome aberrations from primary MEF cells by spectral karyotype analysis (wild-type, n = 21; *Trp53*$^{-/-}$, n = 31; *Rad51d*$^{-/-}$ *Trp53*$^{-/-}$, n = 13 spreads). *Bars*, SE of abnormalities /chromosome for each spread investigated. * indicates statistical significance of *Rad51d*$^{-/-}$ *Trp53*$^{-/-}$ vs. wild-type and *Rad51d*$^{-/-}$ *Trp53*$^{-/-}$ vs. *Trp53*$^{-/-}$ ($p < 0.05$).

To verify that the increase in the number of chromosome abnormalities observed in the *Rad51d*$^{-/-}$ *Trp53*$^{-/-}$ MEFs was due to the absence of *Rad51d*, Giemsa stained metaphase chromosome spreads were investigated from *Rad51d*$^{-/-}$ *Trp53*$^{-/-}$ MEFs that were stably transfected with full length *Rad51d* (*HA-MmRad51d*) (these cell lines were generated by Aaron M. Gruver; for cloning of full length *MmRad51d*, transfection conditions, and screening procedures, see Smiraldo et al., 2005). The number of chromosome abnormalities from two independent *Rad51d*$^{-/-}$ *Trp53*$^{-/-}$ *HA-MmRad51d* clones was compared to the number of chromosome abnormalities from a polyclonal population of *Rad51d*$^{-/-}$ *Trp53*$^{-/-}$ cells transfected with the empty vector (*Rad51d*$^{-/-}$ *Trp53*$^{-/-}$ *pcDNA3.1/Hygro*) (Table III). The *Rad51d*$^{-/-}$ *Trp53*$^{-/-}$ *HA-MmRad51d* MEFs had significantly lower levels of chromatid gaps (1.8-fold) and breaks (3.4-fold) and chromosome end-to-end fusions (2.0-fold), exchanges (3.5-fold), and giant marker chromosomes (13.2-fold) compared to the *Rad51d*$^{-/-}$ *Trp53*$^{-/-}$ *pcDNA3.1/Hygro* MEFs (for *p* values, see Table III). Consistent with data from early passage primary MEFs, no significant difference in the number of chromosome breaks or gaps was observed. Although a direct comparison between the number of chromosome abnormalities in *Rad51d*$^{+/+}$ *Trp53*$^{-/-}$ and *Rad51d*$^{-/-}$ *Trp53*$^{-/-}$ *HA-MmRad51d* was not tested, these data do demonstrate that expression of full length *HA-MmRad51d* (at least) partially complements the chromosomal instability phenotype observed in *Rad51d*$^{-/-}$ *Trp53*$^{-/-}$ MEFs.

Table III. *Chromosome aberrations in high-passage complemented MEF cells*

Genotype	Spreads scored	Total chromosomes	Chromatid[a]		Chromosome[a]				Giant marker chromosomes[a]
			Breaks	Gaps	Breaks	Gaps	Fusions	Exchanges	
Rad51d$^{-/-}$ *Trp53*$^{-/-}$ *HA-MmRad51d*[b]	204	15192	18.56	27.66	3.19	6.75	20.28	10.31	0.70
Rad51d$^{-/-}$ *Trp53*$^{-/-}$ *pcDNA3.1/Hygro*[c]	103	7582	63.31	50.12	7.91	11.87	40.89	35.61	9.23
p value (Mann-Whitney U test)			< 0.001	0.021	0.259	0.175	0.021	< 0.001	0.003

[a] Data represent the total number of aberrations per chromosome x 10^{-4}.

[b] Data are the mean values from two independent *Rad51d*$^{-/-}$ *Trp53*$^{-/-}$ *HA-MmRad51d* cell lines.

[c] The cell line, *Rad51d*$^{-/-}$ *Trp53*$^{-/-}$*pcDNA3.1/Hygro* is a polyclonal population of *Rad51d*$^{-/-}$ *Trp53*$^{-/-}$ cells stably transfected with the *pcDNA3.1/Hygro* vector.

Cells deficient for RAD51D are hypersensitive to DNA damaging agents. Consistent with previous studies, fold sensitivity to DNA damaging agents was determined by comparing D37 values (dose of the DNA damaging agent that corresponds to 37% survival) of mutant (*Rad51d*$^{-/-}$ *Trp53*$^{-/-}$) cells compared to control (*Trp53*$^{-/-}$) cells (Jones et al., 1987; Smiraldo et al., 2005). This type of analysis, however, only considers a single point along the survival curve. To take the entire survival curve into consideration, the area under the curve (integral) for each cell line tested was also calculated (see appendices) and compared. Fold differences based upon "single point" analysis (D37 and D10 values) and "area under the curve" analysis (D100-D37 and D100-D10) were calculated for each DNA damaging agent tested (Table IV). Although the conclusion that RAD51D plays a significant role in DNA repair, particularly of DNA interstrand crosslinks, remains the same, this alternative method for calculating fold sensitivity considers the survival curve rather than a single dose.

Table IV. Fold sensitivity based upon "single point" and "area under the curve" values

Damaging Agent	D37[a]	Integral D100-D37[b]	D10[c]	Integral D100-D10[d]
MMC	17.6	12.8	11.0	11.8
Cisplatin	9.0	10.7	5.9	8.0
MMS	6.3	5.8	3.3	4.7
X-ray	1.5	1.7	1.5	1.6
UV light	1.4	1.6	1.7	1.6

[a] D37, dose of the DNA damaging agent that corresponds to 37% survival
[b] Intergal D100-D37, area under the curve from D100 (untreated cells, dose of the DNA damaging agent that corresponds to 100% survival) to D37
[c] D10, dose of the DNA damaging agent that corresponds to 10% survival
[d] Integral D100-D10, area under the curve from D100 to D10

TELOMERE DYSFUNCTION IN RAD51D-DEFICIENT MOUSE EMBRYONIC FIBROBLASTS

Experimental data presented in this section were either published or in addition to the research article entitled "Telomere Maintenance Requires the RAD51D Recombination/Repair Protein" appearing in *Cell* on April 30, 2004 (Tarsounas et al., 2004). The work described in this article (ibid.) was a collaborative effort between Madalena Tarsounas, Andreas Claas, and Stephen C. West of Cancer Research UK, London Research Institute, Purificación Muñoz and María A. Blasco of the Spanish National Cancer Center, and Douglas L. Pittman and myself of the Medical University of Ohio. Experimental data presented in Figure 6 were collected by Madalena Tarsounas. I performed the studies presented in Figure 7. Chromosome spreads from primary mouse embryonic fibroblasts were made and slides sent to María A. Blasco's laboratory at the Spanish National Cancer Center for Figure 8D and Figure 9. Experimental data presented in Figure 8D are a combination of data that I collected and data collected by Purificación Muñoz. Data presented in Figure 9 were collected by Purificación Muñoz.

Telomeres are nucleoprotein structures at the ends of linear chromosomes that stabilize chromosome termini and allow cells to distinguish natural chromosome ends from DNA DSBs (Zakian, 1995; Wei and Price, 2003; de Lange, 2005). Madalena Tarsounas demonstrated that the RAD51D protein localizes at telomeres in (1) human HeLa cells (telomerase positive) by dual indirect immunofluorescence (Figure 6A) and chromatin immunoprecipitation (ChIP) analysis, (2) human WI38-VA13/2RA cells (telomerase negative) by dual indirect immunofluorescence, and (3) mouse

Figure 6. Localization of RAD51D at Telomeres

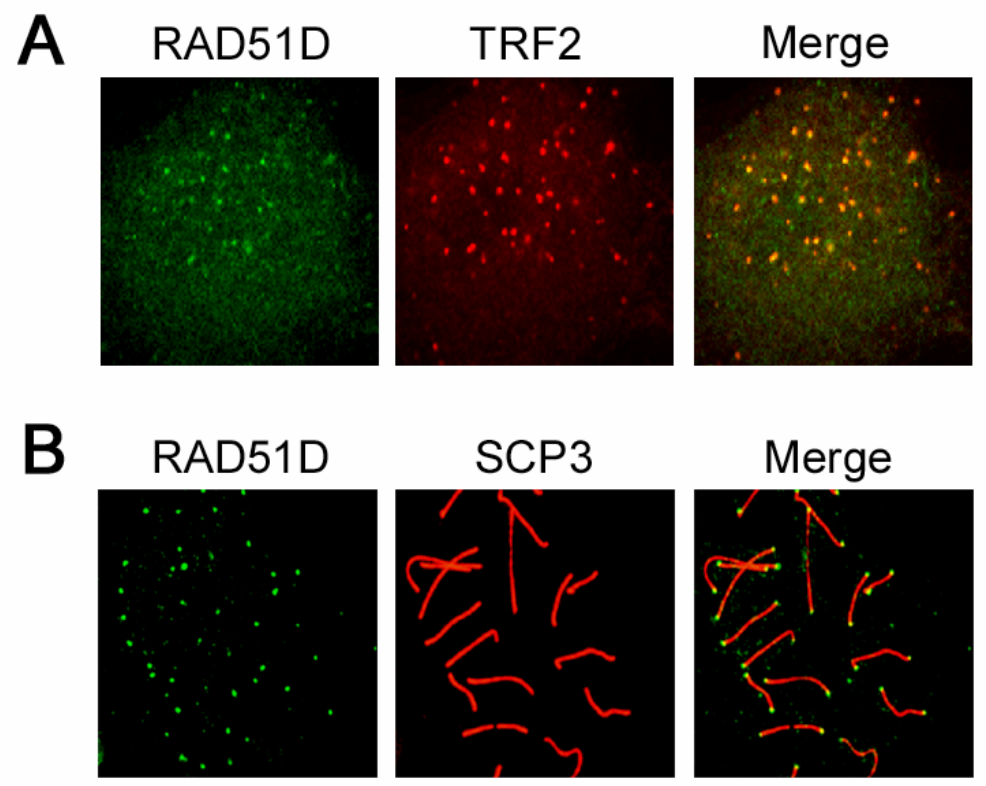

(A) Colocalization of RAD51D (green) with TRF2 (red) in HeLa cells by indirect immunofluorescence. Yellow foci in the merged image indicate colocalization. (B) Localization of RAD51D (green) at telomeres in mouse spermatocytes by indirect immunofluorescence. The SCP3 protein is part of the chromosome core and binds along the entire length of the chromosome (red). The localization of RAD51D at chromosome termini can be visualized in the merged image. Data from Tarsounas et al., 2004.

spermatocytes by dual indirect immunofluorescence (Figure 6B), electron microscopic visualization by immunogold labeling, and ChIP analysis (Tarsounas et al., 2004)

To determine if the RAD51D protein has a functional role at telomeres, Madalena Tarsounas inhibited RAD51D synthesis using siRNA in a telomerase-negative human cell line (Tarsounas et al., 2004). Upon inhibition of RAD51D synthesis, the transfected cells died within 7 days, which is consistent with the cell lethal phenotype of *Rad51d*-

deficient mouse cells (Pittman and Schimenti, 2000). To investigate if telomere dysfunction occurs in the absence of RAD51D, metaphase chromosome spreads were investigated from human cells 5 days after transfection. A 2.5-fold increase in the number of telomere-telomere fusions per metaphase was observed in cells transfected with the RAD51D-specific siRNA (*51DsiRNA*) compared to control cells that were transfected with a control GFP siRNA (*GFPsiRNA*). Additionally, a significant reduction in mean telomere length was observed in the RAD51D-depleted cells. The *51DsiRNA* transfected cells had significantly shorter telomeres (8.71 kb) compared to *GFPsiRNA* transfected cells (10.36 kb). The percentage of short telomeres (< 6 kb) was increased in *51DsiRNA* transfected cells (48.7%) compared to *GFPsiRNA* transfected controls (40.87%), and the percentage of long telomeres (> 20 kb) was decreased in *51DsiRNA* transfected cells (10.5%) compared to *GFPsiRNA* transfected controls (14.90%). Collectively, these data demonstrated that the RAD51D protein functions to protect telomeres from fusion and to maintain telomere length (Tarsounas et al., 2004). However, as noted, "any conclusions drawn from these experiments…must bear the caveat that the cells under analysis would soon become apoptotic, and it is known that apoptotic cells undergo telomere loss (Ramirez et al., 2003)" (Tarsounas et al., 2004). Therefore, to demonstrate that loss of the RAD51D protein confers telomere dysfunction, viable *Rad51d*-deficient cells had to be investigated. Because our lab is currently the only lab successful in making *Rad51d*-deficient cells that are maintainable in culture, we investigated for telomere dysfunction phenotypes in the *Rad51d*$^{-/-}$ *Trp53*$^{-/-}$ MEFs.

When telomeres are left unprotected, DNA repair mechanisms can recognize chromosome ends as DNA damage and act upon these free DNA ends to create intra- or inter-chromosome fusions, resulting in chromosome rings and dicentric chromosomes, respectively. During anaphase, when the centromeres of ring and dicentric chromosomes are pulled to opposite spindle poles, chromatin bridges, referred to as "anaphase bridges" may form. These chromatin bridges can confer chromosome non-disjunction leading to aneuploidy, or chromosome breaks leading to amplification or deletion of chromosome regions in daughter cells (Maser and DePinho, 2002). The anaphase bridge index was determined in primary homozygous wild-type, *Rad51d*$^{+/-}$ *Trp53*$^{+/-}$, *Trp53*$^{-/-}$, and *Rad51d*$^{-/-}$ *Trp53*$^{-/-}$ MEFs (two independent cell lines per genotype) (Figure 7A). The frequency of anaphase bridges was increased 9-fold in *Rad51d*$^{-/-}$ *Trp53*$^{-/-}$ MEFs compared to controls (Figure 7B), suggesting an increase in telomere fusions in the absence of RAD51D.

Figure 7. The Frequency of Anaphase Bridges in Primary MEFs

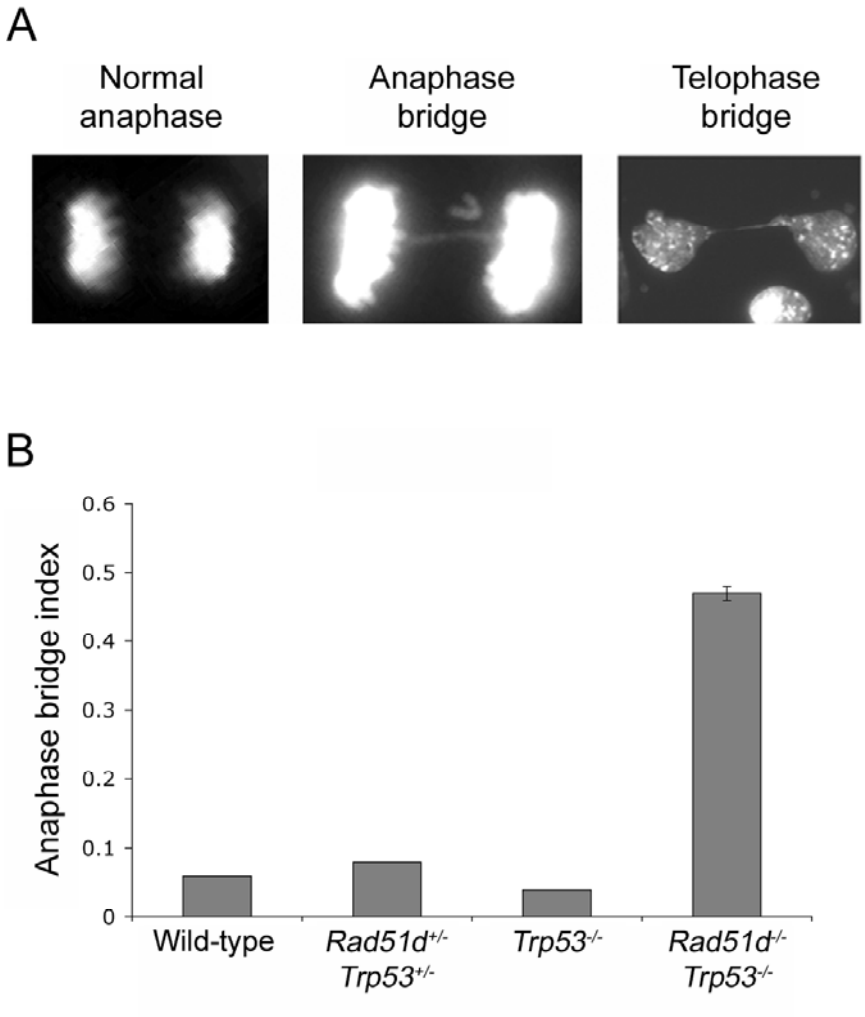

(A) representative picture of a normal anaphase cell, an anaphase cell with a bridge, and a telophase cell with a chromatin bridge. DNA of fixed cells was stained with DAPI. (B) anaphase bridge index of primary MEFs. Anaphase bridge index was calculated as the number of anaphase cells containing a chromatin bridge divided by the total number of anaphase cells investigated for each genotype. *Bars,* SE of the anaphase bridge index of two primary cell cultures for each genotype investigated.

Although an increase in the frequency of anaphase bridges was observed in the *Rad51d*-deficient MEFS, this assay does not distinguish between telomere fusions or DSBs repaired by NHEJ (for example, if two chromosomes are in close proximity and

each contains a DSB in the middle, DNA ends that were not previously linked could be joined by NHEJ resulting in a chromosomal rearrangement/dicentric chromosome). Therefore, to determine if chromosome fusions detected by the presence of anaphase bridges were a result of telomere fusions or chromosome breaks, metaphase chromosome spreads in which the telomeres were fluorescently labeled with a peptide nucleic acid probe were investigated (Figure 8A, B, C). In *Rad51d*$^{-/-}$ *Trp53*$^{-/-}$ MEFs, a 2.4-fold increase of telomere fusions and a 2.5-fold increase of end-to-end fusions were observed compared to *Trp53*$^{-/-}$ controls (Figure 8D) (experimental data in Figure 8D is a combination of data that I collected and data collected by Purificación Muñoz of María A. Blasco's laboratory at the Spanish National Cancer Center, Madrid, Spain). These data demonstrate that the RAD51D protein is essential to protect telomeres from fusion.

Figure 8. Telomere Fusions in Primary MEFs

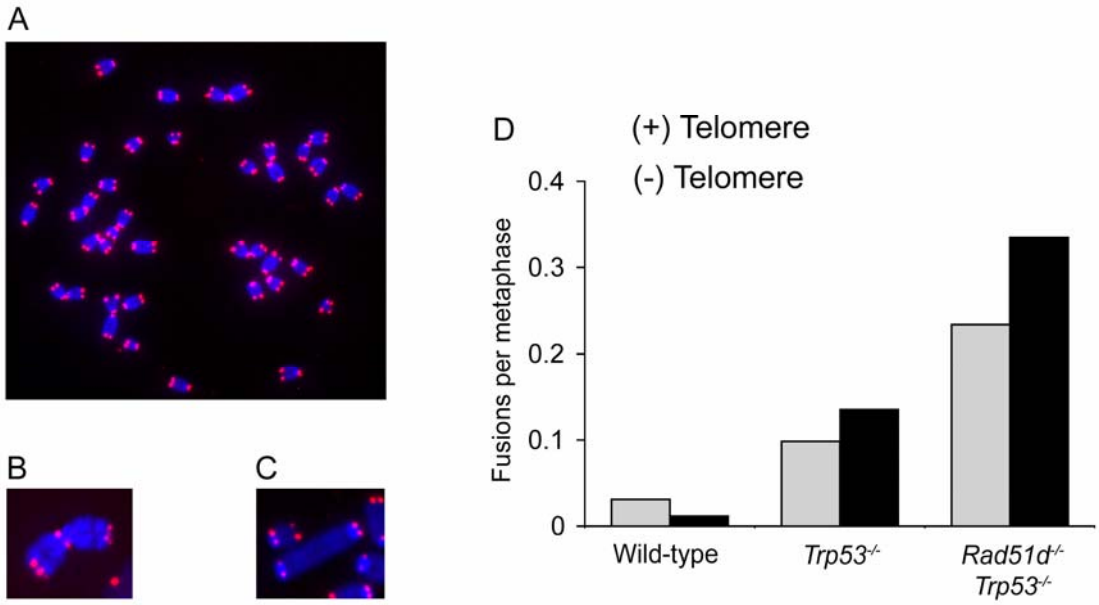

(A) metaphase chromosomes spreads were prepared and DNA stained with DAPI (blue). Telomeres were hybridized with a fluorescently labeled, telomere-specific peptide nucleic acid probe $(CCCTAA)_3$ (red). (B) example of two chromosomes fused together at the p-arm telomeres (this is an example of a "(+) telomere" fusion). (C) example of two chromosomes fused together at the q-arms with no detectable telomere at the fusion point (this is an example of a "(-) telomere" fusion). (D) frequency of chromosome fusions per metaphase that do ((+) telomere) or do not ((-) telomere) contain detectable telomeric DNA at the fusion point.

The identified end-to-end fusions may be caused by DSB repair by NHEJ (as discussed above) or by critically eroded telomeres (critically eroded telomeres would lack detectable signal by fluorescence *in situ* hybridization). Therefore, telomere lengths in primary wild-type, *Trp53*$^{-/-}$, and *Rad51d*$^{-/-}$ *Trp53*$^{-/-}$ MEFs (two independent cell lines per genotype) were investigated by quantitative fluorescence in situ hybridization (Figure 9A) (experiments performed by Purificación Muñoz of María A. Blasco's laboratory at the Spanish National Cancer Center, Madrid, Spain) (Tarsounas et al., 2004). Primary

Rad51d$^{-/-}$ *Trp53*$^{-/-}$ MEFs had significantly shorter telomeres (38.96 kb) compared to wild-type (49.28 kb) and *Trp53*$^{-/-}$ (49.23 kb) controls. The percentage of short telomeres (less than 20 kb) is increased in primary *Rad51d*$^{-/-}$ *Trp53*$^{-/-}$ MEFs (11.52%) compared to wild-type (3.53%) and *Trp53*$^{-/-}$ (3.63%) controls and the percentage of long telomeres (greater than 60 kb) is decreased in primary *Rad51d*$^{-/-}$ *Trp53*$^{-/-}$ MEFs (12.61%) compared to wild-type (23.74%) and *Trp53*$^{-/-}$ (24.02%) controls (Figure 9B). *Rad51d*$^{-/-}$ *Trp53*$^{-/-}$ MEFs also had an increased percentage of signal free (no detectable telomere signal) chromosome ends (1.53%) compared to wild-type (0.71%) and *Trp53*$^{-/-}$ (0.92%) controls. However, this increase in signal free chromosome ends does not correspond to the 2.5-fold increase of end-to-end fusions observed from metaphase spreads. These results demonstrate that the increase in end-to-end fusions was due, in part, to DSB repair by NHEJ. In summary, these data demonstrate that the RAD51D protein is required to protect telomeres from fusion and, in the absence of RAD51D, telomere attrition is accelerated.

Figure 9. Telomere Lengths in Primary MEFs by Fluorescent In Situ Hybridization.

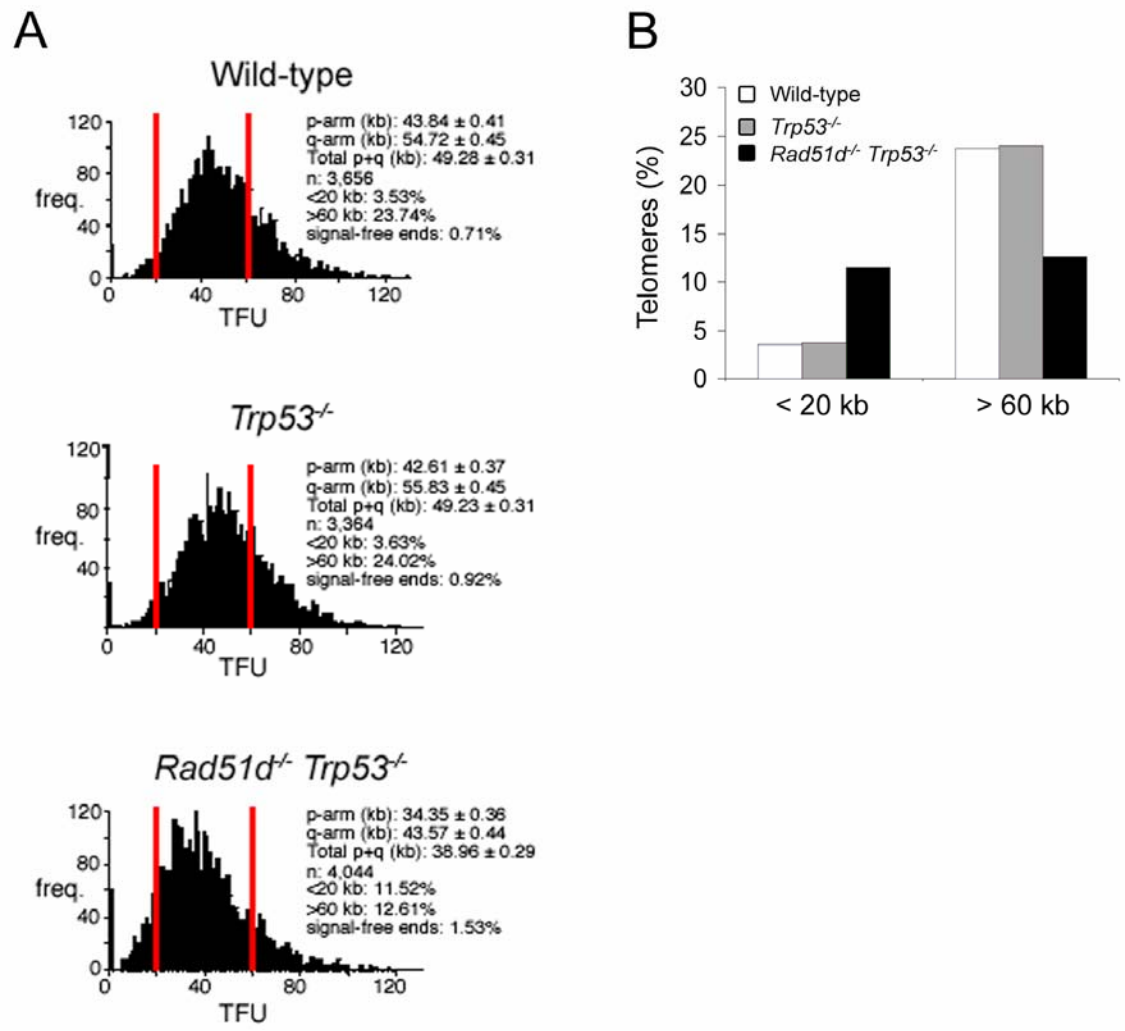

(A) histograms of telomere lengths from wild-type (n = 3656 telomeres), *Trp53*$^{-/-}$ (n = 3364 telomeres), and *Rad51d*$^{-/-}$ *Trp53*$^{-/-}$ (n = 4044 telomeres) MEFs. (B) percentage of short telomeres (<20kb) and long telomeres (>60kb) in wild-type, *Trp53*$^{-/-}$, and *Rad51d*$^{-/-}$ *Trp53*$^{-/-}$ MEFs.

Telomeres function in a number of biological systems: protection of chromosome ends from degradation and DNA repair mechanisms, meiotic chromosome segregation, and chromatin silencing (Zakian, 1995; Greider, 1996). Additionally, telomeres may play a role in preventing uncontrolled cell division because, with each round of cellular division, telomeres become shorter. If telomeres are not protected, the chromosome ends become vulnerable to enzymatic degradation and can be recognized by DNA repair pathways that fuse chromosomes together (Smogorzewska and de Lange, 2004). One model of how telomeres are protected is by forming structures termed T-loops, where the extreme terminal 3′ overhang is tucked into duplex telomeric DNA (Griffith et al., 1999; Stansel et al., 2001). The T-loop is structurally similar to a Holliday junction, suggesting that the mechanism of T-loop formation is similar to how DSBs are repaired by HR. In this conception, T-loop formation is a specialized "intra-chromosomal DNA repair event". The data presented in this Results section demonstrate that the RAD51D protein, which is required for DNA repair by HR, localizes to telomeres and has roles in telomere length maintenance and telomere protection. The RAD51D protein has DNA-stimulated ATPase activity (Braybrooke et al., 2000; Braybrooke et al., 2003) and can promote homologous pairing between single- and double-stranded DNA (Kurumizaka et al., 2002; Yokoyama et al., 2004), making it a candidate for assisting in T-loop formation.

Telomere dysfunction initiates a DNA damage response at chromosome ends, including the activation of ATM and the phosphorylation of histone H2AX (d'Adda di Fagagna et al., 2003; Takai et al., 2003; Hockemeyer et al., 2005). When the telomere-specific TRF2 protein is disrupted, high levels of telomere fusions are observed that,

presumably, occur by the NHEJ repair pathway. Consistent with NHEJ functioning at dysfunctional telomeres, telomere fusions were abrogated in *Trf2*$^{-/-}$ *DNA Ligase IV*-deficient (*Lig4*$^{-/-}$) MEFs (Celli and de Lange, 2005). It is conceivable that the preferred substrates for NHEJ are either blunt-ended DNA or DNA with complementary "sticky ends". Consistent with this proposal, the increase in telomere fusions in the absence of TRF2 or POT1 is associated with the loss of the telomeric single-stranded overhang. Therefore, the presence of the single-stranded overhang at telomeres may act as an additional barrier to prevent telomere fusions; the overhangs of different chromosome ends are not complementary to each other. Based upon this reasoning and the data demonstrating an increase in telomere fusions in the absence of RAD51D, I proposed that the single-stranded telomeric overhang would be lost in the *Rad51d*$^{-/-}$ *Trp53*$^{-/-}$ MEFs. Additionally, I proposed that the dysfunctional telomeres in the *Rad51d*$^{-/-}$ *Trp53*$^{-/-}$ MEFs would initiate a DNA repair response at chromosome ends, conferring increased levels of histone H2AX phosphorylation. The outcomes of experiments that tested these hypotheses are presented in the next chapter.

MANUSCRIPT 2

Preface:

The data presented in this Results section are an extension of the studies describing telomere dysfunction in mouse cells deficient for RAD51D (Tarsounas et al., 2004). This work is a collaborative effort with Abby J. Williams and Susan M. Bailey at the Colorado State University to characterize telomeres in the *Rad51d*-deficient MEFs. Abby J. Williams is currently using a method termed, Chromosome-Orientation Fluorescence In-Situ Hybridization (CO-FISH), which allows for distinction between telomeres that are produced by leading- vs. lagging-strand DNA synthesis, to identify any strand specificity of dysfunctional telomeres (Bailey et al., 2001). Previously, this method was used to demonstrate that, in the absence of TRF2, telomeres that were replicated by leading-strand DNA synthesis had a higher frequency of fusion compared to telomeres replicated by lagging-strand DNA synthesis, suggesting a difference in processing of chromosome ends depending on their mode of replication (Bailey et al., 2001). One fundamental difference between telomeres replicated by leading- vs. lagging-strand DNA synthesis is that, following DNA replication, the telomere replicated by leading-strand synthesis is blunt ended (because DNA polymerase can copy all the way to the end of the chromosome) and the telomere replicated by lagging-strand synthesis will have a 3´-overhang (because of the "end replication problem", see Figure 7, Introduction, pg 36). Because the formation of T-loops likely requires a 3´-overhanging tail, additional processing may be required at telomeres replicated by leading-strand synthesis (Griffith et al., 1999). The following chapter is my contribution to this

continuing collaboration. These data demonstrate that, in *Rad51d*-deficient mouse cells, telomeres have an increased frequency of being detected as DSBs and telomeres have long single-stranded, telomeric 3′ overhangs. When the data collected by Abby J. Williams and myself are combined, it will be interesting see if an association is present between leading- and lagging-strand-specific telomere dysfunction and the long telomeric overhangs.

Characterization of Dysfunctional Telomeres in the Absence of the RAD51D Protein

Phillip G. Smiraldo and Douglas L. Pittman

Department of Physiology, Medical University of Ohio, Toledo, Ohio

Financial Support: The American Cancer Society

Corresponding author:

Douglas L. Pittman

Department of Physiology

Medical University of Ohio

Block Health Science Building

3035 Arlington Avenue

Toledo, OH, 43614-5804

Telephone 419-383-4370

Fax 419-383-6168

Email: dpittman@meduohio.edu

Running Title: Telomere dysfunction in *Rad51d*-deficient mice

Keywords: telomere/homologous recombination/genetic instability/RAD51D/H2AX

Abbreviations: homologous recombination (HR), mouse embryonic fibroblast (MEF)

ABSTRACT

Telomeres are DNA-protein structures that protect chromosome ends from degradation and allow the cell to distinguish chromosome ends from damaged DNA. If telomere integrity is lost, whether due to short telomere lengths or disruption of proteins involved in telomere protection, chromosome ends can be detected as damaged DNA and fused. The RAD51D protein localizes at telomeres and, in *Rad51d*-deficient mouse embryonic fibroblasts (MEFs), an increase in telomere fusions and decreased telomere lengths were observed. Here, we demonstrate a two-fold increase in the percentage of telomere dysfunction-induced γ-H2AX foci in *Rad51d*-deficient MEFs compared to controls. However, because the majority of telomeres in the *Rad51d*-deficient MEFs do not co-localize with γ-H2AX foci, these data suggest that most telomeres are sufficiently masked from DNA repair pathways. To determine if telomere structure is altered in *Rad51d*-deficient cells, we investigated the length of the 3′ overhang using non-denatured/denatured in gel hybridization of DNA from primary mouse embryonic fibroblasts. The *Rad51d*-deficient cells had an approximate 40 percent increase in overhang signal intensity compared to controls. These results imply that RAD51D is required for the regulation of telomeric overhang length.

INTRODUCTION

Telomeres are nucleoprotein structures at the ends of linear chromosomes that stabilize chromosome termini and allow cells to distinguish natural chromosome ends from DNA double-stranded breaks (Zakian, 1995; Wei and Price, 2003; de Lange, 2005). In humans, telomeres are comprised of 5-15 kb of double stranded, tandemly repeated, hexameric sequence; the strand running 5′ to 3′ towards the chromosome end contains the sequence TTAGGG, which is referred to as the G-rich strand. The telomeric G-rich strand in eukaryotes is longer than the complementary C-rich strand, thus forming a single-stranded 3′ overhanging tail at the terminus of each telomere (Makarov et al., 1997; McElligott and Wellinger, 1997). The 3′ overhanging tail is not only the substrate for telomerase, a unique reverse transcriptase-like transferase that synthesizes telomeric repeats on chromosome ends, but it is required for the binding of telomeric single-stranded binding proteins that function to control telomerase activity and to protect chromosome ends from degradation and fusion (Wei and Price, 2003). Proteins that bind specifically to the G-rich overhang include TEBP from the hypotrichous ciliates (Gottschling and Zakian, 1986; Price, 1990), Cdc13 from budding yeast (Lin and Zakian, 1996; Nugent et al., 1996), and the POT1 proteins from fission yeast and mammals (Baumann and Cech, 2001). The human version of POT1 binds specifically to the G-rich overhang sequence 5′-TAGGGTTAG (Baumann and Cech, 2001; Loayza et al., 2004) and has been associated with telomere length regulation (Loayza and De Lange, 2003; Liu et al., 2004; Ye et al., 2004).

One model of how telomeric proteins stabilize chromosome ends is by remodeling telomere DNA into Holliday junction-like structures referred to as t-loops (Griffith et al., 1999). This protective conformation forms when the single-stranded, G-rich overhang invades duplex telomeric DNA and pairs with the complementary C-rich strand. *In vitro*, TRF2, a protein that binds duplex telomeric DNA, remodeled linear telomeres into t-loops (Griffith et al., 1999; Stansel et al., 2001). In cells, expression of a dominant-negative mutant, $TRF2^{\Delta B \Delta M}$, conferred removal of POT1 from telomeres, loss of the single-stranded 3´ overhanging tail, high levels of telomere fusions, and p53-ATM dependent apoptosis (van Steensel et al., 1998; Karlseder et al., 1999). Additionally, reduction of POT1 by RNA interference caused loss of the telomeric overhanging tail, increased levels of telomere fusions, and senescence (Veldman et al., 2004; Hockemeyer et al., 2005; Yang et al., 2005). Combined, these data exemplify the importance of maintaining telomere stability and suggest a fundamental requirement of the 3´ overhanging tail in telomere protection.

One function of the telomeres is to allow the cell to distinguish natural chromosome ends from DNA double-stranded breaks (DSBs). Although the exact mechanism of how cells detect DSBs is not known, one of the earliest events in DSB repair is the phosphorylation of the histone variant H2AX on serine 139 (Rogakou et al., 1998). At the site of the DSB, phosphorylated H2AX (termed γ-H2AX) can be visualized as nuclear foci by immunofluorescence (Rogakou et al., 1998; Rogakou et al., 1999). Nuclear γ-H2AX foci were found to localize at telomeres in cells that were senescent (d'Adda di Fagagna et al., 2003), had critically short telomeres (Hao et al.,

2004), expressed *TRF2*$^{\Delta B \Delta M}$ (Takai et al., 2003), or had reduced levels of POT1 (Hockemeyer et al., 2005), consistent with the proposal that dysfunctional telomeres can be recognized as DSBs.

Although, *in vitro*, purified TRF2 protein was able to reconfigure telomeres into t-loop structures, the reaction is not efficient, suggesting, *in vivo*, TRF2 is assisted by other factors that promote strand invasion of the single-stranded tail during the process of t-loop formation (Griffith et al., 1999; Stansel et al., 2001; de Lange, 2005). RAD51D, a protein required for DNA repair by homologous recombination, was recently demonstrated to function at the telomere (Tarsounas et al., 2004). The RAD51D protein has DNA-stimulated ATPase activity (Braybrooke et al., 2000; Braybrooke et al., 2003) and can promote homologous pairing between single- and double-stranded DNA (Kurumizaka et al., 2002; Yokoyama et al., 2004), making it a candidate for assisting in t-loop formation. Loss of RAD51D conferred extensive chromosome instability, increased telomere fusions, and accelerated telomere attrition (Takata et al., 2001; Tarsounas et al., 2004; Smiraldo et al., 2005). Studying the same *Rad51d*-deficient mouse embryonic fibroblasts investigated previously (Tarsounas et al., 2004; Smiraldo et al., 2005), we observed a two-fold increase in the number of telomere localized γ-H2AX foci in *Rad51d*-deficient MEFs. Additionally, we analyzed the relative length of the 3′ telomeric overhanging tail and demonstrate that *Rad51d*-deficient cells have an approximate 40 percent increase in overhang signal intensity compared to controls. These data suggest that, in the absence of RAD51D, most telomeres are not recognized as

DSBs and that the RAD51D protein is required for the regulation of the extreme telomere termini, specifically, the length of the 3´ telomeric overhang.

MATERIALS AND METHODS

Immunofluorescence

Primary mouse embryonic fibroblasts (MEFs) were generated as described and grown in DMEM supplemented with 7.5% fetal bovine serum, 7.5% newborn calf serum, and antibiotics (Smiraldo et al., 2005). To determine whether γ-H2AX foci localized to telomeres, primary MEFs were seeded onto sterilized glass microscope slides in 100mm plates and grown to subconfluent levels. Two independent primary wild-type, *Trp53*$^{-/-}$, and *Rad51d*$^{-/-}$ *Trp53*$^{-/-}$ MEFs were investigated. The following day, glass slides were removed from 100mm plates and washed twice in 1xPBS. Cells were fixed with 4% paraformaldehyde, permeabilized with a 0.2% Triton X-100 solution, and incubated in block solution (5% dry milk in 1xPBS) for one hour at room temperature. Slides were then incubated in a humid chamber with a 1:600 dilution (diluted in block solution) of anti-phospho-Histone H2AX (Ser139) mouse monoclonal antibody (Upstate) for 3 hours at room temperature. Slides were washed with block solution and incubated in a humid chamber with Oregon Green 488 goat anti-mouse IgG secondary (1:600; Molecular Probes; diluted in block solution) for 1 hour at room temperature. Slides were then washed in 1xPBS for five minutes four times and incubated in 4% paraformaldehyde for 20 min at room temperature, dehydrated through an ethanol series (75%, 85%, 100%) for 2 min at 4°C each, and air-dried. Slides were incubated in 70% formamide solution (70%

formamide, 0.3M NaCl, 0.3M sodium citrate) for 2 min at 75°C, dehydrated through an ethanol series (75%, 85%, 100%) for 2 min at 4°C each, and air-dried. The slides were incubated with the telomere-specific peptide nucleic acid probe Cy3-$(CCCTAA)_3$ (Applied Biosciences) in a humid chamber for 2 hours at room temperature, washed in 70% formamide solution for 15 min at 32°C, and washed with PN buffer (0.1M Na_2HPO_4, 0.05M NaH_2PO_4, 0.1% Triton X-100) for 5 min at room temperature. DNA was stained by incubating slides with 100 ng/ml DAPI for 5 min at room temperature, washed in 1xPBS for 5 min at room temperature three times, covered with a glass coverslip, sealed, and viewed. To determine if γ-H2AX foci localize at telomeres, only cells that were foci-positive were scored. We defined foci-positive cells as those that contained ≥ 5 distinct γ-H2AX foci. The percentage of γ-H2AX foci at telomeres was calculated as [(number of γ-H2AX foci at telomeres) / (number of γ-H2AX foci)] * 100% for each cell. Approximately 50 γ-H2AX foci-positive nuclei were scored for each genotype. Statistical significance of the experimental data was determined by comparing the mean number of γ-H2AX foci at telomeres per cell for each genotype using SPSS® version 11.5 for Windows by ANOVA. Follow-up comparisons were performed using the Tukey HSD post hoc test.

Plug preparation and electrophoresis

Sub-confluent cultures of primary MEFs (two independent homozygous wild-type, one *Rad51d*$^{+/-}$ *Trp53*$^{+/-}$, two independent *Trp53*$^{-/-}$, and two independent *Rad51d*$^{-/-}$ *Trp53*$^{-/-}$ cell lines) were trypsinized, counted by hemacytometer, pelleted by centrifugation for 6 min at 100 RCF, and washed in 1xPBS. After washing, cells were

pelleted by centrifugation for 5 min at 100 RCF and resuspended in 1% low melt agarose at 45°C and $1.6x10^6$ cells cast into 40 μl plug molds. After casting, plugs were incubated overnight at 37°C in a lithium dodecyl sulfate (LDS) solution containing 1% LDS, 100 mM EDTA pH 8.0, and 10 mM Tris pH 8.0 (2.5 ml per plug). Plugs were then washed twice in a 20% NDS solution containing 6.8 mM N-laurylsarcosine, 127 mM EDTA, and 2 mM Tris (two hours per wash) at room temperature (2.5 ml per plug). DNA plugs to be digested by restriction enzyme were washed twice in TE (one hour per wash) at room temperature (2 ml per plug). Plugs were then incubated twice (one hour per incubation) in 1x MboI restriction enzyme buffer at room temperature (200 μl per plug). Each plug was then incubated in 150 μl of 1x MboI buffer with 30U of MboI at 37°C overnight. The following morning, 20 additional units of MboI were added to each tube and incubated at 37°C for 4 hours. DNA plugs were prepared for electrophoresis by washing twice in TE (one hour per wash) at room temperature and once in 0.5xTBE electrophoresis running buffer (one hour) at room temperature. Plugs were loaded into a 1% agarose gel and DNA fragments separated by pulsed field gel electrophoresis (CHEF-DR II apparatus, BioRad) at 6 v/cm for 20 hours with an initial pulse time of 1second and a final pulse time of 10 seconds (chamber temperature maintained at 14°C).

In-gel hybridization

Following electrophoresis, the DNA was stained with ethidium bromide for photography and gels were dried at 50°C for 45 min in preparation for three successive hybridizations. The dried gels were prehybridized in 20 mM NaH_2PO_4, 0.1% SDS, 5x Denhardt's solution, and 5xSSC for one hour at 55°C, and first hybridized with the [γ-

^{32}P]ATP end-labeled oligonucleotide $(TTAGGG)_4$ overnight at 55°C in prehybridization solution. Gels were then washed three times for 20 min in 4xSSC at room temperature and three times for 20 min in 4xSSC, 0.1%SDS at 57°C. Gels were exposed to phoshporimager screens overnight, developed using a Typhoon 8600 Variable Mode Imager (Molecular Dynamics, Amersham Pharmacia Biotech), and radioactive signals quantified (excluding signals from DNA that remained in the wells) using ImageQuant® version 5.2 for Windows. For the second hybridization, gels were prehybridized for one hour at 55°C, hybridized with the [γ-^{32}P]ATP end-labeled oligonucleotide $(CCCTAA)_4$ overnight at 55°C, washed, and exposed to phoshporimager screens overnight, developed, and radioactive signals quantitated. Dried gels were then alkali denatured in 0.6 M NaCl, 0.2 M NaOH for one hour at room temperature, neutralized in 1.5 M NaCl, 0.5 M Tris, for one hour at room temperature, and rinsed in ddH_20 for 30 min at room temperature. For the third hybridization, gels were prehybridized for one hour at 55°C, hybridized with the [γ-^{32}P]ATP end-labeled oligonucleotide $(TTAGGG)_4$ overnight at 55°C, and washed. Gels were exposed to phoshpoimager screens for 5 hours and radioactive signals quantified. Telomere lengths were estimated from radioactive signals of alkali denatured gels hybridized with the end labeled $(TTAGGG)_4$ oligonucleotide, as described (Harley et al., 1990).

Relative G-strand overhang lengths were determined by the following equation, $RS_N / [(TL_C / TL_E) * RS_D]$, where RS_N is the radioactive signal from native gels hybridized with the $(CCCTAA)_4$ oligonucleotide, TL_C is the estimated telomere lengths of the control (homozygous wild-type) cells, TL_E is the estimated telomere lengths of the

experimental (*Rad51d*$^{+/-}$ *Trp53*$^{+/-}$, *Trp53*$^{-/-}$, or *Rad51d*$^{-/-}$ *Trp53*$^{-/-}$) cells, and RS_D is the total radioactive signal from the denatured gels hybridized with the $(TTAGGG)_4$ oligonucleotide. Statistical significance of the experimental data was determined using SPSS® version 11.5 for Windows by ANOVA. Follow-up comparisons were performed using the Tukey HSD post hoc test.

RESULTS

Telomeres protect chromosome ends from degradation and allow the cell to distinguish chromosome ends from damaged DNA. If telomere integrity is lost, chromosome ends can be detected as damaged DNA and fused. Previously, it was demonstrated that the RAD51D protein localizes to telomeres and is required for maintaining telomere stability (Tarsounas et al., 2004). Because an increase in telomere fusions and decreased telomere lengths were observed in primary *Rad51d*-deficient mouse embryonic fibroblasts (MEFs) compared to controls (Tarsounas et al., 2004), the number of γ-H2AX foci that localize to telomeres in non-damaged cells was investigated in primary homozygous wild-type, *Trp53*$^{-/-}$, and *Rad51d*$^{-/-}$ *Trp53*$^{-/-}$ MEFs (Figure 1A). When comparing the percentage of γ-H2AX foci that localize to telomeres, no significant difference was observed between homozygous wild-type and *Trp53*$^{-/-}$ MEFs ($p = 0.929$) (Figure 1B). However, a 2-fold increase in the telomeric localization of γ-H2AX foci was observed in the *Rad51d*$^{-/-}$ *Trp53*$^{-/-}$ MEFs compared to the controls. Although this increase is statistically significant (wild-type vs. *Rad51d*$^{-/-}$ *Trp53*$^{-/-}$ $p = 0.011$; *Trp53*$^{-/-}$ vs. *Rad51d*$^{-/-}$ *Trp53*$^{-/-}$ $p = 0.002$), the majority of telomeres in the *Rad51d*-deficient MEFs did

not have detectable γ-H2AX foci, suggesting that only a subset of telomeres are being recognized as DSBs in the absence of the RAD51D protein.

To determine if chromosome ends are altered in the absence of RAD51D, we determined the relative length of the single-stranded, telomeric 3′ overhangs in *Rad51d*-deficient primary mouse embryonic fibroblasts (MEFs) compared to homozygous wild-type, *Rad51d*$^{+/-}$ *Trp53*$^{+/-}$, or *Trp53*$^{-/-}$ MEFs by utilizing the non-denaturing/denaturing in-gel hybridization technique (Dionne and Wellinger, 1996; Hemann and Greider, 1999). Following electrophoresis, native gels containing non-denatured DNA were first probed with a radioactively labeled $(TTAGGG)_4$ oligonucleotide. This probe is identical to the sequence of the telomeric 3′ overhang. As expected, no signal above background was observed (data not shown) demonstrating that the DNA in the gel was not nicked or denatured during electrophoresis. The possibility that the probe failed was ruled out because the $(TTAGGG)_4$ oligonucleotide was successfully used for a subsequent hybridization (see below). The same gel was then hybridized with a radioactively labeled $(CCCTAA)_4$ oligonucleotide, which is complementary to the 3′ telomeric overhang (Figure 2A). Before electrophoresis, if the plugs containing genomic DNA were pretreated with the single-strand-specific DNA nuclease, mung bean nuclease, overhang signals were absent (data not shown), demonstrating that the radioactively labeled $(CCCTAA)_4$ oligonucleotide was binding to the single-stranded, telomeric 3′ overhangs. Although DNA from the same number of cells of each genotype was used in these experiments, the intensity of the overhang signals of *Rad51d*$^{-/-}$ *Trp53*$^{-/-}$ MEFs could not be directly compared to the intensity of the overhang signals of control cells because

Rad51d-deficient cells have a high level of hypo- and hyperploidy (Smiraldo et al., 2005). To normalize the overhang signal to DNA content, the DNA in the same gel was alkali denatured, hybridized with the radioactively labeled $(TTAGGG)_4$ oligonucleotide, and total radioactive signal quantified for each sample (Figure 2B). Differences of telomere lengths among samples were taken into consideration when calculating the relative length of the telomeric 3´ overhangs (Figure 2C) (Materials and Methods). No significant difference in the relative length of the telomeric overhangs was observed when comparing homozygous wild-type, $Rad51d^{+/-}$ $Trp53^{+/-}$, or $Trp53^{-/-}$ cells ($p > 0.05$). However, the 1.4-fold increase in relative length of the telomeric overhangs in the $Rad51d^{-/-}$ $Trp53^{-/-}$ primary MEFs was significantly different compared to controls (homozygous wild-type vs. $Rad51d^{-/-}$ $Trp53^{-/-}$ $p \leq 0.001$, $Rad51d^{+/-}$ $Trp53^{+/-}$ vs. $Rad51d^{-/-}$ $Trp53^{-/-}$ $p = 0.001$, $Rad51d^{-/-}$ $Trp53^{-/-}$ vs. $Trp53^{-/-}$ $p \leq 0.001$). These results demonstrate that RAD51D is required for proper maintenance of the telomeric 3´ overhangs in mammalian cells.

DISCUSSION

Telomeres function in a number of cellular systems: protection of chromosome ends from degradation and DNA repair mechanisms, meiotic chromosome segregation, and chromatin silencing (Zakian, 1995; Greider, 1996). Additionally, it is proposed that telomeres play a role in preventing uncontrolled cell division (Harley, 1991). With each round of cellular division, telomeres gradually shorten, which theoretically places a limitation on the number of cellular divisions a cell may undergo. If the telomeres are

left unprotected, chromosome ends become vulnerable to enzymatic degradation and can be recognized by DNA repair pathways that fuse chromosomes together (Smogorzewska and de Lange, 2004). One model for telomere protection is forming structures termed t-loops, where the extreme terminal 3′ overhang is tucked into duplex telomeric DNA (Griffith et al., 1999; Stansel et al., 2001). Thus, the stability of the 3′ overhang is critical for telomere protection. Here, we demonstrated that in primary MEFs deficient for the *Rad51d* gene, a small increase in the frequency of γ-H2AX foci at telomeres occurred and the length of the telomeric 3′ overhangs was approximately 40 percent longer compared to control cells. These data suggest that a subset of telomeres is recognized as DNA double-stranded breaks in the absence of RAD51D and that the RAD51D protein is necessary for maintaining normal telomeric 3′ overhang lengths. It is likely that the γ-H2AX foci at telomeres and the long telomeric overhangs are independent events. The 40 percent increase in the 3′ overhang signal intensity in the *Rad51d*-deficient cells suggests that the majority of telomeres have long 3′ overhangs, yet the majority of telomeres are not recognized as DNA double-stranded breaks. The possibility that γ-H2AX foci do localize at telomeres with long overhangs, however, cannot be ruled out.

The increased frequency of telomeres being recognized as DNA double-stranded breaks (as determined by presence of telomere dysfunction induced foci) is relatively small in *Rad51d*-deficient cells compared to those observed when TRF2 or POT1 is disrupted (Takai et al., 2003; Hockemeyer et al., 2005). This suggests that the majority of telomeres in the absence of RAD51D are still protected from DNA repair mechanisms,

even though long telomeric overhangs are observed. Because duplex telomere lengths are decreased in *Rad51d*-deficient cells (Tarsounas et al., 2004), we predict that the increased length of telomeric 3′ overhangs, observed in this study, is a result of enzymatic degradation of the C-rich telomeric strand as opposed to elongation of the G-rich strand by telomerase. Several lines of evidence suggest that a 5′ to 3′ nuclease activity normally occurs at telomeres. First, telomeres replicated by leading strand synthesis have a blunt end. However, single-stranded G-rich tails were observed at all chromosome ends in cells lacking detectable levels of telomerase (Dionne and Wellinger, 1996; Makarov et al., 1997; Hemann and Greider, 1999). Second, with each population doubling, it was estimated that human cells grown in culture lose approximately 100bp (Harley et al., 1990; Counter et al., 1992). This rate of shortening is faster than that expected from the end replication problem of lagging strand synthesis, suggesting that telomere processing occurs following DNA replication. Although the nuclease responsible for the degradation has not been identified, this process is tightly regulated because the C-rich telomeric strand nearly always ends with the sequence ATC-5′ (Sfeir et al., 2005). The TRF2 protein can reconfigure artificial telomeres into T-loops, *in vitro* (Griffith et al., 1999). One possible role of RAD51D at the telomere is to assist the TRF2 protein in the strand invasion step of t-loop formation following DNA replication. In this proposed model, TRF2 is not able to perform strand invasion efficiently in the absence of RAD51D. Potentially, in order for strand invasion to occur, additional enzymatic degradation of the C-rich telomeric strand is required, which would provide more substrate (single-stranded DNA) for TRF2 to form the protective t-loop. This additional

step in t-loop formation may initiate a transient DSB response (the phosphorylation of H2AX), consistent with the small increase in the frequency of γ-H2AX foci at telomeres observed in *Rad51d*-deficient MEFs. If additional 5′ to 3′ nuclease degradation of the C-rich strand occurs in the absence of RAD51D, accelerated telomere attrition would occur as a consequence when these cells divide, consistent with previous studies demonstrating decreased telomere lengths in *Rad51d*-deficient cells (Tarsounas et al., 2004).

The RAD51D protein belongs to a family of RAD51-like proteins that functions to repair damaged DNA by homologous recombination in vertebrates (Thacker, 1999; Thompson and Schild, 2002; West, 2003). When a panel of chicken DT40 knockout cell lines that had deletions of individual genes involved in homologous recombination or non-homologous end joining DNA repair pathways was investigated for telomere problems, depletion of Rad51 conferred an approximate 1.5-fold increase in the relative telomeric 3′ overhang signal intensity (Wei et al., 2002). Interestingly, this increased signal is comparable to that observed in *Rad51d*-deficient primary mouse embryonic fibroblasts. In mammalian cells, there is no evidence that RAD51 plays a role in telomere maintenance (Tarsounas et al., 2004), except in cells that can lengthen telomeres in the absence of telomerase (Yeager et al., 1999). Although telomeric overhang lengths in DT40 cells deficient *Rad51d* have not been investigated, it is possible that RAD51D, in mammals, and Rad51, in *Gallus gallus* (chicken), may perform similar functions at telomeres in a species-specific manner.

Cells that can divide indefinitely have overcome the end replication problem by initiating mechanisms that elongate telomeres. Approximately 90 percent of human

cancers maintain telomere lengths by telomerase, whereas the remaining 10 percent of human cancers are thought to use a homologous recombination mechanism (Kim et al., 1994), demonstrating a correlation between telomeres and cancer. If telomere integrity is lost, whether due to short telomere lengths or disruption of proteins involved in telomere protection, chromosome ends can be detected as damaged DNA and fused, which can initiate the breakage-fusion-bridge (BFB) cycle (for review of the BFB cycle, see (Maser and DePinho, 2002)). The BFB cycle initiates high levels of chromosome instability, conferring duplication and deletion of chromosome regions, hyper- and hypoploidy, and chromosome translocations. Because chromosome instability is associated with the initiation or progression of cancer (Thompson and Schild, 2002), it is likely that disrupting proteins involved in telomere protection will contribute to carcinogenesis. Although disrupting TRF2 confers significantly high levels of telomere problems, the *Trf2*-deficient cells enter senescence and die (even in a *Trp53*$^{-/-}$ background), demonstrating that a complete disruption of this gene is not compatible with life (Celli and de Lange, 2005). A more likely scenario is that missense, nonsense, or deletion mutations that partially disrupt normal TRF2 function will be identified and associated with cancer susceptibility. To date, however, single nucleotide polymorphisms (SNPs) have only been identified in the introns of the TRF2 gene and no susceptibility to disease has been correlated to these SNPs (search performed on 2/13/2006, http://www.ncbi.nlm.nih.gov/SNP gene ID: 7014). Alternatively, a mutation or deletion that confers a mild telomere dysfunction phenotype, like that observed in the viable *Rad51d*-deficient MEFs, will more likely be associated with cancer. Currently, a single

allelic variant of *RAD51D* has been identified (E233G), which changes the glutamic acid at position 233 to glycine, that was more highly represented in high-risk familial breast cancers not associated with defects in *BRCA1* or *BRCA2* genes (Rodriguez-Lopez et al., 2004). It has not been determined, however, if telomere or chromosome stability is affected by RAD51D-E233G.

In summary, these data demonstrate that, in the absence of RAD51D, telomeric 3′ overhang signal intensities were approximately 40 percent higher compared to controls. Previous data demonstrated that the length of the overhang is proportional the rate of telomere shortening (cells with long overhangs lose more telomeric repeats with each cell division) (Huffman et al., 2000), which gives a clue as to why overall telomere lengths are decreased in the absence of RAD51D (Tarsounas et al., 2004). Although it is not known if RAD51D acts alone or as part of a protein complex at telomeres, investigations of protein interactions among RAD51D and telomere-specific proteins will further define the role of RAD51D at chromosome ends and in maintaining genome stability.

REFERENCES

Bailey, S.M., Cornforth, M.N., Kurimasa, A., Chen, D.J., and Goodwin, E.H. (2001). Strand-specific postreplicative processing of mammalian telomeres. Science *293*, 2462-2465.

Baumann, P. and Cech, T.R. (2001). Pot1, the putative telomere end-binding protein in fission yeast and humans. Science *292*, 1171-1175.

Braybrooke, J.P., Li, J.L., Wu, L., Caple, F., Benson, F.E., and Hickson, I.D. (2003). Functional interaction between the Bloom's syndrome helicase and the RAD51 paralog, RAD51L3 (RAD51D). J Biol Chem *278*, 48357-48366.

Braybrooke, J.P., Spink, K.G., Thacker, J., and Hickson, I.D. (2000). The RAD51 Family Member, RAD51L3, is a DNA-stimulated ATPase that Forms a Complex with XRCC2. J Biol Chem *275*, 29100-29106.

Celli, G.B. and de Lange, T. (2005). DNA processing is not required for ATM-mediated telomere damage response after TRF2 deletion. Nature Cell Biology *7*, 712-718.

Counter, C.M., Avilion, A.A., LeFeuvre, C.E., Stewart, N.G., Greider, C.W., Harley, C.B., and Bacchetti, S. (1992). Telomere shortening associated with chromosome instability is arrested in immortal cells which express telomerase activity. Embo J *11*, 1921-1929.

d'Adda di Fagagna, F., Reaper, P.M., Clay-Farrace, L., Fiegler, H., Carr, P., Von Zglinicki, T., Saretzki, G., Carter, N.P., and Jackson, S.P. (2003). A DNA damage checkpoint response in telomere-initiated senescence. Nature *426*, 194-198.

de Lange, T. (2005). Shelterin: the protein complex that shapes and safeguards human telomeres. Genes Dev *19*, 2100-2110.

Dionne, I. and Wellinger, R.J. (1996). Cell cycle-regulated generation of single-stranded G-rich DNA in the absence of telomerase. Proc Natl Acad Sci U S A *93*, 13902-13907.

Gottschling, D.E. and Zakian, V.A. (1986). Telomere proteins: specific recognition and protection of the natural termini of Oxytricha macronuclear DNA. Cell *47*, 195-205.

Greider, C.W. (1996). Telomere length regulation. Annu Rev Biochem *65*, 337-365.

Griffith, J.D., Comeau, L., Rosenfield, S., Stansel, R.M., Bianchi, A., Moss, H., and de Lange, T. (1999). Mammalian telomeres end in a large duplex loop. Cell *97*, 503-514.

Hao, L.Y., Strong, M.A., and Greider, C.W. (2004). Phosphorylation of H2AX at short telomeres in T cells and fibroblasts. J Biol Chem *279*, 45148-45154.

Harley, C.B. (1991). Telomere loss: mitotic clock or genetic time bomb? Mutat Res *256*, 271-282.

Harley, C.B., Futcher, A.B., and Greider, C.W. (1990). Telomeres shorten during ageing of human fibroblasts. Nature *345*, 458-460.

Hemann, M.T. and Greider, C.W. (1999). G-strand overhangs on telomeres in telomerase-deficient mouse cells. Nucleic Acids Res *27*, 3964-3969.

Hockemeyer, D., Sfeir, A.J., Shay, J.W., Wright, W.E., and de Lange, T. (2005). POT1 protects telomeres from a transient DNA damage response and determines how human chromosomes end. Embo J *24*, 2667-2678.

Huffman, K.E., Levene, S.D., Tesmer, V.M., Shay, J.W., and Wright, W.E. (2000). Telomere shortening is proportional to the size of the G-rich telomeric 3'-overhang. J Biol Chem *275*, 19719-19722.

Karlseder, J., Broccoli, D., Dai, Y., Hardy, S., and de Lange, T. (1999). p53- and ATM-dependent apoptosis induced by telomeres lacking TRF2. Science *283*, 1321-1325.

Kim, N.W., Piatyszek, M.A., Prowse, K.R., Harley, C.B., West, M.D., Ho, P.L., Coviello, G.M., Wright, W.E., Weinrich, S.L., and Shay, J.W. (1994). Specific association of human telomerase activity with immortal cells and cancer. Science *266*, 2011-2015.

Kurumizaka, H., Ikawa, S., Nakada, M., Enomoto, R., Kagawa, W., Kinebuchi, T., Yamazoe, M., Yokoyama, S., and Shibata, T. (2002). Homologous pairing and ring and filament structure formation activities of the human Xrcc2:Rad51D complex. J Biol Chem *277*, 14315-14320.

Lin, J.J. and Zakian, V.A. (1996). The Saccharomyces CDC13 protein is a single-strand TG1-3 telomeric DNA-binding protein in vitro that affects telomere behavior in vivo. Proc Natl Acad Sci U S A *93*, 13760-13765.

Liu, D., Safari, A., O'Connor, M.S., Chan, D.W., Laegeler, A., Qin, J., and Songyang, Z. (2004). PTOP interacts with POT1 and regulates its localization to telomeres. Nature Cell Biology *6*, 673-680.

Loayza, D. and de Lange, T. (2003). POT1 as a terminal transducer of TRF1 telomere length control. Nature *423*, 1013-1018.

Loayza, D., Parsons, H., Donigian, J., Hoke, K., and de Lange, T. (2004). DNA binding features of human POT1: a nonamer 5'-TAGGGTTAG-3' minimal binding site, sequence specificity, and internal binding to multimeric sites. J Biol Chem *279*, 13241-13248.

Makarov, V.L., Hirose, Y., and Langmore, J.P. (1997). Long G tails at both ends of human chromosomes suggest a C strand degradation mechanism for telomere shortening. Cell *88*, 657-666.

Maser, R.S. and DePinho, R.A. (2002). Connecting chromosomes, crisis, and cancer. Science *297*, 565-569.

McElligott, R. and Wellinger, R.J. (1997). The terminal DNA structure of mammalian chromosomes. Embo J *16*, 3705-3714.

Nugent, C.I., Hughes, T.R., Lue, N.F., and Lundblad, V. (1996). Cdc13p: a single-strand telomeric DNA-binding protein with a dual role in yeast telomere maintenance. Science *274*, 249-252.

Price, C.M. (1990). Telomere structure in Euplotes crassus: characterization of DNA-protein interactions and isolation of a telomere-binding protein. Mol Cell Biol *10*, 3421-3431.

Rodriguez-Lopez, R., Osorio, A., Ribas, G., Pollan, M., Sanchez-Pulido, L., de la Hoya, M., Ruibal, A., Zamora, P., Arias, J.I., Salazar, R., Vega, A., Martinez, J.I., Esteban-Cardenosa, E., Alonso, C., Leton, R., Urioste Azcorra, M., Miner, C., Armengod, M.E., Carracedo, A., Gonzalez-Sarmiento, R., Caldes, T., Diez, O., and Benitez, J. (2004). The variant E233G of the RAD51D gene could be a low-penetrance allele in high-risk breast cancer families without BRCA1/2 mutations. Int J Cancer *110*, 845-849.

Rogakou, E.P., Boon, C., Redon, C., and Bonner, W.M. (1999). Megabase chromatin domains involved in DNA double-strand breaks in vivo. J Cell Biol *146*, 905-916.

Rogakou, E.P., Pilch, D.R., Orr, A.H., Ivanova, V.S., and Bonner, W.M. (1998). DNA double-stranded breaks induce histone H2AX phosphorylation on serine 139. J Biol Chem *273*, 5858-5868.

Sfeir, A.J., Chai, W., Shay, J.W., and Wright, W.E. (2005). Telomere-end processing the terminal nucleotides of human chromosomes. Mol Cell *18*, 131-138.

Smiraldo, P.G., Gruver, A.M., Osborn, J.C., and Pittman, D.L. (2005). Extensive chromosomal instability in Rad51d-deficient mouse cells. Cancer Res *65*, 2089-2096.

Smogorzewska, A. and de Lange, T. (2004). Regulation of telomerase by telomeric proteins. Annu Rev Biochem *73*, 177-208.

Stansel, R.M., de Lange, T., and Griffith, J.D. (2001). T-loop assembly in vitro involves binding of TRF2 near the 3' telomeric overhang. Embo J *20*, 5532-5540.

Takai, H., Smogorzewska, A., and de Lange, T. (2003). DNA damage foci at dysfunctional telomeres. Curr Biol *13*, 1549-1556.

Takata, M., Sasaki, M.S., Tachiiri, S., Fukushima, T., Sonoda, E., Schild, D., Thompson, L.H., and Takeda, S. (2001). Chromosome instability and defective recombinational repair in knockout mutants of the five Rad51 paralogs. Mol Cell Biol *21*, 2858-2866.

Tarsounas, M., Munoz, P., Claas, A., Smiraldo, P.G., Pittman, D.L., Blasco, M.A., and West, S.C. (2004). Telomere maintenance requires the RAD51D recombination/repair protein. Cell *117*, 337-347.

Thacker, J. (1999). A surfeit of RAD51-like genes? Trends Genet *15*, 166-168.

Thompson, L.H. and Schild, D. (2002). Recombinational DNA repair and human disease. Mutat Res *509*, 49-78.

van Steensel, B., Smogorzewska, A., and de Lange, T. (1998). TRF2 protects human telomeres from end-to-end fusions. Cell *92*, 401-413.

Veldman, T., Etheridge, K.T., and Counter, C.M. (2004). Loss of hPot1 function leads to telomere instability and a cut-like phenotype. Curr Biol *14*, 2264-2270.

Wei, C. and Price, M. (2003). Protecting the terminus: t-loops and telomere end-binding proteins. Cell Mol Life Sci *60*, 2283-2294.

Wei, C., Skopp, R., Takata, M., Takeda, S., and Price, C.M. (2002). Effects of double-strand break repair proteins on vertebrate telomere structure. Nucleic Acids Res *30*, 2862-2870.

West, S.C. (2003). Molecular views of recombination proteins and their control. Nature Reviews. Molecular Cell Biology *4*, 435-445.

Yang, Q., Zheng, Y.L., and Harris, C.C. (2005). POT1 and TRF2 cooperate to maintain telomeric integrity. Mol Cell Biol *25*, 1070-1080.

Ye, J.Z., Hockemeyer, D., Krutchinsky, A.N., Loayza, D., Hooper, S.M., Chait, B.T., and de Lange, T. (2004). POT1-interacting protein PIP1: a telomere length regulator that recruits POT1 to the TIN2/TRF1 complex. Genes Dev *18*, 1649-1654.

Yeager, T.R., Neumann, A.A., Englezou, A., Huschtscha, L.I., Noble, J.R., and Reddel, R.R. (1999). Telomerase-negative immortalized human cells contain a novel type of promyelocytic leukemia (PML) body. Cancer Res *59*, 4175-4179.

Yokoyama, H., Sarai, N., Kagawa, W., Enomoto, R., Shibata, T., Kurumizaka, H., and Yokoyama, S. (2004). Preferential binding to branched DNA strands and strand-annealing activity of the human Rad51B, Rad51C, Rad51D and Xrcc2 protein complex. Nucleic Acids Res *32*, 2556-2565.

Zakian, V.A. (1995). Telomeres: beginning to understand the end. Science *270*, 1601-1607.

Figure 1. Localization of γ-H2AX foci at telomeres in primary mouse embryonic fibroblasts.

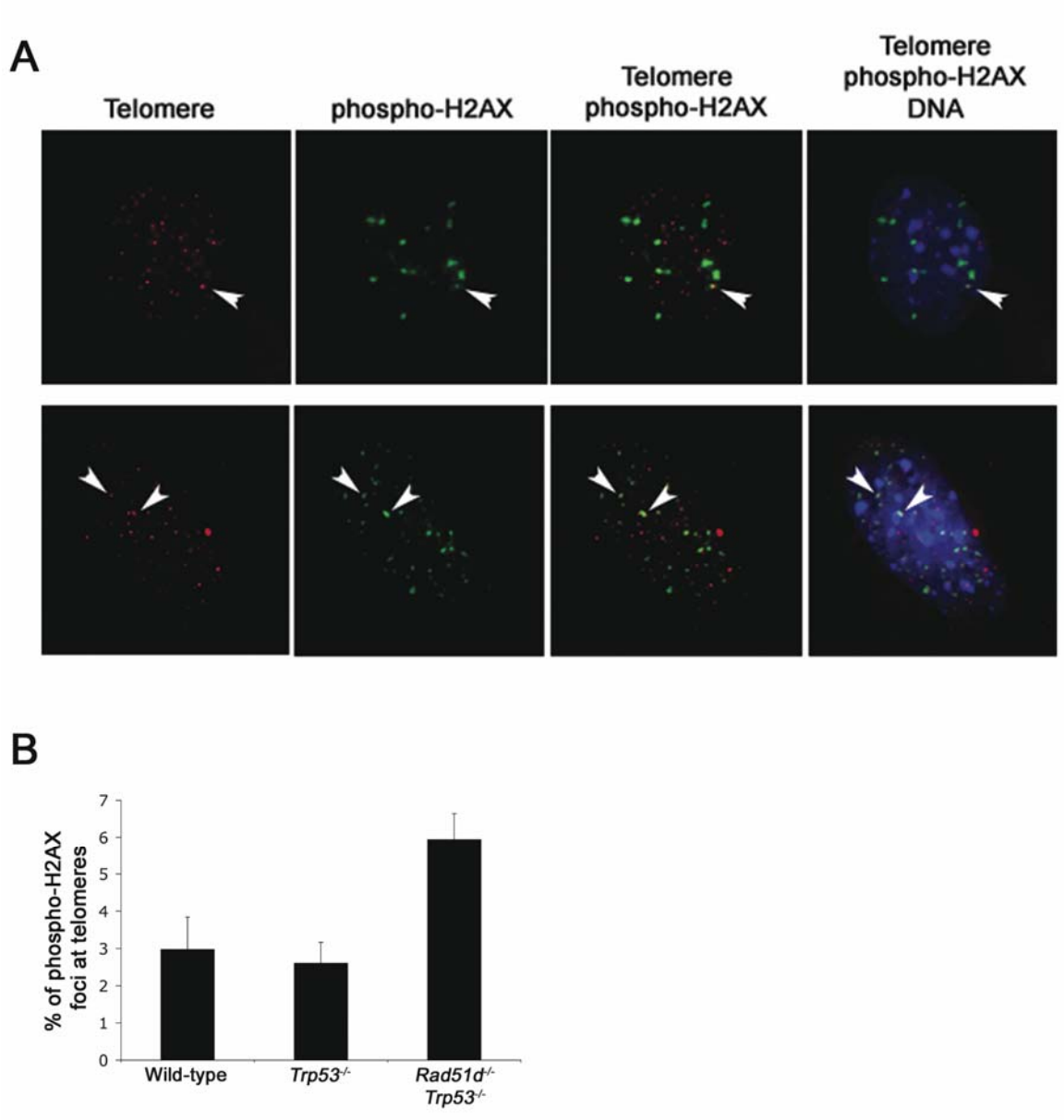

Figure 2. Comparison of relative telomeric 3´ overhang lengths in primary mouse embryonic fibroblasts.

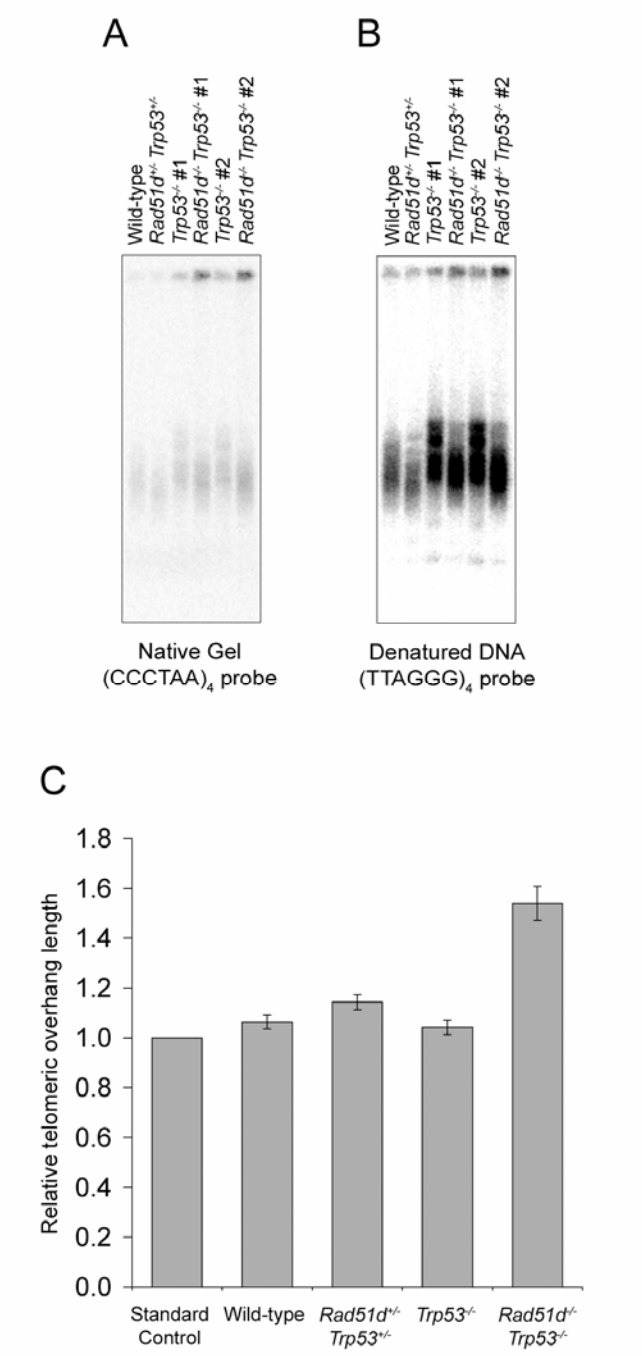

FIGURE LEGENDS

Figure 1. Localization of γ-H2AX foci at telomeres in primary mouse embryonic fibroblasts (MEFs). (**A**) Representative images of primary MEFs. Telomeric DNA is labeled with a fluorescently labeled peptide nucleic acid probe (red), γ-H2AX is immunolabeled by indirect immunofluorescence (green), and DNA is stained with DAPI (blue). White arrowheads demonstrate the localization of γ-H2AX foci at telomeres. (**B**) Percentage of γ-H2AX foci at telomeres in homozygous wild-type (n = 51 nuclei scored), *Trp53*$^{-/-}$ (n = 58 nuclei scored), and *Rad51d*$^{-/-}$ *Trp53*$^{-/-}$ (n = 59 nuclei scored) cells.

Figure 2. Comparison of relative telomeric 3′ overhang lengths in primary mouse embryonic fibroblasts (MEFs). Radioactively labeled oligonucleotide in-gel hybridizations to MboI digested genomic DNA isolated from primary MEFs. (**A**) Native gel hybridized with $(CCCTAA)_4$ probe. (**B**) The DNA from the same gel was alkali denatured and hybridized with $(TTAGGG)_4$ probe. (**C**) Relative G-strand overhang lengths were determined by the following equation, $RS_N / [(TL_C / TL_E) * RS_D]$, where RS_N is the radioactive signal from native gels hybridized with the $(CCCTAA)_4$ oligonucleotide, TL_C is the estimated telomere lengths of the control (homozygous wild-type) cells, TL_E is the estimated telomere lengths of the experimental (*Rad51d*$^{+/-}$ *Trp53*$^{+/-}$, *Trp53*$^{-/-}$, or *Rad51d*$^{-/-}$ *Trp53*$^{-/-}$) cells, and RS_D is the total radioactive signal from the denatured gels hybridized with the $(TTAGGG)_4$ oligonucleotide. Telomere lengths were estimated from radioactive signals of alkali denatured gels hybridized with the

$(TTAGGG)_4$ oligonucleotide, as described (Harley et al., 1990). Error bars are the standard error of the mean from at least three independent experiment.

MANUSCRIPT 3

Preface:

The ideas for the work presented in this section came about from weekly lab meetings among the faculty and students in the Department of Physiology, Medical University of Ohio. This work was a collaborative effort with Lauren Gerard Koch and Steven L. Britton (both of whom are currently faculty at the University of Michigan). During these meetings, it was evident that rats selectively bred based upon low aerobic running capacity were emerging as models that display multiple cardiovascular and metabolic disease risks when young adults (Wisloff et al., 2005). Around the same time, reports from human studies described a correlation between patients with short telomere lengths and the development of age-related diseases; however, the cause-effect relationship was not known. Because age-related diseases are genetically complex and determined by the expression of combinations of allelic variants sensitive to a given environment (Mootha et al., 2003), animal models to test their relationship with telomere lengths are limiting. With the availability of low and high capacity running rats as genetically complex disease models, we were able to test the hypothesis that rats selectively bred based upon their low aerobic running capacity have shorter telomeres compared to rats selectively bred based upon their high aerobic running capacity. As an initial test, I measured telomere lengths in adult rat fibroblasts (ARFs), which were generated by Charbel F. Maskiny, Medical University of Ohio. Interestingly, telomere lengths in the ARFs derived from the low capacity running rats (LCRs) (43.86 ± 0.44 kb) were significantly longer than telomere lengths in the ARFs derived from high capacity

running rats (42.06 ± 0.31 kb) ($p = 0.016$). Caution was taken about drawing conclusions from these data because of the concern that the telomere lengths in cells that have been extensively passaged in culture may not represent the telomere lengths in the rats. Therefore, telomere lengths were measured from heart, kidney, liver, spleen, skeletal muscle, and white blood cells from LCR and HCR rats. Lori Gilligan and Ashley Duvall of the University of Michigan extracted whole blood samples from the rats and the samples transferred to me for processing. This work, presented below, will be submitted for publication.

Telomere Lengths are Independent of Disease Risks and Age in Rat Models of Low and High Aerobic Capacity

Phillip G. Smiraldo[1], Lauren Gerard Koch[2], Steven L. Britton[2], and Douglas L. Pittman[1]

[1] Department of Physiology, Pharmacology, Metabolism, and Cardiovascular Sciences, Medical University of Ohio, 3035 Arlington Avenue, Toledo, Ohio 43614-5804, USA.

[2] Department of Physical Medicine and Rehabilitation, University of Michigan, 1500 East Medical Center Drive, Ann Arbor, Michigan 48109-0718, USA.

Financial Support: NIH grants HL 64270 and RR 17718

Corresponding Author:

Phillip G. Smiraldo

Department of Physiology, Pharmacology, Metabolism, and Cardiovascular Sciences

Medical University of Ohio

Block Health Science Building

3035 Arlington Avenue

Toledo, OH, 43614-5804

Telephone 419-383-4102

Fax 419-383-6168

Email: psmiraldo@meduohio.edu

Running Title: Telomere lengths in high and low capacity running rats

Keywords: telomere/aerobic running capacity/aging

Abbreviations: high capacity running (HCR), low capacity running (LCR), telomere restriction fragment (TRF)

Abstract

In somatic cells, telomeres, the DNA protein complexes at the ends of chromosomes, shorten with each cellular division. This progressive decrease in telomere length is proposed to be a mechanism for cellular aging. In human studies, decreased telomere lengths have been correlated to the development of age-related diseases; however, the cause-effect relationship is not known. Rats selectively bred based upon their low aerobic running capacity have emerged as models that display multiple cardiovascular and metabolic disease risks when young adults. To determine if the disease phenotype of low capacity running (LCR) rats is associated with decreased telomere lengths, we compared the lengths of telomere restriction fragments from heart, kidney, liver, spleen, and skeletal muscle tissues isolated from high capacity running (HCR) and LCR young adult rats, and from white blood cells derived from young adult, middle-aged, and old HCR and LCR rats. Mean telomere length from liver tissue was significantly shorter in LCR relative to HCR rats, but telomeres were not critically eroded. Telomeres from heart, kidney, spleen, or skeletal muscle did not differ in length between the LCR and HCR rats and telomeres from white blood cells did not differ between HCR and LCR rats at the ages investigated. These data demonstrate that, in this animal model, the development of metabolic risk factors is independent of differences in telomere length.

1. Introduction

Telomeres are nucleoprotein complexes found at the terminal ends of all eukaryotic chromosomes. In humans, telomeres are composed of 5-15kb of tandemly repeated 5′-TTAGGG hexamers and, with each round of cellular division, telomeres become shorter in length (Harley et al., 1990; Allsopp et al., 1992; Allsopp et al., 1995). Telomere length, therefore, is proposed to be an indicator of replicative history and replicative potential of somatic cells (Harley, 1991). Consistent with this proposal, in humans, older individuals have shorter telomeres compared to younger individuals (Harley et al., 1992) and critically eroded telomeres induce cellular senescence (Wright and Shay, 1992; Counter, 1996; de Lange, 1998; Hemann et al., 2001; Zou et al., 2004). These data suggest telomere length not only functions in aging at the cellular level but, presumably in aging at the tissue, organ, and systemic levels.

Recent data have demonstrated an association between short telomeres and age-related diseases. In humans, decreased telomere lengths have been correlated with increased pulse pressure (Jeanclos et al., 2000; Benetos et al., 2001), atherosclerosis (Samani et al., 2001; Obana et al., 2003; Benetos et al., 2004), heart failure (Oh et al., 2003), type 1 and type 2 diabetes (Jeanclos et al., 1998; Adaikalakoteswari et al., 2005), insulin resistance (Gardner et al., 2005), obesity (Valdes et al., 2005), and stress (Epel et al., 2004). Whether or not short telomeres are a cause or a consequence of these pathologies, however, remains to be established (Serrano and Andres, 2004). Mice in which telomeres are critically short due to a targeted gene disruption in telomerase have phenotypes characteristic of premature aging and disease, including infertility, graying of

hair, alopecia, impaired wound healing, small intestine and spleen atrophy, reduced proliferation of T and B lymphocytes, cancer predisposition, and increased levels of heart failure (Blasco et al., 1997; Lee et al., 1998; Herrera et al., 1999; Rudolph et al., 1999; Franco et al., 2002; Leri et al., 2003; Wong et al., 2003; Poch et al., 2004). However, because age-related diseases are genetically complex and determined by the expression of combinations of allelic variants sensitive to a given environment (Mootha et al., 2003), animal models to test the relationship of short telomeres and onset of disease are limiting.

Telomere lengths and telomerase expression are tissue-specifically regulated in rats. In adult rats, telomerase expression is either low or not detectable in the heart, kidney, brain, or spleen, whereas telomerase expression is detectable in the testis and liver (Borges and Liew, 1997; Golubovskaya et al., 1997). Although telomerase is detectable in the rat liver, telomere lengths decrease with age in this tissue (Cherif et al., 2003), suggesting that telomerase expression levels are not sufficient to maintain telomere lengths. Telomere shortening as a result of aging is also observed in rat kidney, pancreas, lung, and a subgroup of cardiac myocytes (Jennings et al., 1999; Kajstura et al., 2000; Cherif et al., 2003). Telomeres of rodents are relatively long compared to humans (Harley et al., 1990; Kipling and Cooke, 1990; Lejnine et al., 1995) and thus provide useful substrate to test for a robust relationship between telomere length and age-related disease as a general feature of mammals.

Rats that were selectively bred based upon low or high intrinsic aerobic running capacity, have recently emerged as models for investigating cardiovascular and metabolic risk factors (Britton and Koch, 2005; Wisloff et al., 2005). After 11 generations of

selective breeding, the low capacity running (LCR) rats had higher mean blood pressures, increased insulin-resistance, and increased levels of weight gain compared to the high capacity running (HCR) rats (Wisloff et al., 2005). Maintenance of the differences for metabolic risk factors between LCR and HCR was confirmed in generation 13 rats (Thyfault et al., 2005). Because the LCR rats had phenotypes suggestive of age-related diseases, we hypothesized that telomeres from LCR rats would be significantly shorter compared to telomeres from HCR rats. To determine if the disease-phenotype of the LCR rats is associated with telomere defects like that observed in humans, telomere lengths in heart, kidney, liver, spleen, and skeletal muscle were measured from LCR and HCR young adult rats. In the liver, mean telomere length was significantly decreased in the LCR rats, but telomeres were not critically eroded. Additionally, no significant difference was observed in the other four tissues examined. To determine if telomere lengths differ across age, telomere lengths were measured from white blood cells of young adult, middle-aged, and old LCR and HCR rats. Neither mean telomere lengths at the ages investigated nor rates of telomere shortening were different between LCR and HCR rats. These data demonstrate that, in this animal model, the development of cardiovascular and metabolic risks can develop independent of global differences in telomere length.

2. Material and methods

2.1. Plug preparation and electrophoresis

All animal procedures were done in compliance with federal and institutional guidelines. For investigation of telomere lengths in heart, kidney, liver, spleen, and

skeletal muscle, the sample consisted of six male low capacity running (LCR) rats and six male high capacity running (HCR) rats (Wisloff et al., 2005), all of which were 33 to 36 weeks of age at euthanasia. Fresh tissue samples of liver (~0.6g), spleen (~0.5g), left ventricle (~0.5g), kidney (~0.5g), and left quadriceps (~0.5g) were isolated, minced, and incubated in 10ml of 0.04% collagenase, type II (Worthington Biochemical) in DMEM for two hours at 37°C (during this incubation, samples were pipetted up and down every 30min to dissociate tissues). For white blood cell analysis, blood was drawn from live rats into EDTA-coated collection tubes. Tissue/cell suspensions were washed three times by pelleting cells at 150 RCF (relative centrifugal force) for five minutes and resuspending cells in 5ml 1xPBS. After washing, cells were pelleted by centrifugation for 5 minutes at 150 RCF and resuspended in three pellet volumes of 1.33% low melt agarose at 45°C and 40µl of suspension cast into plug molds. Additionally, as a standard control, cells from an established mouse embryonic fibroblast cell line were cast into low melt agarose plugs ($1.6x10^6$ cells/plug). Because telomere lengths may change as mouse embryonic fibroblasts are passaged in culture, enough plugs were generated from a single passage of fibroblasts to be used as standards in all subsequent experiments. After casting, plugs were incubated overnight at 37°C in a lithium dodecyl sulfate (LDS) solution containing 1% LDS, 100mM EDTA pH 8.0, and 10 mM Tris pH 8.0 (2.5 ml per plug). Plugs were then washed twice in a 20% NDS solution containing 6.8mM N-laurylsarcosine, 127 mM EDTA, and 2mM Tris (two hours per wash) at room temperature (2.5 ml per plug). DNA plugs to be digested by restriction enzyme (including a plug from the mouse embryonic fibroblast cells for each experiment) were

washed twice in TE (one hour per wash) at room temperature (2ml per plug). Plugs were then incubated twice (one hour per incubation) in 1x MboI restriction enzyme buffer at room temperature (200µl per plug). Each plug was then incubated in 150µl of 1x MboI buffer with 30U of MboI at 37°C overnight. The following morning, 20 additional units of MboI were added to each tube and incubated at 37°C for 4 hours. DNA plugs were prepared for electrophoresis by washing twice in TE (one hour per wash) at room temperature and once in 0.5xTBE electrophoresis running buffer (one hour) at room temperature. Plugs were loaded into a 1% agarose gel and DNA fragments separated by pulsed field gel electrophoresis (CHEF-DR II apparatus, BioRad) at 6 v/cm for 20 hours with an initial pulse time of 1 second and a final pulse time of 10 seconds (chamber temperature maintained at 14°C).

2.2. In-gel hybridization

Following electrophoresis, the DNA was stained with ethidium bromide for photography, and gels were dried at 50°C for 45 minutes. Dried gels were incubated in 0.6 M NaCl, 0.2 M NaOH for one hour at room temperature to alkali denature DNA, incubated in neutralization solution, 1.5 M NaCl, 0.5 M Tris, for one hour at room temperature, and rinsed in ddH_20 for 30 min at room temperature. The dried gels were prehybridized in 20 mM NaH_2PO_4, 0.1% SDS, 5x Denhardt's solution, and 5xSSC for one hour at 55°C, and hybridized with the [γ-^{32}P]ATP end-labeled oligonucleotide $(TTAGGG)_4$ overnight at 55°C in prehybridization solution. Gels were then washed three times for 20 min in 4xSSC at room temperature and three times for 20 min in 4xSSC, 0.1% SDS at 57°C. Gels were exposed to phoshporimager screens for five hours,

developed using a Typhoon 8600 Variable Mode Imager (Molecular Dynamics, Amersham Pharmacia Biotech), and radioactive signals quantified (excluding signals from DNA that remained in the wells) using ImageQuant® version 5.2 for Windows. Telomere lengths were estimated from radioactive signals of alkali denatured gels hybridized with the end labeled $(TTAGGG)_4$ oligonucleotide, as described (Harley et al., 1990). To directly compare telomere lengths that were determined from separate gels, all rat telomere lengths were normalized to the control mouse embryonic fibroblast cell line. To compare telomere signals in quadrants, percent signal intensities for the regions 194.0-145.5kb, 145.5-48.5kb, 48.5-15.0kb, and less than 15.0kb were calculated as described (Jennings et al., 1999).

Statistical significance of mean telomere lengths was determined using SPSS® version 11.5 for Windows by independent-samples *t* test. Linear trendlines were added using Microsoft® Excel:mac v.X. Statistical difference between rates of telomere shortening was determined using the GLM procedure in SAS v9.1 by ANCOVA.

3. Results

Telomere length is influenced by both genetic and environmental factors, and decreased telomere lengths have been associated with multiple age-related diseases in humans, including cardiovascular disease, insulin resistance, and obesity (von Zglinicki and Martin-Ruiz, 2005). To control for differences in telomere lengths due to gender and age (Harley et al., 1992; Jeanclos et al., 2000; Benetos et al., 2001; Cherif et al., 2003), telomere lengths from heart, kidney, spleen, liver, and skeletal muscle were measured from an age-matched population of six HCR and six LCR males by telomere restriction

fragment (TRF) analysis. DNA from each tissue was digested with the MboI restriction enzyme, resolved by pulsed field gel electrophoresis, alkali denatured, and hybridized with a radioactively end-labeled $(TTAGGG)_4$ oligonucleotide (Fig. 1a, and data not shown). Telomeres from inbred rat strains are approximately 50kb in length (Lejnine et al., 1995). To avoid inefficient depurination and transfer of high molecular weight DNA fragments onto a membrane, in-gel hybridization was preferred over traditional Southern blot methods (Hemann and Greider, 1999). Comparing telomere lengths between HCR rats and LCR rats, no significant difference was observed between heart, kidney, spleen, or skeletal muscle ($p > 0.05$) (Fig. 1b). In the liver, mean telomere length was significantly shorter in the LCR rats (54.77 ± 1.16 kb) compared to HCR rats (58.41 ± 0.98 kb) ($p = 0.030$), suggesting accelerated telomere attrition in the liver may contribute to the metabolic disease phenotype in the LCR rats. To directly compare telomere lengths that were determined from separate gels, all rat telomere lengths were normalized to a control mouse embryonic fibroblast cell line, which was included in each experiment (data not shown). Cellular replicative senescence due to telomere erosion is caused by the shortest telomere(s), not by mean telomere length (Hemann et al., 2001; Zou et al., 2004). Therefore, telomere signal intensities ranging from 194.0 to 145.5 kb, 145.5 to 48.5 kb, 48.5 to 15.0 kb, and less than 15.0 kb were compared (Fig. 1c). In the liver, a significant increase in signal intensity was observed for the 48.5 to 15.0 kb quadrant of LCR rats compared to HCR rats ($p = 0.036$). Significant differences between LCR and HCR rats were not observed in the remaining quadrants from the liver ($p > 0.05$) or in any quadrants from the other tissues examined ($p > 0.05$) (data not shown).

Although only slight differences in telomere length between young adult LCR and HCR rats were observed in the previous experiments, we proposed that telomere length differences would be more pronounced in aged animals. To test this hypothesis, telomere lengths from white blood cells were measured by TRF analysis in three different age populations: young adult males (mean age = 191 ± 5.83 days), middle-aged males (mean age = 340 ± 5.06 days), and old males (mean age = 759 ± 17.9 days). Comparing HCR and LCR rats, no significant difference in mean telomere length was observed in white blood cells from the ages investigated ($p > 0.05$) (Fig. 2a) and rates of telomere attrition were not different between LCR (-10.2 bp/day) and HCR rats (-7.9 bp/day) ($p = 0.8817$) (Fig. 2b). Additionally, there were no significant differences when telomere signal intensities from white blood cells, ranging from 194.0 to 145.5 kb, 145.5 to 48.5 kb, 48.5 to 15.0 kb, and less than 15.0 kb, were compared ($p > 0.05$) (Fig. 2c and data not shown). To verify the results from the male populations, telomere lengths of white blood cells from old female rats (four LCR rats and four HCR rats, mean age = 772 ± 26.8 days) were measured. No significant difference in mean telomere length (LCR = 55.9 ± 2.64 kb: HCR = 58.0 ± 2.60 kb, $p = 0.598$) or in signal intensity quadrants (data not shown, $p > 0.05$) was observed.

4. Discussion

Telomere stability is necessary for cell viability, and previous studies demonstrated that with each cell division, telomeres become decreased in length (Harley et al., 1990; Allsopp et al., 1992; Allsopp et al., 1995). Eventually, telomeres are eroded to critically short lengths and cells enter senescence (Wright and Shay, 1992; Counter,

1996; de Lange, 1998; Hemann et al., 2001; Zou et al., 2004). This mechanism of counting cell divisions theoretically protects complex organisms from cancer and also determines, at the cellular level, biological age. Consistent with telomeres playing a role in aging, in general, older individuals have shorter telomeres compared to younger individuals (Harley et al., 1992). However, the trigger for cell senescence by short telomeres is not known. In humans, decreased telomere lengths have been associated with multiple age-related diseases, including cardiovascular disease, insulin resistance, and obesity (von Zglinicki and Martin-Ruiz, 2005). Rats selectively bred, based upon aerobic running capacity, are new rodent models to investigate cardiac and metabolic risk factors (Britton and Koch, 2005; Wisloff et al., 2005). In the present study, we demonstrated that telomere lengths between high capacity running (HCR) rats and low capacity running (LCR) rats, with the exception of the liver, were not significantly different, suggesting the "early" disease phenotypes in LCR rats are independent of telomere length differences.

Mean telomere length in the liver was significantly decreased in the LCR rats compared to the HCR rats. When investigating the signal intensity of telomeres that were less than 15.0 kb in length, no difference was observed between LCR rats and HCR rats, demonstrating that the decrease in mean telomere length was not due to a significant change in critically short telomeres. Telomere lengths were also slightly, but not statistically significant, decreased in heart, kidney, and spleen of young adult LCR rats compared to HCR rats and in white blood cells of middle-aged and old male LCR rats compared to HCR rats. While the exact physiological or pathological significance of a 3-

4 kb decrease in telomeres that are 50 kb in length is not known (Lee et al., 1998), recent work suggests small changes may have functional consequence. Humans have telomeres about 7 kb in length. Valdes and colleagues (Valdes et al., 2005) report that, in women, telomeres decline 0.027 kb/year of age (range 18 to 76). In addition, they report that telomeres of obese women are 0.240 kb shorter than those of lean women, and that smoking accelerates telomere attrition at a rate of 0.005 kb per pack-year (Valdes et al., 2005).

When human fibroblasts are grown under hyperoxic conditions, telomere shortening occurs at a faster rate, suggesting telomeres are sensitive to oxidative damage (Petersen et al., 1998; von Zglinicki, 1998). Additionally, oxidative stress preferentially damages DNA at polyguanosine sequences, making each G-triplet of the telomeric hexamer (5′-TTAGGG-3′) a target for oxidative damage (Oikawa and Kawanishi, 1999). Therefore, the ability of organisms to detoxify free radicals, which are produced endogenously or environmentally, contributes to telomere length regulation (von Zglinicki, 1998; von Zglinicki, 2000). Because aging is associated with increased rates of mitochondrial oxygen free radical production (Sohal et al., 1995; de Grey, 1997; Lucas and Szweda, 1999), it will be of interest to investigate if the LCR and HCR rats differ in their production of free radicals or tolerance to oxidative damage.

In summary, there is no uniform connection between decreased telomere lengths and early metabolic disease in male LCR rats. Data from human studies do demonstrate an association, however the cause-effect relationship has not been determined (von Zglinicki and Martin-Ruiz, 2005). The data presented here suggest that, in this animal

model, the development of metabolic disease is independent of telomere length differences. Investigating the ability of LCR and HCR rats to cope with oxidative insults will provide additional insight into the age-related diseases and telomere length relationship.

Acknowledgements

We gratefully acknowledge support from a Helen and Harold McMaster Endowment, the expert care of our rat colony provided by Lori Gilligan and Ashley Duvall, and, for statistical advice, Dr. Sadik Khuder. Supported by NIH grants HL16497 and RR17710 to LGK and SLB.

References

Adaikalakoteswari, A., Balasubramanyam, M., and Mohan, V. (2005). Telomere shortening occurs in Asian Indian Type 2 diabetic patients. Diabetic Medicine *22*, 1151-1156.

Allsopp, R.C., Chang, E., Kashefi-Aazam, M., Rogaev, E.I., Piatyszek, M.A., Shay, J.W., and Harley, C.B. (1995). Telomere shortening is associated with cell division in vitro and in vivo. Exp Cell Res *220*, 194-200.

Allsopp, R.C., Vaziri, H., Patterson, C., Goldstein, S., Younglai, E.V., Futcher, A.B., Greider, C.W., and Harley, C.B. (1992). Telomere length predicts replicative capacity of human fibroblasts. Proc Natl Acad Sci U S A *89*, 10114-10118.

Benetos, A., Gardner, J.P., Zureik, M., Labat, C., Xiaobin, L., Adamopoulos, C., Temmar, M., Bean, K.E., Thomas, F., and Aviv, A. (2004). Short telomeres are associated with increased carotid atherosclerosis in hypertensive subjects. Hypertension *43*, 182-185.

Benetos, A., Okuda, K., Lajemi, M., Kimura, M., Thomas, F., Skurnick, J., Labat, C., Bean, K., and Aviv, A. (2001). Telomere length as an indicator of biological aging: the gender effect and relation with pulse pressure and pulse wave velocity. Hypertension *37*, 381-385.

Blasco, M.A., Lee, H.W., Hande, M.P., Samper, E., Lansdorp, P.M., DePinho, R.A., and Greider, C.W. (1997). Telomere shortening and tumor formation by mouse cells lacking telomerase RNA. Cell *91*, 25-34.

Borges, A., and Liew, C.C. (1997). Telomerase activity during cardiac development. J Mol Cell Cardiol *29*, 2717-2724.

Britton, S.L., and Koch, L.G. (2005). Animal models of complex diseases: An initial strategy. IUBMB Life *57*, 631-638.

Cherif, H., Tarry, J.L., Ozanne, S.E., and Hales, C.N. (2003). Ageing and telomeres: a study into organ- and gender-specific telomere shortening. Nucleic Acids Res *31*, 1576-1583.

Counter, C.M. (1996). The roles of telomeres and telomerase in cell life span. Mutat Res *366*, 45-63.

de Grey, A.D. (1997). A proposed refinement of the mitochondrial free radical theory of aging. Bioessays *19*, 161-166.

de Lange, T. (1998). Telomeres and senescence: ending the debate. Science *279*, 334-335.

Epel, E.S., Blackburn, E.H., Lin, J., Dhabhar, F.S., Adler, N.E., Morrow, J.D., and Cawthon, R.M. (2004). Accelerated telomere shortening in response to life stress. Proc Natl Acad Sci U S A *101*, 17312-17315.

Franco, S., Segura, I., Riese, H.H., and Blasco, M.A. (2002). Decreased B16F10 melanoma growth and impaired vascularization in telomerase-deficient mice with critically short telomeres. Cancer Res *62*, 552-559.

Gardner, J.P., Li, S., Srinivasan, S.R., Chen, W., Kimura, M., Lu, X., Berenson, G.S., and Aviv, A. (2005). Rise in insulin resistance is associated with escalated telomere attrition. Circulation *111*, 2171-2177.

Golubovskaya, V.M., Presnell, S.C., Hooth, M.J., Smith, G.J., and Kaufmann, W.K. (1997). Expression of telomerase in normal and malignant rat hepatic epithelia. Oncogene *15*, 1233-1240.

Harley, C.B. (1991). Telomere loss: mitotic clock or genetic time bomb? Mutat Res *256*, 271-282.

Harley, C.B., Futcher, A.B., and Greider, C.W. (1990). Telomeres shorten during ageing of human fibroblasts. Nature *345*, 458-460.

Harley, C.B., Vaziri, H., Counter, C.M., and Allsopp, R.C. (1992). The telomere hypothesis of cellular aging. Experimental Gerontology *27*, 375-382.

Hemann, M.T., and Greider, C.W. (1999). G-strand overhangs on telomeres in telomerase-deficient mouse cells. Nucleic Acids Res *27*, 3964-3969.

Hemann, M.T., Strong, M.A., Hao, L.Y., and Greider, C.W. (2001). The shortest telomere, not average telomere length, is critical for cell viability and chromosome stability. Cell *107*, 67-77.

Herrera, E., Samper, E., Martin-Caballero, J., Flores, J.M., Lee, H.W., and Blasco, M.A. (1999). Disease states associated with telomerase deficiency appear earlier in mice with short telomeres. Embo J *18*, 2950-2960.

Jeanclos, E., Krolewski, A., Skurnick, J., Kimura, M., Aviv, H., Warram, J.H., and Aviv, A. (1998). Shortened telomere length in white blood cells of patients with IDDM. Diabetes *47*, 482-486.

Jeanclos, E., Schork, N.J., Kyvik, K.O., Kimura, M., Skurnick, J.H., and Aviv, A. (2000). Telomere length inversely correlates with pulse pressure and is highly familial. Hypertension *36*, 195-200.

Jennings, B.J., Ozanne, S.E., Dorling, M.W., and Hales, C.N. (1999). Early growth determines longevity in male rats and may be related to telomere shortening in the kidney. FEBS Lett *448*, 4-8.

Kajstura, J., Pertoldi, B., Leri, A., Beltrami, C.A., Deptala, A., Darzynkiewicz, Z., and Anversa, P. (2000). Telomere shortening is an in vivo marker of myocyte replication and aging. Am J Pathol *156*, 813-819.

Kipling, D., and Cooke, H.J. (1990). Hypervariable ultra-long telomeres in mice. Nature *347*, 400-402.

Lee, H.W., Blasco, M.A., Gottlieb, G.J., Horner, J.W., 2nd, Greider, C.W., and DePinho, R.A. (1998). Essential role of mouse telomerase in highly proliferative organs. Nature *392*, 569-574.

Lejnine, S., Makarov, V.L., and Langmore, J.P. (1995). Conserved nucleoprotein structure at the ends of vertebrate and invertebrate chromosomes. Proc Natl Acad Sci U S A *92*, 2393-2397.

Leri, A., Franco, S., Zacheo, A., Barlucchi, L., Chimenti, S., Limana, F., Nadal-Ginard, B., Kajstura, J., Anversa, P., and Blasco, M.A. (2003). Ablation of telomerase and telomere loss leads to cardiac dilatation and heart failure associated with p53 upregulation. Embo J *22*, 131-139.

Lucas, D.T., and Szweda, L.I. (1999). Declines in mitochondrial respiration during cardiac reperfusion: age-dependent inactivation of alpha-ketoglutarate dehydrogenase. Proc Natl Acad Sci U S A *96*, 6689-6693.

Mootha, V.K., Lindgren, C.M., Eriksson, K.F., Subramanian, A., Sihag, S., Lehar, J., Puigserver, P., Carlsson, E., Ridderstrale, M., Laurila, E., Houstis, N., Daly, M.J., Patterson, N., Mesirov, J.P., Golub, T.R., Tamayo, P., Spiegelman, B., Lander, E.S., Hirschhorn, J.N., Altshuler, D., and Groop, L.C. (2003). PGC-1alpha-responsive genes involved in oxidative phosphorylation are coordinately downregulated in human diabetes. Nature Genetics *34*, 267-273.

Obana, N., Takagi, S., Kinouchi, Y., Tokita, Y., Sekikawa, A., Takahashi, S., Hiwatashi, N., Oikawa, S., and Shimosegawa, T. (2003). Telomere shortening of peripheral blood mononuclear cells in coronary disease patients with metabolic disorders. Intern. Med. *42*, 150-153.

Oh, H., Wang, S.C., Prahash, A., Sano, M., Moravec, C.S., Taffet, G.E., Michael, L.H., Youker, K.A., Entman, M.L., and Schneider, M.D. (2003). Telomere attrition and Chk2 activation in human heart failure. Proc Natl Acad Sci U S A *100*, 5378-5383.

Oikawa, S., and Kawanishi, S. (1999). Site-specific DNA damage at GGG sequence by oxidative stress may accelerate telomere shortening. FEBS Lett *453*, 365-368.

Petersen, S., Saretzki, G., and von Zglinicki, T. (1998). Preferential accumulation of single-stranded regions in telomeres of human fibroblasts. Exp Cell Res *239*, 152-160.

Poch, E., Carbonell, P., Franco, S., Diez-Juan, A., Blasco, M.A., and Andres, V. (2004). Short telomeres protect from diet-induced atherosclerosis in apolipoprotein E-null mice. Faseb J *18*, 418-420.

Rudolph, K.L., Chang, S., Lee, H.W., Blasco, M., Gottlieb, G.J., Greider, C., and DePinho, R.A. (1999). Longevity, stress response, and cancer in aging telomerase-deficient mice. Cell *96*, 701-712.

Samani, N.J., Boultby, R., Butler, R., Thompson, J.R., and Goodall, A.H. (2001). Telomere shortening in atherosclerosis. Lancet *358*, 472-473.

Serrano, A.L., and Andres, V. (2004). Telomeres and cardiovascular disease: does size matter? Circ Res *94*, 575-584.

Sohal, R.S., Agarwal, S., and Sohal, B.H. (1995). Oxidative stress and aging in the Mongolian gerbil (Meriones unguiculatus). Mech. Ageing Dev. *81*, 15-25.

Thyfault, J.P., Noland, R.C., Coburn, L.E., Henes, S.T., Britton, S.L., Koch, L.G., Dohm, L., Cortright, R.N., and Lust, R.M. (2005). Effects of a high fat diet on glycogen synthesis rates in skeletal muscle of rats bred for low and high (LCR and HCR) endurance capacity. Experimental Biology meeting abstracts. The FASEB Journal *19*, Abstract # 665.19.

Valdes, A.M., Andrew, T., Gardner, J.P., Kimura, M., Oelsner, E., Cherkas, L.F., Aviv, A., and Spector, T.D. (2005). Obesity, cigarette smoking, and telomere length in women. Lancet *366*, 662-664.

von Zglinicki, T. (1998). Telomeres: influencing the rate of aging. Ann N Y Acad Sci *854*, 318-327.

von Zglinicki, T. (2000). Role of oxidative stress in telomere length regulation and replicative senescence. Ann N Y Acad Sci *908*, 99-110.

von Zglinicki, T., and Martin-Ruiz, C.M. (2005). Telomeres as biomarkers for ageing and age-related diseases. Curr. Mol. Med. *5*, 197-203.

Wisloff, U., Najjar, S.M., Ellingsen, O., Haram, P.M., Swoap, S., Al-Share, Q., Fernstrom, M., Rezaei, K., Lee, S.J., Koch, L.G., and Britton, S.L. (2005). Cardiovascular risk factors emerge after artificial selection for low aerobic capacity. Science *307*, 418-420.

Wong, K.K., Maser, R.S., Bachoo, R.M., Menon, J., Carrasco, D.R., Gu, Y., Alt, F.W., and DePinho, R.A. (2003). Telomere dysfunction and Atm deficiency compromises organ homeostasis and accelerates ageing. Nature *421*, 643-648.

Wright, W.E., and Shay, J.W. (1992). The two-stage mechanism controlling cellular senescence and immortalization. Experimental Gerontology *27*, 383-389.

Zou, Y., Sfeir, A., Gryaznov, S.M., Shay, J.W., and Wright, W.E. (2004). Does a sentinel or a subset of short telomeres determine replicative senescence? Mol. Biol. Cell *15*, 3709-3718.

Figure 1. Telomere lengths in LCR and HCR rats.

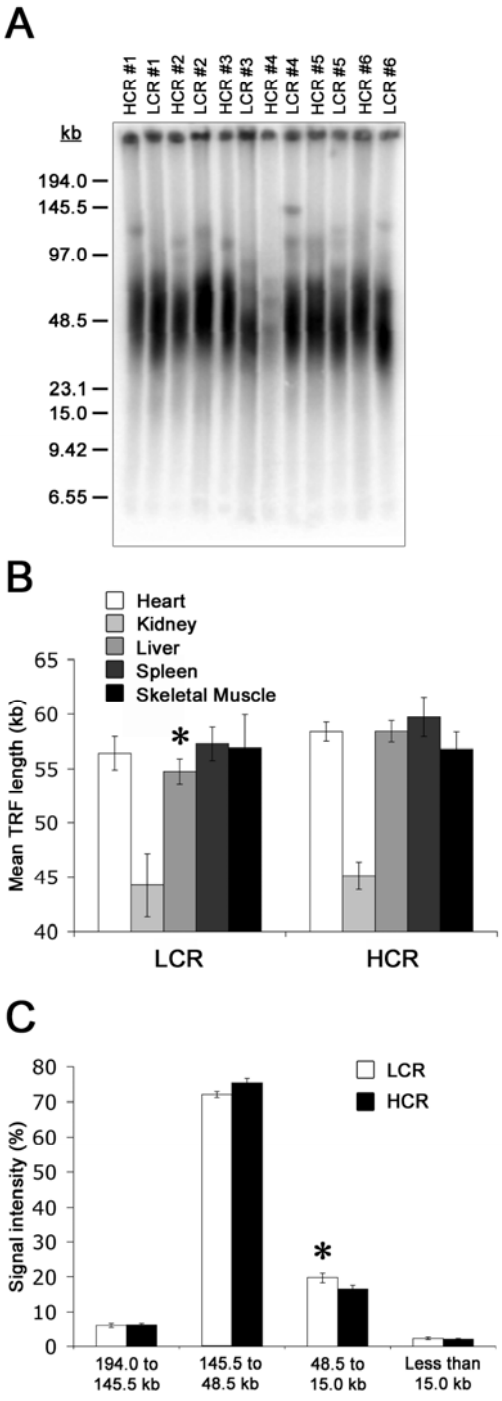

Figure 2. Telomere lengths from white blood cells in LCR and HCR rats.

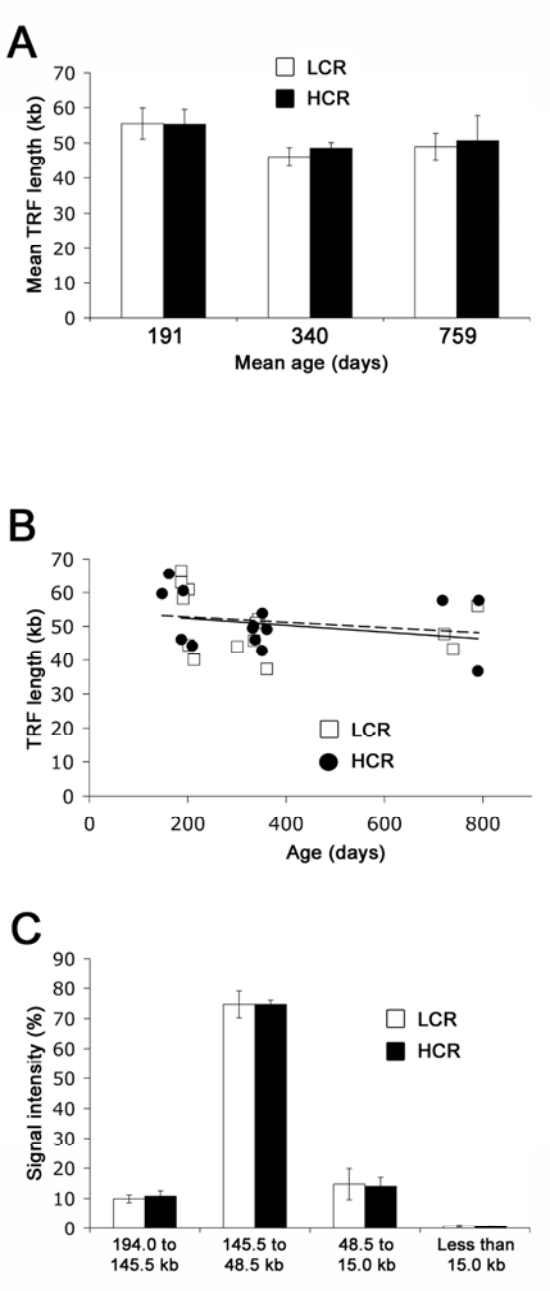

Figure legends

Fig. 1. Examination of telomere lengths in age matched low capacity running (LCR) and high capacity running (HCR) rats. (A) Representative image of digested DNA fragments separated by pulse field gel electrophoresis and hybridized with the radioactively end-labeled, telomere-specific, $(TTAGGG)_4$ oligonucleotide. Samples shown are DNA isolated from the spleens of LCR and HCR rats. (B) Mean telomere lengths from telomere restriction fragment analysis were determined as described (Harley et al., 1990) from each tissue. * indicates statistically significant difference in LCR rats compared to corresponding tissue from HCR rats. Error bars indicate the standard error of the mean from the six animals investigated from each group. (C) Signal intensity quadrants were determined, as described (Jennings et al., 1999). Data shown are from liver samples. * indicates statistically significant difference in the quadrant between LCR and HCR rats. Error bars indicate the standard error of the mean from the six animals investigated from each group.

Fig. 2. Examination of telomere lengths from white blood cells in low capacity running (LCR) and high capacity running (HCR) rats. (A) Mean telomere lengths from white blood cells were determined by telomere restriction fragment analysis from young adult (mean age of 191 days, six LCR and six HCR rats), middle-aged (mean age of 340 days, six LCR and six HCR rats), and old (mean age of 759 days, three LCR and three HCR rats) male rats. Error bars indicate the standard error of the mean from the animals investigated in each group. (B) Telomere

lengths from white blood cells of each male rat investigated. Dashed trendline represents the linear decrease of telomere length from white blood cells over time for HCR rats (y = -0.0079x + 54.364). Solid trendline represents the linear decrease of telomere length from white blood cells over time for LCR rats (y = -0.0102x + 54.432). (C) Signal intensity quadrants were determined, as described (Jennings et al., 1999). Data shown are from middle-aged adult (mean age 340 days) rats. Error bars indicate the standard error of the mean from the six animals investigated from each group.

DISCUSSION

Homologous recombination is a DNA repair pathway that fixes complex forms of DNA damage (such as ICLs and DSBs), maintains chromosome stability, and increases genetic diversity. In mammals, DNA structures that protect the ends of linear chromosomes (telomeres) resemble HR intermediates, suggesting the protein machinery that functions in HR has roles in telomere protection. This thesis has described research towards characterizing mouse cells deficient for the *Rad51d* gene and has demonstrated that the RAD51D protein is necessary for repairing DNA damage and maintaining both chromosome and telomere stability. Data in the first chapter of the Results section demonstrate that, at the cellular level, a disruption of the *Rad51d* gene confers an increase in gross chromosomal abnormalities, hypersensitivity to DNA damaging agents, a reduced ability to form RAD51 foci following irradiation, and decreased levels of sister chromatid exchange following treatment with the DNA interstrand crosslinking agent, mitomycin C. Data in the second chapter of the Results section demonstrate that the RAD51D protein protects telomeres, and in the absence of RAD51D, an increase in telomere fusions and accelerated telomere attrition occurs. The third chapter of the Results section demonstrates that telomeres in *Rad51d*-deficient MEFs have long telomeric 3′ overhangs and an increased frequency of being recognized as DSBs. Because previous studies have demonstrated telomere shortening as a result of aging (Harley et al., 1992), the data in the fourth chapter of the Results section tests the association of short telomere lengths and genetically complex age-related diseases in rats selectively bred based upon aerobic running capacity. This was the first study to

investigate such an association and, surprisingly, no correlation was demonstrated in this animal model. In this chapter, I will discuss the data presented in the dissertation focusing on RAD51D and conclude with speculative models for the repair of interstrand crosslinks during DNA replication and multiple models for telomere dysfunction in *Rad51d*-deficient cells.

Rad51d-deficient mice die at approximately 10.5 days post conception (dpc), demonstrating the importance of RAD51D for embryo and cell viability. *Rad51d*$^{-/-}$ mouse embryo phenotypes include delayed development, posterior truncation, decreased brain vesicle size, and disorganized limb buds, suggesting increased levels of cell death by necrosis or apoptosis. Additionally, cells derived from *Rad51d*$^{-/-}$ mouse embryos failed to propagate in culture (Pittman and Schimenti, 2000). To determine whether absence of the *Trp53* gene (the gene that encodes the p53 tumor suppressor protein) would rescue embryonic lethality of *Rad51d*$^{-/-}$ mice, I crossed the *Rad51d* disruption into a *Trp53*-deficient background. Eliminating the *Trp53* gene was sufficient to prolong the lifespan of *Rad51d*-deficient mouse embryos up to 6 days and rescue *Rad51d*$^{-/-}$ cell lethality. *Rad51d*$^{-/-}$ *Trp53*$^{-/-}$ mouse embryos are developmentally delayed and had non-consistent phenotypes of varying severity (including blood pooling, tissue necrosis, femele-specific exencephaly, and spinal and craniofacial malformations), which is suggestive of random mutations in developmental regulatory genes (Smiraldo et al., 2005). Previous reports also describe partial bypass of embryonic lethality by a *Trp53* deficiency in mice carrying targeted disruptions in HR repair genes. Mice deficient for *Rad51* or *Rad51b* die during early gestation (6.5-8.5 dpc) (Lim and Hasty, 1996; Tsuzuki

et al., 1996; Shu et al., 1999) and when crossed into a *Trp53*$^{-/-}$ background, embryo lethality was bypassed at least 1-2 days (Lim and Hasty, 1996; Shu et al., 1999). *Brca1* or *Brca2* null mouse embryos die approximately 7.5-12.5 dpc (Gowen et al., 1996; Hakem et al., 1996; Liu et al., 1996; Ludwig et al., 1997; Sharan et al., 1997; Suzuki et al., 1997) and, as observed in the *Rad51* knockout mouse, embryo lethality was bypassed approximately 1-2 days by a *Trp53*-disruption (Ludwig et al., 1997). These results demonstrate that HR proteins play a vital role maintaining cell viability during high rates of cell proliferation, such as embryogenesis.

In humans, heritable mutations in the *BRCA1* or *BRCA2* genes significantly increase susceptibility of women to developing breast or ovarian cancer (Thompson and Schild, 2002). As models to investigate how defects in the *Brca1* or *Brca2* genes confer cancer susceptibility, tissue-specific (conditional) disruptions in mice were generated (Xu et al., 1999a; Jonkers et al., 2001). Mice carrying a mammary gland-specific disruption of *Brca1* had abnormal ductal development and developed mammary gland tumors that were associated with aneuploidy and chromosomal rearrangements. Tumor formation in these mice was accelerated in a *Trp53* heterozygous (*Trp53*$^{+/-}$) background, and cancer cells frequently had loss of heterozygosity at the *Trp53* allele (Xu et al., 1999a). In *Brca2*-conditional disruption mice, tumor formation only occurred in a *Trp53*-deficient (*Trp53*$^{-/-}$) background (Jonkers et al., 2001). These data demonstrated that, in the absence of *Brca1* or *Brca2*, disruption of the p53 pathway is critical for cancer formation. Because cells deficient for *Rad51d* have similar phenotypes to cells deficient for *Brca1* or *Brca2*, including chromosome instability, hypersensitivity to DNA damaging agents, and

decreased HR activities (see Table III, Literature, pg. 30), I propose that a *Rad51d* deficiency contributes to breast cancer susceptibility. To test this hypothesis, a mammary gland-specific disruption of the *Rad51d* gene should be generated in mice and the frequency of tumor formation determined. It is possible that, like the tissue-specific *Brca2* disruption, tumor formation in the absence of *Rad51d* may require the absence of the p53 protein. Therefore, the frequency of mammary tumor formation in mice carrying the *Rad51d* conditional disruption should be investigated in a $Trp53^{+/-}$ or $Trp53^{-/-}$ background. If an increase in tumor formation occurs in the absence of RAD51D, these data would implicate the RAD51D protein as a genome "caretaker" necessary to prevent carcinogenesis. However, because mice deficient for *Rad51d*, *Brca1*, or *Brca2* are not viable (Gowen et al., 1996; Hakem et al., 1996; Liu et al., 1996; Ludwig et al., 1997; Sharan et al., 1997; Suzuki et al., 1997; Pittman and Schimenti, 2000), complete disruptions of *BRCA1*, *BRCA2*, or *RAD51D* in the human population are likely not compatible with life. Instead, heritable defects in *BRCA1* or *BRCA2* that cause frameshift, missense, nonsense, or deletion mutations are observed that confer cancer predisposition (Peto et al., 1999) (OMIM 113705; OMIM 600185: http://www.ncbi.nlm.nih.gov/omim). Within the human *RAD51D* gene, 69 single nucleotide polymorphisms (SNPs) have been identified, six are located in untranslated regions of the gene, 57 are located in introns, and six are located in exons (of the six located in exons, five are missense mutations and one is a silent mutation) (http://www.ncbi.nlm.nih.gov/SNP: gene ID:5892, search performed on February 16, 2006). One of the allelic variants of *RAD51D*, conferred by a SNP that changes the

glutamic acid at position 233 to glycine, was more highly represented in high-risk familial breast cancers not associated with defects in *BRCA1* or *BRCA2* genes (Rodriguez-Lopez et al., 2004). Therefore, it will be of interest to determine how this mutation affects the function of the RAD51D protein in maintaining genome stability or DNA repair and if mice carrying this mutation can be used as models to study the initiation and progression of cancer.

Potential Mechanisms of RAD51D in DNA Repair

Rad51d-deficient MEFs are hypersensitive to DNA damaging agents, demonstrating a role for RAD51D in DNA repair. Following exposure to ionizing radiation, RAD51 proteins accumulate at the sites of DNA damage to form foci that are visible by immunofluorescence (Haaf et al., 1995; Raderschall et al., 1999). Consistent with this observation, in MEFs that are wild-type or heterozygous for *Rad51d*, RAD51 foci form after treatment with 10 Gy of ionizing radiation. However, in *Rad51d*-deficient MEFs, RAD51 foci did not form (Smiraldo et al., 2005), demonstrating a role for RAD51D in the formation of the RAD51 nucleoprotein filaments. These data are consistent with the absence of RAD51 foci formation following treatment with ionizing radiation in chicken DT40 cells or mammalian cells deficient for the *Rad51*-like genes: *Rad51b*, *Rad51c*, *Rad51d*, *Xrcc2*, or *Xrcc3* (see Table III, Literature, pg. 30). The RAD51 protein interacts directly with the breast cancer susceptibility protein, BRCA2, at BRC motifs (Pellegrini et al., 2002). The BRCA2 protein contains eight BRC motifs, each motif being 30-40 amino acids in length (Bork et al., 1996). It is proposed that the BRCA2/RAD51 complex localizes to damaged DNA, and BRCA2 functions to load

RAD51 onto ss-DNA (Pellegrini et al., 2002). Consistent with this proposal, *BRCA2* mutant cells are defective for the formation of ionizing radiation-induced RAD51 foci (Yuan et al., 1999; Yu et al., 2000). Recent *in vitro* data demonstrate that RAD51 proteins or protein complexes can slide along ds-DNA molecules and stop at the DNA terminus (Graneli et al., 2006). Therefore, a potential model to describe the formation of RAD51 foci is that the RAD51-like proteins (1) direct BRCA2/RAD51 to sites of DNA damage, (2) prepare the site of DNA damage for BRCA2/RAD51 docking, or (3) interact with BRCA2 to unload RAD51 onto DNA. Once RAD51 is bound to DNA, it may translocate along the DNA towards the damaged site, where it accumulates to form a nucleoprotein filament. In *Rad51d*-deficient MEFs, there was only a 1.5-fold increased sensitivity to ionizing radiation compared to controls (based upon colony survival analyses), even though a dramatic decrease in the ability to form RAD51 foci was observed. This small increase in sensitivity to ionizing radiation is consistent with that observed in cells deficient in other HR genes (see Table III, Literature, pg. 30). One possible explanation is that in the absence of HR, the NHEJ pathway repairs the damaged DNA. Although it is proposed that HR is preferred in S and G2 phases of the cell cycle and NHEJ is preferred in G1 or G0 phases of the cell cycle (Johnson and Jasin, 2001), NHEJ may be able to function in S and G2 in the absence of HR to maintain cell viability. The NHEJ pathway, however, can be error prone conferring deletions or chromosome translocations, both of which are significantly increased in the *Rad51d*-deficient MEFs (see Figure 5, Results, pg. 104). It is not likely, however, that HR repair mechanisms can compensate for the absence of NHEJ in G1 or G0 because, in these

stages of the cell cycle, no sister chromatid is present for HR to use as a template. Consistent with this proposal, cells deficient for the NHEJ genes, *LigaseIV*, *DNA-PKcs*, or *Ku70* are approximately 4-fold more sensitive to IR compared to control cells (Gu et al., 1997; Frank et al., 1998), even though HR repair was still functional (Sonoda et al., 1999; Mills et al., 2004).

Rad51d-deficient MEFs were most sensitive to interstrand crosslinking agents, which is consistent with HR as a primary repair pathway of DNA ICLs and with that observed in cells deficient in other HR genes (see Table III, Literature, pg. 30). Models of the repair of ICLs by HR, however, are limiting. One model does not include a strand invasion/homologous pairing step (Dronkert and Kanaar, 2001). If correct, much of the known activities of RAD51 and the RAD51-related proteins would not be required for ICL repair. This would be surprising given the data from biochemical studies of the RAD51 family members (Table I, Literature, pg. 27), the hypersensitivity of cells deficient for HR genes to ICL damage (Table III, Literature, pg. 30), and the formation of RAD51 foci in response to ICL lesions (Hussain et al., 2003). A different model predicts that the damaged nucleotides affected by the ICLs are simply excised by the nucleotide excision repair pathway to form a DSB (Dronkert and Kanaar, 2001). The DSB then is repaired by HR using the sister chromatid as a replication template like that described in the DSBR model (Figure 2, Literature, pg. 12) or the SDSA model (Figure 3, Literature, pg. 13). These models are sufficient to describe ICL repair only if the damage occurs after DNA replication. During DNA replication, however, the covalent bonds caused by ICL lesions likely stall DNA replication because the parental strands cannot be separated.

One model that describes ICL repair during DNA replication proposes that the nucleotides affected by the damage are excised by nucleotide excision repair to form a DSB. Because no sister chromatid is present to use as a template, the DSB is repaired by HR using the non-sister, homologous chromosome (Dronkert and Kanaar, 2001). If this model is correct, an increase in the rate of loss of heterozygosity (LOH) would be expected. For example, if the homologous chromosome that is used as a template contains a mutation, that mutation will be copied to the damaged chromosome. In Figure 12, I propose a model for ICL repair when the replication machinery encounters an ICL during DNA replication. As opposed to previously published models that predict that the non-sister, homologous chromosome is used as a replication template for ICL repair (Dronkert and Kanaar, 2001), the model in Figure 12 does not require the non-sister homologous chromosome and, therefore, would not confer potential LOH. In this model, the nucleotide excision repair (NER) pathway and the HR repair pathway cooperate to repair the ICL at the stalled replication fork. Consistent with the involvement of NER in ICL repair, cells deficient for genes involved in NER, such as *ERCC1* or *ERCC4/XPF*, are hypersensitive to ICL agents (De Silva et al., 2000). The ERCC1 and ERCC4/XPF proteins form a complex that functions as an endonuclease (de Laat et al., 1998) and, in *ERCC1*-deficient cells, incision of the DNA phosphate backbone at ICL lesions is reduced (Larminat and Bohr, 1994). The HR machinery would be required to go from step 3 to step 4 where the newly replicated strands are separated from the parental strands and re-annealed to each other to form the regressed forks. This fork regression would be required to allow the NER machinery access to excise and remove the damaged

nucleotides to form a DSB. The HR proteins would be required to go from step 4 to step 5 to resolve the regressed forks and re-anneal the newly replicated strands with the parental strands. Additionally, the HR machinery would be required for the strand invasion of the newly replicated leading strands into the sister chromatids in step 6 to step 7 to form two Holliday junctions. The mechanistic understanding of Holliday junction resolution in mammals is not known (West, 1997). It is possible that Holliday junctions are resolved by BLM and/or WRN; both of which are helicases that can unwind four-way DNA structures that mimic Holliday junctions (Karow et al., 1997; Constantinou et al., 2000; Mohaghegh et al., 2001). This model for ICL repair is similar to the DSBR model (Figure 2, Literature, pg. 12) in that two, four-way Holliday junctions are formed. Depending on how the Holliday junctions are resolved, crossover and non-crossover products would be expected, consistent with the increase in sister chromatid exchange in *Rad51d*-proficient cells in response to treatment with the interstrand crosslinking agent, mitomycin C (see Results Figure 2C, pg. 95). Because multiple strand annealing, base pairing, and resolution steps by HR are required for the model described in Figure 12, cells deficient for RAD51D are not able to repair ICLs, consistent with (1) the inability to induce SCE frequencies upon challenge with mitomycin C and (2) the hypersensitivity to interstrand crosslinking agents observed in the *Rad51d*$^{-/-}$ *Trp53*$^{-/-}$ MEFs.

Figure 12. Interstrand Crosslink Repair During DNA Replication

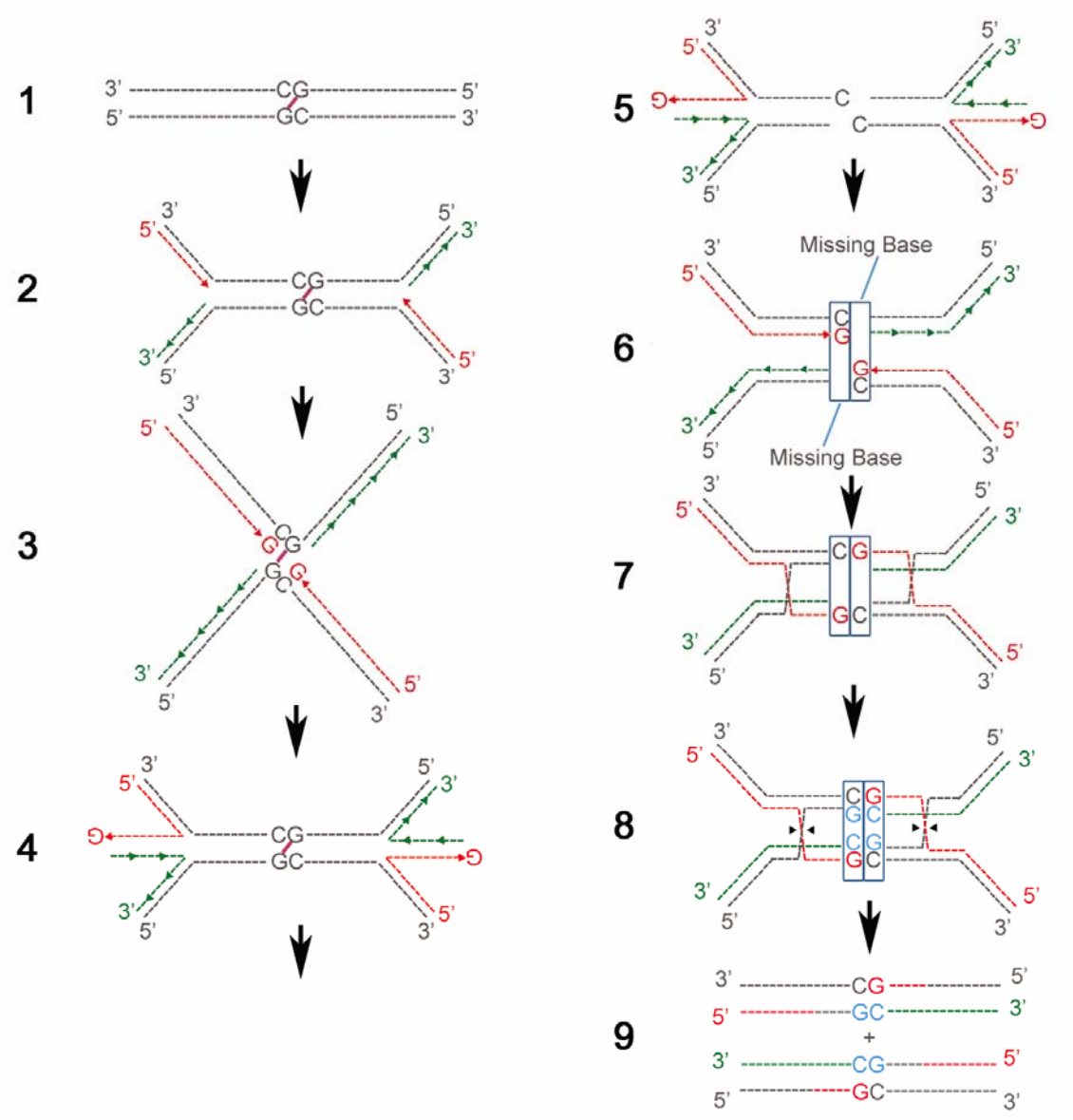

Interstrand crosslink (ICL) repair during DNA replication. Step 1, double gray lines represent parental DNA. The ICL, shown as a line between the guanine residues, is an example of a cisplatin adduct that typically forms an ICL between guanines in the sequence d(GpC) (Dronkert and Kanaar, 2001). Step 2, two DNA replication forks approach the ICL. Red line represents leading strand DNA synthesis and green line represents lagging strand DNA synthesis. Step 3, DNA replication forks proceed all of the way to the ICL, but parental stands cannot be separated. Step 4, newly synthesized strands pair and reverse branch migrate to form Holliday junction-like structures, also

known as a regressed fork (chicken foot). Step 5, the guanine residues that are linked by the ICL are removed by the nucleotide excision repair pathway to form a DSB. Step 6, the regressed forks are resolved and the parental and daughter strands re-anneal. A missing base pair in both sister chromatids remains at the site of the damage. Step 7, the 3′ tail of the daughter strands replicated by leading strand synthesis (red lines) invade the sister chromatid, displace the parental strands (gray lines), and pair to the daughter strands replicated by lagging strand synthesis (green lines). The displaced parental strands (gray lines) pair with the original parental strands on the sister chromatid (gray lines). This forms two Holliday junctions. Step 8, new bases are added to fill in the single stranded gaps (shown in blue). The double Holliday junctions are resolved by cleaving the crossed DNA strands (shown as small gray arrowheads). Step 9, DNA replication/repair is complete. Both daughter strands (sister chromatids) are identical to the original parental DNA.

Spontaneous sister chromatid exchange (SCE) levels were not affected by loss of *Rad51d* in mouse cells (Figure 2C, Results, pg. 95). These data were previously interpreted as, in mouse cells, RAD51D is not essential for the rescue of stalled replication forks during DNA replication, but is critical for DNA strand invasion of the homologous sister chromatid during the repair of ICLs (Smiraldo et al., 2005). Based upon the evidence that the BCDX2 (RAD51B-RAD51C-RAD51D-XRCC2) complex functions during branch migration (Y. Liu et al., 2004) and the direct interaction of RAD51D with the BLM helicase protein (Braybrooke et al., 2003), the increase in spontaneous chromosome aberrations in *Rad51d*-deficient cells was predicted to be a result from failure to resolve HR-associated intermediates as opposed to defects in strand invasion. As an alternative conclusion, the two proposed models for DNA DSBs repair are considered, DSBR (Figure 2, Literature, pg. 12) and SDSA (Figure 3, Literature, pg. 13). The products from the DSBR model are gene conversion with or without crossover whereas the products from the SDSA model are only gene conversion without crossover.

The SCE assay only detects crossover products and, therefore, measures DSBR but does not measure SDSA. It is possible that, in the absence of RAD51D, HR repair of stalled replication forks or DSBs by SDSA is defective. This phenotype would be undetectable by measuring SCE frequencies and also would contribute to the increase of spontaneous gross structural chromosome abnormalities observed in *Rad51d*-deficient mouse cells. If the strand invasion step of SDSA or the resolution SDSA intermediates is defective in the absence of RAD51D, an increase in chromatid gaps and breaks would be expected as opposed to chromosome gaps and breaks because, in the SDSA model, only one of the sister chromatids is ever broken. This hypothesis is consistent with the significant increase in chromatid gaps and breaks, but not chromosome gaps and breaks, observed in the *Rad51d*$^{-/-}$ *Trp53*$^{-/-}$ MEFs compared to controls (see Table 2, Results, pg. 99). An alternative method to test HR levels in cells is to use the I-*Sce*I endonuclease DSB repair system (reviewed in Johnson and Jasin, 2001). In this system, two defective neomycin phosphotransferase genes (one contains a 5′ truncation and the other is disrupted by insertion of the 18 bp I-*Sce*I endonuclease site) are integrated into the mammalian genome. The cells then are transiently transfected with a plasmid that will express the I-*Sce*I endonuclease. If gene conversion occurs by repairing the I-*Sce*I endonuclease cut site by HR, the cells will become neomycin resistant. If the I-*Sce*I endonuclease cut site is repaired by NHEJ, the cell will remain neomycin sensitive. This system measures gene conversion (which occurs in the DSBR model, Figure 2, Literature, pg. 12 and the SDSA model, Figure 3, Literature, pg. 13) rather than crossover frequencies. Assuming that the RAD51D protein is involved in repairing spontaneous DSBs by SDSA, HR levels in the

Rad51d-deficient MEFs will be decreased compared to controls using the I-*Sce*I endonuclease DSB repair system.

In the *Rad51d*-deficient MEFs, a significant increase in the percentage of mitotic cells containing more than two centrosomes was observed compared to controls (see Results Figure 3C, pg. 96). This was attributable to a pathway named "mitotic catastrophe," which is gaining attention as a mechanism to eliminate cells with chromosome instability. Damaged DNA, such as DSBs, within the genome of a cell in G2 normally confers delayed entry into mitosis, presumably so that the damage is repaired. It is proposed that, like transcription, DNA repair activities are absent during mitosis because of the condensed condition of the chromatin (Gottesfeld and Forbes, 1997; Morrison and Rieder, 2004). Therefore, repair of DNA damage during G2 is critical to prevent aberrant mitosis, which could confer deletion or amplification of chromosome regions or aneuploidy to daughter cells. If DNA damage is present in G2, the ATM kinase undergoes autophosphorylation and becomes activated to initiate a signal cascade to stop progression into mitosis (Bakkenist and Kastan, 2003). The DNA damage signal is communicated to CHK2 directly by ATM or indirectly by mediator proteins, such as 53BP1 (for review, see Sancar et al., 2004). Additionally, ATM can activate p53, which in turn stimulates transcription of the CDK inhibitor, p21 (Kastan and Lim, 2000; Bakkenist and Kastan, 2003). Although the p53 protein is not required for the initiation of the G2 arrest, it is required to ensure that the arrest is maintained until DNA repair is complete (Bunz et al., 1998). If this G2 checkpoint is circumvented, the cell will enter into mitosis with damaged chromosomes (Bunz et al., 1998). During the metaphase

stage of mitosis, chromosomes are aligned to form the metaphase plate and each chromosome kinetochore is attached to the spindle. When this process is complete, the anaphase promoting complex will cleave the securin proteins (these proteins holds sister chromatids together) allowing sister chromatid separation during anaphase. However, if chromosomes fail to form along the metaphase plate or if the kinetochores are not attached to the spindle poles, the anaphase promoting complex is inhibited (Hagting et al., 2002). If the chromosome alignment problems are not resolved, the cell will enter a "mitotic catastrophe" state. This status is associated with the amplification and/or fragmentation of centrosomes, which results in a mitotic cell that contains more than two functional centrosomes (normal mitotic cells contain two centrosomes) (Heald et al., 1993). As this cell continues through mitosis, the chromosomes will be pulled in more than two directions leaving daughter cells micronucleated or with less than the appropriated amount of DNA. These defective daugher cells are either non-viable or eliminated by apoptosis following cytokinesis (Castedo et al., 2002). Evidence from studies of human cancer cell lines demonstrate that after treatment with irradiation, a significant increase in the percentage of mitotic cells contain more than two centrosomes compared to untreated cells, suggesting that mitotic catastrophe can be activated by the presence of DSBs (Sato et al., 2000). Consistent with this proposal, mammalian cell lines carrying disruptions in the DSB repair proteins *BRCA1*, *BRCA2*, *Mre11*, *Xrcc2*, or *Xrcc3*, demonstrate centrosome amplification/fragmentation that, presumably, is coupled to the chromosome instability phenotype associated with these mutants (Tutt et al., 1999; Xu et al., 1999b; Yamaguchi-Iwai et al., 1999; Griffin et al., 2000). The chromosome

instability in *Rad51d*$^{-/-}$ *Trp53*$^{-/-}$ MEFs likely initiates an arrest at the G2 checkpoint, consistent with the increased percentage of *Rad51d*$^{-/-}$ *Trp53*$^{-/-}$ MEFs (19.2%) compared *Trp53*$^{-/-}$ MEFs (14.7%) in G2 (Figure 1D, Results, pg. 94). However, because the p53 protein is required to maintain the G2 arrest (Bunz et al., 1998), the *Rad51d*$^{-/-}$ *Trp53*$^{-/-}$ MEFs with damaged chromosomes continue into mitosis and initiate mitotic catastrophe. The increased percentage of sub-G1 cell signals from FACS analysis (Figure 1D, Results, pg. 94) would be consistent with micronucleated and dead cells following abnormal mitosis due to centrosome amplification/fragmentation in the *Rad51d*$^{-/-}$ *Trp53*$^{-/-}$ MEFs. Although the mitotic catastrophe pathway explains why cells with chromosomal instability have centrosome abnormalities, definitive answers to fundamental questions need addressed. For example, (1) do broken chromosomes initiate mitotic catastrophe? (2) when chromosomes are in the condensed state, how are they monitored for DNA damage? (3) what proteins monitor for chromosome damage during mitosis? and (4) what proteins are involved in the amplification/fragmentation of centrosomes?

These data discussed have implemented the RAD51D protein in DNA repair by HR. Based upon these data, I have proposed that RAD51D is necessary to repair stalled replication forks by the SDSA model for DSB repair. In the absence of RAD51D, SDSA repair is absent, which confers an increase in chromatid gaps and breaks. Because these chromosome abnormalities are not repaired in the absence of RAD51D, mitotic catastrophe is triggered as these cells progress through mitosis. Additionally, a model for the accurate repair of ICLs during DNA replication has been proposed. The next sections

discuss the potential roles of RAD51D at telomeres and two models of telomere dysfunction in RAD51D-deficient MEFs are proposed.

The RAD51D Protein Maintains Telomere Stability

In addition to its role in DNA repair, the RAD51D protein localizes to telomeres and functions to maintain telomere stability. Mouse embryonic fibroblasts lacking RAD51D have shorter telomeres and an increased frequency of telomere fusions (Tarsounas et al., 2004), both of which likely contribute to the embryonic lethal phenotype of *Rad51d*-deficient mice. Although a deficiency in other proteins that maintain telomere stability, such as TRF2 (van Steensel et al., 1998; Celli and de Lange, 2005), POT1 (Hockemeyer et al., 2005; Yang et al., 2005), Ku70 (Wei et al., 2002), Ku80 (Samper et al., 2000), or DNA-PKcs (Goytisolo et al., 2001), confer an increase in telomere fusions and/or accelerated telomere shortening, a disruption of the *Rad51d* gene is unique in that long telomeric single-stranded overhangs are observed in mutant cells. Two potential models of telomere dysfunction will be described that take into consideration the decrease in telomere lengths, the increase in telomere fusions, and the long telomeric 3′ overhangs observed in *Rad51d*-deficient MEFs.

In chromatin immunoprecipitation analyses, antibodies specific to RAD51D, but not RAD51 or the RAD51D interacting proteins RAD51C and XRCC2, pulled down significant levels of telomeric DNA. These data suggest that RAD51D is unique among the RAD51-family members by maintaining genomic integrity by telomere protection (Tarsounas et al., 2004). RAD51D, however, is not the only HR protein that is involved in telomere maintenance. Mouse embryonic fibroblasts deficient for *Rad54* have

decreased telomere lengths and increased levels of telomere fusions compared to wild-type controls, suggesting the RAD54 protein plays a role in telomere length maintenance and in telomere capping (Jaco et al., 2003). Biochemical analyses demonstrate that the RAD54 protein has ds-DNA-specific ATPase activity (Swagemakers et al., 1998) and the ability to translocate along duplex DNA to partially relax supercoiled DNA, suggesting that RAD54 is involved in chromatin remodeling (Tan et al., 1999; Ristic et al., 2001). Based upon the data from biochemical studies, it is proposed that the RAD54 protein alters chromatin structure at the telomere to allow for T-loop formation following DNA replication or for T-loop resolution before DNA replication (Jaco et al., 2003). The BLM helicase protein localizes to telomeres (Schawalder et al., 2003), potentially through the direct interaction of BLM with TRF2 (Opresko et al., 2002), BLM with POT1 (Opresko et al., 2005), or BLM with RAD51D (Braybrooke et al., 2003). Cells derived from patients with Bloom syndrome have accelerated telomere attrition *in vitro* (Klapper et al., 2001), and $Blm^{-/-}$ mice have shorter telomeres than controls (Du et al., 2004), demonstrating that BLM plays a role in telomere length maintenance. Biochemical analyses demonstrate that BLM is a DNA-stimulated ATPase, has 3′ to 5′ helicase activity, and is able to unwind synthetic Holliday junctions *in vitro* (Karow et al., 1997; Braybrooke et al., 2003). These biochemical properties of the BLM protein suggest that it is involved in branch migration of the T-loop or in the resolution of the protective T-loop structure prior to DNA replication. In addition to its role in unwinding ds-DNA, the BLM helicase protein unwinds G-quartets (also referred to as G4-DNA) (Sun et al., 1998). A G-quartet is a stable four-stranded DNA secondary structure stabilized by

Hoogsteen bonding between runs of guanines. Hoogsteen bonding (base pairing) is a non-Watson-Crick variation of base-pairing between nucleotides (Sen and Gilbert, 1988). Although G-quartets have not been observed *in vivo*, the stability and rapid formation under physiological salt concentrations *in vitro* suggest that these structures exist in cells (Sen and Gilbert, 1988). The G-rich telomeric strand is made up of tandem repeats of the sequence 5′-TTAGGG-3′ and is longer than the complementary C-rich telomeric strand, thus forming a single-stranded 3′ tail on the end of each chromosome. Because the single-stranded telomeric tail is G-rich, the BLM helicase may be required to remove G-quartets at telomeres.

Although, *in vitro*, purified TRF2 protein was able to reconfigure telomeres into T-loop structures, the reaction is not efficient, suggesting, *in vivo*, TRF2 is assisted by other factors that promote strand invasion of the single-stranded tail during the process of T-loop formation (Griffith et al., 1999; Stansel et al., 2001; de Lange, 2005). The RAD51D protein has DNA-stimulated ATPase activity (Braybrooke et al., 2000; Braybrooke et al., 2003) and can promote homologous pairing between single- and double-stranded DNA molecules (Kurumizaka et al., 2002; Yokoyama et al., 2004), making RAD51D a potential candidate for T-loop formation. In cells that express the dominant negative *TRF2*$^{\Delta B \Delta M}$ gene or are deficient for *Trf2*, most telomeres are recognized as DNA DSBs, as determined by the presence of γ-H2AX foci at telomeres, and high levels of telomere fusions are observed (van Steensel et al., 1998; Takai et al., 2003; Celli and de Lange, 2005). Because purified TRF2 reconfigures artificial telomeres into T-loops, the cell phenotypes observed when *TRF2* is disrupted suggest that

telomeres are unable to form the protective T-loops in the absence of the TRF2 protein. Compared to the *TRF2* disruption cell phenotypes, the increase in telomere fusions and γ-H2AX foci at telomeres in *Rad51d*-deficient MEFs is relatively small. These data suggest that the majority of telomeres in the *Rad51d*-deficient MEFs are still able to form the protective T-loops and that the RAD51D protein may function as an accessory factor to TRF2 in T-loop formation. Consistent with this proposal, the telomeric localization of TRF2 was normal in the *Rad51d*-deficient MEFs (Tarsounas et al., 2004). Because telomere lengths are decreased in *Rad51d*-deficient cells (Tarsounas et al., 2004), yet long telomeric 3′ overhangs were observed, one potential explanation is that excessive enzymatic degradation of the C-rich telomeric strand occurs. Several lines of evidence suggest that a 5′ to 3′ nuclease activity normally occurs at telomeres. First, telomeres replicated by leading strand synthesis have a blunt end. However, single-stranded G-rich tails were observed at all chromosome ends (Dionne and Wellinger, 1996; Makarov et al., 1997; Hemann and Greider, 1999). Second, with each population doubling, it was estimated that human cells grown in culture lose approximately 100 bp (Harley et al., 1990; Counter et al., 1992). This rate of shortening is faster than that expected from the end replication problem of lagging strand synthesis (see Figure 7, Literature, pg. 36), suggesting that telomere processing occurs following DNA replication. Although the nuclease responsible for the degradation has not been identified, this process is tightly regulated because the C-rich telomeric strand nearly always ends with the sequence ATC-5′ (Sfeir et al., 2005). I propose RAD51D assists TRF2 in the strand invasion step of T-loop formation (Figure 13). In this model, TRF2 is not able to perform strand invasion

Figure 13. Model of Telomere Dysfunction in *Rad51d*-deficient MEFs

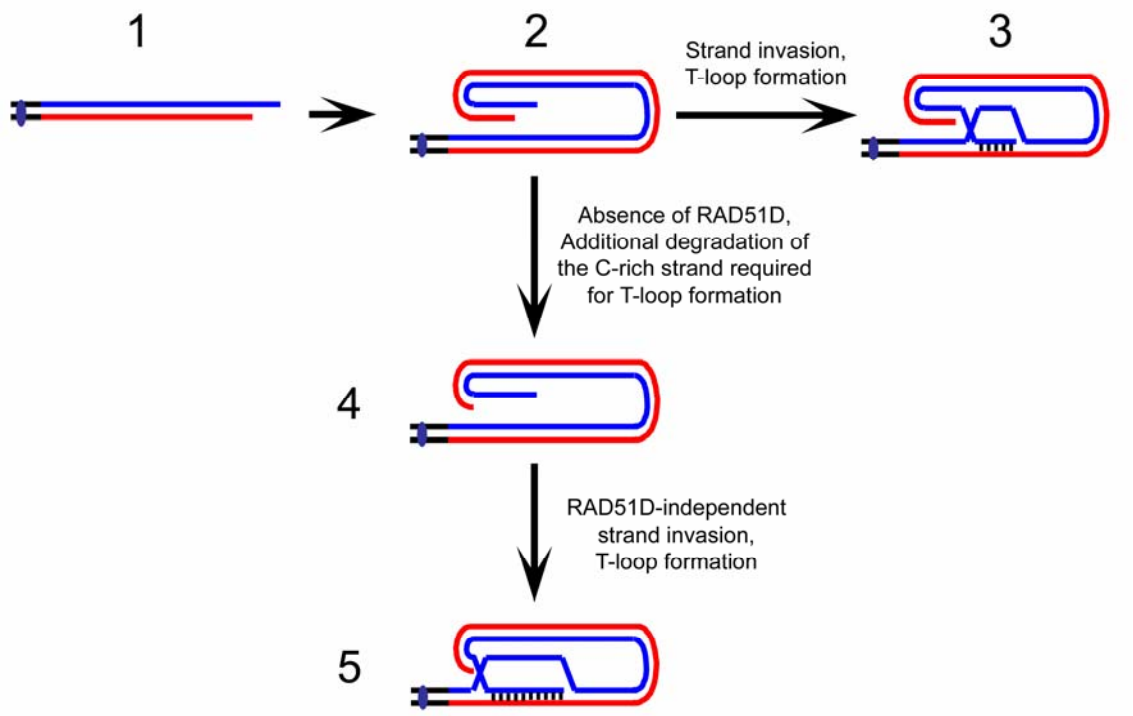

Model of telomere dysfunction in *Rad51d*-deficient MEFs. The blue lines represent the G-rich telomeric strand and the red lines represent the C-rich telomeric strand. The double black lines and the black oval represent non-telomeric DNA and the centromere, respectively. Normal T-loop formation is shown along the top (steps 1 through 3). In step 2 to 4, TRF2 is unable to form the protective T-loop efficiently in the absence of RAD51D. Therefore, additional 5′ to 3′ exonuclease degradation occurs to form a long telomeric 3′ overhang. With a longer substrate (ss-DNA), TRF2 is able to perform strand invasion to form the protective T-loop structure (step 4 to 5).

efficiently in the absence of RAD51D. Potentially, in order for strand invasion to occur, additional enzymatic degradation of the C-rich telomeric strand is required, which would provide more substrate (single-stranded DNA) for TRF2 to form the protective T-loop. This additional step in T-loop formation may initiate a transient DSB response (the phosphorylation of H2AX), consistent with the small increase in the frequency of γ-H2AX foci at telomeres observed in *Rad51d*-deficient MEFs. If additional 5′ to 3′

nuclease degradation of the C-rich strand occurs in the absence of RAD51D, accelerated telomere attrition would occur as a consequence when these cells divide, consistent with previous studies demonstrating decreased telomere lengths in *Rad51d*-deficient cells (Tarsounas et al., 2004).

An alternative model for the RAD51D protein at telomeres, based upon the direct interaction of RAD51D with BLM (Braybrooke et al., 2003), predicts that it is involved in the resolution of T-loops prior to DNA replication. This model, however, makes two assumptions. First, regarding the T-loop structure, the C-rich strand of the invading terminus pairs with the displaced D-loop. This pairing may occur normally if branch migration occurs at the T-loop and would likely stabilize the T-loop structure. The second assumption is that the RAD51D protein has the ability to re-anneal ss-DNA molecules that are homologous. In support of the second assumption, one biochemical activity of the RecA protein in *E. coli* is the renaturation of homologous ss-DNA to form ds-DNA. In these experiments, purified RecA protein was incubated with complementary single-stranded oligonucleotides. The DNA products from this reaction were double-stranded and resistant to the single-stranded DNA nuclease, S1 nuclease (Weinstock et al., 1979). Therefore, in addition to the RecA protein performing the strand invasion step during HR, RecA may be required in later stages of HR, for example, to re-anneal ss-DNA molecules following Holliday junction resolution. In mammalian cells, the RAD51-like proteins have been implicated in the late stages of HR (Y. Liu et al., 2004). RAD51D binds directly to BLM (Braybrooke et al., 2003), the BCDX2 complex (RAD51B-RAD51C-RAD51D, XRCC2) binds to synthetic Holliday junctions implying

that it can participate in the migration of joint structures in the cell (Yokoyama et al., 2004), and the RAD51C-XRCC3 heterodimer or the BCDX2 complex can perform branch migration and resolution of synthetic Holliday junctions (Y. Liu et al., 2004). Because RAD51C, the RAD51D-XRCC2 heterodimer, and the RAD51C-XRCC3 heterodimer are each able to perform homologous pairing (Kurumizaka et al., 2001, 2002; Lio et al., 2003) (see Table I, Literature, pg. 27), one could predict that each of these proteins or protein complexes, like RecA in *E. coli*, has ss-DNA re-annealing properties. The second model of telomere dysfunction in *Rad51d*-deficient MEFs predicts that the RAD51D protein functions to re-anneal the G- and C-rich telomeric strands after the resolution of the T-loop structure (Figure 14). Immediately after the T-loop is resolved, the G- and C-rich strands are in a single-stranded state and the single-stranded G-rich DNA may form G-quartets. Because of this secondary structure, the single-stranded C-rich DNA is inappropriately annealed. The BLM protein can resolve the G-quartet but, in the absence of RAD51D, the C-rich DNA is not annealed properly. As a consequence, the loop in the C-rich DNA may stall and terminate DNA replication at the end of the chromosome before the telomere is completely replicated, which would confer accelerated telomere shortening with each cell division.

Figure 14. Model of Telomere Dysfunction in *Rad51d*-deficient MEFs

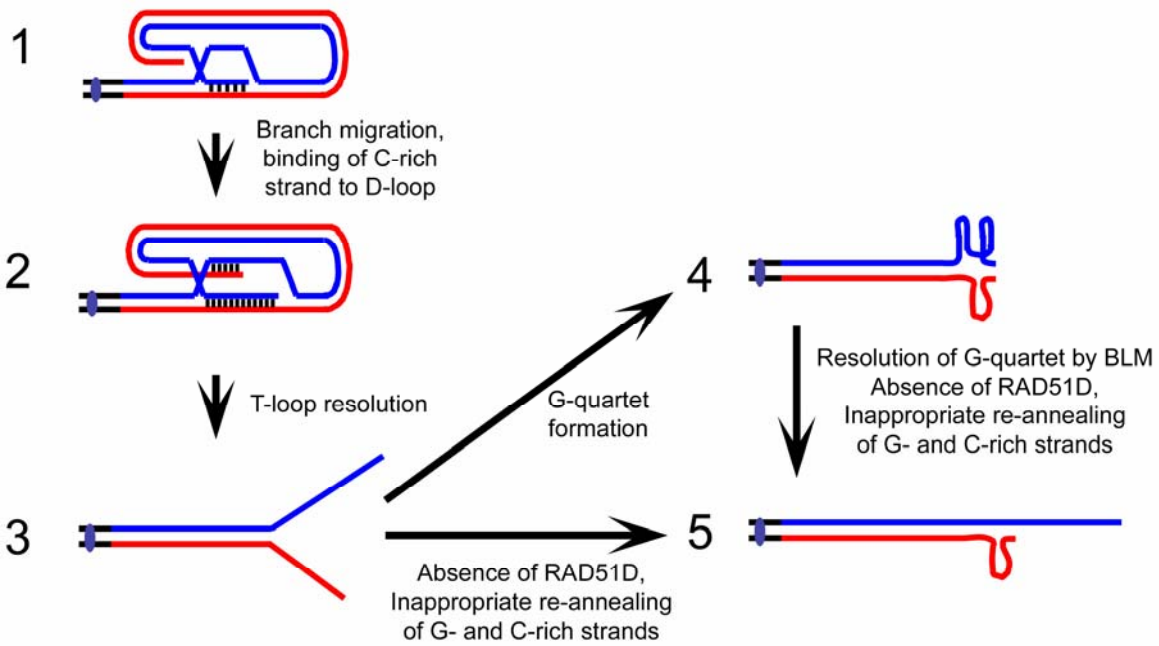

Model of telomere dysfunction in *Rad51d*-deficient MEFs. The blue lines represent the G-rich telomeric strand and the red lines represent the C-rich telomeric strand. The double black lines and the black oval represent non-telomeric DNA and the centromere, respectively. Step 1 to 2, following strand invasion and pairing of the single-stranded overhang into duplex DNA, branch migration occurs causing the C-rich strand to pair to the displaced D-loop. Step 2 to 3, the T-loop is resolved and the G- and C-rich strands are in a single-stranded state. Step 3 to 4, the G-rich strand may form G-quartets causing the C-rich strand to anneal inappropriately. Step 4 to 5, the G-quartet is resolved by BLM but, in the absence of RAD51D, the C-rich strand does not re-anneal to the G-rich strand properly. Step 3 to 5, alternatively, if G-quartets do not occur *in vivo*, the C- and G-rich strands do not anneal properly in the absence of RAD51D.

The following experiments will help to determine if RAD51D functions to assist TRF2 in T-loop formation (as proposed in Figure 13) or if RAD51D functions in the renaturation of G- and C-rich telomeric strands after T-loop resolution (as proposed in Figure 14). When purified human TRF2 protein is incubated with an artificial telomere, approximately 20% of the telomeres were remodeled into T-loops (viewed using electron

microscopy) (Griffith et al., 1999). If RAD51D assists TRF2 in T-loop formation, the addition of purified RAD51D to the TRF2/artificial telomere mixture should either increase the percentage of T-loops or increase the rate of T-loop formation (supporting proposal in Figure 13). Additionally, telomeres could be isolated from *Rad51d*$^{-/-}$ *Trp53*$^{-/-}$ and *Trp53*$^{-/-}$ MEFs, viewed by electron microscopy, and the percentage of telomeres in the T-loop formation quantified. If T-loops are not observed or are observed at decreased frequencies in the *Rad51d*$^{-/-}$ *Trp53*$^{-/-}$ MEFs, this would support that RAD51D assists TRF2 in T-loop formation, as proposed in Figure 13. If T-loops are present in the *Rad51d*$^{-/-}$ *Trp53*$^{-/-}$ MEFs, the length of the D-loop (which would correspond to the length of the single-stranded telomeric overhang) can be estimated by incubating the samples with the *E. coli* SSB (single-stranded DNA binding) protein. More SSB protein binding to the D-loop would correlate to long telomeric single-stranded overhangs (supporting proposal in Figure 13). Additionally, it may be possible to visualize DNA secondary structures at the termini of telomeres from *Rad51d*$^{-/-}$ *Trp53*$^{-/-}$ MEFs that are not in the T-loop formation (testing proposal in Figure 14). A final experiment is to determine if the last nucleotide on the C-rich telomeric strand is altered in the absence of RAD51D, using a method called "C-STELA" (for a schematic diagram, see Figure 15). In human cells, the C-rich telomeric strand nearly always ends with the sequence, ATC-5′ (Sfeir et al., 2005). C-STELA relies on PCR amplification of the entire telomere. Therefore, instead of using *Rad51d*$^{-/-}$ *Trp53*$^{-/-}$ and *Trp53*$^{-/-}$ MEFs (which have telomeres 40-50 kb in length), human cells (which have telomeres approximately 10 kb in length) with RAD51D synthesis inhibited by siRNA would have to be investigated. If the last nucleotides on the

Figure 15. Identifying the C-strand Terminal Nucleotides by C-STELA

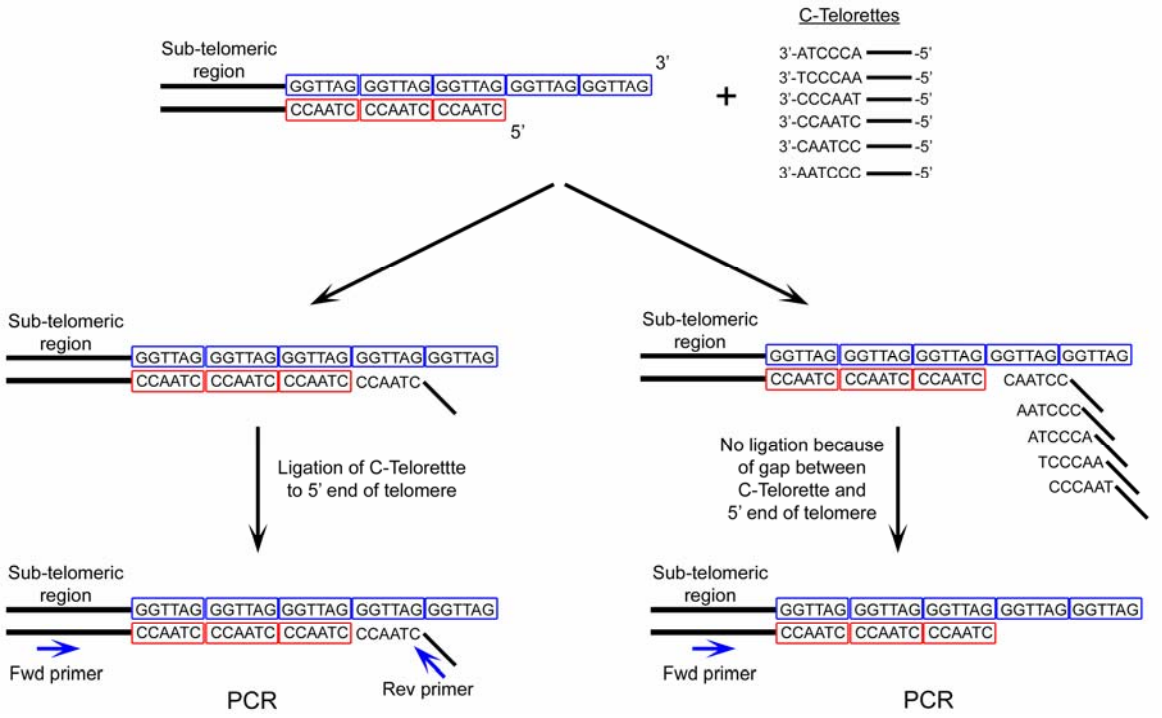

Identifying the C-strand terminal nucleotides by C-STELA. In six separate reactions, the six individual "C-telorettes", each containing a permutation of the telomeric sequence (3´-AATCCC-5´) and a non-complementary tail of known sequence (represented as a black line on the 5´ end of the C-telorette), are incubated with telomeric DNA. Only the C-telorette that anneals adjacent to the last base of the C-rich strand will be ligated to the telomere end (left). C-telorettes that do not anneal adjacent to the last base of the C-rich strand are not ligated to the telomere end (right). The products then undergo PCR amplification using a forward primer that is located in the sub-telomeric region and a reverse primer that is identical to the tail on the C-telorette (primers are represented as blue arrows). In this figure, exponential PCR amplification will only occur if the C-telorette is ligated to the telomere end (left). By this method, it was determined that the C-rich telomeric strand nearly always ends with the sequence, ATC-5´ (Sfeir et al., 2005). Figure was re-drawn with modifications from Sfeir et al., 2005.

C-rich strand are not ATC-5´, this would suggest nuclease degradation of the C-rich strand occurs in the absence of RAD51D (supporting the proposed model in Figure 13).

However, if the last nucleotides on the C-rich strand remain unchanged, this would

support the proposed model of telomere dysfunction in the absence of RAD51D described in Figure 14.

It is proposed by Wang et al. (2004) that, in addition to the "end replication problem," an alternative mechanism for telomere shortening can occur. It was demonstrated in human and mouse cells that a sudden decrease in length of individual telomeres can occur. The products from this sudden loss of individual telomeres included a short linear telomere at the chromosome end and a large circular DNA molecule containing the telomeric repeats. It was proposed that, instead of "unwinding" the T-loop (prior to DNA replication), the circular T-loop is cleaved off (Wang et al., 2004). Expression of $TRF2^{\Delta B}$, a mutant version of TRF2 that lacks the N-terminal basic domain, stimulates the cleavage of T-loops and confers accelerated telomere loss. Therefore, it is proposed that the N-terminal basic domain of TRF2 prevents cleavage of the T-loops by repressing proteins that cut the DNA of Holliday junction-like structures. As opposed to a mutant version of TRF2 that lacks both the N-terminal basic domain and the DNA binding domain ($TRF2^{\Delta B\Delta M}$), the mutant version of TRF2 that lacks only the N-terminal basic domain ($TRF2^{\Delta B}$) retains the ability to bind telomeric DNA and form T-loops on artificial telomeres *in vitro* (van Steensel et al., 1998; Wang et al., 2004). Additionally, cells expressing $TRF2^{\Delta B}$ have normal telomeric ss-overhang lengths and no increase in telomere fusions is observed. Therefore, the telomere dysfunction observed upon expression of $TRF2^{\Delta B}$ (telomere loss) is distinct compared to the telomere dysfunction observed upon expression of $TRF2^{\Delta B\Delta M}$ (loss of the telomeric ss-overhang, increase in telomere fusions) in mammalian cells (Wang et al., 2004). The cleavage of the T-loop in

cells expressing *TRF2*$^{\Delta B}$ is dependent upon the presence of the RAD51-like protein, XRCC3 (Wang et al., 2004), consistent with the role of the XRCC3-RAD51C heterodimer in resolving Holliday junctions *in vitro* (Y. Liu et al., 2004). Although the XRCC3 protein, by itself, does not have nuclease activity, it may bind to Holliday junction-like structures for the recruitment of a nuclease. The RAD51D protein was not required for the cleavage of T-loops in MEFs expressing *TRF2*$^{\Delta B}$ (Wang et al., 2004), suggesting that the potential resolution of Holliday junction activities by RAD51D are different compared to the resolution activities of XRCC3. One potential explanation is that RAD51D, together with the BLM helicase, promotes branch migration and the unwinding of Holliday junctions and T-loops (like the SDSA model, see Figure 3, Literature, pg. 13), whereas XRCC3 promotes cleavage of DNA strands in Holliday junctions and T-loops (like the DSBR model, see Figure 2, Literature, pg. 12).

Alternative Telomere Lengthening

The exact role(s) of the RAD51D protein at telomeres in immortalized cells that use the ALT pathway is not clear. Recall that ALT-positive cells do not express detectable levels of telomerase, which would be required to maintain telomere lengths (Yeager et al., 1999). Instead, ALT-positive cells use a HR mechanism for telomere elongation (see Figure 11, Literature, pg. 56) (for overview of ALT in yeast, see Literature, pgs. 39-41: for overview of ALT in mammalian cells, see Literature, pgs. 54-57). The localization of RAD51 at telomeres in ALT-positive cells, but not telomerase-positive cells, supports this idea (Yeager et al., 1999; Tarsounas et al., 2004). Madalena Tarsounas demonstrated the localization of RAD51D with the TRF2 protein at telomeres

in ALT-positive cells (Tarsounas et al., 2004). One explanation for RAD51D at telomeres in ALT cells is for HR-mediated telomere elongation. A second explanation for RAD51D at telomeres in ALT cells is for telomere protection, like that in the telomerase-positive MEFs. When RAD51D synthesis was inhibited by siRNA in ALT-positive cells, an increase in the number of telomere-telomere fusions and accelerated telomere shortening was observed compared to controls (Tarsounas et al., 2004). These phenotypes are similar to those observed in the telomerase-positive *Rad51d*-deficient MEFs, suggesting that RAD51D performs the same telomere protection functions in ALT-positive and telomerase-positive cells. In these experiments, however, the potential role of RAD51D in ALT was not tested. Because RAD51D is required for the localization of RAD51 to DNA repair foci in response to DNA damage (ionizing radiation) (see Figures 3A and 3B, Results, pg. 96), I hypothesize that RAD51D is also required for the localization of RAD51 to telomeres in ALT-positive cells. I predict that, if RAD51D synthesis is inhibited by siRNA in ALT-positive cells, RAD51 foci would not be visible at telomeres. Therefore, in addition to the roles of RAD51D in telomere protection (see above) (Tarsounas et al., 2004), these data would suggest that RAD51D is also required for ALT.

Telomere Lengths and Disease in Humans

It is proposed that telomere length may be used as a biomarker to predict the probability of developing age-related diseases in humans. Recent data demonstrate a correlation between patients with short telomeres and the development of hypertension (Jeanclos et al., 2000; Benetos et al., 2004), type 1 and type 2 diabetes (Jeanclos et al.,

1998; Adaikalakoteswari et al., 2005), and obesity (Valdes et al., 2005). Consistent with the hypothesis that short telomeres correlate to cardiac risk factors, mice in which telomeres are critically short due to a targeted gene disruption in telomerase have increased levels of heart failure (Leri et al., 2003). One concern with the human studies (Ibid.) is that telomere lengths were measured only in white blood cells, and not, for example, in the heart tissue. Therefore, a clear link between heart failure and short telomere lengths in this tissue cannot be concluded. It is likely that telomere lengths in white blood cells do represent the biological age rather than the chronological age of the patient. Because diseases develop as humans age, it is no surprise that biologically older individuals (patients with short telomeres) have an increased risk for developing these diseases. We tested the hypothesis that short telomeres associate with age-related diseases in rats selectively bred based upon low aerobic running capacity compared to rats selectively bred based upon high aerobic running capacity. Telomere lengths were measured in white blood cells and in heart, kidney, liver, spleen, skeletal muscle tissues from these animals, however, no significant difference in telomere length was observed between the low and high capacity running rats. These data demonstrated that, in this animal model, the development of metabolic risk factors is independent of differences in telomere length. In humans, it will be interesting to determine if biologically older patients (short telomeres) carry heritable mutations in genes that are required to maintain telomere length (for example RAD51D). A genetic mutation that confers accelerated telomere shortening would increase the rate of biological aging and, therefore, likely predispose these patients to developing age-related diseases.

Closing Remarks

In this thesis, I have described work towards understanding the importance of maintaining genome stability by characterizing mouse cells deficient for the *Rad51d* gene. These studies have demonstrated multiple roles of the RAD51D protein in the repair of DNA damage by HR and in telomere protection. From the data collected, it is interesting to speculate how RAD51D functions in these cellular processes, however, additional work, such as the experiments suggested in the Discussion, will be required to fully understand the mechanistic functions of RAD51D in these cellular processes. The knowledge and tools generated from this work will help provide a better understanding of RAD51D, and the machinery required for HR and telomere protection.

REFERENCES

Aaronson, S.A. and Todaro, G.J. (1968). Development of 3T3-like lines from Balb/c mouse embryo cultures: transformation susceptibility to SV40. J Cell Physiol *72*, 141-148.

Abbott, D.W., Freeman, M.L., and Holt, J.T. (1998). Double-strand break repair deficiency and radiation sensitivity in BRCA2 mutant cancer cells. J Natl Cancer Inst *90*, 978-985.

Abbott, D.W., Thompson, M.E., Robinson-Benion, C., Tomlinson, G., Jensen, R.A., and Holt, J.T. (1999). BRCA1 expression restores radiation resistance in BRCA1-defective cancer cells through enhancement of transcription-coupled DNA repair. J Biol Chem *274*, 18808-18812.

Aboussekhra, A., Chanet, R., Adjiri, A., and Fabre, F. (1992). Semidominant suppressors of Srs2 helicase mutations of Saccharomyces cerevisiae map in the RAD51 gene, whose sequence predicts a protein with similarities to procaryotic RecA proteins. Mol Cell Biol *12*, 3224-3234.

Adaikalakoteswari, A., Balasubramanyam, M., and Mohan, V. (2005). Telomere shortening occurs in Asian Indian Type 2 diabetic patients. Diabet Med *22*, 1151-1156.

Alani, E., Thresher, R., Griffith, J.D., and Kolodner, R.D. (1992). Characterization of DNA-binding and strand-exchange stimulation properties of y-RPA, a yeast single-strand-DNA-binding protein. J Mol Biol *227*, 54-71.

Albala, J.S., Thelen, M.P., Prange, C., Fan, W., Christensen, M., Thompson, L.H., and Lennon, G.G. (1997). Identification of a novel human RAD51 homolog, RAD51B. Genomics *46*, 476-479.

Allsopp R.C., Chang E., Kashefi-Aazam M., Rogaev E.I., Piatyszek M.A., Shay J.W., and Harley C.B. (1995). Telomere shortening is associated with cell division in vitro and in vivo. Exp Cell Res *220*, 194-200.

Allsopp R.C., Vaziri H., Patterson C., Goldstein S., Younglai E.V., Futcher A.B., Greider C.W., and Harley C.B. (1992). Telomere length predicts replicative capacity of human fibroblasts. Proc Natl Acad Sci U S A *89*, 10114-10118.

Artandi S.E., Chang S., Lee S.L., Alson S., Gottlieb G.J., Chin L., and DePinho R.A. (2000). Telomere dysfunction promotes non-reciprocal translocations and epithelial cancers in mice. Nature *406*, 641-645.

Auerbach, A.D., Adler, B., and Chaganti, R.S. (1981). Prenatal and postnatal diagnosis and carrier detection of Fanconi anemia by a cytogenetic method. Pediatrics *67*, 128-135.

Bailey, S.M., Cornforth, M.N., Kurimasa, A., Chen, D.J., and Goodwin, E.H. (2001). Strand-specific postreplicative processing of mammalian telomeres. Science *293*, 2462-2465.

Bailey, S.M., Meyne, J., Chen, D.J., Kurimasa, A., Li, G.C., Lehnert, B.E., and Goodwin, E.H. (1999). DNA double-strand break repair proteins are required to cap the ends of mammalian chromosomes. Proc Natl Acad Sci U S A *96*, 14899-14904.

Bakkenist, C.J. and Kastan, M.B. (2003). DNA damage activates ATM through intermolecular autophosphorylation and dimer dissociation. Nature *421*, 499-506.

Barlow, C., Hirotsune, S., Paylor, R., Liyanage, M., Eckhaus, M., Collins, F., Shiloh, Y., Crawley, J.N., Ried, T., Tagle, D., and Wynshaw-Boris, A. (1996). Atm-deficient mice: a paradigm of ataxia telangiectasia. Cell *86*, 159-171.

Barlund, M., Monni, O., Kononen, J., Cornelison, R., Torhorst, J., Sauter, G., Kallioniemi, O.-P., and Kallioniemi, A. (2000). Multiple genes at 17q23 undergo amplification and overexpression in breast cancer. Cancer Res *60*, 5340-5344.

Barnes D.E., Stamp G., Rosewell I., Denzel A., and Lindahl T. (1998). Targeted disruption of the gene encoding DNA ligase IV leads to lethality in embryonic mice. Curr Biol *8*, 1395-1398.

Basile, G., Aker, M., and Mortimer, R.K. (1992). Nucleotide sequence and transcriptional regulation of the yeast recombinational repair gene RAD51. Mol Cell Biol *12*, 3235-3246.

Bassing, C.H. and Alt, F.W. (2004). The cellular response to general and programmed DNA double strand breaks. DNA Repair (Amst) *3*, 781-796.

Baumann, P., Benson, F.E., and West, S.C. (1996). Human Rad51 protein promotes ATP-dependent homologous pairing and strand transfer reactions in vitro. Cell *87*, 757-766.

Baumann, P. and Cech, T.R. (2001). Pot1, the putative telomere end-binding protein in fission yeast and humans. Science *292*, 1171-1175.

Baumann, P. and West, S.C. (1997). The human Rad51 protein: polarity of strand transfer and stimulation by hRP-A. Embo J *16*, 5198-5206.

Beamish, H., Kedar, P., Kaneko, H., Chen, P., Fukao, T., Peng, C., Beresten, S., Gueven, N., Purdie, D., Lees-Miller, S., Ellis, N., Kondo, N., and Lavin, M.F. (2002). Functional link between BLM defective in Bloom's syndrome and the ataxia-telangiectasia-mutated protein, ATM. J Biol Chem *277*, 30515-30523.

Benedict C.L., Gilfillan S., Thai T.H., and Kearney J.F. (2000). Terminal deoxynucleotidyl transferase and repertoire development. Immunol Rev *175*, 150-157.

Benetos, A., Gardner, J.P., Zureik, M., Labat, C., Xiaobin, L., Adamopoulos, C., Temmar, M., Bean, K.E., Thomas, F., and Aviv, A. (2004). Short telomeres are associated with increased carotid atherosclerosis in hypertensive subjects. Hypertension *43*, 182-185.

Benetos, A., Okuda, K., Lajemi, M., Kimura, M., Thomas, F., Skurnick, J., Labat, C., Bean, K., and Aviv, A. (2001). Telomere length as an indicator of biological aging: the gender effect and relation with pulse pressure and pulse wave velocity. Hypertension *37*, 381-385.

Benson, F.E., Baumann, P., and West, S.C. (1998). Synergistic actions of Rad51 and Rad52 in recombination and DNA repair. Nature *391*, 401-404.

Benson, F.E., Stasiak, A., and West, S.C. (1994). Purification and characterization of the human Rad51 protein, an analogue of E. coli RecA. Embo J *13*, 5764-5771.

Bernards A., Michels P.A., Lincke C.R., and Borst P. (1983). Growth of chromosome ends in multiplying trypanosomes. Nature *303*, 592-597.

Bezzubova, O., Silbergleit, A., Yamaguchi-Iwai, Y., Takeda, S., and Buerstedde, J.M. (1997). Reduced X-ray resistance and homologous recombination frequencies in a RAD54-/- mutant of the chicken DT40 cell line. Cell *89*, 185-193.

Bhattacharyya, A., Ear, U.S., Koller, B.H., Weichselbaum, R.R., and Bishop, D.K. (2000). The breast cancer susceptibility gene BRCA1 is required for subnuclear assembly of Rad51 and survival following treatment with the DNA cross-linking agent cisplatin. J Biol Chem *275*, 23899-23903.

Bilaud, T., Brun, C., Ancelin, K., Koering, C.E., Laroche, T., and Gilson, E. (1997). Telomeric localization of TRF2, a novel human telobox protein. Nat Genet *17*, 236-239.

Bischof, O., Kim, S.H., Irving, J., Beresten, S., Ellis, N.A., and Campisi, J. (2001). Regulation and localization of the Bloom syndrome protein in response to DNA damage. J Cell Biol *153*, 367-380.

Blackburn, E.H. (1991). Structure and function of telomeres. Nature *350*, 569-573.

Blasco, M.A., Lee, H.W., Hande, M.P., Samper, E., Lansdorp, P.M., DePinho, R.A., and Greider, C.W. (1997). Telomere shortening and tumor formation by mouse cells lacking telomerase RNA. Cell *91*, 25-34.

Bodnar, A.G., Ouellette, M., Frolkis, M., Holt, S.E., Chiu, C.P., Morin, G.B., Harley, C.B., Shay, J.W., Lichtsteiner, S., and Wright, W.E. (1998). Extension of life-

span by introduction of telomerase into normal human cells. Science *279*, 349-352.

Borges A., and Liew C.C. (1997). Telomerase activity during cardiac development. J Mol Cell Cardiol *29*, 2717-2724.

Bork, P., Blomberg, N., and Nilges, M. (1996). Internal repeats in the BRCA2 protein sequence. Nat Genet *13*, 22-23.

Boswell R.E., Klobutcher L.A., and Prescott D.M. (1982). Inverted terminal repeats are added to genes during macronuclear development in Oxytricha nova. Proc Natl Acad Sci U S A *79*, 3255-3259.

Boulton, S.J. and Jackson, S.P. (1996). Identification of a Saccharomyces cerevisiae Ku80 homologue: roles in DNA double strand break rejoining and in telomeric maintenance. Nucleic Acids Res *24*, 4639-4648.

Braybrooke, J.P., Li, J.L., Wu, L., Caple, F., Benson, F.E., and Hickson, I.D. (2003). Functional interaction between the Bloom's syndrome helicase and the RAD51 paralog, RAD51L3 (RAD51D). J Biol Chem *278*, 48357-48366.

Braybrooke, J.P., Spink, K.G., Thacker, J., and Hickson, I.D. (2000). The RAD51 Family Member, RAD51L3, is a DNA-stimulated ATPase that Forms a Complex with XRCC2. J Biol Chem *275*, 29100-29106.

Bressan, D.A., Baxter, B.K., and Petrini, J.H. (1999). The Mre11-Rad50-Xrs2 protein complex facilitates homologous recombination-based double-strand break repair in Saccharomyces cerevisiae. Mol Cell Biol *19*, 7681-7687.

Britton S.L., and Koch L.G. (2005). Animal models of complex diseases: An initial strategy. IUBMB Life *57*, 631-638.

Broccoli, D., Smogorzewska, A., Chong, L., and de Lange, T. (1997). Human telomeres contain two distinct Myb-related proteins, TRF1 and TRF2. Nat Genet *17*, 231-235.

Brown, E.J. and Baltimore, D. (2000). ATR disruption leads to chromosomal fragmentation and early embryonic lethality. Genes Dev *14*, 397-402.

Bryan, T.M., Englezou, A., Gupta, J., Bacchetti, S., and Reddel, R.R. (1995). Telomere elongation in immortal human cells without detectable telomerase activity. Embo J *14*, 4240-4248.

Bunz, F., Dutriaux, A., Lengauer, C., Waldman, T., Zhou, S., Brown, J.P., Sedivy, J.M., Kinzler, K.W., and Vogelstein, B. (1998). Requirement for p53 and p21 to sustain G2 arrest after DNA damage. Science *282*, 1497-1501.

Burma, S., Chen, B.P., Murphy, M., Kurimasa, A., and Chen, D.J. (2001). ATM phosphorylates histone H2AX in response to DNA double-strand breaks. J Biol Chem *276*, 42462-42467.

Cartwright, R., Dunn, A.M., Simpson, P.J., Tambini, C.E., and Thacker, J. (1998). Isolation of novel human and mouse genes of the recA/RAD51 recombination-repair gene family. Nucleic Acids Res *26*, 1653-1659.

Castedo, M., Perfettini, J.L., Roumier, T., and Kroemer, G. (2002). Cyclin-dependent kinase-1: linking apoptosis to cell cycle and mitotic catastrophe. Cell Death Differ *9*, 1287-1293.

Celeste, A., Petersen, S., Romanienko, P.J., Fernandez-Capetillo, O., Chen, H.T., Sedelnikova, O.A., Reina-San-Martin, B., Coppola, V., Meffre, E., Difilippantonio, M.J., Redon, C., Pilch, D.R., Olaru, A., Eckhaus, M., Camerini-Otero, R.D., Tessarollo, L., Livak, F., Manova, K., Bonner, W.M., Nussenzweig, M.C., and Nussenzweig, A. (2002). Genomic instability in mice lacking histone H2AX. Science *296*, 922-927.

Celli, G.B. and de Lange, T. (2005). DNA processing is not required for ATM-mediated telomere damage response after TRF2 deletion. Nature Cell Biology *7*, 712-718.

Chaganti, R.S., Schonberg, S., and German, J. (1974). A manyfold increase in sister chromatid exchanges in Bloom's syndrome lymphocytes. Proc Natl Acad Sci U S A *71*, 4508-4512.

Chakhparonian, M. and Wellinger, R.J. (2003). Telomere maintenance and DNA replication: how closely are these two connected? Trends Genet *19*, 439-446.

Chan, C.S. and Tye, B.K. (1983). Organization of DNA sequences and replication origins at yeast telomeres. Cell *33*, 563-573.

Chan S.R., and Blackburn E.H. (2004). Telomeres and telomerase. Philos Trans R Soc Lond B Biol Sci *359*, 109-121.

Chen C.F., Chen P.L., Zhong Q., Sharp Z.D., and Lee W.H. (1999). Expression of BRC repeats in breast cancer cells disrupts the BRCA2-Rad51 complex and leads to radiation hypersensitivity and loss of G(2)/M checkpoint control. J Biol Chem *274*, 32931-32935.

Chen P.L., Chen C.F., Chen Y., Xiao J., Sharp Z.D., and Lee W.H. (1998). The BRC repeats in BRCA2 are critical for RAD51 binding and resistance to methyl methanesulfonate treatment. Proc Natl Acad Sci U S A *95*, 5287-5292.

Chen, Q., Ijpma, A., and Greider, C.W. (2001). Two survivor pathways that allow growth in the absence of telomerase are generated by distinct telomere recombination events. Mol Cell Biol *21*, 1819-1827.

Cherif H., Tarry J.L., Ozanne S.E., and Hales C.N. (2003). Ageing and telomeres: a study into organ- and gender-specific telomere shortening. Nucleic Acids Res *31*, 1576-1583.

Chester, N., Kuo, F., Kozak, C., O'Hara, C.D., and Leder, P. (1998). Stage-specific apoptosis, developmental delay, and embryonic lethality in mice homozygous for a targeted disruption in the murine Bloom's syndrome gene. Genes Dev *12*, 3382-3393.

Chiang, Y.J., Kim, S.H., Tessarollo, L., Campisi, J., and Hodes, R.J. (2004). Telomere-associated protein TIN2 is essential for early embryonic development through a telomerase-independent pathway. Mol Cell Biol *24*, 6631-6634.

Chin L., Artandi S.E., Shen Q., Tam A., Lee S.L., Gottlieb G.J., Greider C.W., and DePinho R.A. (1999). p53 deficiency rescues the adverse effects of telomere loss and cooperates with telomere dysfunction to accelerate carcinogenesis. Cell *97*, 527-538.

Chong, L., van Steensel, B., Broccoli, D., Erdjument-Bromage, H., Hanish, J., Tempst, P., and de Lange, T. (1995). A human telomeric protein. Science *270*, 1663-1667.

Ciapponi, L., Cenci, G., Ducau, J., Flores, C., Johnson-Schlitz, D., Gorski, M.M., Engels, W.R., and Gatti, M. (2004). The Drosophila Mre11/Rad50 complex is to prevent both telomeric fusion and chromosome breakage. Curr Biol *14*, 1360-1366.

Cleaver J.E. (1990). Do we know the cause of xeroderma pigmentosum? Carcinogenesis *11*, 875-882.

Cliby, W.A., Roberts, C.J., Cimprich, K.A., Stringer, C.M., Lamb, J.R., Schreiber, S.L., and Friend, S.H. (1998). Overexpression of a kinase-inactive ATR protein causes sensitivity to DNA-damaging agents and defects in cell cycle checkpoints. Embo J *17*, 159-169.

Collins A.M., Sewell W.A., and Edwards M.R. (2003). Immunoglobulin gene rearrangement, repertoire diversity, and the allergic response. Pharmacol Ther *100*, 157-170.

Connolly, B., Parsons, C.A., Benson, F.E., Dunderdale, H.J., Sharples, G.J., Lloyd, R.G., and West, S.C. (1991). Resolution of Holliday junctions in vitro requires the Escherichia coli ruvC gene product. Proc Natl Acad Sci U S A *88*, 6063-6067.

Connolly, B. and West, S.C. (1990). Genetic recombination in Escherichia coli: Holliday junctions made by RecA protein are resolved by fractionated cell-free extracts. Proc Natl Acad Sci U S A *87*, 8476-8480.

Constantinou, A., Tarsounas, M., Karow, J.K., Brosh, R.M., Bohr, V.A., Hickson, I.D., and West, S.C. (2000). Werner's syndrome protein (WRN) migrates Holliday junctions and co-localizes with RPA upon replication arrest. EMBO Rep *1*, 80-84.

Cortez, D., Wang, Y., Qin, J., and Elledge, S.J. (1999). Requirement of ATM-dependent phosphorylation of brca1 in the DNA damage response to double-strand breaks. Science *286*, 1162-1166.

Counter C.M. (1996). The roles of telomeres and telomerase in cell life span. Mutat Res *366*, 45-63.

Counter, C.M., Avilion, A.A., LeFeuvre, C.E., Stewart, N.G., Greider, C.W., Harley, C.B., and Bacchetti, S. (1992). Telomere shortening associated with chromosome instability is arrested in immortal cells which express telomerase activity. Embo J *11*, 1921-1929.

Cox, M.M. and Lehman, I.R. (1982). recA protein-promoted DNA strand exchange. Stable complexes of recA protein and single-stranded DNA formed in the presence of ATP and single-stranded DNA binding protein. J Biol Chem *257*, 8523-8532.

d'Adda di Fagagna, F., Reaper, P.M., Clay-Farrace, L., Fiegler, H., Carr, P., Von Zglinicki, T., Saretzki, G., Carter, N.P., and Jackson, S.P. (2003). A DNA damage checkpoint response in telomere-initiated senescence. Nature *426*, 194-198.

Davies, A.A., Masson, J.Y., McIlwraith, M.J., Stasiak, A.Z., Stasiak, A., Venkitaraman, A.R., and West, S.C. (2001). Role of BRCA2 in control of the RAD51 recombination and DNA repair protein. Mol Cell *7*, 273-282.

de Grey A.D. (1997). A proposed refinement of the mitochondrial free radical theory of aging. Bioessays *19*, 161-166.

de Klein, A., Muijtjens, M., van Os, R., Verhoeven, Y., Smit, B., Carr, A.M., Lehmann, A.R., and Hoeijmakers, J.H. (2000). Targeted disruption of the cell-cycle checkpoint gene ATR leads to early embryonic lethality in mice. Curr Biol *10*, 479-482.

de Laat, W.L., Appeldoorn, E., Jaspers, N.G., and Hoeijmakers, J.H. (1998). DNA structural elements required for ERCC1-XPF endonuclease activity. J Biol Chem *273*, 7835-7842.

de Lange, T. (2005). Shelterin: the protein complex that shapes and safeguards human telomeres. Genes Dev *19*, 2100-2110.

de Lange T. (1998). Telomeres and senescence: ending the debate. Science *279*, 334-335.

de Lange, T., Shiue, L., Myers, R.M., Cox, D.R., Naylor, S.L., Killery, A.M., and Varmus, H.E. (1990). Structure and variability of human chromosome ends. Mol Cell Biol *10*, 518-527.

De Silva, I.U., McHugh, P.J., Clingen, P.H., and Hartley, J.A. (2000). Defining the roles of nucleotide excision repair and recombination in the repair of DNA interstrand cross-links in mammalian cells. Mol Cell Biol *20*, 7980-7990.

Deans, B., Griffin, C.S., Maconochie, M., and Thacker, J. (2000). Xrcc2 is required for genetic stability, embryonic neurogenesis and viability in mice. Embo J *19*, 6675-6685.

Deans, B., Griffin, C.S., O'Regan, P., Jasin, M., and Thacker, J. (2003). Homologous recombination deficiency leads to profound genetic instability in cells derived from xrcc2-knockout mice. Cancer Res *63*, 8181-8187.

Deutscher M.P. (1984). Processing of tRNA in prokaryotes and eukaryotes. CRC Crit Rev Biochem *17*, 45-71.

Digweed, M., Reis, A., and Sperling, K. (1999). Nijmegen breakage syndrome: consequences of defective DNA double strand break repair. Bioessays *21*, 649-656.

Dionne, I. and Wellinger, R.J. (1996). Cell cycle-regulated generation of single-stranded G-rich DNA in the absence of telomerase. Proc Natl Acad Sci U S A *93*, 13902-13907.

Dokudovskaya, S.S., Petrov, A.V., Dontsova, O.A., and Bogdanov, A.A. (1997). Telomerase is an unusual RNA-containing enzyme. A review. Biochemistry *62*, 1206-1215.

Dong, Z., Zhong, Q., and Chen, P.L. (1999). The Nijmegen breakage syndrome protein is essential for Mre11 phosphorylation upon DNA damage. J Biol Chem *274*, 19513-19516.

Dosanjh, M.K., Collins, D.W., Fan, W., Lennon, G.G., Albala, J.S., Shen, Z., and Schild, D. (1998). Isolation and characterization of RAD51C, a new human member of the RAD51 family of related genes. Nucleic Acids Res *26*, 1179-1184.

Dronkert, M.L. and Kanaar, R. (2001). Repair of DNA interstrand cross-links. Mutat Res *486*, 217-247.

Du, X., Shen, J., Kugan, N., Furth, E.E., Lombard, D.B., Cheung, C., Pak, S., Luo, G., Pignolo, R.J., DePinho, R.A., Guarente, L., and Johnson, F.B. (2004). Telomere

shortening exposes functions for the mouse Werner and Bloom syndrome genes. Mol Cell Biol *24*, 8437-8446.

Dunham, M.A., Neumann, A.A., Fasching, C.L., and Reddel, R.R. (2000). Telomere maintenance by recombination in human cells. Nat Genet *26*, 447-450.

Dunkern T.R. and Kaina B. (2002). Cell proliferation and DNA breaks are involved in ultraviolet light-induced apoptosis in nucleotide excision repair-deficient Chinese hamster cells. Mol Biol Cell *13*, 348-361.

Elson, A., Wang, Y., Daugherty, C.J., Morton, C.C., Zhou, F., Campos-Torres, J., and Leder, P. (1996). Pleiotropic defects in ataxia-telangiectasia protein-deficient mice. Proc Natl Acad Sci U S A *93*, 13084-13089.

Epel, E.S., Blackburn, E.H., Lin, J., Dhabhar, F.S., Adler, N.E., Morrow, J.D., and Cawthon, R.M. (2004). Accelerated telomere shortening in response to life stress. Proc Natl Acad Sci U S A *101*, 17312-17315.

Essers, J., Hendriks, R.W., Swagemakers, S.M., Troelstra, C., de Wit, J., Bootsma, D., Hoeijmakers, J.H., and Kanaar, R. (1997). Disruption of mouse RAD54 reduces ionizing radiation resistance and homologous recombination. Cell *89*, 195-204.

Ferguson, D.O. and Holloman, W.K. (1996). Recombinational repair of gaps in DNA is asymmetric in Ustilago maydis and can be explained by a migrating D-loop model. Proc Natl Acad Sci USA *93*, 5419-5424.

Fiorentini, P., Huang, K.N., Tishkoff, D.X., Kolodner, R.D., and Symington, L.S. (1997). Exonuclease I of Saccharomyces cerevisiae functions in mitotic recombination in vivo and in vitro. Mol Cell Biol *17*, 2764-2773.

Franco S., Segura I., Riese H.H., and Blasco M.A. (2002). Decreased B16F10 melanoma growth and impaired vascularization in telomerase-deficient mice with critically short telomeres. Cancer Res *62*, 552-559.

Frank, K.M., Sekiguchi, J.M., Seidl, K.J., Swat, W., Rathbun, G.A., Cheng, H.L., Davidson, L., Kangaloo, L., and Alt, F.W. (1998). Late embryonic lethality and impaired V(D)J recombination in mice lacking DNA ligase IV. Nature *396*, 173-177.

Frank K.M., Sharpless N.E., Gao Y., Sekiguchi J.M., Ferguson D.O., Zhu C., Manis J.P., Horner J., DePinho R.A., and Alt F.W. (2000). DNA ligase IV deficiency in mice leads to defective neurogenesis and embryonic lethality via the p53 pathway. Mol Cell *5*, 993-1002.

French, C.A., Masson, J.Y., Griffin, C.S., O'Regan, P., West, S.C., and Thacker, J. (2002). Role of Mammalian RAD51L2 (RAD51C) in Recombination and Genetic Stability. J Biol Chem *277*, 19322-19330.

Game, J.C. and Mortimer, R.K. (1974). A genetic study of x-ray sensitive mutants in yeast. Mutat Res *24*, 281-292.

Gangloff, S., McDonald, J.P., Bendixen, C., Arthur, L., and Rothstein, R. (1994). The yeast type I topoisomerase Top3 interacts with Sgs1, a DNA helicase homolog: a potential eukaryotic reverse gyrase. Mol Cell Biol *14*, 8391-8398.

Gao Y., Ferguson D.O., Xie W., Manis J.P., Sekiguchi J., Frank K.M., Chaudhuri J., Horner J., DePinho R.A., and Alt F.W. (2000). Interplay of p53 and DNA-repair

protein XRCC4 in tumorigenesis, genomic stability and development. Nature *404*, 897-900.

Gao Y., Sun Y., Frank K.M., Dikkes P., Fujiwara Y., Seidl K.J., Sekiguchi J.M., Rathbun G.A., Swat W., Wang J., Bronson R.T., Malynn B.A., Bryans M., Zhu C., Chaudhuri J., Davidson L., Ferrini R., Stamato T., Orkin S.H., Greenberg M.E., and Alt F.W. (1998). A critical role for DNA end-joining proteins in both lymphogenesis and neurogenesis. Cell *95*, 891-902.

Gardner, J.P., Li, S., Srinivasan, S.R., Chen, W., Kimura, M., Lu, X., Berenson, G.S., and Aviv, A. (2005). Rise in insulin resistance is associated with escalated telomere attrition. Circulation *111*, 2171-2177.

Gasior, S.L., Olivares, H., Ear, U., Hari, D.M., Weichselbaum, R., and Bishop, D.K. (2001). Assembly of RecA-like recombinases: distinct roles for mediator proteins in mitosis and meiosis. Proc Natl Acad Sci U S A *98*, 8411-8418.

Gilfillan S., Dierich A., Lemeur M., Benoist C., and Mathis D. (1993). Mice lacking TdT: mature animals with an immature lymphocyte repertoire. Science *261*, 1175-1178.

Godthelp, B.C., Wiegant, W.W., van Duijn-Goedhart, A., Scharer, O.D., van Buul, P.P., Kanaar, R., and Zdzienicka, M.Z. (2002). Mammalian Rad51C contributes to DNA cross-link resistance, sister chromatid cohesion and genomic stability. Nucleic Acids Res *30*, 2172-2182.

Golubovskaya V.M., Presnell S.C., Hooth M.J., Smith G.J., and Kaufmann W.K. (1997). Expression of telomerase in normal and malignant rat hepatic epithelia. Oncogene *15*, 1233-1240.

Gottesfeld, J.M. and Forbes, D.J. (1997). Mitotic repression of the transcriptional machinery. Trends Biochem Sci *22*, 197-202.

Gottschling D.E., and Zakian V.A. (1986). Telomere proteins: specific recognition and protection of the natural termini of Oxytricha macronuclear DNA. Cell *47*, 195-205.

Gowen, L.C., Johnson, B.L., Latour, A.M., Sulik, K.K., and Koller, B.H. (1996). Brca1 deficiency results in early embryonic lethality characterized by neuroepithelial abnormalities. Nat Genet *12*, 191-194.

Goytisolo, F.A., Samper, E., Edmonson, S., Taccioli, G.E., and Blasco, M.A. (2001). The absence of the dna-dependent protein kinase catalytic subunit in mice results in anaphase bridges and in increased telomeric fusions with normal telomere length and G-strand overhang. Mol Cell Biol *21*, 3642-3651.

Graneli, A., Yeykal, C.C., Robertson, R.B., and Greene, E.C. (2006). Long-distance lateral diffusion of human Rad51 on double-stranded DNA. Proc Natl Acad Sci U S A.

Gravel, S., Larrivee, M., Labrecque, P., and Wellinger, R.J. (1998). Yeast Ku as a regulator of chromosomal DNA end structure. Science *280*, 741-744.

Greider C.W. (1996). Telomere length regulation. Annu Rev Biochem *65*, 337-365.

Greider C.W., and Blackburn E.H. (2004). Tracking telomerase. Cell *116*, S83-86.

Greider C.W., and Blackburn E.H. (1989). A telomeric sequence in the RNA of Tetrahymena telomerase required for telomere repeat synthesis. Nature *337*, 331-337.

Greider C.W., and Blackburn E.H. (1987). The telomere terminal transferase of Tetrahymena is a ribonucleoprotein enzyme with two kinds of primer specificity. Cell *51*, 887-898.

Greider C.W., and Blackburn E.H. (1985). Identification of a specific telomere terminal transferase activity in Tetrahymena extracts. Cell *43*, 405-413.

Griffin, C.S., Simpson, P.J., Wilson, C.R., and Thacker, J. (2000). Mammalian recombination-repair genes XRCC2 and XRCC3 promote correct chromosome segregation. Nat Cell Biol *2*, 757-761.

Griffith, J.D., Comeau, L., Rosenfield, S., Stansel, R.M., Bianchi, A., Moss, H., and de Lange, T. (1999). Mammalian telomeres end in a large duplex loop. Cell *97*, 503-514.

Grobelny, J.V., Godwin, A.K., and Broccoli, D. (2000). ALT-associated PML bodies are present in viable cells and are enriched in cells in the G(2)/M phase of the cell cycle. J Cell Sci *24*, 4577-4585.

Gu, Y., Jin, S., Gao, Y., Weaver, D.T., and Alt, F.W. (1997). Ku70-deficient embryonic stem cells have increased ionizing radiosensitivity, defective DNA end-binding activity, and inability to support V(D)J recombination. Proc Natl Acad Sci U S A *94*, 8076-8081.

Gupta, R.C., Folta-Stogniew, E., and Radding, C.M. (1999). Human Rad51 protein can form homologous joints in the absence of net strand exchange. J Biol Chem *274*, 1248-1256.

Haaf, T., Golub, E.I., Reddy, G., Radding, C.M., and Ward, D.C. (1995). Nuclear foci of mammalian Rad51 recombination protein in somatic cells after DNA damage and its localization in synaptonemal complexes. Proc Natl Acad Sci U S A *92*, 2298-2302.

Habu, T., Taki, T., West, A., Nishimune, Y., and Morita, T. (1996). The mouse and human homologs of DMC1, the yeast meiosis-specific homologous recombination gene, have a common unique form of exon-skipped transcript in meiosis. Nucleic Acids Res *24*, 470-477.

Hagting, A., Den Elzen, N., Vodermaier, H.C., Waizenegger, I.C., Peters, J.M., and Pines, J. (2002). Human securin proteolysis is controlled by the spindle checkpoint and reveals when the APC/C switches from activation by Cdc20 to Cdh1. J Cell Biol *157*, 1125-1137.

Hakem, R., de la Pompa, J.L., Sirard, C., Mo, R., Woo, M., Hakem, A., Wakeham, A., Potter, J., Reitmair, A., Billia, F., Firpo, E., Hui, C.C., Roberts, J., Rossant, J., and Mak, T.W. (1996). The tumor suppressor gene Brca1 is required for embryonic cellular proliferation in the mouse. Cell *85*, 1009-1023.

Hall, S.D., Kane, M.F., and Kolodner, R.D. (1993). Identification and characterization of the Escherichia coli RecT protein, a protein encoded by the recE region that promotes renaturation of homologous single-stranded DNA. J Bacteriol *175*, 277-287.

Hao L.Y., Strong M.A., and Greider C.W. (2004). Phosphorylation of H2AX at short telomeres in T cells and fibroblasts. J Biol Chem *279*, 45148-45154.

Hara, E., Tsurui, H., Shinozaki, A., Nakada, S., and Oda, K. (1991). Cooperative effect of antisense-Rb and antisense-p53 oligomers on the extension of life span in human diploid fibroblasts, TIG-1. Biochem Biophys Res Commun *179*, 528-534.

Harley C.B. (1991). Telomere loss: mitotic clock or genetic time bomb? Mutat Res *256*, 271-282.

Harley, C.B., Futcher, A.B., and Greider, C.W. (1990). Telomeres shorten during ageing of human fibroblasts. Nature *345*, 458-460.

Harley, C.B., Vaziri, H., Counter, C.M., and Allsopp, R.C. (1992). The telomere hypothesis of cellular aging. Exp Gerontol *27*, 375-382.

Harrington L. (2003). Biochemical aspects of telomerase function. Cancer Lett *194*, 139-154.

Harvey M., Sands A.T., Weiss R.S., Hegi M.E., Wiseman R.W., Pantazis P., Giovanella B.C., Tainsky M.A., Bradley A., and Donehower L.A. (1993). In vitro growth characteristics of embryo fibroblasts isolated from p53-deficient mice. Oncogene *8*, 2457-2467.

Hays, S.L., Firmenich, A.A., and Berg, P. (1995). Complex formation in yeast double-strand break repair: participation of Rad51, Rad52, Rad55, and Rad57 proteins. Proc Natl Acad Sci U S A *92*, 6925-6929.

Heald, R., McLoughlin, M., and McKeon, F. (1993). Human wee1 maintains mitotic timing by protecting the nucleus from cytoplasmically activated Cdc2 kinase. Cell *74*, 463-474.

Hefferin, M.L. and Tomkinson, A.E. (2005). Mechanism of DNA double-strand break repair by non-homologous end joining. DNA Repair (Amst) *4*, 639-648.

Helleday, T. (2003). Pathways for mitotic homologous recombination in mammalian cells. Mutat Res *532*, 103-115.

Hemann, M.T. and Greider, C.W. (1999). G-strand overhangs on telomeres in telomerase-deficient mouse cells. Nucleic Acids Res *27*, 3964-3969.

Hemann M.T., Strong M.A., Hao L.Y., and Greider C.W. (2001). The shortest telomere, not average telomere length, is critical for cell viability and chromosome stability. Cell *107*, 67-77.

Herrera E., Samper E., Martin-Caballero J., Flores J.M., Lee H.W., and Blasco M.A. (1999). Disease states associated with telomerase deficiency appear earlier in mice with short telomeres. Embo J *18*, 2950-2960.

Higgins, N.P., Kato, K., Strauss, B. (1976). A model for replication repair in mammalian cells. J Mol Biol *101*, 417-425.

Hockemeyer, D., Sfeir, A.J., Shay, J.W., Wright, W.E., and de Lange, T. (2005). POT1 protects telomeres from a transient DNA damage response and determines how human chromosomes end. Embo J *24*, 2667-2678.

Houghtaling, B.R., Cuttonaro, L., Chang, W., and Smith, S. (2004). A dynamic molecular link between the telomere length regulator TRF1 and the chromosome end protector TRF2. Curr Biol *14*, 1621-1631.

Hsu, H.L., Gilley, D., Blackburn, E.H., and Chen, D.J. (1999). Ku is associated with the telomere in mammals. Proc Natl Acad Sci U S A *96*, 12454-12458.

Hu, P., Beresten, S.F., van Brabant, A.J., Ye, T.Z., Pandolfi, P.P., Johnson, F.B., Guarente, L., and Ellis, N.A. (2001). Evidence for BLM and Topoisomerase IIIalpha interaction in genomic stability. Hum Mol Genet *10*, 1287-1298.

Huffman K.E., Levene S.D., Tesmer V.M., Shay J.W., and Wright W.E. (2000). Telomere shortening is proportional to the size of the G-rich telomeric 3'-overhang. J Biol Chem *275*, 19719-19722.

Hussain, S., Witt, E., Huber, P.A., Medhurst, A.L., Ashworth, A., and Mathew, C.G. (2003). Direct interaction of the Fanconi anaemia protein FANCG with BRCA2/FANCD1. Hum Mol Genet *12*, 2503-2510.

Ingraham, S.E., Lynch, R.A., Kathiresan, S., Buckler, A.J., and Menon, A.G. (1999). hREC2, a RAD51-like gene, is disrupted by t(12;14) (q15;q24.1) in a uterine leiomyoma. Cancer Genet Cytogenet *115*, 56-61.

Ivanov, E.L., Sugawara, N., White, C.I., Fabre, F., and Haber, J.E. (1994). Mutations in XRS2 and RAD50 delay but do not prevent mating-type switching in Saccharomyces cerevisiae. Mol Cell Biol *14*, 3414-3425.

Jacks T., Remington L., Williams B.O., Schmitt E.M., Halachmi S., Bronson R.T., and Weinberg R.A. (1994). Tumor spectrum analysis in p53-mutant mice. Curr Biol *4*, 1-7.

Jaco, I., Munoz, P., Goytisolo, F., Wesoly, J., Bailey, S., Taccioli, G., and Blasco, M.A. (2003). Role of mammalian Rad54 in telomere length maintenance. Mol Cell Biol *23*, 5572-5580.

Jeanclos, E., Krolewski, A., Skurnick, J., Kimura, M., Aviv, H., Warram, J.H., and Aviv, A. (1998). Shortened telomere length in white blood cells of patients with IDDM. Diabetes *47*, 482-486.

Jeanclos, E., Schork, N.J., Kyvik, K.O., Kimura, M., Skurnick, J.H., and Aviv, A. (2000). Telomere length inversely correlates with pulse pressure and is highly familial. Hypertension *36*, 195-200.

Jennings B.J., Ozanne S.E., Dorling M.W., and Hales C.N. (1999). Early growth determines longevity in male rats and may be related to telomere shortening in the kidney. FEBS Lett *448*, 4-8.

Johnson, F.B., Lombard, D.B., Neff, N.F., Mastrangelo, M.A., Dewolf, W., Ellis, N.A., Marciniak, R.A., Yin, Y., Jaenisch, R., and Guarente, L. (2000). Association of the Bloom syndrome protein with topoisomerase IIIalpha in somatic and meiotic cells. Cancer Res *60*, 1162-1167.

Johnson, R.D. and Jasin, M. (2001). Double-strand-break-induced homologous recombination in mammalian cells. Biochem Soc Trans *29*, 196-201.

Johnson, R.D. and Symington, L.S. (1995). Functional differences and interactions among the putative RecA homologs Rad51, Rad55, and Rad57. Mol Cell Biol *15*, 4843-4850.

Jones, N.J., Cox, R., and Thacker, J. (1987). Isolation and cross-sensitivity of X-ray-sensitive mutants of V79-4 hamster cells. Mutat Res *183*, 279-286.

Jonkers, J., Meuwissen, R., van der Gulden, H., Peterse, H., van der Valk, M., and Berns, A. (2001). Synergistic tumor suppressor activity of BRCA2 and p53 in a conditional mouse model for breast cancer. Nat Genet *29*, 418-425.

Kajstura J., Pertoldi B., Leri A., Beltrami C.A., Deptala A., Darzynkiewicz Z., and Anversa P. (2000). Telomere shortening is an in vivo marker of myocyte replication and aging. Am J Pathol *156*, 813-819.

Kang, J., Bronson, R.T., and Xu, Y. (2002). Targeted disruption of NBS1 reveals its roles in mouse development and DNA repair. Embo J *21*, 1447-1455.

Karlseder, J., Broccoli, D., Dai, Y., Hardy, S., and de Lange, T. (1999). p53- and ATM-dependent apoptosis induced by telomeres lacking TRF2. Science *283*, 1321-1325.

Karlseder, J., Kachatrian, L., Takai, H., Mercer, K., Hingorani, S., Jacks, T., and de Lange, T. (2003). Targeted deletion reveals an essential function for the telomere length regulator Trf1. Mol Cell Biol *23*, 6533-6541.

Karlseder, J., Smogorzewska, A., and de Lange, T. (2002). Senescence induced by altered telomere state, not telomere loss. Science *295*, 2446-2449.

Karow, J.K., Chakraverty, R.K., and Hickson, I.D. (1997). The Bloom's syndrome gene product is a 3'-5' DNA helicase. J Biol Chem *272*, 30611-30614.

Kass-Eisler, A. and Greider, C.W. (2000). Recombination in telomere-length maintenance. Trends Biochem Sci *25*, 200-204.

Kastan, M.B. and Lim, D.S. (2000). The many substrates and functions of ATM. Nat Rev Mol Cell Biol *1*, 179-186.

Kato, M., Yano, K., Matsuo, F., Saito, H., Katagiri, T., Kurumizaka, H., Yoshimoto, M., Kasumi, F., Akiyama, F., Sakamoto, G., Nagawa, H., Nakamura, Y., and Miki, Y. (2000). Identification of Rad51 alteration in patients with bilateral breast cancer. J Hum Genet *45*, 133-137.

Kawabata M. and Saeki K. (1999). Multiple alternative transcripts of the human homologue of the mouse TRAD/R51H3/RAD51D gene, a member of the rec A/RAD51 gene family. Biochem Biophys Res Commun *257*, 156-162.

Kawabata, M. and Saeki, K. (1998). Sequence analysis and expression of a novel mouse homolog of Escherichia coli recA gene. Biochim Biophys Acta *1398*, 353-358.

Kim, N.W., Piatyszek, M.A., Prowse, K.R., Harley, C.B., West, M.D., Ho, P.L., Coviello, G.M., Wright, W.E., Weinrich, S.L., and Shay, J.W. (1994). Specific association of human telomerase activity with immortal cells and cancer. Science *266*, 2011-2015.

Kim, S.H., Kaminker, P., and Campisi, J. (1999). TIN2, a new regulator of telomere length in human cells. Nat Genet *23*, 405-412.

Kipling D., and Cooke H.J. (1990). Hypervariable ultra-long telomeres in mice. Nature *347*, 400-402.

Klapper, W., Parwaresch, R., and Krupp, G. (2001). Telomere biology in human aging and aging syndromes. Mech Ageing Dev *122*, 695-712.

Kohn, P.H., Whang-Peng, J., and Levis, W.R. (1982). Chromosomal instability in ataxia telangiectasia. Cancer Genet Cytogenet *6*, 289-302.

Komori T., Okada A., Stewart V., and Alt F.W. (1993). Lack of N regions in antigen receptor variable region genes of TdT-deficient lymphocytes. Science *261*, 1171-1175.

Kowalczykowski, S.C., Dixon, D.A., Eggleston, A.K., Lauder, S.D., and Rehrauer, W.M. (1994). Biochemistry of homologous recombination in Escherichia coli. Microbiol Rev *58*, 401-465.

Kowalczykowski, S.C. and Krupp, R.A. (1987). Effects of Escherichia coli SSB protein on the single-stranded DNA-dependent ATPase activity of Escherichia coli RecA protein. Evidence that SSB protein facilitates the binding of RecA protein to regions of secondary structure within single-stranded DNA. J Mol Biol *193*, 97-113.

Kraakman-van der Zwet, M., Overkamp, W.J., van Lange, R.E., Essers, J., van Duijn-Goedhart, A., Wiggers, I., Swaminathan, S., van Buul, P.P., Errami, A., Tan, R.T., Jaspers, N.G., Sharan, S.K., Kanaar, R., and Zdzienicka, M.Z. (2002). Brca2 (XRCC11) deficiency results in radioresistant DNA synthesis and a higher frequency of spontaneous deletions. Mol Cell Biol *22*, 669-679.

Krogh, B.O. and Symington, L.S. (2004). Recombination proteins in yeast. Annu Rev Genet *38*, 233-271.

Kurumizaka, H., Ikawa, S., Nakada, M., Eda, K., Kagawa, W., Takata, M., Takeda, S., Yokoyama, S., and Shibata, T. (2001). Homologous-pairing activity of the human DNA-repair proteins Xrcc3.Rad51C. Proc Natl Acad Sci U S A *98*, 5538-5543.

Kurumizaka, H., Ikawa, S., Nakada, M., Enomoto, R., Kagawa, W., Kinebuchi, T., Yamazoe, M., Yokoyama, S., and Shibata, T. (2002). Homologous pairing and ring and filament structure formation activities of the human Xrcc2:Rad51D complex. J Biol Chem *277*, 14315-14320.

Larminat, F. and Bohr, V.A. (1994). Role of the human ERCC-1 gene in gene-specific repair of cisplatin-induced DNA damage. Nucleic Acids Res *22*, 3005-3010.

Laroche, T., Martin, S.G., Gotta, M., Gorham, H.C., Pryde, F.E., Louis, E.J., and Gasser, S.M. (1998). Mutation of yeast Ku genes disrupts the subnuclear organization of telomeres. Curr Biol *8*, 653-656.

Lavin, M.F. and Khanna, K.K. (1999). ATM: the protein encoded by the gene mutated in the radiosensitive syndrome ataxia-telangiectasia. Int J Radiat Biol *75*, 1201-1214.

Le, S., Moore, J.K., Haber, J.E., and Greider, C.W. (1999). RAD50 and RAD51 define two pathways that collaborate to maintain telomeres in the absence of telomerase. Genetics *152*, 143-152.

Lebel, M., Spillare, E.A., Harris, C.C., and Leder, P. (1999). The Werner syndrome gene product co-purifies with the DNA replication complex and interacts with PCNA and topoisomerase I. J Biol Chem *274*, 37795-37799.

Lee, H.W., Blasco, M.A., Gottlieb, G.J., Horner, J.W., 2nd, Greider, C.W., and DePinho, R.A. (1998). Essential role of mouse telomerase in highly proliferative organs. Nature *392*, 569-574.

Lejnine S., Makarov V.L., and Langmore J.P. (1995). Conserved nucleoprotein structure at the ends of vertebrate and invertebrate chromosomes. Proc Natl Acad Sci U S A *92*, 2393-2397.

Lendvay, T.S., Morris, D.K., Sah, J., Balasubramanian, B., and Lundblad, V. (1996). Senescence mutants of Saccharomyces cerevisiae with a defect in telomere replication identify three additional EST genes. Genetics *144*, 1399-1412.

Leri, A., Franco, S., Zacheo, A., Barlucchi, L., Chimenti, S., Limana, F., Nadal-Ginard, B., Kajstura, J., Anversa, P., and Blasco, M.A. (2003). Ablation of telomerase and telomere loss leads to cardiac dilatation and heart failure associated with p53 upregulation. Embo J *22*, 131-139.

Levy-Lahad, E., Lahad, A., Eisenberg, S., Dagan, E., Paperna, T., Kasinetz, L., Catane, R., Kaufman, B., Beller, U., Renbaum, P., and Gershoni-Baruch, R. (2001). A single nucleotide polymorphism in the RAD51 gene modifies cancer risk in BRCA2 but not BRCA1 carriers. Proc Natl Acad Sci U S A *98*, 3232-3236.

Li, B., Oestreich, S., and de Lange, T. (2000). Identification of human Rap1: implications for telomere evolution. Cell *101*, 471-483.

Lim, D.S. and Hasty, P. (1996). A mutation in mouse rad51 results in an early embryonic lethal that is suppressed by a mutation in p53. Mol Cell Biol *16*, 7133-7143.

Lin J.J., and Zakian V.A. (1996). The Saccharomyces CDC13 protein is a single-strand TG1-3 telomeric DNA-binding protein in vitro that affects telomere behavior in vivo. Proc Natl Acad Sci U S A *93*, 13760-13765.

Lingner, J., Hughes, T.R., Shevchenko, A., Mann, M., Lundblad, V., and Cech, T.R. (1997). Reverse transcriptase motifs in the catalytic subunit of telomerase. Science *276*, 561-567.

Lio, Y.C., Mazin, A.V., Kowalczykowski, S.C., and Chen, D.J. (2003). Complex formation by the human Rad51B and Rad51C DNA repair proteins and their activities in vitro. J Biol Chem *278*, 2469-2478.

Lio, Y.C., Schild, D., Brenneman, M.A., Redpath, J.L., and Chen, D.J. (2004). Human Rad51C deficiency destabilizes XRCC3, impairs recombination, and radiosensitizes S/G2-phase cells. J Biol Chem *279*, 42313-42320.

Liu, C.Y., Flesken-Nikitin, A., Li, S., Zeng, Y., and Lee, W.H. (1996). Inactivation of the mouse Brca1 gene leads to failure in the morphogenesis of the egg cylinder in early postimplantation development. Genes Dev *10*, 1835-1843.

Liu, D., O'Connor, M.S., Qin, J., and Songyang, Z. (2004a). Telosome, a mammalian telomere-associated complex formed by multiple telomeric proteins. J Biol Chem *279*, 51338-51342.

Liu, D., Safari, A., O'Connor, M.S., Chan, D.W., Laegeler, A., Qin, J., and Songyang, Z. (2004b). PTOP interacts with POT1 and regulates its localization to telomeres. Nature Cell Biology *6*, 673-680.

Liu, N., Lamerdin, J.E., Tebbs, R.S., Schild, D., Tucker, J.D., Shen, M.R., Brookman, K.W., Siciliano, M.J., Walter, C.A., Fan, W., Narayana, L.S., Zhou, Z.Q., Adamson, A.W., Sorensen, K.J., Chen, D.J., Jones, N.J., and Thompson, L.H. (1998). XRCC2 and XRCC3, new human Rad51-family members, promote

chromosome stability and protect against DNA cross-links and other damages. Mol Cell *1*, 783-793.

Liu, N., Schild, D., Thelen, M.P., and Thompson, L.H. (2002). Involvement of Rad51C in two distinct protein complexes of Rad51 paralogs in human cells. Nucleic Acids Res *30*, 1009-1015.

Liu, Y., Masson, J.Y., Shah, R., O'Regan, P., and West, S.C. (2004). RAD51C is required for Holliday junction processing in mammalian cells. Science *303*, 243-246.

Loayza D., and De Lange T. (2003). POT1 as a terminal transducer of TRF1 telomere length control. Nature *423*, 1013-1018.

Loayza D., Parsons H., Donigian J., Hoke K., and de Lange T. (2004). DNA binding features of human POT1: a nonamer 5'-TAGGGTTAG-3' minimal binding site, sequence specificity, and internal binding to multimeric sites. J Biol Chem *279*, 13241-13248.

Lucas D.T., and Szweda L.I. (1999). Declines in mitochondrial respiration during cardiac reperfusion: age-dependent inactivation of alpha-ketoglutarate dehydrogenase. Proc Natl Acad Sci U S A *96*, 6689-6693.

Ludwig, T., Chapman, D.L., Papaioannou, V.E., and Efstratiadis, A. (1997). Targeted mutations of breast cancer susceptibility gene homologs in mice: lethal phenotypes of Brca1, Brca2, Brca1/Brca2, Brca1/p53, and Brca2/p53 nullizygous embryos. Genes Dev *11*, 1226-1241.

Lundblad, V. and Blackburn, E.H. (1993). An alternative pathway for yeast telomere maintenance rescues est1- senescence. Cell *73*, 347-360.

Luo, G., Santoro, I.M., McDaniel, L.D., Nishijima, I., Mills, M., Youssoufian, H., Vogel, H., Schultz, R.A., and Bradley, A. (2000). Cancer predisposition caused by elevated mitotic recombination in Bloom mice. Nat Genet *26*, 424-429.

Luo, G., Yao, M.S., Bender, C.F., Mills, M., Bladl, A.R., Bradley, A., and Petrini, J.H. (1999). Disruption of mRad50 causes embryonic stem cell lethality, abnormal embryonic development, and sensitivity to ionizing radiation. Proc Natl Acad Sci U S A *96*, 7376-7381.

Maacke, H., Opitz, S., Jost, K., Hamdorf, W., Henning, W., Kruger, S., Feller, A.C., Lopens, A., Diedrich, K., Schwinger, E., and Sturzbecher, H.W. (2000). Over-expression of wild-type Rad51 correlates with histological grading of invasive ductal breast cancer. Int J Cancer *88*, 907-913.

MacKay, V. and Linn, S. (1974). The mechanism of degradation of duplex deoxyribonucleic acid by the recBC enzyme of Escherichia coli K-12. J Biol Chem *249*, 4286-4294.

Maizels N., Weiner A.M., Yue D., and Shi P.Y. (1999). New evidence for the genomic tag hypothesis: archaeal CCA-adding enzymes and tDNA substrates. Biol Bull *196*, 331-333.

Makarov, V.L., Hirose, Y., and Langmore, J.P. (1997). Long G tails at both ends of human chromosomes suggest a C strand degradation mechanism for telomere shortening. Cell *88*, 657-666.

Maser, R.S. and DePinho, R.A. (2002). Connecting chromosomes, crisis, and cancer. Science *297*, 565-569.

Maser, R.S., Monsen, K.J., Nelms, B.E., and Petrini, J.H. (1997). hMre11 and hRad50 nuclear foci are induced during the normal cellular response to DNA double-strand breaks. Mol Cell Biol *17*, 6087-6096.

Masson, J.Y., Stasiak, A.Z., Stasiak, A., Benson, F.E., and West, S.C. (2001a). Complex formation by the human RAD51C and XRCC3 recombination repair proteins. Proc Natl Acad Sci U S A *98*, 8440-8446.

Masson, J.Y., Tarsounas, M.C., Stasiak, A.Z., Stasiak, A., Shah, R., McIlwraith, M.J., Benson, F.E., and West, S.C. (2001b). Identification and purification of two distinct complexes containing the five RAD51 paralogs. Genes Dev *15*, 3296-3307.

Matullo, G., Guarrera, S., Carturan, S., Peluso, M., Malaveille, C., Davico, L., Piazza, A., and Vineis, P. (2001). DNA repair gene polymorphisms, bulky DNA adducts in white blood cells and bladder cancer in a case-control study. Int J Cancer *92*, 562-567.

Mazin, A.V., Bornarth, C.J., Solinger, J.A., Heyer, W.D., and Kowalczykowski, S.C. (2000). Rad54 protein is targeted to pairing loci by the Rad51 nucleoprotein filament. Mol Cell *6*, 583-592.

McElligott R., and Wellinger R.J. (1997). The terminal DNA structure of mammalian chromosomes. Embo J *16*, 3705-3714.

McEntee, K., Weinstock, G.M., and Lehman, I.R. (1981a). Binding of the recA protein of Escherichia coli to single- and double-stranded DNA. J Biol Chem *256*, 8835-8844.

McEntee, K., Weinstock, G.M., and Lehman, I.R. (1981b). DNA and nucleoside triphosphate binding properties of recA protein from Escherichia coli. Prog Nucleic Acid Res Mol Biol *26*, 265-279.

Miller K.A., Sawicka D., Barsky D., and Albala J.S. (2004). Domain mapping of the Rad51 paralog protein complexes. Nucleic Acids Res *32*, 169-178.

Miller, K.A., Yoshikawa, D.M., McConnell, I.R., Clark, R., Schild, D., and Albala, J.S. (2002). RAD51C interacts with RAD51B and is central to a larger protein complex in vivo exclusive of RAD51. J Biol Chem *277*, 8406-8411.

Mills, K.D., Ferguson, D.O., Essers, J., Eckersdorff, M., Kanaar, R., and Alt, F.W. (2004). Rad54 and DNA Ligase IV cooperate to maintain mammalian chromatid stability. Genes Dev *18*, 1283-1292.

Miyazaki, T., Bressan, D.A., Shinohara, M., Haber, J.E., and Shinohara, A. (2004). In vivo assembly and disassembly of Rad51 and Rad52 complexes during double-strand break repair. Embo J *23*, 939-949.

Mohaghegh, P., Karow, J.K., Brosh Jr, R.M., Jr., Bohr, V.A., and Hickson, I.D. (2001). The Bloom's and Werner's syndrome proteins are DNA structure-specific helicases. Nucleic Acids Res *29*, 2843-2849.

Mootha, V.K., Lindgren, C.M., Eriksson, K.F., Subramanian, A., Sihag, S., Lehar, J., Puigserver, P., Carlsson, E., Ridderstrale, M., Laurila, E., Houstis, N., Daly, M.J., Patterson, N., Mesirov, J.P., Golub, T.R., Tamayo, P., Spiegelman, B., Lander, E.S., Hirschhorn, J.N., Altshuler, D., and Groop, L.C. (2003). PGC-1alpha-

responsive genes involved in oxidative phosphorylation are coordinately downregulated in human diabetes. Nat Genet *34*, 267-273.

Morin G.B. (1989). The human telomere terminal transferase enzyme is a ribonucleoprotein that synthesizes TTAGGG repeats. Cell *59*, 521-529.

Morrison, C. and Rieder, C.L. (2004). Chromosome damage and progression into and through mitosis in vertebrates. DNA Repair (Amst) *3*, 1133-1139.

Morrison, C., Sonoda, E., Takao, N., Shinohara, A., Yamamoto, K., and Takeda, S. (2000). The controlling role of ATM in homologous recombinational repair of DNA damage. Embo J *19*, 463-471.

Moynahan, M.E., Pierce, A.J., and Jasin, M. (2001). BRCA2 is required for homology-directed repair of chromosomal breaks. Mol Cell *7*, 263-272.

Nejedly K., Kittner R., Pospisilova S., and Kypr J. (2001). Crosslinking of the complementary strands of DNA by UV light: dependence on the oligonucleotide composition of the UV irradiated DNA. Biochim Biophys Acta *1517*, 365-375.

Nugent C.I., Hughes T.R., Lue N.F., and Lundblad V. (1996). Cdc13p: a single-strand telomeric DNA-binding protein with a dual role in yeast telomere maintenance. Science *274*, 249-252.

O'Connor, M.S., Safari, A., Liu, D., Qin, J., and Songyang, Z. (2004). The human Rap1 protein complex and modulation of telomere length. J Biol Chem *279*, 28585-28591.

O'Driscoll, M., Gennery, A.R., Seidel, J., Concannon, P., and Jeggo, P.A. (2004). An overview of three new disorders associated with genetic instability: LIG4

syndrome, RS-SCID and ATR-Seckel syndrome. DNA Repair (Amst) *3*, 1227-1235.

Obana, N., Takagi, S., Kinouchi, Y., Tokita, Y., Sekikawa, A., Takahashi, S., Hiwatashi, N., Oikawa, S., and Shimosegawa, T. (2003). Telomere shortening of peripheral blood mononuclear cells in coronary disease patients with metabolic disorders. Intern Med *42*, 150-153.

Ogawa, T., Yu, X., Shinohara, A., and Egelman, E.H. (1993). Similarity of the yeast RAD51 filament to the bacterial RecA filament. Science *259*, 1896-1899.

Oh, H., Wang, S.C., Prahash, A., Sano, M., Moravec, C.S., Taffet, G.E., Michael, L.H., Youker, K.A., Entman, M.L., and Schneider, M.D. (2003). Telomere attrition and Chk2 activation in human heart failure. Proc Natl Acad Sci U S A *100*, 5378-5383.

Oikawa S., and Kawanishi S. (1999). Site-specific DNA damage at GGG sequence by oxidative stress may accelerate telomere shortening. FEBS Lett *453*, 365-368.

Opresko, P.L., Mason, P.A., Podell, E.R., Lei, M., Hickson, I.D., Cech, T.R., and Bohr, V.A. (2005). POT1 stimulates RecQ helicases WRN and BLM to unwind telomeric DNA substrates. J Biol Chem *280*, 32069-32080.

Opresko, P.L., von Kobbe, C., Laine, J.P., Harrigan, J., Hickson, I.D., and Bohr, V.A. (2002). Telomere-binding protein TRF2 binds to and stimulates the Werner and Bloom syndrome helicases. J Biol Chem *277*, 41110-41119.

Pastink A., Eeken J.C., and Lohman P.H. (2001). Genomic integrity and the repair of double-strand DNA breaks. Mutat Res *480-481*, 37-50.

Patel, K.J., Yu, V.P., Lee, H., Corcoran, A., Thistlethwaite, F.C., Evans, M.J., Colledge, W.H., Friedman, L.S., Ponder, B.A., and Venkitaraman, A.R. (1998). Involvement of Brca2 in DNA repair. Mol Cell *1*, 347-357.

Paull, T.T. and Gellert, M. (1998). The 3' to 5' exonuclease activity of Mre 11 facilitates repair of DNA double-strand breaks. Mol Cell *1*, 969-979.

Paull, T.T., Rogakou, E.P., Yamazaki, V., Kirchgessner, C.U., Gellert, M., and Bonner, W.M. (2000). A critical role for histone H2AX in recruitment of repair factors to nuclear foci after DNA damage. Curr Biol *10*, 886-895.

Pellegrini, L., Yu, D.S., Lo, T., Anand, S., Lee, M., Blundell, T.L., and Venkitaraman, A.R. (2002). Insights into DNA recombination from the structure of a RAD51-BRCA2 complex. Nature *420*, 287-293.

Petersen S., Saretzki G., and von Zglinicki T. (1998). Preferential accumulation of single-stranded regions in telomeres of human fibroblasts. Exp Cell Res *239*, 152-160.

Peto, J., Collins, N., Barfoot, R., Seal, S., Warren, W., Rahman, N., Easton, D.F., Evans, C., Deacon, J., and Stratton, M.R. (1999). Prevalence of BRCA1 and BRCA2 gene mutations in patients with early-onset breast cancer. J Natl Cancer Inst *91*, 943-949.

Petukhova, G., Van Komen, S., Vergano, S., Klein, H., and Sung, P. (1999). Yeast Rad54 promotes Rad51-dependent homologous DNA pairing via ATP hydrolysis-driven change in DNA double helix conformation. J Biol Chem *274*, 29453-29462.

Pierce, A.J., Stark, J.M., Araujo, F.D., Moynahan, M.E., Berwick, M., and Jasin, M. (2001). Double-strand breaks and tumorigenesis. Trends Cell Biol *11*, S52-59.

Pittman, D.L., Cobb, J., Schimenti, K.J., Wilson, L.A., Cooper, D.M., Brignull, E., Handel, M.A., and Schimenti, J.C. (1998a). Meiotic prophase arrest with failure of chromosome synapsis in mice deficient for Dmc1, a germline-specific RecA homolog. Mol Cell *1*, 697-705.

Pittman, D.L. and Schimenti, J.C. (2000). Midgestation lethality in mice deficient for the RecA-related gene, Rad51d/Rad51l3. Genesis *26*, 167-173.

Pittman, D.L., Weinberg, L.R., and Schimenti, J.C. (1998b). Identification, characterization, and genetic mapping of Rad51d, a new mouse and human RAD51/RecA-related gene. Genomics *49*, 103-111.

Poch E., Carbonell P., Franco S., Diez-Juan A., Blasco M.A., and Andres V. (2004). Short telomeres protect from diet-induced atherosclerosis in apolipoprotein E-null mice. Faseb J *18*, 418-420.

Price C.M. (1990). Telomere structure in Euplotes crassus: characterization of DNA-protein interactions and isolation of a telomere-binding protein. Mol Cell Biol *10*, 3421-3431.

Radding, C.M. (1991). Helical interactions in homologous pairing and strand exchange driven by RecA protein. J Biol Chem *266*, 5355-5358.

Raderschall, E., Golub, E.I., and Haaf, T. (1999). Nuclear foci of mammalian recombination proteins are located at single-stranded DNA regions formed after DNA damage. Proc Natl Acad Sci U S A *96*, 1921-1926.

Ramirez, R., Carracedo, J., Jimenez, R., Canela, A., Herrera, E., Aljama, P., and Blasco, M.A. (2003). Massive telomere loss is an early event of DNA damage-induced apoptosis. J Biol Chem *278*, 836-842.

Register, J.C. and Griffith, J. (1985). The direction of RecA protein assembly onto single strand DNA is the same as the direction of strand assimilation during strand exchange. J Biol Chem *260*, 12308-12312.

Resnick, M.A. (1976). The repair of double-strand breaks in DNA: a model involving recombination. J Theor Biol *56*, 97-106.

Rijkers, T., Van Den Ouweland, J., Morolli, B., Rolink, A.G., Baarends, W.M., Van Sloun, P.P., Lohman, P.H., and Pastink, A. (1998). Targeted inactivation of mouse RAD52 reduces homologous recombination but not resistance to ionizing radiation. Mol Cell Biol *18*, 6423-6429.

Ristic, D., Wyman, C., Paulusma, C., and Kanaar, R. (2001). The architecture of the human Rad54-DNA complex provides evidence for protein translocation along DNA. Proc Natl Acad Sci U S A *98*, 8454-8460.

Rodriguez-Lopez, R., Osorio, A., Ribas, G., Pollan, M., Sanchez-Pulido, L., de la Hoya, M., Ruibal, A., Zamora, P., Arias, J.I., Salazar, R., Vega, A., Martinez, J.I., Esteban-Cardenosa, E., Alonso, C., Leton, R., Urioste Azcorra, M., Miner, C., Armengod, M.E., Carracedo, A., Gonzalez-Sarmiento, R., Caldes, T., Diez, O., and Benitez, J. (2004). The variant E233G of the RAD51D gene could be a low-penetrance allele in high-risk breast cancer families without BRCA1/2 mutations. Int J Cancer *110*, 845-849.

Rogakou E.P., Boon C., Redon C., and Bonner W.M. (1999). Megabase chromatin domains involved in DNA double-strand breaks in vivo. J Cell Biol *146*, 905-916.

Rogakou E.P., Pilch D.R., Orr A.H., Ivanova V.S., and Bonner W.M. (1998). DNA double-stranded breaks induce histone H2AX phosphorylation on serine *139*. J Biol Chem 273, 5858-5868.

Rosselli, F., Briot, D., and Pichierri, P. (2003). The Fanconi anemia pathway and the DNA interstrand cross-links repair. Biochimie *85*, 1175-1184.

Rudolph, K.L., Chang, S., Lee, H.W., Blasco, M., Gottlieb, G.J., Greider, C., and DePinho, R.A. (1999). Longevity, stress response, and cancer in aging telomerase-deficient mice. Cell *96*, 701-712.

Sah V.P., Attardi L.D., Mulligan G.J., Williams B.O., Bronson R.T., and Jacks T. (1995). A subset of p53-deficient embryos exhibit exencephaly. Nat Genet *10*, 175-180.

Samani, N.J., Boultby, R., Butler, R., Thompson, J.R., and Goodall, A.H. (2001). Telomere shortening in atherosclerosis. Lancet *358*, 472-473.

Samper, E., Goytisolo, F.A., Slijepcevic, P., van Buul, P.P., and Blasco, M.A. (2000). Mammalian Ku86 protein prevents telomeric fusions independently of the length of TTAGGG repeats and the G-strand overhang. EMBO Rep *1*, 244-252.

Sancar, A., Lindsey-Boltz, L.A., Unsal-Kacmaz, K., and Linn, S. (2004). Molecular mechanisms of mammalian DNA repair and the DNA damage checkpoints. Annu Rev Biochem *73*, 39-85.

Sato, N., Mizumoto, K., Nakamura, M., Ueno, H., Minamishima, Y.A., Farber, J.L., and Tanaka, M. (2000). A possible role for centrosome overduplication in radiation-induced cell death. Oncogene *19*, 5281-5290.

Savage J. (1975). Classification and relationships of induced chromosomal structural changes. Journal of Medical Genetics *12*, 103-122.

Schawalder, J., Paric, E., and Neff, N.F. (2003). Telomere and ribosomal DNA repeats are chromosomal targets of the bloom syndrome DNA helicase. BMC Cell Biol *4*, 15.

Schild, D., Lio, Y.C., Collins, D.W., Tsomondo, T., and Chen, D.J. (2000). Evidence for simultaneous protein interactions between human Rad51 paralogs. J Biol Chem *275*, 16443-16449.

Schoenmakers, E.F., Huysmans, C., and Van de Ven, W.J. (1999). Allelic knockout of novel splice variants of human recombination repair gene RAD51B in t(12;14) uterine leiomyomas. Cancer Res *59*, 19-23.

Schurer H., Schiffer S., Marchfelder A., and Morl M. (2001). This is the end: processing, editing and repair at the tRNA 3'-terminus. Biol Chem *382*, 1147-1156.

Sen, D. and Gilbert, W. (1988). Formation of parallel four-stranded complexes by guanine-rich motifs in DNA and its implications for meiosis. Nature *334*, 364-366.

Serrano A.L., and Andres V. (2004). Telomeres and cardiovascular disease: does size matter? Circ Res *94*, 575-584.

Sfeir, A.J., Chai, W., Shay, J.W., and Wright, W.E. (2005). Telomere-end processing the terminal nucleotides of human chromosomes. Mol Cell *18*, 131-138.

Shackelford, R.E., Kaufmann, W.K., and Paules, R.S. (1999). Cell cycle control, checkpoint mechanisms, and genotoxic stress. Environ Health Perspect *107 Suppl 1*, 5-24.

Shampay J., Szostak J.W., and Blackburn E.H. (1984). DNA sequences of telomeres maintained in yeast. Nature *310*, 154-157.

Sharan, S.K., Morimatsu, M., Albrecht, U., Lim, D.S., Regel, E., Dinh, C., Sands, A., Eichele, G., Hasty, P., and Bradley, A. (1997). Embryonic lethality and radiation hypersensitivity mediated by Rad51 in mice lacking Brca2. Nature *386*, 804-810.

Shay, J.W. (1997). Telomerase in human development and cancer. J Cell Physiol *173*, 266-270.

Shay, J.W., Pereira-Smith, O.M., and Wright, W.E. (1991). A role for both RB and p53 in the regulation of human cellular senescence. Exp Cell Res *196*, 33-39.

Shen, S.X., Weaver, Z., Xu, X., Li, C., Weinstein, M., Chen, L., Guan, X.Y., Ried, T., and Deng, C.X. (1998). A targeted disruption of the murine Brca1 gene causes gamma-irradiation hypersensitivity and genetic instability. Oncogene *17*, 3115-3124.

Shen, Z., Cloud, K.G., Chen, D.J., and Park, M.S. (1996). Specific interactions between the human RAD51 and RAD52 proteins. J Biol Chem *271*, 148-152.

Shu, Z., Smith, S., Wang, L., Rice, M.C., and Kmiec, E.B. (1999). Disruption of muREC2/RAD51L1 in mice results in early embryonic lethality which can be partially rescued in a p53(-/-) background. Mol Cell Biol *19*, 8686-8693.

Sigurdsson, S., Van Komen, S., Bussen, W., Schild, D., Albala, J.S., and Sung, P. (2001). Mediator function of the human Rad51B-Rad51C complex in Rad51/RPA-catalyzed DNA strand exchange. Genes Dev *15*, 3308-3318.

Singer, M.S. and Gottschling, D.E. (1994). TLC1: template RNA component of Saccharomyces cerevisiae telomerase. Science *266*, 404-409.

Slupianek, A., Gurdek, E., Koptyra, M., Nowicki, M.O., Siddiqui, K.M., Groden, J., and Skorski, T. (2005). BLM helicase is activated in BCR/ABL leukemia cells to modulate responses to cisplatin. Oncogene *24*, 3914-3922.

Slupianek A., Schmutte C., Tombline G., Nieborowska-Skorska M., Hoser G., Nowicki M.O., Pierce A.J., Fishel R., and Skorski T. (2001). BCR/ABL regulates mammalian RecA homologs, resulting in drug resistance. Mol Cell *8*, 795-806.

Smiraldo, P.G. (2004). Telomerase: a mystery by name alone. IUBMB Life *56*, 573-574.

Smiraldo, P.G., Gruver, A.M., Osborn, J.C., and Pittman, D.L. (2005). Extensive chromosomal instability in Rad51d-deficient mouse cells. Cancer Res *65*, 2089-2096.

Smogorzewska A., and de Lange T. (2004). Regulation of telomerase by telomeric proteins. Annu Rev Biochem *73*, 177-208.

Snouwaert, J.N., Gowen, L.C., Latour, A.M., Mohn, A.R., Xiao, A., DiBiase, L., and Koller, B.H. (1999). BRCA1 deficient embryonic stem cells display a decreased

homologous recombination frequency and an increased frequency of non-homologous recombination that is corrected by expression of a brca1 transgene. Oncogene *18*, 7900-7907.

Sohal R.S., Agarwal S., and Sohal B.H. (1995). Oxidative stress and aging in the Mongolian gerbil (Meriones unguiculatus). Mech. Ageing Dev. *81*, 15-25.

Solinger, J.A. and Heyer, W.D. (2001). Rad54 protein stimulates the postsynaptic phase of Rad51 protein-mediated DNA strand exchange. Proc Natl Acad Sci U S A *98*, 8447-8453.

Solinger, J.A., Kiianitsa, K., and Heyer, W.D. (2002). Rad54, a Swi2/Snf2-like recombinational repair protein, disassembles Rad51:dsDNA filaments. Mol Cell *10*, 1175-1188.

Song, B. and Sung, P. (2000). Functional interactions among yeast Rad51 recombinase, Rad52 mediator, and replication protein A in DNA strand exchange. J Biol Chem *275*, 15895-15904.

Song, K., Jung, D., Jung, Y., Lee, S.G., and Lee, I. (2000). Interaction of human Ku70 with TRF2. FEBS Lett *481*, 81-85.

Sonoda, E., Sasaki, M.S., Buerstedde, J.M., Bezzubova, O., Shinohara, A., Ogawa, H., Takata, M., Yamaguchi-Iwai, Y., and Takeda, S. (1998). Rad51-deficient vertebrate cells accumulate chromosomal breaks prior to cell death. Embo J *17*, 598-608.

Sonoda, E., Sasaki, M.S., Morrison, C., Yamaguchi-Iwai, Y., Takata, M., and Takeda, S. (1999). Sister chromatid exchanges are mediated by homologous recombination in vertebrate cells. Mol Cell Biol *19*, 5166-5169.

Stansel, R.M., de Lange, T., and Griffith, J.D. (2001). T-loop assembly in vitro involves binding of TRF2 near the 3' telomeric overhang. Embo J *20*, 5532-5540.

Stewart, G.S., Maser, R.S., Stankovic, T., Bressan, D.A., Kaplan, M.I., Jaspers, N.G., Raams, A., Byrd, P.J., Petrini, J.H., and Taylor, A.M. (1999). The DNA double-strand break repair gene hMRE11 is mutated in individuals with an ataxia-telangiectasia-like disorder. Cell *99*, 577-587.

Strathern, J.N., Klar, A.J., and Hicks, J.B. (1982). Homothallic switching of yeast mating type cassettes is initiated by a double-stranded cut in the MAT locus. Cell *31*, 183-192.

Sugawara, N., Wang, X., and Haber, J.E. (2003). In vivo roles of Rad52, Rad54, and Rad55 proteins in Rad51-mediated recombination. Mol Cell *12*, 209-219.

Sugiyama, T. and Kowalczykowski, S.C. (2002). Rad52 protein associates with replication protein A (RPA)-single-stranded DNA to accelerate Rad51-mediated displacement of RPA and presynaptic complex formation. J Biol Chem *277*, 31663-31672.

Sun, H., Karow, J.K., Hickson, I.D., and Maizels, N. (1998). The Bloom's syndrome helicase unwinds G4 DNA. J Biol Chem *273*, 27587-27592.

Sung, P. (1994). Catalysis of ATP-dependent homologous DNA pairing and strand exchange by yeast RAD51 protein. Science *265*, 1241-1243.

Sung, P. (1997). Yeast Rad55 and Rad57 proteins form a heterodimer that functions with replication protein A to promote DNA strand exchange by Rad51 recombinase. Genes Dev *11*, 1111-1121.

Sung, P. and Robberson, D.L. (1995). DNA strand exchange mediated by a RAD51-ssDNA nucleoprotein filament with polarity opposite to that of RecA. Cell *82*, 453-461.

Suzuki, A., de la Pompa, J.L., Hakem, R., Elia, A., Yoshida, R., Mo, R., Nishina, H., Chuang, T., Wakeham, A., Itie, A., Koo, W., Billia, P., Ho, A., Fukumoto, M., Hui, C.C., and Mak, T.W. (1997). Brca2 is required for embryonic cellular proliferation in the mouse. Genes Dev *11*, 1242-1252.

Swagemakers, S.M., Essers, J., de Wit, J., Hoeijmakers, J.H., and Kanaar, R. (1998). The human RAD54 recombinational DNA repair protein is a double-stranded DNA-dependent ATPase. J Biol Chem *273*, 28292-28297.

Szostak J.W., and Blackburn E.H. (1982). Cloning yeast telomeres on linear plasmid vectors. Cell *29*, 245-255.

Szostak, J.W., Orr-Weaver, T.L., Rothstein, R.J., and Stahl, F.W. (1983). The double-strand break repair model for recombination. Cell *33*, 25-35.

Takada S., Kelkar A., and Theurkauf W.E. (2003). Drosophila checkpoint kinase 2 couples centrosome function and spindle assembly to genomic integrity. Cell *113*, 87-99.

Takahashi, T., Nagai, N., Oda, H., Ohama, K., Kamada, N., and Miyagawa, K. (2001). Evidence for RAD51L1/HMGIC fusion in the pathogenesis of uterine leiomyoma. Genes Chromosomes Cancer *30*, 196-201.

Takai, H., Smogorzewska, A., and de Lange, T. (2003). DNA damage foci at dysfunctional telomeres. Curr Biol *13*, 1549-1556.

Takao, N., Kato, H., Mori, R., Morrison, C., Sonada, E., Sun, X., Shimizu, H., Yoshioka, K., Takeda, S., and Yamamoto, K. (1999). Disruption of ATM in p53-null cells causes multiple functional abnormalities in cellular response to ionizing radiation. Oncogene *18*, 7002-7009.

Takata, M., Sasaki, M.S., Sonoda, E., Fukushima, T., Morrison, C., Albala, J.S., Swagemakers, S.M., Kanaar, R., Thompson, L.H., and Takeda, S. (2000). The rad51 paralog Rad51B promotes homologous recombinational repair. Mol Cell Biol *20*, 6476-6482.

Takata, M., Sasaki, M.S., Sonoda, E., Morrison, C., Hashimoto, M., Utsumi, H., Yamaguchi-Iwai, Y., Shinohara, A., and Takeda, S. (1998). Homologous recombination and non-homologous end-joining pathways of DNA double-strand break repair have overlapping roles in the maintenance of chromosomal integrity in vertebrate cells. Embo J *17*, 5497-5508.

Takata, M., Sasaki, M.S., Tachiiri, S., Fukushima, T., Sonoda, E., Schild, D., Thompson, L.H., and Takeda, S. (2001). Chromosome instability and defective recombinational repair in knockout mutants of the five Rad51 paralogs. Mol Cell Biol *21*, 2858-2866.

Tan, T.L., Essers, J., Citterio, E., Swagemakers, S.M., de Wit, J., Benson, F.E., Hoeijmakers, J.H., and Kanaar, R. (1999). Mouse Rad54 affects DNA conformation and DNA-damage-induced Rad51 foci formation. Curr Biol *9*, 325-328.

Tarsounas, M., Munoz, P., Claas, A., Smiraldo, P.G., Pittman, D.L., Blasco, M.A., and West, S.C. (2004). Telomere maintenance requires the RAD51D recombination/repair protein. Cell *117*, 337-347.

Tauchi, H., Kobayashi, J., Morishima, K., van Gent, D.C., Shiraishi, T., Verkaik, N.S., vanHeems, D., Ito, E., Nakamura, A., Sonoda, E., Takata, M., Takeda, S., Matsuura, S., and Komatsu, K. (2002). Nbs1 is essential for DNA repair by homologous recombination in higher vertebrate cells. Nature *420*, 93-98.

Taylor, A. and Smith, G.R. (1980). Unwinding and rewinding of DNA by the RecBC enzyme. Cell *22*, 447-457.

Teng, S.C. and Zakian, V.A. (1999). Telomere-telomere recombination is an efficient bypass pathway for telomere maintenance in Saccharomyces cerevisiae. Mol Cell Biol *19*, 8083-8093.

Thacker, J. (1999). A surfeit of RAD51-like genes? Trends Genet *15*, 166-168.

Thacker, J. (2005). The RAD51 gene family, genetic instability and cancer. Cancer Lett *219*, 125-135.

Thacker, J., Tambini, C.E., Simpson, P.J., Tsui, L.C., and Scherer, S.W. (1995). Localization to chromosome 7q36.1 of the human XRCC2 gene, determining sensitivity to DNA-damaging agents. Hum Mol Genet *4*, 113-120.

Thompson, L.H. (1998). Chinese hamster cells meet DNA repair: an entirely acceptable affair. Bioessays *20*, 589-597.

Thompson, L.H. and Schild, D. (1999). The contribution of homologous recombination in preserving genome integrity in mammalian cells. Biochimie *81*, 87-105.

Thompson, L.H. and Schild, D. (2001). Homologous recombinational repair of DNA ensures mammalian chromosome stability. Mutat Res *477*, 131-153.

Thompson, L.H. and Schild, D. (2002). Recombinational DNA repair and human disease. Mutat Res *509*, 49-78.

Thyfault J.P., Noland R.C., Coburn L.E., Henes S.T., Britton S.L., Koch L.G., Dohm L., Cortright R.N., and Lust R.M. (2005). Effects of a high fat diet on glycogen synthesis rates in skeletal muscle of rats bred for low and high (LCR and HCR) endurance capacity. Experimental Biology meeting abstracts. The FASEB Journal *19*, Abstract # 665.19.

Todaro, G.J. and Green, H. (1963). Quantitative studies of the growth of mouse embryo cells in culture and their development into established lines. J Cell Biol *17*, 299-313.

Tombline, G. and Fishel, R. (2002). Biochemical characterization of the human RAD51 protein. I. ATP hydrolysis. J Biol Chem *277*, 14417-14425.

Tombline, G., Heinen, C.D., Shim, K.S., and Fishel, R. (2002). Biochemical characterization of the human RAD51 protein. III. Modulation of DNA binding by adenosine nucleotides. J Biol Chem *277*, 14434-14442.

Trujillo, K.M. and Sung, P. (2001). DNA structure-specific nuclease activities in the Saccharomyces cerevisiae Rad50*Mre11 complex. J Biol Chem *276*, 35458-35464.

Trujillo, K.M., Yuan, S.S., Lee, E.Y., and Sung, P. (1998). Nuclease activities in a complex of human recombination and DNA repair factors Rad50, Mre11, and p95. J Biol Chem *273*, 21447-21450.

Tsaneva, I.R., Muller, B., and West, S.C. (1992). ATP-dependent branch migration of Holliday junctions promoted by the RuvA and RuvB proteins of E. coli. Cell *69*, 1171-1180.

Tsubouchi, H. and Ogawa, H. (1998). A novel mre11 mutation impairs processing of double-strand breaks of DNA during both mitosis and meiosis. Mol Cell Biol *18*, 260-268.

Tsuzuki, T., Fujii, Y., Sakumi, K., Tominaga, Y., Nakao, K., Sekiguchi, M., Matsushiro, A., Yoshimura, Y., and MoritaT (1996). Targeted disruption of the Rad51 gene leads to lethality in embryonic mice. Proc Natl Acad Sci U S A *93*, 6236-6240.

Tutt, A., Gabriel, A., Bertwistle, D., Connor, F., Paterson, H., Peacock, J., Ross, G., and Ashworth, A. (1999). Absence of Brca2 causes genome instability by chromosome breakage and loss associated with centrosome amplification. Curr Biol *9*, 1107-1110.

Valdes, A.M., Andrew, T., Gardner, J.P., Kimura, M., Oelsner, E., Cherkas, L.F., Aviv, A., and Spector, T.D. (2005). Obesity, cigarette smoking, and telomere length in women. Lancet *366*, 662-664.

van Brabant, A.J., Stan, R., and Ellis, N.A. (2000). DNA helicases, genomic instability, and human genetic disease. Annu Rev Genomics Hum Genet *1*, 409-459.

van Gent, D.C., Hoeijmakers, J.H., and Kanaar, R. (2001). Chromosomal stability and the DNA double-stranded break connection. Nat Rev Genet *2*, 196-206.

Van Komen, S., Petukhova, G., Sigurdsson, S., Stratton, S., and Sung, P. (2000). Superhelicity-driven homologous DNA pairing by yeast recombination factors Rad51 and Rad54. Mol Cell *6*, 563-572.

van Steensel, B. and de Lange, T. (1997). Control of telomere length by the human telomeric protein TRF1. Nature *385*, 740-743.

van Steensel, B., Smogorzewska, A., and de Lange, T. (1998). TRF2 protects human telomeres from end-to-end fusions. Cell *92*, 401-413.

Veldman, T., Etheridge, K.T., and Counter, C.M. (2004). Loss of hPot1 function leads to telomere instability and a cut-like phenotype. Curr Biol *14*, 2264-2270.

von Zglinicki T. (2000). Role of oxidative stress in telomere length regulation and replicative senescence. Ann N Y Acad Sci *908*, 99-110.

von Zglinicki T. (1998). Telomeres: influencing the rate of aging. Ann N Y Acad Sci *854*, 318-327.

von Zglinicki T., and Martin-Ruiz C.M. (2005). Telomeres as biomarkers for ageing and age-related diseases. Curr. Mol. Med. *5*, 197-203.

Wallis, J.W., Chrebet, G., Brodsky, G., Rolfe, M., and Rothstein, R. (1989). A hyper-recombination mutation in S. cerevisiae identifies a novel eukaryotic topoisomerase. Cell *58*, 409-419.

Wang, R.C., Smogorzewska, A., and de Lange, T. (2004). Homologous recombination generates T-loop-sized deletions at human telomeres. Cell *119*, 355-368.

Wang, Z.G., Ruggero, D., Ronchetti, S., Zhong, S., Gaboli, M., Rivi, R., and Pandolfi, P.P. (1998). PML is essential for multiple apoptotic pathways. Nat Genet *20*, 266-272.

Wei, C. and Price, M. (2003). Protecting the terminus: t-loops and telomere end-binding proteins. Cell Mol Life Sci *60*, 2283-2294.

Wei, C., Skopp, R., Takata, M., Takeda, S., and Price, C.M. (2002). Effects of double-strand break repair proteins on vertebrate telomere structure. Nucleic Acids Res *30*, 2862-2870.

Weinstock, G.M., McEntee, K., and Lehman, I.R. (1979). ATP-dependent renaturation of DNA catalyzed by the recA protein of Escherichia coli. Proc Natl Acad Sci U S A *76*, 126-130.

West S.C. (2003). Molecular views of recombination proteins and their control. Nature Reviews. Molecular Cell Biology *4*, 435-445.

West, S.C. (1997). Processing of recombination intermediates by the RuvABC proteins. Annu Rev Genet *31*, 213-244.

West, S.C., Cassuto, E., and Howard-Flanders, P. (1981). recA protein promotes homologous-pairing and strand-exchange reactions between duplex DNA molecules. Proc Natl Acad Sci U S A *78*, 2100-2104.

West, S.C., Cassuto, E., Mursalim, J., and Howard-Flanders, P. (1980). Recognition of duplex DNA containing single-stranded regions by recA protein. Proc Natl Acad Sci U S A *77*, 2569-2573.

West, S.C. and Connolly, B. (1992). Biological roles of the Escherichia coli RuvA, RuvB and RuvC proteins revealed. Mol Microbiol *6*, 2755-2759.

Weterings, E. and van Gent, D.C. (2004). The mechanism of non-homologous end-joining: a synopsis of synapsis. DNA Repair (Amst) *3*, 1425-1435.

Wiese, C., Collins, D.W., Albala, J.S., Thompson, L.H., Kronenberg, A., and Schild, D. (2002). Interactions involving the Rad51 paralogs Rad51C and XRCC3 in human cells. Nucleic Acids Res *30*, 1001-1008.

Winsey, S.L., Haldar, N.A., Marsh, H.P., Bunce, M., Marshall, S.E., Harris, A.L., Wojnarowska, F., and Welsh, K.I. (2000). A variant within the DNA repair gene XRCC3 is associated with the development of melanoma skin cancer. Cancer Res *60*, 5612-5616.

Wisloff U., Najjar S.M., Ellingsen O., Haram P.M., Swoap S., Al-Share Q., Fernstrom M., Rezaei K., Lee S.J., Koch L.G., and Britton S.L. (2005). Cardiovascular risk factors emerge after artificial selection for low aerobic capacity. Science *307*, 418-420.

Wolner, B., van Komen, S., Sung, P., and Peterson, C.L. (2003). Recruitment of the recombinational repair machinery to a DNA double-strand break in yeast. Mol Cell *12*, 221-232.

Wong A.K., Pero R., Ormonde P.A., Tavtigian S.V., and Bartel P.L. (1997). RAD51 interacts with the evolutionarily conserved BRC motifs in the human breast cancer susceptibility gene brca2. J Biol Chem *272*, 31941-31944.

Wong K.K., Maser R.S., Bachoo R.M., Menon J., Carrasco D.R., Gu Y., Alt F.W., and DePinho R.A. (2003). Telomere dysfunction and Atm deficiency compromises organ homeostasis and accelerates ageing. Nature *421*, 643-648.

Wood, R.D., Mitchell, M., Sgouros, J., and Lindahl, T. (2001). Human DNA repair genes. Science *291*, 1284-1289.

Wright, J.A., Keegan, K.S., Herendeen, D.R., Bentley, N.J., Carr, A.M., Hoekstra, M.F., and Concannon, P. (1998). Protein kinase mutants of human ATR increase sensitivity to UV and ionizing radiation and abrogate cell cycle checkpoint control. Proc Natl Acad Sci U S A *95*, 7445-7450.

Wright W.E., and Shay J.W. (1992). The two-stage mechanism controlling cellular senescence and immortalization. Experimental Gerontology *27*, 383-389.

Wu, G.J., Sinclair, C.S., Paape, J., Ingle, J.N., Roche, P.C., James, C.D., and Couch, F.J. (2000). 17q23 amplifications in breast cancer involve the PAT1, RAD51C, PS6K, and SIGma1B genes. Cancer Res *60*, 5371-5375.

Wu, L., Davies, S.L., Levitt, N.C., and Hickson, I.D. (2001). Potential role for the BLM helicase in recombinational repair via a conserved interaction with RAD51. J Biol Chem *276*, 19375-19381.

Wu, L., Davies, S.L., North, P.S., Goulaouic, H., Riou, J.F., Turley, H., Gatter, K.C., and Hickson, I.D. (2000). The Bloom's syndrome gene product interacts with topoisomerase III. J Biol Chem *275*, 9636-9644.

Wu, X., Ranganathan, V., Weisman, D.S., Heine, W.F., Ciccone, D.N., O'Neill, T.B., Crick, K.E., Pierce, K.A., Lane, W.S., Rathbun, G., Livingston, D.M., and Weaver, D.T. (2000). ATM phosphorylation of Nijmegen breakage syndrome protein is required in a DNA damage response. Nature *405*, 477-482.

Xia, F., Taghian, D.G., DeFrank, J.S., Zeng, Z.C., Willers, H., Iliakis, G., and Powell, S.N. (2001). Deficiency of human BRCA2 leads to impaired homologous recombination but maintains normal nonhomologous end joining. Proc Natl Acad Sci U S A *98*, 8644-8649.

Xu, X., Wagner, K.U., Larson, D., Weaver, Z., Li, C., Ried, T., Hennighausen, L., Wynshaw-Boris, A., and Deng, C.X. (1999a). Conditional mutation of Brca1 in mammary epithelial cells results in blunted ductal morphogenesis and tumour formation. Nat Genet *22*, 37-43.

Xu, X., Weaver, Z., Linke, S.P., Li, C., Gotay, J., Wang, X.W., Harris, C.C., Ried, T., and Deng, C.X. (1999b). Centrosome amplification and a defective G2-M cell cycle checkpoint induce genetic instability in BRCA1 exon 11 isoform-deficient cells. Mol Cell *3*, 389-395.

Xu, Y., Ashley, T., Brainerd, E.E., Bronson, R.T., Meyn, M.S., and Baltimore, D. (1996). Targeted disruption of ATM leads to growth retardation, chromosomal

fragmentation during meiosis, immune defects, and thymic lymphoma. Genes Dev *10*, 2411-2422.

Yamaguchi-Iwai, Y., Sonoda, E., Buerstedde, J.M., Bezzubova, O., Morrison, C., Takata, M., Shinohara, A., and Takeda, S. (1998). Homologous recombination, but not DNA repair, is reduced in vertebrate cells deficient in RAD52. Mol Cell Biol *18*, 6430-6435.

Yamaguchi-Iwai, Y., Sonoda, E., Sasaki, M.S., Morrison, C., Haraguchi, T., Hiraoka, Y., Yamashita, Y.M., Yagi, T., Takata, M., Price, C., Kakazu, N., and Takeda, S. (1999). Mre11 is essential for the maintenance of chromosomal DNA in vertebrate cells. Embo J *18*, 6619-6629.

Yang, H., Jeffrey, P.D., Miller, J., Kinnucan, E., Sun, Y., Thoma, N.H., Zheng, N., Chen, P.L., Lee, W.H., and Pavletich, N.P. (2002). BRCA2 function in DNA binding and recombination from a BRCA2-DSS1-ssDNA structure. Science *297*, 1837-1848.

Yang, Q., Zheng, Y.L., and Harris, C.C. (2005). POT1 and TRF2 cooperate to maintain telomeric integrity. Mol Cell Biol *25*, 1070-1080.

Yannone, S.M., Roy, S., Chan, D.W., Murphy, M.B., Huang, S., Campisi, J., and Chen, D.J. (2001). Werner syndrome protein is regulated and phosphorylated by DNA-dependent protein kinase. J Biol Chem *276*, 38242-38248.

Ye, J.Z., Donigian, J.R., van Overbeek, M., Loayza, D., Luo, Y., Krutchinsky, A.N., Chait, B.T., and de Lange, T. (2004a). TIN2 binds TRF1 and TRF2

simultaneously and stabilizes the TRF2 complex on telomeres. J Biol Chem *279*, 47264-47271.

Ye, J.Z., Hockemeyer, D., Krutchinsky, A.N., Loayza, D., Hooper, S.M., Chait, B.T., and de Lange, T. (2004b). POT1-interacting protein PIP1: a telomere length regulator that recruits POT1 to the TIN2/TRF1 complex. Genes Dev *18*, 1649-1654.

Yeager, T.R., Neumann, A.A., Englezou, A., Huschtscha, L.I., Noble, J.R., and Reddel, R.R. (1999). Telomerase-negative immortalized human cells contain a novel type of promyelocytic leukemia (PML) body. Cancer Res *59*, 4175-4179.

Yokoyama, H., Sarai, N., Kagawa, W., Enomoto, R., Shibata, T., Kurumizaka, H., and Yokoyama, S. (2004). Preferential binding to branched DNA strands and strand-annealing activity of the human Rad51B, Rad51C, Rad51D and Xrcc2 protein complex. Nucleic Acids Res *32*, 2556-2565.

Yu G.L., Bradley J.D., Attardi L.D., and Blackburn E.H. (1990). In vivo alteration of telomere sequences and senescence caused by mutated Tetrahymena telomerase RNAs. Nature *344*, 126-132.

Yu, V.P., Koehler, M., Steinlein, C., Schmid, M., Hanakahi, L.A., van Gool, A.J., West, S.C., and Venkitaraman, A.R. (2000). Gross chromosomal rearrangements and genetic exchange between nonhomologous chromosomes following BRCA2 inactivation. Genes Dev *14*, 1400-1406.

Yuan, S.S., Lee, S.Y., Chen, G., Song, M., Tomlinson, G.E., and Lee, E.Y. (1999). BRCA2 is required for ionizing radiation-induced assembly of Rad51 complex in vivo. Cancer Res *59*, 3547-3551.

Yun, J., Zhong, Q., Kwak, J.Y., and Lee, W.H. (2005). Hypersensitivity of Brca1-deficient MEF to the DNA interstrand crosslinking agent mitomycin C is associated with defect in homologous recombination repair and aberrant S-phase arrest. Oncogene *24*, 4009-4016.

Zakian, V.A. (1995). Telomeres: beginning to understand the end. Science *270*, 1601-1607.

Zhong, Z., Shiue, L., Kaplan, S., and de Lange, T. (1992). A mammalian factor that binds telomeric TTAGGG repeats in vitro. Mol Cell Biol *12*, 4834-4843.

Zhu, J., Petersen, S., Tessarollo, L., and Nussenzweig, A. (2001). Targeted disruption of the Nijmegen breakage syndrome gene NBS1 leads to early embryonic lethality in mice. Curr Biol *11*, 105-109.

Zhu, X.D., Kuster, B., Mann, M., Petrini, J.H., and Lange, T. (2000). Cell-cycle-regulated association of RAD50/MRE11/NBS1 with TRF2 and human telomeres. Nat Genet *25*, 347-352.

Zou Y., Sfeir A., Gryaznov S.M., Shay J.W., and Wright W.E. (2004). Does a sentinel or a subset of short telomeres determine replicative senescence? Mol. Biol. Cell *15*, 3709-3718.

APPENDIX A

IUBMB Life. 2004 Sep;56(9):573-4

Telomerase: A Mystery By Name Alone

An Invited Commentary

Phillip G. Smiraldo

Department of Physiology and Cardiovascular Genomics, Medical College of Ohio, Toledo, OH 43614, USA

Corresponding author:

Phillip G. Smiraldo

Department of Physiology and Cardiovascular Genomics

Medical College of Ohio

Block Health Science Building

3035 Arlington Avenue

Toledo, OH, 43614-5804

Telephone 419-383-4102

Fax 419-383-6168

Email: psmiraldo@mco.edu

Running Title: Telomerase: What's In A Name?

Names are given to all things in attempt to describe and classify them based upon the most current knowledge. As more insight is acquired through experimentation, the classification and nomenclature must also be updated accordingly. Unfortunately, as scientists speed forward gaining immense amounts of information, the name game, from whole organisms to enzymes, fails to evolve at the same rate. This commentary focuses on an enzyme that, besides having its roots in single celled, pond-dwelling organisms, has been implemented in two of most studied topics in medicine, aging and cancer. This enzyme, as we currently know it, is telomerase. By name alone, most cell biologists know the basic roles of telomerase in cells. However, young scientists and newcomers to the field are offered little help by the name "telomerase", except that it performs some catalytic function at the telomere. With such an ambiguous name, one may consider telomerase functioning to cleave, elongate, fuse, protect, replicate, separate, or perform any other imaginable role at telomeres. A full review on telomerase is beyond the scope of this letter (for full reviews, see (*1*-*3*)); rather, I will highlight some of its unique enzymatic properties and focus on how the current nomenclature for "telomerase" should be refined.

Telomeres, the ends of linear chromosomes, are unique structures that stabilize chromosome termini and allow cells to distinguish natural chromosome ends from damaged DNA. Telomeric DNA is composed of long stretches of a simple, tandemly repeated, G/C-rich sequence that can extend for several kilobases. However, due to the chromosome "end replication problem", telomeres become progressively shortened with each round of DNA replication, thus placing a limit on the number of divisions a cell may

undergo. In spite of this, eukaryotic cells that can divide indefinitely, such as cancers and single-celled organisms, exist, suggesting that the replication of chromosome ends can occur by a different means than that of conventional DNA replication enzymes.

In the early 1980s, a number of elegant experiments demonstrated that a unique mechanism existed that added tandem telomeric repeat sequences to eukaryotic chromosome termini (*4-6*). Although multiple hypotheses for this mechanism were considered, in 1984, Shampay et al. proposed that the chromosome elongation phenomenon occurred by terminal transferase-like activities (*7*) and, a little less than a year later, Carol Greider and Elizabeth Blackburn reported novel enzymatic activity from Tetrahymena cell free extracts that added telomeric repeats onto synthetic telomere primers (*8*). A similar enzymatic activity was later identified in human cells (*9*), thus making "telomere terminal transferase" (later abbreviated to its more common name, "telomerase") emerge as the primary factor for telomere elongation.

Although the formal name "telomere terminal transferase" is a more informative name to describe its mechanistic function, this nomenclature seems to have been lost from the literature over the past 19 years. However, because telomerase is quite unique when compared to other classical transferases, perhaps the gradual weaning of classifying telomerase as a transferase was no mistake. To identify some of these fundamental differences, we briefly compared telomerase with two popular transferases, terminal deoxynucleotidyl transferase, which functions in increasing immune system diversity, and tRNA nucleotidyl transferase, which is required for translation in all cells.

The immune system has evolved the ability to respond to almost all foreign antigens. The process of rearranging gene segments from the variable (V), diversity (D), and joining (J) sets creates this immunological diversity (abbreviated as V(D)J recombination). In addition, the processing of recombining gene segment ends produces junctional diversity, which further enhances the immune system repertoire. The primary role of terminal deoxynucleotidyl transferase (TdT) is to increase immunoglobulin heavy chain diversity by adding up to 15 nucleotides in random order to both the D_H-J_H and V_H-D_HJ_H joints (*10, 11*). Although TdT is not required for a functional immune system, in its absence, the immunological diversity is substantially decreased (*12, 13*). Based upon this simple understanding, the most obvious difference between telomerase and TdT is that telomerase adds nucleotides in a specific order to the ends of chromosomes whereas TdT adds nucleotides in a random order to the ends of gene segments.

Mature tRNAs always have the sequence 'CCA' at their 3′-termini. This three-nucleotide sequence is the site for aminoacylation and, therefore, is essential for transferring the amino acid to the growing polypeptide chain during protein synthesis. While some bacterial tRNA genes encode the CCA terminus, most organisms rely on the posttranscriptional addition of the CCA triplet (*14*). The enzyme responsible for synthesis of the 3′-terminal CCA sequence on tRNA molecules is ATP(CTP):tRNA nucleotidyltransferase (CCase) (*14, 15*). Like telomerase, CCase adds nucleotides in a sequence-specific order to its target substrate. Interestingly, from a functional evolutionary standpoint, it has been suggested that CCase may have served as the "original telomerase" to regenerate 3′ termini during RNA replication, despite a lack of

amino acid sequence similarity (*16*). This consideration, however, amplifies one difference between these enzymes; the target substrates for telomerase and CCase are DNA and tRNA, respectively.

How does telomerase, without error, repeatedly add the same sequence to chromosome ends? In the late 1980's and early 1990's, several reports demonstrated that telomere terminal transferase uses an RNA component, which is encoded for in a respective gene, as a template for telomere synthesis (*9, 17-19*). This RNA component is essential, as a targeted disruption of the RNA encoding gene in mice disrupted telomerase activity (*20*). The evidence that telomerase uses an RNA template for telomere elongation is the most significant difference when comparing telomerase to TdT or CCase: the latter two enzymes add nucleotides in a template-independent manner. Finally, because telomerase uses RNA as a template, a new nomenclature for this ribonucleoprotein was adopted, "telomerase reverse transcriptase". This name is still confusing, as this enzyme does not reverse transcribe all RNA molecules nor does it reverse transcribe *telomerase*.

What does one name an enzyme that elongates telomeres by transferring nucleotides to chromosome ends in a sequence-specific manner using an RNA template? Is "telomere reverse transcriptase-like terminal transferase" appropriate? Although this name would be more descriptive, it is still quite a complicated nomenclature. To still encompass all of this enzyme's unique properties and to state that this enzyme elongates telomeres, perhaps "telomere elongase" or "telomere synthase" would be more fitting.

REFERENCES

1 Chan, S. R., and Blackburn, E. H. (2004) Telomeres and telomerase, Philos. Trans. R. Soc. Lond. B. Biol. Sci. 359, 109-121.

2 Greider, C. W., and Blackburn, E. H. (2004) Tracking telomerase, Cell 116, S83-86.

3 Harrington, L. (2003) Biochemical aspects of telomerase function, Cancer Lett. 194, 139-154.

4 Boswell, R. E., Klobutcher, L. A., and Prescott, D. M. (1982) Inverted terminal repeats are added to genes during macronuclear development in Oxytricha nova, Proc. Natl. Acad. Sci. U. S. A. 79, 3255-3259.

5 Szostak, J. W., and Blackburn, E. H. (1982) Cloning yeast telomeres on linear plasmid vectors, Cell 29, 245-255.

6 Bernards, A., Michels, P. A., Lincke, C. R., and Borst, P. (1983) Growth of chromosome ends in multiplying trypanosomes, Nature 303, 592-597.

7 Shampay, J., Szostak, J. W., and Blackburn, E. H. (1984) DNA sequences of telomeres maintained in yeast, Nature 310, 154-157.

8 Greider, C. W., and Blackburn, E. H. (1985) Identification of a specific telomere terminal transferase activity in Tetrahymena extracts, Cell 43, 405-413.

9 Morin, G. B. (1989) The human telomere terminal transferase enzyme is a ribonucleoprotein that synthesizes TTAGGG repeats, Cell 59, 521-529.

10 Collins, A. M., Sewell, W. A., and Edwards, M. R. (2003) Immunoglobulin gene rearrangement, repertoire diversity, and the allergic response, Pharmacol. Ther. 100, 157-170.

11 Benedict, C. L., Gilfillan, S., Thai, T. H., and Kearney, J. F. (2000) Terminal deoxynucleotidyl transferase and repertoire development, Immunol. Rev. 175, 150-157.

12 Gilfillan, S., Dierich, A., Lemeur, M., Benoist, C., and Mathis, D. (1993) Mice lacking TdT: mature animals with an immature lymphocyte repertoire, Science 261, 1175-1178.

13 Komori, T., Okada, A., Stewart, V., and Alt, F. W. (1993) Lack of N regions in antigen receptor variable region genes of TdT-deficient lymphocytes, Science 261, 1171-1175.

14 Schurer, H., Schiffer, S., Marchfelder, A., and Morl, M. (2001) This is the end: processing, editing and repair at the tRNA 3'-terminus, Biol. Chem. 382, 1147-1156.

15 Deutscher, M. P. (1984) Processing of tRNA in prokaryotes and eukaryotes, CRC Crit. Rev. Biochem. 17, 45-71.

16 Maizels, N., Weiner, A. M., Yue, D., and Shi, P. Y. (1999) New evidence for the genomic tag hypothesis: archaeal CCA-adding enzymes and tDNA substrates, Biol. Bull. 196, 331-333; discussion 333-334.

17 Greider, C. W., and Blackburn, E. H. (1987) The telomere terminal transferase of Tetrahymena is a ribonucleoprotein enzyme with two kinds of primer specificity, Cell 51, 887-898.

18 Greider, C. W., and Blackburn, E. H. (1989) A telomeric sequence in the RNA of Tetrahymena telomerase required for telomere repeat synthesis, Nature 337, 331-337.

19 Yu, G. L., Bradley, J. D., Attardi, L. D., and Blackburn, E. H. (1990) In vivo alteration of telomere sequences and senescence caused by mutated Tetrahymena telomerase RNAs, Nature 344, 126-132.

20 Blasco, M. A., Lee, H. W., Hande, M. P., Samper, E., Lansdorp, P. M., DePinho, R. A., and Greider, C. W. (1997) Telomere shortening and tumor formation by mouse cells lacking telomerase RNA, Cell 91, 25-34.

APPENDIX B: LABORATORY PROTOCOLS

GENOTYPING MICE FROM EAR-PUNCH TISSUE

Reagents and Materials:

PBND buffer

500ml H_2O
1.87g KCl (Fisher, BP366-500)
5ml of 1M Tris-HCl Stock
1.25ml of 1M stock $MgCl_2$
50mg gelatin
2.25ml NONIDET P-40 (Amresco, E109)
2.25ml Tween 20 (Fisher, BP337)
Sterilize by autoclaving

Proteinase K (10mg/ml)

1. After "ear-punching" mouse, collect tissue from ear punch tool (1mm diameter) and place into a 1.5ml microfuge tube.
2. Add 150µl 1x PBND buffer to each tube.
3. Add 1µl of Proteinase K (10mg/ml) to each tube.
4. Incubate samples at 55°C overnight.
5. Place tubes at 100°C for 10min to inactivate Proteinase K.
6. Set up PCR reaction using 0.5µl of DNA sample for each reaction.

ESTABLISHING PRIMARY MOUSE EMBRYONIC FIBROBLASTS FROM E13.5-15.5 MICE

Reagents and Materials:

Primary mouse embryonic fibroblast (MEF) growth medium
- 400ml of DMEM
- 37.5ml of FBS
- 37.5ml of NCS
- 25ml of ES cell qualified complete mix

1 x phosphate buffered saline (PBS)
- 1000ml sterile H_2O
- 1 packet of PBS powder
- Filter sterilize (0.22 micron filter)

Tissue homogenizer (Fisher, Tissuemiser 15-338-55)

1. After dissection, place embryo in a snap-cap tube with 3ml of ice-cold 1xPBS. Keep tube on ice while continuing with dissections.
2. In the tissue culture hood, remove PBS with sterile pipette.
3. Place 4ml of primary mouse embryonic fibroblast (MEF) growth medium (37°C) into each snap-cap tube with the embryo.
4. Sterilize tissue homogenizer by dipping it into 70% ethanol and turning it on 3/4 speed for 10sec.
5. Dip homogenizer into sterile 1xPBS and turn it on 3/4 speed for 10sec to rinse off ethanol.
6. Homogenize embryo in primary MEF growth medium at 3/4 speed for 4sec.
7. Before homogenizing next embryo, sterilize tissue homogenizer by dipping it into 70% ethanol and turning it on to 3/4 speed for 10sec.
8. Dip homogenizer into sterile 1xPBS and turn it on to 3/4 speed for 10sec to rinse off ethanol.
9. For each additional embryo, repeat steps 6-8.
10. Transfer each homogenized embryo and primary MEF growth medium (4ml) to a 60mm plate.
11. Place plates in 37° incubator, 5% CO_2.

SOUTHERN BLOTTING

Reagents and Materials:

10xTBE
- 800ml H_2O
- 108g Tris base
- 55g Boric acid
- 3.75g EDTA
- Adjust pH to 8.3
- Add H_2O to bring final volume to 1000ml

1xTBE
- 900ml H_2O
- 100ml 10xTBE

Denaturing solution
- 800ml H_2O
- 87.5g NaCl
- 20g NaOH
- Add H_2O to bring final volume to 1000ml

Neutralizing solution
- 800ml H_2O
- 87.5g NaCl
- 60.5g Tris base
- Adjust pH to 7.6
- Add H_2O to bring final volume to 1000ml

20xSSC
- 800ml H_2O
- 175.25g NaCl
- 88.25g Na Citrate
- Adjust pH to 7.7
- Add H_2O to bring final volume to 1000ml

10xSSC
- 500ml H_2O
- 500ml 20xSSC

100x Denhardts reagent
- 85ml H_2O
- 2g Ficoll
- 2g PVP
- 2g BSA
- Add H_2O to bring final volume to 100ml

Hybridization solution
- 595ml H_2O
- 300ml 20xSSC
- 20ml 0.5M EDTA
- 50ml 100x Denhardts reagent
- 10ml Sheared salmon sperm (1mg/ml)
- 25ml 20% SDS

1xSSC 0.1% SDS
- 945ml H_2O
- 50ml 20xSSC
- 5ml 20% SDS

0.1xSSC 0.1% SDS
- 990ml H_2O
- 5ml 20xSSC
- 5ml 20% SDS

Whatman 3MM paper

Nylon membrane (Nytran Supercharge (SPC), Schleicher & Schuell, 10416280)

1. Digest 3-5µg of DNA with appropriate restriction enzyme.
2. Separate DNA fragments by electrophoresis on a 0.8% agarose gel at 2-3volts/cm for 15h in 1xTBE.
3. Take picture of gel with a ruler next to the DNA ladder.
4. Incubate gel in 0.2M HCl for 15min at room temperature with shaking.
5. Rinse gel with H_2O.
6. Incubate gel in denaturing solution for 30min at room temperature with shaking.
7. Rinse gel with H_2O.
8. Incubate gel in neutralizing solution for 30min at room temperature with shaking.

Capillary transfer

9. Set up large transfer station containing approximately 1000ml of 10xSSC.
    a. Allow transfer stone to become saturated with 10xSSC.

b. Wet one sheet of Whatman 3MM with 10xSSC and lay across the transfer stone (the Whatman 3MM should cover the entire stone).
c. Place gel on the Whatman paper and remove air bubbles under gel.
d. Incubate nylon membrane in H_2O for 5min.
e. Place membrane on top of gel and remove air bubbles.
f. Wet two sheets of Whatman 3MM with 10xSSC and place on top of membrane and remove air bubbles.
g. Place two dry sheets of Whatman 3MM on top of previous wet Whatman papers.
h. Stack paper towels on top of dry Whatman papers.
i. Cover stack with Plexiglas plate and add approximately 500g of weight.

10. Allow transfer station to sit 8h / overnight.
11. Tear down transfer station, remove membrane with forceps, and rinse membrane in neutralizing solution.
12. Allow membrane to dry by placing it on a sheet of Whatman 3MM.
13. UV crosslink DNA onto membrane with 600J/m^2 using a UV Stratalinker.

Hybridization

14. Pre-hybridize membrane in 15ml hybridization solution for 1h at 63°C in rotation oven.
15. Denature radioactively labeled DNA probe for 5min at 100°C.
16. Immediately place probe on ice for 5min.
17. Replace hybridization solution on membrane with fresh 15ml hybridization solution.
18. Add radioactive probe and incubate overnight at 63°C in rotation oven.

Washing

19. Discard radioactive hybridization solution in waste container.
20. Remove membrane with forceps and place in a Tupperware container.
21. Wash membrane two times in 1xSSC 0.1% SDS for 20min at room temperature with shaking.
22. Wash membrane two times in 0.1xSSC 0.1% SDS for 20min at 65°C with constant shaking.
23. Place membrane on dry Whatman 3MM, but do not let it dry completely.
24. Wrap membrane in plastic wrap and expose to film.

ESTABLISHING HIGH PASSAGE CELL LINES FROM PRIMARY MEF CULTURES

Mouse embryonic fibroblasts (MEFs) that are *Trp53*-deficient can be passaged through crisis by splitting cultures 1:3 as cells reach 100% confluence.

For MEFs that are not *Trp53*-deficient, use the 3T3 protocol (Todaro and Green, 1963; Aaronson and Todaro, 1968) to passage primary MEFs through crisis (below).

1. Begin with primary MEFs (≤ passage 3) growing in primary MEF growth medium (4ml) (for medium recipe, see pg. 272) on a 60mm plate.
2. After three days, trypsinize and count cells by hemacytometer.
3. To a new 60mm plate, seed cells at 3 x 10^5 cells per plate in primary MEF growth medium (4ml).
4. Three days after plating, repeat steps 2-3.
5. Continue with this procedure until MEFs have reached passage 10. The cells can then be passaged by splitting cultures 1:3 as the cells reach 100% confluence.

CELL GROWTH CURVE ANALYSIS

Reagents and Materials:

Primary MEF growth medium (pg. 272)

Isotone (Coulter Beckman, 8546719)

Coulter Counter vials (Fisher, 3-341-13)

1. Seed primary MEFs onto a 6-well plate at $8x10^4$ cells per well in primary MEF growth medium (2ml/well).
2. Twenty-four hours after plating, trypsinize (use 0.3ml of trypsin for each well) one well and re-suspend cells in 3ml of primary MEF growth medium.
3. In a Coulter counter vial, add 200µl of cell suspension to 10ml of isotone and gently mix.
4. Prior to sample analysis, fill a clean Coulter counter vial with 10ml of isotone. Load the vial into the Coulter counter and press the Start button. Continue to flush the Coulter counter with the clean isotone until the background registers less than 30 counts. Remove the vial from the Coulter counter.
5. For sample analysis, load the Coulter counter vial containing the cell sample into the Coulter counter and press the Start button. The Coulter counter determines the number of cells in 0.5ml of isotone and will display the number of cells.

   Determine the total number of cells that were trypsinized from the well.

   (Number of cells displayed on Coulter counter / Volume of cell suspension analyzed by the Coulter counter) * (Isotone volume of cell sample / Volume of trypsinized cells in medium added to isotone) * (Volume of medium used to re-suspend cells) = total number of cells in the single well

   For example, assume the Coulter counter displayed 1500 cells.

   (1500cells / 0.5ml) * (10ml / 0.2ml) * 3ml = 4.5×10^5 total cells in the single well.

6. Continue steps 2-5 every twenty-four hours until completion of experiment (full experiment typically lasts 120h).

FLOW CYTOMETRY TO DETERMINE DNA CONTENT IN PRIMARY MEFs

Reagents and Materials:

Citrate buffer

Dissolve 85.50g Sucrose and 11.76g NaCitrate in 800ml of deionized water
Add 50.0ml of DMSO
Bring final volume to 1000ml with deionized water
Adjust pH to 7.6
Filter sterilize (0.45micron filter)
Store at 4°C in sterile bottle
*expires at 6 months

Stock solution

Dissolve 2.0g NaCitrate, 2.0ml NONIDET P-40 (Sigma 74385), 1.04g Spermine (Sigma S-2876), and 0.12g Tris in a final volume of 2000ml deionized water
Adjust pH to 7.6
Filter sterilize (0.45 micron filter)
Store at 4°C in sterile bottle
*Expires at 1 year

Solution A

Dissolve 15 mg trypsin (Sigma T-0303) in 500ml of stock solution
Adjust pH to 7.6
Filter sterilize (0.45 micron filter)
Store in frozen aliquots (10ml)
*Expires at 1 year

Solution B

Dissolve 250mg trypsin inhibitor (Sigma T-9253) and 50mg RNase (Worthington 5650) in 500ml of stock solution
Adjust pH to 7.6
Filter sterilize (0.45 micron filter)
Store in frozen aliquots (10ml)
*Expires at 1 year

Solution C

Dissolve 208mg propidium iodide (Sigma P-4170) and 580mg Spermine (Sigma S-2876) in 500ml of stock solution
Adjust pH to 7.6
Filter sterilize (0.45 micron filter)
Store protected from light at 4°C
*Expires at 1 year

Experiment for a 100mm plate of cells (grown in 10ml medium). The cells must be actively dividing to get an accurate measurement of cell cycle. Do not use cells that are 100% confluent.

Freezing cells

1. Trypsinize (cells must be in a single cell suspension) and count cells by hemacytometer.
2. Transfer cell suspension to a 15ml tube and centrifuge (tabletop, swinging bucket centrifuge) at 100 RCF for 3min to pellet cells.
3. Aspirate medium.
4. Re-suspend cell pellet in citrate buffer at a cell concentration of 5 x 10^6 cells/ml (proper cell concentration is very important).
5. Transfer 200µl of cells suspension to a freezer vial.
6. Place cells/vials at -80°C indefinitely (Do not place cells in a "freezing container". The cells will not be viable after freezing and are not to be re-grown).

Analysis

7. Remove cells from freezer and allow them to thaw (on the benchtop) to room temperature.
8. Upon thawing, remove 100µl of cell sample and place in a 15ml Falcon tube.
9. Add 450µl of solution A to each tube and incubate for 10min at 25°C with gentle mixing.
10. Add 375µl of solution B to each tube and incubate for 20min at 25°C with gentle mixing.
11. Add 375µl of solution C to each tube (keep in dark), gently vortex, and incubate in dark for a minimum of 15min at 25°C.
12. Re-suspend nuclei and filter through a 30 micron nylon mesh into a flow cytometer tube (12x75mm polystyrene culture tube).
13. Analyze samples according to instructions (Tom Sawyer, Flow Cytometry Specialist, Medical University of Ohio, Department of Pathology, 419-383-4212).

PREPARATION OF METAPHASE CHROMOSOME SPREADS

Reagents and Materials:

Hypotonic solution
- 50.0ml H_2O
- 0.28g KCl (Fisher, BP366-500)
- Make fresh for each use

Fixative solution
- 19.5ml absolute methanol
- 6.5ml glacial acetic acid
- Make fresh for each use

Giemsa stain
- 94ml of H_2O
- 4ml of Giemsa stain (Harleco, EM Science, L620-32)
- 2ml of methanol
- *Gravity filter through Whatman filter paper (Whatman, 15.0cm Ashless 40, catalog 1440 150)

1. Treat a 60mm plate (containing 4ml of medium) of actively dividing cells with 8µl of Colcemid (at 10µg/ml) for 2h at 37°C (final concentration of Colcemid in medium is 0.02µg/ml).
2. Wash plate with 1x PBS and trypsinize. Re-suspend cells in 3ml of growth medium by pipetting up and down 10-15 times.
3. Transfer cell suspension to a 15ml tube, spin (tabletop, swinging bucket centrifuge) for 3min at 100 RCF. Aspirate all but the last 200µl of medium. Finger-flick tube to re-suspend cells.
4. Add 1ml of hypotonic solution; flick tube again to re-suspend. Add 3ml of hypotonic solution. Leave at room temperature for 6-12min.
5. Centrifuge (tabletop, swinging bucket centrifuge) tube for 5min at 100 RCF. Remove supernatant and flick tub to re-suspend cell pellet.
6. Add 1ml of fixative solution (fix) and finger-flick tube to re-suspend. Add 3ml of fix.
7. Repeat Steps 5 and 6 three times.
8. After last spin, re-suspend cells in 1ml of fix and finger-flick tube.
9. Test-drop cells onto one slide from about 12in above slide. View slide under phase-contrast microscope to check cell density and to determine if cells are bursting (if the cells are bursting, you will see chromosome spreads). If cells are too dense, add more fix and finger-flick to re-suspend. If there is not enough spreads present, spin again and re-suspend in 0.5ml fix. If no chromosome spreads are observed, try dropping cells from 24in above slide.
10. Drop remaining slides and allow them to dry at room temperature.

11. Giemsa stain slides for 8min in Coplin jar.
12. Rinse slides twice in distilled water and air-dry.
13. Examine spreads under oil immersion using a 100x objective (1000x magnification total).

SISTER CHROMATID EXCHANGE

Reagents and Materials:

Cell growth medium (SCE medium)
- 416ml McCoy's 5A medium (Cellgro, 10-050-CV)
- 75ml newborn calf serum
- 5ml Pen-Strep
- 4ml L-glutamine

2 mM BrdU
- 10ml H_2O
- 0.006142g BrdU (Sigma, B5002-250)
- Filter-sterilize (0.22 micron filter)
- Distribute in 1ml aliquots in the dark and store at –20^{o}C

Hypotonic solution
- 45.5ml H_2O
- 2.5ml newborn calf serum
- 1ml 100mg/ml KCl
- 1ml 100mg/ml sodium citrate

Carnoy's fixative
- 19.5ml absolute methanol
- 6.5ml glacial acetic acid
- Make fresh for each use

100x Hoechst 33258 dye
- 10ml H_2O
- 0.5mg Hoechst 33258 (Sigma, B1155-100)
- Store in the dark at 4^{o}C
- Good for ~2 weeks

Sorensen's buffer
- 500ml H_2O
- 47.57g Na_2HPO_4
- 45.56g KH_2PO_4
- pH to 6.8. Store at room temperature

10x Hoechst working solution
- 45ml 1x Sorensen's buffer
- 5ml 100x Hoechst 33258
- Keep in the dark and make fresh for each use

20X SSC

500ml H_2O
87.65g NaCl
44.13g sodium citrate

Gurr buffer

1000ml H_2O
1 tablet Gurr buffer (BDH Laboratory Supplies, 331992P)
pH to 6.8

4% Giemsa stain

48ml Gurr buffer
2ml Giemsa stain (Harleco, EM Science, L620-32)

1. Seed a T-75 flask with $1x10^6$ cells, suspended in 18ml of SCE Medium.
2. Add with 75µl of 2mM BrdU (10µM final concentration). Turn lights off while working with BrdU.
3. Incubate at 37°C for 2 cell cycles (You must know the doubling time of each cell line used in this experiment. This should be determined by performing a growth curve analysis for each cell line. The protocol is described on pg. 277).
4. Add 36µl of 10µg/ml Colcemid 2h before the end of the second cycle (final concentration of Colcemid in medium is 0.02µg/ml). Incubate 2h. During this time, warm hypotonic solution to 37°C.
5. Wash plate with 1x PBS and trypsinize. Re-suspend cells in 6ml of growth medium by pipetting up and down 10-15 times.
6. Transfer cell suspension to a 15ml tube and centrifuge (tabletop, swinging bucket centrifuge) for 3min at 100 RCF. Aspirate all but the last 200µl of medium. Finger-flick tube to re-suspend cells.
7. Add 6ml of warm hypotonic solution dropwise. Flick tube to re-suspend cells after each 1ml.
8. Incubate tube at 37°C for 15min.
9. Centrifuge (tabletop, swinging bucket centrifuge) tube for 5min at 100 RCF. Gently remove supernatant and flick tube to re-suspend cell pellet.
10. Add 5ml of cold (4°C) Carnoy's fixative dropwise. Finger-flick tube after each 1ml.
11. Repeat steps 9-10 three times.
12. After last spin, re-suspend cells in 1ml of fix and finger-flick tube.
13. Test-drop cells onto one slide from about 12in above slide. View slide under phase-contrast microscope to check cell density and to determine if cells are bursting (if the cells are bursting, you will see chromosome spreads). If cells are too dense, add more fix and finger-flick to re-suspend. If there is not enough spreads present, spin again and re-suspend in 0.5ml fix. If no chromosome spreads are observed, try dropping cells from 24in above slide.

14. Drop remaining slides. Let dry at room temperature in the dark.
15. Age the slides for 48h in the dark at room temperature.

Harlequin Staining (performed in the dark)

16. Stain slides in 1x Hoechst working solution for 20min at room temperature. Rinse slides and air-dry. Meanwhile, preheat the slide warmer to 65 ^{o}C.
17. Place a drop of 10x Sorensen's buffer onto each slide, and add a coverslip.
18. Place the slides on the slide warmer (65 ^{o}C) and expose to blacklight for 20min. The bulb should be ~2in away from the slides.
19. Remove the coverslips and rinse in H_2O. Air-dry.
20. Place a drop of 20x SSC onto each slide and add a coverslip. Incubate on slide warmer (65 ^{o}C) for 20min.
21. Remove coverslips and rinse in H_2O. Air-dry.
22. Stain slides in 4% Giemsa for 5min. Rinse in two separate beakers of ddH_2O, and air-dry.
23. Examine spreads under oil immersion using a 100x objective (1000x magnification total) to determine differential staining of sister-chromatids.

* To determine the frequency of DNA damage induced SCEs, DNA damaging agent should be added for one cell cycle prior to harvesting.

IMMUNOFLUORESCENCE OF CENTROSOMES

Reagents and Materials:

Monoclonal anti-γ-tubulin CY3 conjugate (Sigma, item C-7604)

Monoclonal anti-α-tubulin FITC conjugate clone DM1A (Sigma, item F-2168)

Absolute methanol (4°C)

Acetone (4°C)

1 x phosphate buffered saline (PBS)
1000ml sterile H_2O
1 packet of PBS powder
Filter sterilize (0.22 micron filter)

1xPBS 1%BSA
100ml 1xPBS
1g BSA
Make fresh for each use

20X SSC
500ml H_2O
87.65g NaCl
44.13g sodium citrate

2xSSC 0.1% Tween 20
190ml H_2O
10ml 20xSSC
100µl Tween 20 (Fisher, BP337)

DAPI stock solution (100µg/ml)
10ml H_2O
1mg DAPI powder (Sigma, D9542)

DAPI working solution
50ml 2xSSC 0.1% Tween 20
100µl of DAPI stock solution

1. Place sterilized round glass coverslips (18mm in diameter) into each well of a 12-well plate. Seed $8x10^4$ MEFs into each well (feed cells with 1ml medium/well).
2. Incubate overnight at 37°C. This allows cells to become semi-confluent (70-80%) for fixation.

3. Remove medium and wash with 1xPBS two times (1ml/well for each wash).
4. Add 1 ml of cold methanol to each well and place at –20°C for 10min.
5. Aspirate methanol.
6. Add 1 ml of cold acetone to each well and place at –20°C for 1min.
7. Remove acetone.
8. Wash each well 2 times with 1ml of 1xPBS 1%BSA.
9. Re-hydrate cells in 1ml of 1xPBS 1%BSA for 45min at room temperature.
10. Dilute gamma tubulin Ab (Sigma) 1:600 in 1xPBS 1%BSA.
11. Add 300µl of diluted Ab to each coverslip.
12. Incubate at RT for 60min.
13. Remove antibody and wash 3 times with 1ml of 1xPBS 1%BSA (five min. per wash).
14. Dilute alpha tubulin Ab (Sigma) 1:300 in 1xPBS 1%BSA.
15. Add 300µl of diluted Ab to each coverslip.
16. Incubate at room temperature for 60min.
17. Remove antibody and wash 3 times with 1ml of 1xPBS 1%BSA (five min. per wash).
18. Wash one time with 1ml of 1xPBS.
19. Add 300µl of DAPI (100ng/ml) stain to each coverslip and incubate at room temperature for 10min.
20. Remove DAPI stain and wash with 1ml of 1xPBS 1%BSA three times.
21. Remove coverslips from wells (one at a time).
22. Touch edge of coverslip to paper towel.
23. Place one drop of anti-fade solution (Dako Cytomation Fluorescent Mounting Medium, Dako, item 53023) to slide before mounting.
24. Place coverslip on slide (with cells facing down) directly on top of drop of anti-fade solution.
25. Incubate slides in the dark at room temperature for 30min.
26. Seal coverslips onto slides with nail polish.
27. Slides can be viewed immediately or stored at 4°C.

PROCEDURE FOR GIEMSA STAINING MEF COLONIES

Reagents and Materials:

Giemsa stain
232.5ml H_2O
10ml methanol
7.5ml Giemsa stain (Harleco, EM Science, L620-32)

1. Aspirate growth medium from 150mm tissue culture dish.
2. Wash culture dish with 20ml of 1x PBS twice.
3. Add 20ml of ice cold methanol (gently). Leave cells at room temperature for 20min.
4. Aspirate methanol and allow plates to air-dry.
5. Add 20ml of Giemsa stain to dish. Incubate at room temperature for 30min.
6. Remove Giemsa stain and place Giemsa solution in waste container.
7. Rinse dish with 20ml of single distilled water.
8. Remove water rinse and allow plates to air-dry at room temperature.
9. Count Giemsa-stained colonies (as a standard, a colony consists of >50 cells).

TREATING MOUSE EMBRYONIC FIBROBLASTS WITH ULTRAVIOLET LIGHT

Reagents and Materials:

UV Stratalinker® 2400 (Stratagene)

Mouse embryonic fibroblast (MEF) growth medium
400ml of DMEM
75.0ml of NCS
25ml of ES cell qualified complete mix

1x phosphate buffered saline (PBS)
1000ml sterile H_2O
1 packet of PBS powder
Filter sterilize (0.22 micron filter)

1. Seed MEFs onto a 6-well plate at approximately 750 (*Trp53*$^{-/-}$) to 3000 (*Rad51d*$^{-/-}$ *Trp53*$^{-/-}$) cells per well (use 2ml of growth medium per well).
2. Place plates into the 37°C incubator, overnight.
3. Aspirate and discard growth medium from each well.
4. Place 0.5ml of 1xPBS into each well (just enough to cover the cells).
5. Place the 6-well plates into the UV Stratalinker® 2400 (Stratagene) and remove the plate lid.
6. Close the UV Stratalinker® 2400 door and input the dose (see UV Stratalinker® 2400 owners manual) (any dose above 25J/m^2 is lethal to all cells).
7. After treatment, aspirate and discard 1xPBS.
8. Feed cells with fresh medium (2ml/well) and place cells into 37°C incubator.
9. Incubate cells in the 37°C incubator for 8-10 days to allow colonies to form (feed cells with fresh medium every two days).
10. Stain and count colonies (see pg. 287 for protocol).

TREATING MOUSE EMBRYONIC FIBROBLASTS WITH IONIZING RADIATION

Reagents and Materials:

Clinac 1800 X-Ray machine (400cGy/min)

Mouse embryonic fibroblast (MEF) growth medium
400ml of DMEM
75.0ml of NCS
25ml of ES cell qualified complete mix

1. Seed MEFs onto a 6-well plate at approximately 750 (*Trp53*$^{-/-}$) to 3000 (*Rad51d*$^{-/-}$ *Trp53*$^{-/-}$) cells per well (use 2ml of growth medium per well).
2. Place plates into the 37°C incubator, overnight.
3. Remove plates from the incubator and take them to the hospital radiation facility.
4. Give the plates to the radiation specialist for treatment (any dose above 10Gy is lethal to all cells).
5. The cells should be treated from the bottom of the plate (the plate lid should not be removed from the plate).
6. After treatment, transfer cells to the tissue culture hood and aspirate (discard) growth medium.
7. Feed cells with fresh medium (2ml/well) and place cells into 37°C incubator.
8. Incubate cells in the 37°C incubator for 8-10 days to allow colonies to form (feed cells with fresh medium every two days).
9. Stain and count colonies (see pg. 287 for protocol).

DETECTING ANAPHASE BRIDGES IN PRIMARY MEFs

Reagents and Materials:

1x phosphate buffered saline (PBS)
- 1000ml sterile H_2O
- 1 packet of PBS powder
- Filter sterilize (0.22 micron filter)

3xphosphate buffered saline (PBS)
- 333ml sterile H_2O
- 1 packet of PBS powder
- Filter sterilize (0.22 micron filter)

4% paraformaldehyde
- 66ml H_2O heated to 60°C
- 4g paraformaldehyde (Sigma, P-6148)
- 1 drop of 2M NaOH
- Continue at 60°C with stirring until solution becomes clear
- Add 33ml of 3xPBS
- pH to 7.2
- Filter sterilize (0.22 micron filter)
- Store at 4°C

1xPBS 0.3% Triton X
- 100ml 1xPBS
- 300µl Triton X 100 (Fisher, BP151)

20X SSC
- 500ml H_2O
- 87.65g NaCl
- 44.13g sodium citrate

2xSSC 0.1% Tween 20
- 190ml H_2O
- 10ml 20xSSC
- 100µl Tween 20 (Fisher, BP337)

DAPI stock solution (100µg/ml)
- 10ml H_2O
- 1mg DAPI powder (Sigma, D9542)

DAPI working solution

50ml 2xSSC 0.1% Tween 20
100µl of DAPI stock solution

1. Place sterilized round glass coverslips (18mm in diameter) into each well of a 12-well plate. Seed $8x10^4$ MEFs into each well (feed cells with 1ml medium/well).
2. Incubate overnight at 37°C. This allows cells to become semi-confluent (70-80%) for fixation.
3. Remove medium and wash twice with 1xPBS.
4. Fix cells using 4% paraformaldehyde for 20min at 4°C.
5. Wash twice with 1x PBS.
6. Add 0.5ml of 0.3% Triton x in 1xPBS for 10min at 4°C.
7. Wash twice with 1xPBS.
8. Remove all 1xPBS.
9. Add 150µl of DAPI working solution to each well and place in dark for 10min at room temperature.
10. Wash slides twice with 1x PBS (1ml/well for each wash).
11. Remove coverslips from wells (one at a time).
12. Touch edge of coverslip to paper towel.
13. Place one drop of anti-fade solution (Dako Cytomation Fluorescent Mounting Medium, Dako, item 53023) to slide before mounting.
14. Place coverslip on slide (with cells facing down) directly on top of drop of anti-fade solution.
15. Incubate slides in the dark at room temperature for 30min.
16. Seal coverslips onto slides with nail polish.
17. Slides can be viewed immediately or stored at 4°C.

LABELING TELOMERES FROM METAPHASE SPREADS WITH A FLUORESCENT PEPTIDE NUCLEIC ACID PROBE

Reagents and Materials:

Telomere peptide nucleic acid (PNA) probe-Cy3. Applied Biosystems, Catalog number 4337107

Hypotonic solution
- 50.0ml H_2O
- 0.28g KCl (Fisher, BP366-500)
- Make fresh for each use

Fixative solution
- 19.5ml absolute methanol
- 6.5ml glacial acetic acid
- Make fresh for each use

100% ethanol

85% ethanol
- 15ml H_2O
- 85ml 100% ethanol

70% ethanol
- 30ml H_2O
- 70ml 100% ethanol

20X SSC
- 500ml H_2O
- 87.65g NaCl
- 44.13g sodium citrate

20X SSC 1% Tween 20
- 100ml 20X SSC
- 1ml Tween 20 (Fisher, BP337)
- pH to 7.2

2X SSC 0.1% Tween 20
- 90ml H_2O
- 10ml 20X SSC 1% Tween 20

1 x phosphate buffered saline (PBS)
1000ml sterile H_2O
1 packet of PBS powder
Filter sterilize (0.22 micron filter)

1xPBS 0.1% Tween 20
100ml 1x PBS
1ml Tween 20 (Fisher, BP337)

10% Pepsin stock solution
10ml H_2O
1g pepsin (Acros, 41707)
store at -20°C

0.005% Pepsin working solution
50ml 0.01M HCl
25µl 10% pepsin stock solution

DAPI stock solution (100µg/ml)
10ml H_2O
1mg DAPI powder (Sigma, D9542)

DAPI working solution
50ml 2xSSC 0.1% Tween 20
100µl of DAPI stock solution

1. Treat each 60mm plate (each plate contains 4ml medium) of actively dividing cells with 8µl of Colcemid (at 10µg/ml) for 2h at 37°C (final concentration of Colcemid in medium is 0.02µg/ml).
2. Wash plate with 1xPBS and trypsinize. Re-suspend cells in 3ml of growth medium by pipetting up and down 10-15 times.
3. Transfer cell suspension to a 15ml tube and centrifuge (tabletop, swinging bucket centrifuge) for 3 min at 100 RCF. Aspirate all but the last 200µl of medium. Finger-flick tube to re-suspend cells.
4. Add 1ml of hypotonic solution; flick tube again to re-suspend. Add 3ml of hypotonic solution. Leave at room temperature for 6-12min.
5. Centrifuge (tabletop, swinging bucket centrifuge) tube for 5min at 100 RCF. Remove supernatant and flick tube to re-suspend cell pellet.
6. Add 1ml of fixative solution (fix), finger-flick tube to re-suspend. Add 3ml of fix.
7. Repeat Steps 5 and 6 three times.
8. After last spin, re-suspend cells in 1ml of fix and finger-flick tube.
9. Test-drop cells onto one slide from about 12in above slide. View slide under phase-contrast microscope to check cell density and to determine if cells are bursting (if the cells are bursting, you will see chromosome spreads). If cells are

too dense, add more fix and finger-flick to re-suspend. If there is not enough spreads present, spin again and re-suspend in 0.5ml fix. If no chromosome spreads are observed, try dropping cells from 24in above slide.

10. Drop remaining slides. Let dry at room temperature.
11. Place the slide in 0.005% Pepsin Working Solution for 7.5min at 37°C.
12. Wash slide in 1xPBS pH7.0-7.5 for 5min.
13. Dehydrate the slide through a cold ethanol series (aqueous 70%, 85%, 100%)
14. Air-dry slides.
15. Apply 12µl of the PNA probe to the target area of the slide.
16. Immediately cover with a large coverslip and allow the solution to spread evenly under the coverslip.
17. Place the slide(s) into the humid incubator (Tupperware container containing wet paper towels) (70°C) for 7min.
18. Place the slide into another humid chamber (Tupperware container containing wet paper towels) at room temp.
19. Incubate in the dark for 30min.
20. Immerse the slide in 1xPBS 0.1% Tween 20 wash solution at room temperature to remove coverslips.
21. Transfer slide to 1xPBS 0.1% Tween 20 wash solution at 57°C and wash for 20min.
22. Rinse slide in 2xSSC 0.1% Tween 20 wash solution for 1min at room temperature.
23. Add 20µl of DAPI working solution (100ng/ml) to each slide and cover with large coverslip.
24. Incubate at room temp for 5min.
25. Rinse slide in 2xSSC 0.1% Tween 20 to remove coverslip.
26. Touch slide of slide to a paper towel to remove excess wash solution.
27. Apply one drop of mounting medium (Dako Cytomation Fluorescent Mounting Medium, Dako, item 53023) to slide and cover with a coverslip.
28. Place slide in the dark for 30min at room temp.
29. Seal coverslip with nail polish.
30. View slide or place at 4°C (in slide box to keep away from light).

LABELING γ-H2AX AND TELOMERES FOR IMMUNOFLUORESCENCE

Reagents and Materials:

1°Antibody: Anti-phospho-Histone H2AX (Ser139), clone JBW301, mouse monoclonal IgG_1. Upstate, Catalog number 05-636.

2°Antibody: Oregon Green 488 goat anti-mouse IgG. Molecular Probes, Catalog number 06380.

Telomere peptide nucleic acid (PNA) probe-Cy3. Applied Biosystems, Catalog number 4337107

4% paraformaldehyde
- 66 ml H_2O heated to 60°C
- 4 g paraformaldehyde (Sigma, P-6148)
- 1 drop of 2M NaOH
- Continue at 60°C with stirring until solution becomes clear
- 33 ml 3xPBS
- pH to 7.2
- Filter sterilize (0.22 micron filter)
- Store at 4°C

1xPBS 0.2% Triton X
- 100 ml 1xPBS
- 200 µl Triton X 100 (Fisher, BP151)

1xPBS 5% milk
- 100 ml 1xPBS
- 5 g powdered milk

20xSSC
- 800 ml H_2O
- 175.25 g NaCl
- 88.25 g Na Citrate
- Adjust pH to 7.7
- Add H_2O to bring final volume to 1000 ml

70% Formamide solution
- 10 ml H_2O
- 5 ml 20xSSC
- 35 ml formamide

PN Buffer (0.1M Na_2HPO_4, 0.05M NaH_2PO_4, 0.1% triton X)

1000 ml H_2O
26.8 g $Na_2HPO_4 \cdot 7H_2O$
6.9 g $NaH_2PO_4 \cdot H_2O$
1 ml Triton X 100 (Fisher, BP151)

Sterilize glass microscope slide by dipping in 100% ethanol, blotting off excess ethanol, and passing through flame. When ethanol is burned off completely, place slide into a 100mm tissue culture plate.

From a confluent 100mm plate of actively dividing MEFs, trypsinize, and plate at a 1:3 or 1:4 (depending on rate of cell division of the MEFs) onto the plate containing the glass microscope slide. Plates containing glass slides will require more medium than normal (instead of 10 ml of medium, use 20 ml). Place plates in incubator overnight.

Cells must be grown to semi-confluence on glass slide. If cells are the appropriate density (70-80% confluence), continue on with fixing and labeling. If not, place them back into incubator and wait an additional 24 hours.

Fixation and immuno-labeling γ-H2AX

1. Remove slide from plate and dip into (wash) a coplan jar containing 1xPBS.
2. Remove slide and wash through another coplan jar containing 1xPBS.
3. Place slide into a coplan jar containing 4% paraformaldehyde (in 1x PBS) for 20min at room temperature.
4. Wash slides in 1xPBS for 10min at room temperature.
5. Place slide into 0.2% Triton X (in 1x PBS) for 10min at room temperature.
6. Soak slides in 1xPBS 5%Milk (made fresh from powder) for 45min at room temperature.
7. Dilute anti-γ-H2AX Ab in 1xPBS 5%Milk 1:600 (you need 500µl per slide).
8. Lay slide into a humid chamber (Tupperware container containing wet paper towels) on top of a PCR grid and add 500µl of diluted Ab to each slide (be sure to cover the whole slide with the Ab).
9. Incubate 1h at room temperature in humid chamber.
10. Remove primary Ab and wash in 1xPBS for 5min at room temperature.
11. Wash slide in 1xPBS 5%milk for 5min at room temperature.
12. Dilute secondary Ab in 1xPBS 5%milk 1:600 (you need 500µl per slide).
13. Lay slide into a humid chamber (Tupperware container containing wet paper towels) on top of a PCR grid and add 500µl of diluted Ab to each slide (be sure to cover the whole slide with the Ab).
14. Incubate at RT in the dark in a humid chamber for 1h.
15. Remove secondary Ab and wash 4 times in 1xPBS for 5min at room temperature.

Labeling telomeres with peptide nucleic acid (PNA) probe

16. Place slide into a coplan jar containing 4% paraformaldehyde (in 1x PBS) for 20min at room temperature.
17. Dehydrate slides through the cold (4°C) ethanol series (75%, 85%, 100%): 2min in each ethanol solution.
18. Allow slides to air-dry completely.
19. Denature slides in 70% formamide solution for 2min at 75°C.
20. Dehydrate slides through the cold (4°C) ethanol series (75%, 85%, 100%): 2min in each ethanol solution.
21. Allow slides to air-dry completely.
22. Apply 10µl of telomere PNA probe to the center of the slide and cover area with a large glass coverslip (try to avoid air bubbles between the slide and coverslip).
23. Lay slide into a humid chamber (Tupperware container containing wet paper towels) on top of a PCR grid for 2h at room temperature.
24. Wash slide in 70% formamide solution (be sure to remove coverslip, it should fall off when slide is placed in this wash) for 15min at 32°C.
25. Wash slide in PN buffer for 5min at room temperature.

Staining DNA with DAPI

26. Add 500µl of DAPI stain (100ng/ml) to each slide and incubate for 10min at room temperature.
27. Remove DAPI stain and wash in 1xPBS for 5min at room temperature three times.
28. Add one drop of anti-fade reagent (Dako Cytomation Fluorescent Mounting Medium, Dako, item 53023) to the center of the slide and cover with a glass coverslip.
29. Allow slides to sit in dark at room temperature for 30min.
30. Seal with nail polish. View immediately or store at 4°C.

ESTIMATING TELOMERE LENGTHS BY TELOMERE RESTRICTION FRAGMENT ANALYSIS IN MEF CELLS

Reagents and Materials:

1M Tris
- 1000ml H_2O
- 121g Tris
- pH to 8.0

0.5M EDTA
- 1000ml H_2O
- 186g EDTA
- pH to 8.0

TE Buffer
- 990ml H_2O
- 10ml 1M Tris
- 0.2ml 0.5M EDTA

2% Low melt agarose
- 100ml TE Buffer
- 2g low melt agarose

Lithium dodecyl sulfate (LDS) solution
- 400ml H_2O
- 5g lithium dodecyl sulfate (Sigma, L9781)
- 100ml 0.5M EDTA
- 5ml 1M Tris

20% NDS solution
- 372ml H_2O
- 1ml 1M Tris
- 0.9228g N-laurylsarcosine (Sigma, L5000)
- 127ml 0.5M EDTA

Alkali denaturing solution
- 250ml H_2O
- 8.7g NaCl
- 2g NaOH

Neutralizing solution

250ml H_2O
21.9g NaCl
15.1g Tris

10x TBE buffer

800ml H_2O
108g Tris
55g boric acid
40ml 0.5M EDTA

0.5x TBE buffer

1900ml H_2O
100ml 10x TBE buffer

Hybridization solution

145ml H_2O
0.621g NaH_2PO_4
1.125ml 20% SDS
22.5ml of 50x Denhardt's solution
56.25ml 20x SSC

G-rich telomere probe

$(TTAGGG)_4$ oligonucleotide (IDT, Inc.)
Dilute oligonucleotide in sterile H2O to a final concentration of 2μM

1. Trypsinize, count, and pellet cells (tabletop, swinging bucket centrifuge) (100 RCF for 6min). Aspirate off medium.
2. Re-suspend pellet in 1xPBS so cell conc. is 1.67×10^6 cells/ml.
3. Place 1ml of cell suspension (1.67×10^6 cells) into a 1.5ml microfuge tube.
4. Spin cells down to pellet at 100 RCF for 5min.
5. Aspirate off PBS. Mix equal volume of 2% low melt agarose (LMA) and TE in a separate tube (50°C).
6. Transfer 40μl of LMA/TE mixture to the cell pellet, re-suspend, and transfer to a 200μl PCR tube.
7. Place samples at 4°C for 15min.
8. Open caps of PCR tubes. Using a pair of scissors, snip off very bottom of PCR tube and use a toothpick to push plug into a falcon tube containing LDS solution. As a standard, use 3ml/plug.
9. Incubate at 37°C overnight.
10. Remove plugs from LDS solution.
11. Wash the plugs at room temperature for 2h in 20% NDS solution (2.5ml/plug).

12. Discard 20% NDS and replace with fresh 20% NDS solution (2.5ml/plug). Incubate at room temperature for 2h (plugs can be stored at 4°C in 20% NDS solution until ready for DNA digestion).
13. DNA plugs to be digested, incubate at room temperature in TE for 1h (2ml/plug).
14. Remove TE and replace with fresh TE (2ml/plug). Incubate at room temperature for 1h.
15. Remove TE.
16. Place plugs in individual 1.5ml microfuge tubes.
17. Incubate plugs for 1hr in 1xMbo1 restriction enzyme buffer at room temperature (200µl/plug).
18. Remove buffer.
19. Incubate plugs for 1h in 1xMbo1 restriction enzyme buffer at room temperature (200µl/plug).
20. Remove buffer and make digestion mix.
    Per plug
    a. 92µl H_2O
    b. 15µl 10x RE buffer
    c. 3µl RE MboI (New England Biolabs, R0147L)
    d. Final volume is 150µl (including 40µl plug)
21. Incubate at 37°C overnight.
22. Add 2µl of Mbo1 enzyme to each plug. Place at 37°C for 4-5h.
23. Discard restriction enzyme mix.
24. Prepare all plugs for electrophoresis by washing each plug in 4 ml of TE for 1h at room temperature.
25. Remove TE and add a fresh 4ml of TE, wash at room temperature for 1h.
26. Remove TE and incubate plugs for 1h at room temperature in 4ml of 0.5xTBE.
27. Load plugs into wells of the gel (1.2% agarose gel) and then cover each well with 1% LMA at 50°C.
28. Place whole gel at 4°C for 15min.
29. Run gel using pulsed field gel electrophoresis in 2500ml of 0.5x TBE (20h at a constant 6v/cm (200 V), ramping pulse times from 1 to 10sec. Keep run temperatures at 14°C).
30. Post-stain gel in 0.5xTBE (approximately 200ml) with 4µl of EtBr for 1h.
31. Take picture of gel with ruler.
32. Dry gel for 1h at 50°C.
33. Take picture of gel with ruler.
34. Alkali denature DNA by placing gel in denaturing solution for 1h at room temperature with constant shaking.
35. Neutralize by placing gel in neutralizing solution for 1h at room temperature with constant shaking.
36. Place gel in H_2O for 30min at room temperature with constant shaking.
37. Pre-hybridize gel in 10ml of hybridization solution in “seal-a-meal” bag at 55°C for 1h.
38. Make up radioactively labeled probe by mixing

a. 2.5µl DNA fragment (at 2µM. 5pmol) "G-rich probe"
b. 5.0µl 5x Forward reaction buffer (Invitrogen, Y02295)
c. 1.0µl T4 polynucleotide kinase (10U) (Invitrogen, 18004-010)
d. 2.5µl [γ-^{32}P]ATP (10µCi/µl, 3000Ci/mmol)
e. 14.0µl H_2O

39. Incubate probe at 37°C for 15min.
40. Stop labeling reaction by adding EDTA for a final conc. of 5mM (for final volume of 200µl, add 175µl of 5.7mM EDTA).
41. Determine initial radioactive counts per min (CPM).
42. Make G25 sephadex column. (Add 3ml of sephadex mixture to spin column and spin at 575 RCF for 1.5min.
43. Add radioactive probe to G25 sephadex column and centrifuge (tabletop, swinging bucket centrifuge) at 575 RCF for 1.5min.
44. Determine final probe CPM (determine % incorporation).
45. Replace pre-hybridization solution with fresh 10ml of hybridization solution.
46. Add labeled probe to gel, seal bag, seal inside a second bag, and incubate with shaking overnight in Tupperware container at 55°C.
47. Cut off corner of bag and use pipette to remove radioactive hybridization solution and discard into liquid waste container.
48. Place gel in medium sized Tupperware container.
49. Wash gel with 333ml of 4xSSC for 20min at RT on shaker three times.
50. Wash gel with 333ml of 4xSSC 0.1%SDS for 20min at 57°C with shaking three times.
51. Blot gel dry with Whatman papers.
52. Wrap gel in plastic wrap and expose to phosphoimager screen for 3h – overnight at room temperature.
53. Develop film and quantify radioactive signals. Telomere lengths are determined as described by Harley et al., 1990.

DETERMINING RELATIVE TELOMERIC OVERHANG LENGTH IN PRIMARY MOUSE EMBRYONIC FIBROBLASTS

Reagents and Materials:

1M Tris
- 1000ml H_2O
- 121g Tris
- pH to 8.0

0.5M EDTA
- 1000ml H_2O
- 186g EDTA
- pH to 8.0

TE Buffer
- 990ml H_2O
- 10ml 1M Tris
- 0.2ml 0.5M EDTA

2% Low melt agarose
- 100ml TE Buffer
- 2g low melt agarose

Lithium dodecyl sulfate (LDS) solution
- 400ml H_2O
- 5g lithium dodecyl sulfate (Sigma, L9781)
- 100ml 0.5M EDTA
- 5ml 1M Tris

20% NDS solution
- 372ml H_2O
- 1ml 1M Tris
- 0.9228g N-laurylsarcosine (Sigma, L5000)
- 127ml 0.5M EDTA

Alkali denaturing solution
- 250ml H_2O
- 8.7g NaCl
- 2g NaOH

Neutralizing solution

250ml H_2O
21.9g NaCl
15.1g Tris

10x TBE buffer

800ml H_2O
108g Tris
55g boric acid
40ml 0.5M EDTA

0.5x TBE buffer

1900ml H_2O
100ml 10x TBE buffer

Hybridization solution

145ml H_2O
0.621g NaH_2PO_4
1.125ml 20% SDS
22.5ml of 50x Denhardt's solution
56.25ml 20x SSC

G-rich telomere probe

$(TTAGGG)_4$ oligonucleotide (IDT, Inc.)
Dilute oligonucleotide in sterile H2O to a final concentration of 2μM

C-rich telomere probe

$(CCCTAA)_4$ oligonucleotide (IDT, Inc.)
Dilute oligonucleotide in sterile H2O to a final concentration of 2μM

1. Trypsinize, count, and pellet cells (tabletop, swinging bucket centrifuge) (100 RCF for 6min). Aspirate off medium.
2. Re-suspend pellet in 1xPBS so cell conc. is 1.67×10^6 cells/ml.
3. Place 1ml of cell suspension (1.67×10^6 cells) into a 1.5ml microfuge tube.
4. Pellet cells at 100 RCF for 5min.
5. Aspirate off PBS. Mix equal volume of 2% low melt agarose (LMA) and TE in a separate tube (50°C).
6. Transfer 40μl of LMA/TE mixture to the cell pellet, re-suspend, and transfer to a 200μl PCR tube.
7. Place samples at 4°C for 15min.
8. Open caps of PCR tubes. Using a pair of scissors, snip off very bottom of PCR tube and use a toothpick to push plug into a falcon tube containing LDS solution. As a standard, use 3ml/plug.
9. Incubate at 37°C overnight.

10. Remove plugs from LDS solution.
11. Wash the plugs at room temperature for 2h in 20% NDS solution (2.5ml/plug).
12. Discard 20% NDS and replace with fresh 20% NDS solution (2.5ml/plug). Incubate at room temperature for 2h (plugs can be stored at 4°C in 20% NDS solution until ready for DNA digestion).
13. DNA plugs to be digested, incubate at room temperature in TE for 1h (2ml/plug).
14. Remove TE and replace with fresh TE (2ml/plug). Incubate at room temperature for 1h.
15. Remove TE.
16. Place plugs in individual 1.5ml microfuge tubes.
17. Incubate plugs for 1h in 1xMbo1 restriction enzyme buffer at room temperature (200µl/plug).
18. Remove buffer.
19. Incubate plugs for 1h in 1xMbo1 restriction enzyme buffer @ RT (200µl/plug).
20. Remove buffer and make digestion mix.
    Per plug
    a. 92µl H_2O
    b. 15µl 10x RE buffer
    c. 3µl RE MboI (New England Biolabs, R0147L)
    d. Final volume should be 150µl (including 40µl plug)
21. Incubate at 37°C overnight.
22. Add 2µl of Mbo1 enzyme to each plug. Place at 37°C for 4-5h.
23. Discard restriction enzyme mix.
24. Prepare all plugs for electrophoresis by washing each plug in 4 ml of TE for 1h at room temperature.
25. Remove TE and add a fresh 4ml of TE, wash at room temperature for 1h.
26. Remove TE and incubate plugs for 1h at room temperature in 4ml of 0.5xTBE.
27. Load plugs into wells of the gel (1.2% agarose gel) and then cover with 1% LMA at 50°C.
28. Place whole gel at 4°C for 15min.
29. Run gel using pulsed field gel electrophoresis in 2500ml of 0.5x TBE (20h at a constant 6v/cm (200 V), ramping pulse times from 1 to 10sec. Keep run temperatures at 14°C).
30. Post-stain gel in 0.5xTBE (approximately 200ml) with 4µl of EtBr for 1h.
31. Take picture of gel with ruler.
32. Dry gel for 1h at 50°C.
33. Take picture of gel with ruler.
34. Pre-hybridize gel in 10ml of hybridization solution in "seal-a-meal" bag at 55°C for 1h.
35. Make up radioactively labeled probe by mixing
    a. 2.5µl DNA fragment (at 2µM. 5pmol) "G-rich probe"
    b. 5.0µl 5x Forward reaction buffer (Invitrogen, Y02295)
    c. 1.0µl T4 polynucleotide kinase (10U) (Invitrogen, 18004-010)
    d. 2.5µl [γ-^{32}P]ATP (10uCi/µl, 3000Ci/mmol)

e. 14.0µl H_2O

36. Incubate probe at 37°C for 15min.
37. Stop labeling reaction by adding EDTA for a final conc. of 5mM (for final volume of 200µl, add 175µl of 5.7mM EDTA).
38. Determine initial radioactive counts per min (CPM).
39. Make G25 sephadex column. (Add 3ml of sephadex mixture to spin column and spin at 575 RCF for 1.5min.
40. Add radioactive probe to G25 sephadex column and centrifuge (tabletop, swinging bucket centrifuge) at 575 RCF for 1.5min.
41. Determine final probe CPM (determine % incorporation).
42. Replace pre-hybridization solution with fresh 10ml of hybridization solution.
43. Add labeled probe to gel, seal bag, seal inside a second bag, incubate with shaking overnight in Tupperware container at 55°C.
44. Cut off corner of bag and use pipette to remove radioactive hybridization solution and discard into liquid waste container.
45. Place gel in medium sized Tupperware container.
46. Wash gel with 333ml of 4xSSC for 20min at RT on shaker three times.
47. Wash gel with 333ml of 4xSSC 0.1%SDS for 20min at 57°C with shaking three times.
48. Blot gel dry with Whatman papers.
49. Wrap gel in plastic wrap and expose to phosphoimager screen for 3h – overnight at room temperature.
50. Develop film and quantify any radioactive signal.
51. Pre-hybridize gel in 10ml of hybridization solution in "seal-a-meal" bag at 55°C for 1h.
52. Make up radioactively labeled probe by mixing
    a. 2.5µl DNA fragment (at 2µM. 5pmol) "C-rich probe"
    b. 5.0µl 5x Forward reaction buffer (Invitrogen, Y02295)
    c. 1.0µl T4 polynucleotide kinase (10U) (Invitrogen, 18004-010)
    d. 2.5µl [γ-^{32}P]ATP (10uCi/ul, 3000Ci/mmol)
    e. 14.0µl H_2O
53. Incubate probe at 37°C for 15min.
54. Stop labeling reaction by adding EDTA for a final conc. of 5mM (for final volume of 200µl, add 175µl of 5.7mM EDTA).
55. Determine initial radioactive counts per min (CPM).
56. Make G25 sephadex column. (Add 3ml of sephadex mixture to spin column and spin at 575 RCF for 1.5min.
57. Add radioactive probe to G25 sephadex column and centrifuge (tabletop, swinging bucket centrifuge) at 575 RCF for 1.5min.
58. Determine final probe CPM (determine % incorporation).
59. Replace pre-hybridization solution with fresh 10ml of hybridization solution.
60. Add labeled probe to gel, seal bag, seal inside a second bag, incubate with shaking overnight in Tupperware container at 55°C.

61. Cut off corner of bag and use pipette to remove radioactive hybridization solution and discard into liquid waste container.
62. Place gel in medium sized Tupperware container.
63. Wash gel with 333ml of 4xSSC for 20min at RT on shaker three times.
64. Wash gel with 333ml of 4xSSC 0.1%SDS for 20min at 57°C with shaking three times.
65. Blot gel dry with Whatman papers.
66. Wrap gel in plastic wrap and expose to phosphoimager screen for 3h – overnight at room temperature.
67. Develop film and quantify any radioactive signal.
68. Alkali denature DNA by placing gel in denaturing solution for 1h at room temperature with constant shaking.
69. Neutralize by placing gel in neutralizing solution for 1h at room temperature with constant shaking.
70. Place gel in H_2O for 30min at room temperature with constant shaking.
71. Pre-hybridize gel in 10ml of hybridization solution in "seal-a-meal" bag at 55°C for 1h.
72. Make up radioactively labeled probe by mixing
    a. 2.5µl DNA fragment (at 2µM. 5pmol) "G-rich probe"
    b. 5.0µl 5x Forward reaction buffer (Invitrogen, Y02295)
    c. 1.0µl T4 polynucleotide kinase (10U) (Invitrogen, 18004-010)
    d. 2.5µl [γ-^{32}P]ATP (10uCi/µl, 3000Ci/mmol)
    e. 14.0µl H_2O
73. Incubate probe at 37°C for 15min.
74. Stop labeling reaction by adding EDTA for a final conc. of 5mM (for final volume of 200µl, add 175µl of 5.7mM EDTA).
75. Determine initial radioactive counts per min (CPM).
76. Make G25 sephadex column. (Add 3ml of sephadex mixture to spin column and spin at 575 RCF for 1.5min.
77. Add radioactive probe to G25 sephadex column and centrifuge (tabletop, swinging bucket centrifuge) at 575 RCF for 1.5min.
78. Determine final probe CPM (determine % incorporation).
79. Replace pre-hybridization solution with fresh 10 ml of hybridization solution.
80. Add labeled probe to gel, seal bag, seal inside a second bag, incubate with shaking overnight in Tupperware container at 55°C.
81. Cut off corner of bag and use pipette to remove radioactive hybridization solution and discard into liquid waste container.
82. Place gel in medium sized Tupperware container.
83. Wash gel with 333ml of 4xSSC for 20min at RT on shaker three times.
84. Wash gel with 333ml of 4xSSC 0.1%SDS for 20min at 57°C with shaking three times.
85. Blot gel dry with Whatman papers.
86. Wrap gel in plastic wrap and expose to phosphoimager screen for 3h – overnight at room temperature.

87. Develop film and quantify any radioactive signal.
88. Determine relative G-strand overhang lengths by the following equation, RS_N / [(TL_C / TL_E) * RS_D], where RS_N is the radioactive signal from native gels hybridized with the $(CCCTAA)_4$ oligonucleotide, TL_C is the estimated telomere lengths of the control (homozygous wild-type) cells, TL_E is the estimated telomere lengths of the experimental (*Rad51d*$^{+/-}$ *Trp53*$^{+/-}$, *Trp53*$^{-/-}$, or *Rad51d*$^{-/-}$ *Trp53*$^{-/-}$) cells, and RS_D is the total radioactive signal from the denatured gels hybridized with the $(TTAGGG)_4$ oligonucleotide. Telomere lengths are determined as described by Harley et al., 1990.

ESTIMATING TELOMERE LENGTHS FROM ANIMAL TISSUES

Reagents and Materials:

1M Tris
- 1000ml H_2O
- 121g Tris
- pH to 8.0

0.5M EDTA
- 1000ml H_2O
- 186g EDTA
- pH to 8.0

TE Buffer
- 990ml H_2O
- 10ml 1M Tris
- 0.2ml 0.5M EDTA

2% Low melt agarose
- 100ml TE Buffer
- 2g low melt agarose

Lithium dodecyl sulfate (LDS) solution
- 400ml H_2O
- 5g lithium dodecyl sulfate (Sigma, L9781)
- 100ml 0.5M EDTA
- 5ml 1M Tris

20% NDS solution
- 372ml H_2O
- 1ml 1M Tris
- 0.9228g N-laurylsarcosine (Sigma, L5000)
- 127ml 0.5M EDTA

Alkali denaturing solution
- 250ml H_2O
- 8.7g NaCl
- 2g NaOH

Neutralizing solution
250ml H_2O
21.9g NaCl
15.1g Tris

10x TBE buffer
800ml H_2O
108g Tris
55g boric acid
40ml 0.5M EDTA

0.5x TBE buffer
1900ml H_2O
100ml 10x TBE buffer

Hybridization solution
145ml H_2O
0.621g NaH_2PO_4
1.125ml 20% SDS
22.5ml of 50x Denhardt's solution
56.25ml 20x SSC

0.04% collagenase II in DMEM
250ml DMEM
0.1g collagenase II
make fresh each time

G-rich telomere probe
$(TTAGGG)_4$ oligonucleotide (IDT, Inc.)
Dilute oligonucleotide in sterile H2O to a final concentration of 2μM

Tissue dissociation protocol can be used for heart, kidney, liver, spleen, or skeletal muscle.
Isolate fresh tissue samples of left ventricle (~0.5g), kidney (~0.5g), liver (~0.6g), spleen (~0.5g), and left quadriceps (~0.5g).

1. Wash tissue sample 3 times with 1xPBS.
2. Mince tissue with a razor blade.
3. Incubate tissue in a 15ml falcon tube containing 8ml of DMEM, 0.04% collagenase II.
4. Mix and incubate at 37°C for 2h (mix/pipette every 30min).
5. Centrifuge at 100 RCF for 5min (tabletop, swinging bucket centrifuge) to pellet cells.
6. Discard supernatant.

7. Re-suspend tissue samples in 5ml of 1xPBS.
8. Repeat steps 5-7 twice.
9. After final spin, aspirate all 1xPBS.
10. Add 1 pellet volume of TE buffer to sample.
11. Add 2 pellet volumes of 2% low melt agarose to sample.
12. Mix.
13. Transfer 40µl of cell mixture to a 200µl PCR tube.
14. Place at 4°C for 15min.
15. Incubate plugs in LDS solution overnight at 37°C (3.0ml/plug).
16. Remove plugs from LDS solution.
17. Wash the plugs at room temperature for 2h in 20% NDS solution (2.5ml/plug).
18. Discard 20% NDS and replace with fresh 20% NDS solution (2.5ml/plug). Incubate at room temperature for 2h (plugs can be stored at 4°C in 20% NDS solution until ready for DNA digestion).
19. DNA plugs to be digested, incubate at room temperature in TE for 1h (2ml/plug).
20. Remove TE and replace with fresh TE (2 ml/plug). Incubate at room temperature for 1h.
21. Remove TE.
22. Place plugs in individual 1.5ml microfuge tubes.
23. Incubate plugs for 1h in 1xMbo1 restriction enzyme buffer at room temperature (200µl/plug).
24. Remove buffer.
25. Incubate plugs for 1h in 1xMbo1 restriction enzyme buffer @ RT (200µl/plug).
26. Remove buffer and make digestion mix.
    Per plug
    a. 92µl H_2O
    b. 15µl 10x RE buffer
    c. 3µl RE MboI (New England Biolabs, R0147L)
    d. Final volume should be 150µl (including 40µl plug)
27. Incubate at 37°C overnight.
28. Add 2µl of Mbo1 enzyme to each plug. Place at 37°C for 4-5h.
29. Discard restriction enzyme mix.
30. Prepare all plugs for electrophoresis by washing each plug in 4ml of TE for 1h at room temperature.
31. Remove TE and add a fresh 4ml of TE, wash at room temperature for 1h.
32. Remove TE and incubate plugs for 1h at room temperature in 4ml of 0.5xTBE.
33. Load plugs into wells of the gel (1.2% agarose gel) and then cover each well with 1% LMA at 50°C.
34. Place whole gel at 4°C for 15min.
35. Run gel using pulsed field gel electrophoresis in 2500ml of 0.5x TBE (20h at a constant 6v/cm (200 V), ramping pulse times from 1 to 10sec. Keep run temperatures at 14°C).
36. Post-stain gel in 0.5xTBE (approximately 200ml) with 4µl of EtBr for 1h.
37. Take picture of gel with ruler.

38. Dry gel for 1h at 50°C.
39. Take picture of gel with ruler.
40. Alkali denature DNA by placing gel in denaturing solution for 1h at room temperature with constant shaking.
41. Neutralize by placing gel in neutralizing solution for 1 hr at room temperature with constant shaking.
42. Place gel in H_2O for 30min at room temperature with constant shaking.
43. Pre-hybridize gel in 10ml of hybridization solution in "seal-a-meal" bag at 55°C for 1h.
44. Make up radioactively labeled probe by mixing
    a. 2.5µl DNA fragment (at 2µM. 5pmol) "G-rich probe"
    b. 5.0µl 5x Forward reaction buffer (Invitrogen, Y02295)
    c. 1.0µl T4 polynucleotide kinase (10U) (Invitrogen, 18004-010)
    d. 2.5µl [γ-^{32}P]ATP (10uCi/µl, 3000Ci/mmol)
    e. 14.0µl H_2O
45. Incubate probe at 37°C for 15min.
46. Stop labeling reaction by adding EDTA for a final conc. of 5mM (for final volume of 200µl, add 175µl of 5.7mM EDTA).
47. Determine initial radioactive counts per min (CPM).
48. Make G25 sephadex column. (Add 3ml of sephadex mixture to spin column and spin at 575 RCF for 1.5min.
49. Add radioactive probe to G25 sephadex column and centrifuge (tabletop, swinging bucket centrifuge) at 575 RCF for 1.5min.
50. Determine final probe CPM (determine % incorporation).
51. Replace pre-hybridize solution with fresh 10ml of hybridization solution.
52. Add labeled probe to gel, seal bag, seal inside a second bag, incubate with shaking overnight in Tupperware container at 55°C.
53. Cut off corner of bag and use pipette to remove radioactive hybridization solution and discard into liquid waste container.
54. Place gel in medium sized Tupperware container.
55. Wash gel with 333ml of 4xSSC for 20min at RT on shaker three times.
56. Wash gel with 333ml of 4xSSC 0.1%SDS for 20min at 57°C with shaking three times.
57. Blot gel dry with Whatman papers.
58. Wrap gel in plastic wrap and expose to phosphoimager screen for 3h – overnight at room temperature.
59. Develop film and quantify any radioactive signal. Telomere lengths are determined as described by Harley et al., 1990.

ESTIMATING TELOMERE LENGTHS FROM RAT BLOOD SAMPLES

Reagents and Materials:

1M Tris
- 1000ml H_2O
- 121g Tris
- pH to 8.0

0.5M EDTA
- 1000ml H_2O
- 186g EDTA
- pH to 8.0

TE Buffer
- 990ml H_2O
- 10ml 1M Tris
- 0.2ml 0.5M EDTA

2% Low melt agarose
- 100ml TE Buffer
- 2g low melt agarose

Lithium dodecyl sulfate (LDS) solution
- 400ml H_2O
- 5g lithium dodecyl sulfate (Sigma, L9781)
- 100ml 0.5M EDTA
- 5ml 1M Tris

20% NDS solution
- 372ml H_2O
- 1ml 1M Tris
- 0.9228g N-laurylsarcosine (Sigma, L5000)
- 127ml 0.5M EDTA

Alkali denaturing solution
- 250ml H_2O
- 8.7g NaCl
- 2g NaOH

Neutralizing solution
250ml H_2O
21.9g NaCl
15.1g Tris

10x TBE buffer
800ml H_2O
108g Tris
55g boric acid
40ml 0.5M EDTA

0.5x TBE buffer
1900ml H_2O
100ml 10x TBE buffer

Hybridization solution
145ml H_2O
0.621g NaH_2PO_4
1.125ml 20% SDS
22.5ml of 50x Denhardt's solution
56.25ml 20x SSC

G-rich telomere probe
$(TTAGGG)_4$ oligonucleotide (IDT, Inc.)
Dilute oligonucleotide in sterile H2O to a final concentration of 2μM

Approximately 250-500μl of blood was drawn from rats into EDTA coated blood collection tubes and stored at 4°C. At start of procedure, large blood clots were observed in each tube.

1. Transfer blood samples (including clotted blood) into 1.5ml microfuge tubes.
2. Add 500μl of TE buffer to each tube and finger flick or lightly vortex samples.
3. Place tubes onto bench top to allow clotted blood to settle to the bottom of the tube.
4. Remove supernatant from each tube and transfer it to a fresh 1.5ml microfuge tube.
5. Centrifuge supernatants at 800 RCF (tabletop, swinging bucket centrifuge) for 5min to pellet cells.
6. Remove supernatant.
7. Re-suspend cells in 500μl of TE buffer.
8. Repeat steps 5-7 twice.
9. After final spin, aspirate all TE buffer.
10. Add 1 pellet volume of TE buffer to sample.
11. Add 2 pellet volumes of 2% low melt agarose to sample.

12. Mix.
13. Transfer 40µl of cell mixture to 200µl PCR tubes (cast as many plugs as possible).
14. Place at 4°C for 15min.
15. Incubate plugs in LDS solution overnight at 37°C (3.0ml/plug).
16. Remove plugs from LDS solution.
17. Wash the plugs at room temperature for 2 hr in 20% NDS solution (2.5ml/plug).
18. Discard 20% NDS and replace with fresh 20% NDS solution (2.5ml/plug). Incubate at room temperature for 2h (plugs can be stored at 4°C in 20% NDS solution until ready for DNA digestion).
19. DNA plugs to be digested, incubate at room temperature in TE for 1h (2ml/plug).
20. Remove TE and replace with fresh TE (2ml/plug). Incubate at room temperature for 1 hr.
21. Remove TE.
22. Place plugs in individual 1.5ml microfuge tubes.
23. Incubate plugs for 1 hr in 1xMbo1 restriction enzyme buffer at room temperature (200µl/plug).
24. Remove buffer.
25. Incubate plugs for 1 hr in 1xMbo1 restriction enzyme buffer @ RT (200µl/plug).
26. Remove buffer and make digestion mix.
    Per plug
    a. 92µl H_2O
    b. 15µl 10x RE buffer
    c. 3µl RE MboI (New England Biolabs, R0147L)
    d. Final volume should be 150µl (including 40µl plug)
27. Incubate at 37°C overnight.
28. Add 2µl of Mbo1 enzyme to each plug. Place at 37°C for 4-5h.
29. Discard restriction enzyme mix.
30. Prepare all plugs for electrophoresis by washing each plug in 4ml of TE for 1h at room temperature.
31. Remove TE and add a fresh 4ml of TE, wash at room temperature for 1h.
32. Remove TE and incubate plugs for 1h at room temperature in 4ml of 0.5xTBE.
33. Load plugs into wells of the gel (1.2% agarose gel) and then cover with 1% LMA at 50°C.
34. Place whole gel at 4°C for 15min.
35. Run gel using pulsed field gel electrophoresis in 2500ml of 0.5x TBE (20h at a constant 6v/cm (200 V), ramping pulse times from 1 to 10sec. Keep run temperatures at 14°C).
36. Post-stain gel in 0.5xTBE with 4µl of EtBr for 1h.
37. Take picture of gel with ruler.
38. Dry gel for 1h at 50°C.
39. Take picture of gel with ruler.
40. Alkali denature DNA by placing gel in denaturing solution for 1h at room temperature with constant shaking.

41. Neutralize by placing gel in neutralizing solution for 1h at room temperature with constant shaking.
42. Place gel in H_2O for 30min at room temperature with constant shaking.
43. Pre-hybridize gel in 10 ml of hybridization solution in "seal-a-meal" bag at 55°C for 1h.
44. Make up radioactively labeled probe by mixing
    a. 2.5µl DNA fragment (at 2µM. 5pmol) "G-rich probe"
    b. 5.0µl 5x Forward reaction buffer (Invitrogen, Y02295)
    c. 1.0µl T4 polynucleotide kinase (10U) (Invitrogen, 18004-010)
    d. 2.5µl [γ-^{32}P]ATP (10uCi/µl, 3000Ci/mmol)
    e. 14.0µl H_2O
45. Incubate probe at 37°C for 15min.
46. Stop labeling reaction by adding EDTA for a final conc. of 5mM (for final volume of 200µl, add 175µl of 5.7mM EDTA).
47. Determine initial radioactive counts per min (CPM).
48. Make G25 sephadex column. (Add 3ml of sephadex mixture to spin column and spin at 575 RCF for 1.5min.
49. Add radioactive probe to G25 sephadex column and centrifuge (tabletop, swinging bucket centrifuge) at 575 RCF for 1.5min.
50. Determine final probe CPM (determine % incorporation).
51. Replace pre-hybridization solution with fresh 10ml of hybridization solution.
52. Add labeled probe to gel, seal bag, seal inside a second bag, incubate with shaking overnight in Tupperware container at 55°C.
53. Cut off corner of bag and use pipette to remove radioactive hybridization solution and discard into liquid waste container.
54. Place gel in medium sized Tupperware container.
55. Wash gel with 333ml of 4xSSC for 20min at RT on shaker three times.
56. Wash gel with 333ml of 4xSSC 0.1%SDS for 20min at 57°C with shaking three times.
57. Blot gel dry with Whatman papers.
58. Wrap gel in plastic wrap and expose to phosphoimager screen for 3h – overnight at room temperature.
59. Develop film and quantify any radioactive signal. Telomere lengths are determined as described by Harley et al., 1990.

DETERMINING AREA UNDER THE CURVE FOR ANY f(x)

Reagents and Materials:

Texas Instruments TI-81 graphing calculator

This program is used to determine the area under the curve (integral) for any function of "x" [f(x)]. Write program exactly as written.

Program name: SIMPSON

```
:Disp_"L.ENDPOINT_(A)"
:Input_A
:Disp_"R.ENDPOINT_(B)"
:Input_B
:Disp_"PARABOLAS"
:Input_P
:(B-A)/(2P)→H
:A→X
:Y1→S
:1→J
:Lbl_1
:X+H→X
:S+4Y1→S
:X+H→X
:S+2Y1→S
:IS>(J,P-1)
:GOTO_1
:X+H→X
:S+4Y1→S
:X+H→X
:S+Y1→S
:HS/3→C
:Disp_"INTEGRAL"
:Disp_C
```

Example:
Determine the area under the curve of the equation [$y=2x^3+34x^2-16x+9$] from x=2 to x=5.

On the calculator, input the f(x) into Y_1

$:Y_1=(2x^3)+(34x^2)-(16x)+9$

Run program "SIMPSON"

Input “2” when asked for the “L.ENDPOINT”
Input “5” when asked for the “R.ENDPOINT”
Input “75” when asked for the number of “PARABOLAS” (75 means that the calculator will draw 75 “arcs” under the curve, determine the area for each “arc”, add all of the “arc” areas together, and give you the estimated area under the curve). 75 parabolas is a standard value and should be used for determining any integral (lower than 75 is calculated faster but will have slightly more error, higher than 75 will be calculated slowly but will be more accurate).

Press “ENTER” and wait for approximately 5 sec

The answer is 1489.5

Therefore, for the f(x), $y=2x^3+34x^2-16x+9$. The area under the curve from x=2 to x=5 equals 1489.5 $units^2$

ABSTRACT

The process of homologous genetic recombination is essential for increasing genetic diversity, maintaining chromosome and telomere structure, and repairing DNA damage. A homozygous targeted disruption of *Rad51d*, a gene required for homologous recombination (HR), confers embryonic and cell lethality in mice. In the absence of *Rad51d*, elevated levels of genome instability likely result in p53 activation and programmed cell death. As described in this thesis, a p53 deletion is sufficient to extend the lifespan of *Rad51d*-deficient embryos by up to 6 days, rescue the *Rad51d*-deficient cell lethal phenotype, and, for the first time, permit the characterization of mammalian cells deficient for *Rad51d*.

The *Rad51d*$^{-/-}$ *Trp53*$^{-/-}$ mouse embryonic fibroblasts (MEFs) exhibited extensive chromosome instability including aneuploidy, chromosome fragments, deletions, and complex rearrangements. Additionally, loss of *Rad51d* resulted in increased levels of centrosome fragmentation, which is likely a consequence of mitotic catastrophe initiated by chromosome instability in the mutant cells. Consistent with the role of RAD51D in HR-mediated repair of DNA damage, *Rad51d*-deficient cells were hypersensitive to DNA-damaging agents, particularly interstrand crosslinks, had reduced levels of radiation-induced RAD51-focus formation, and had decreased levels of DNA damage-induced sister chromatid exchange. These findings support a crucial role for the RAD51D protein in normal development, recombination, and DNA repair.

In addition to its role in DNA repair, the RAD51D protein localizes at telomeres, DNA-protein structures that protect chromosome ends. Decreased telomere lengths and

increased levels of anaphase bridging and telomere fusions were observed in primary *Rad51d*-deficient cells. Additionally, telomeres in the *Rad51d*$^{-/-}$ *Trp53*$^{-/-}$ MEFs had an increased frequency of being detected as DNA damage, as determined by the telomeric localization of γ-H2AX foci, and had long single-stranded telomeric 3′ overhangs. These data demonstrate that RAD51D functions to protect telomeres against attrition and fusion, potentially by assisting in the formation or resolution of telomeric T-loop structures.

The novel findings presented here and the tools that have been generated lay the groundwork for continued investigations to determine the mechanistic roles of RAD51D in maintaining genome stability, which may underlie protection against carcinogenesis.